

Synthesis and Biological Activity of Multifunctional Sensor/Effector Catalysts

Dissertation

zur Erlangung des Grades
des Doktors der Naturwissenschaften
der Naturwissenschaftlich-Technischen Fakultät III
Chemie, Pharmazie, Bio- und Werkstoffwissenschaften
der Universität des Saarlandes

Von

Saad Shaaban

Saarbrücken

November 2010

Tag des Kolloquiums: 08.02.2011, 14:15 Uhr.

Dekan: Prof. Dr. Stefan Diebels.

Berichterstatter: Jun. –Prof. Dr. C. Jacob.

Prof. Dr. Bernhardt.

Vorsitz: Prof. Dr. C. Jacob.

Akad. Mitarbeiter: Dr. L. A. Ba-Bernardi.

Diese Dissertation wurde in der Zeit von Dezember 2006 bis November 2010 unter Anleitung von **Jun.-Prof. Dr. Claus Jacob** im Arbeitskreis für Bioorganische Chemie, Fachrichtung Pharmazie der Universität des Saarlandes durchgeführt.

Bei Herr Prof. Dr. Claus Jacob möchte ich mich für die Überlassung des Themas und die wertvollen Anregungen und Diskussionen herzlich bedanken.

Dedicated to my loving Parents

I would like to dedicate my thesis to my mother and father.

I also want to dedicate my thesis to my loving wife, daughters and brothers.

“And We have enjoined on man to be dutiful and good to his parents. His mother bore him in weakness and hardship upon weakness and hardship, and his weaning is in two years give thanks to Me and to your parents, unto Me is the final destination”. [Quran 31.14]

Abstract

Increased generation of reactive oxygen species (ROS) and an altered redox status have long been observed in several types of cancer. This biochemical property of cancer cells might be exploited for therapeutic benefits since it might be possible to preferentially eliminate these cells by pharmacological ROS insults. Compounds able to modulate the intracellular redox state of cells have been developed, which effectively, yet also selectively, appear to kill cancer cells. Among the various agents employed to modulate the intracellular redox state of cells, certain redox catalysts containing quinone and chalcogen moieties have shown considerable promise since they are non-toxic on their own yet develop an effective, often selective cytotoxicity. A simple synthetic method based on the Passerini and Ugi multicomponent reactions has been developed for the synthesis of multifunctional redox catalysts. This method allowed the synthesis of a representative set of agents combining two, three or even four redox centres in one molecule in a good yield.

When incubated with cancer cells these multifunctional agents inhibited cell proliferation and induced both cell cycle delay and apoptotic cell death in low, often sub-micromolar concentrations. The cause was obviously OS, which was reflected by an enhanced ROS level together with a significant decrease in reduced glutathione. Interestingly, some of these redox active compounds showed quite low toxicity with normal human fibroblasts and endothelial cells, supporting the notion that such compounds might have a selective anticancer activity. Chemogenomic assays using a mutant library of *Saccharomyces cerevisiae* were used to look for chemical-genetic interactions. Analyzing the resulting chemical-genetic interaction profiles afforded a set of sensitive mutants. The corresponding knocked out genes of these mutants play a major role in the antioxidant defence system and are pivotal for the removal of toxic oxidants. Therefore, deletion of the respective genes might cause an OS sensitive phenotype of the mutant. These observations were in excellent agreement with the other cell-based assay performed as a part of this study. Finally, some of these compounds showed a potent antimicrobial activity evaluated against different fungal and bacterial strains.

Kurzdarstellung

Seit langem wird in mehreren Krebsarten eine erhöhte Generierung von reaktiven Sauerstoffspezies (ROS) und ein veränderter Redox-Status beobachtet. Diese biochemische Eigenschaft von Krebszellen könnte für therapeutische Zwecke genutzt werden, indem diese Zellen durch eine weitere Erhöhung des ROS-Levels eliminiert werden können. Wirkstoffe, die den intrazellulären Redox-Status der Zellen modulieren, wurden hier entwickelt. Diese können effektiv aber auch selektiv Krebszellen abtöten. Von den verschiedenen untersuchten Substanzen sind vor allem Redoxkatalysatoren, die Quinone- und Chalcogenreste enthalten, Erfolg versprechend. Sie sind an sich nicht toxisch, zeigen aber eine effektive und selektive Zytotoxizität. Für die Synthese von solchen multifunktionalen Redoxkatalysatoren wurde eine einfache synthetische Methode basierend auf den Passerini und Ugi Multikomponenten Reaktionen entwickelt. Diese Methode ermöglicht die Synthese eines repräsentativen Satzes von Substanzen mit hoher Ausbeute. Diese Substanzen enthalten zwei, drei oder sogar vier Redox-Zentren in einem Molekül.

Diese multifunktionalen Substanzen inhibieren die Zellproliferation in Krebszelllinien. Im niedrigen micromolaren Konzentrationsbereich hemmen sie den Zellzyklus und induzieren Apoptose. Diese Wirkung wurde durch oxidativen Stress (OS) vermittelt, was durch einen erhöhten ROS-Level zusammen mit einer deutlichen Abnahme von reduziertem Glutathion belegt werden konnte. Interessanterweise zeigen diese redox-aktiven Substanzen nur geringe toxische Effekte in primären humanen Fibroblasten sowie Endothelzellen, was die Annahme unterstützt, dass diese Substanzen einen selektiven Effekt auf Tumorzellen haben. Um chemo-genetische Wechselwirkungen dieser Stoffe zu identifizieren, wurden Experimente mit einer Bibliothek von *Saccharomyces cerevisiae* Mutanten durchgeführt. Dabei wurden mehrere Mutanten entdeckt, die sensitiv auf diese Stoffe reagieren. Die in diesen Mutanten deletierten Gene sind besonders bei der antioxidativen Kontrolle der Zellen von Bedeutung und spielen eine Schlüsselrolle bei der Beseitigung von toxischen Oxidantien. Die Deletion solcher Gene kann zu einem Phänotyp führen, der besonders empfindlich auf oxidativen Stress reagiert. Diese Ergebnisse stützen und bestärken die aus den zellbasierten Experimenten gewonnenen Daten. Schließlich zeigen einige dieser Substanzen eine starke antimikrobielle Aktivität gegen verschiedene Pilz- und Bakterienstämme.

Abbreviations

OS	Oxidative stress
ROS	Reactive oxygen species
MCR	Multicomponent reactions
P-3CR	Passerini three component reactions
U-4CR	Ugi four component reactions
U-4CC	Ugi four component condensation
CDCl₃	Chloroform
CH₂Cl₂	Dichloromethane
¹³C NMR	Carbon Nuclear magnetic resonance
d	Duplet
dd	Duplet of duplet
DMF	Dimethyl formamide
DMSO	Dimethyl sulfoxide
EtOH	Ethanol
g	Gram
¹H NMR	Proton Nuclear Magnetic Resonance
hr	Hour/hours
IC₅₀	50 % inhibition concentration
Kg	Kilogram
l	Litre
LC-MS	Liquid chromatography-mass spectroscopy
m/z	Mass to charge ratio
m	Multiplet
MeOH	Methanol
mg	Milligram
min	Minute
ml	Millilitre
MTT	3-(4,5-dimethylthiazol-2-yl)-2,5-diphenyl tetrazolium bromide
NADPH	Nicotinamide adenine dinucleotide phosphate

n.d.	Not determined
NMR	Nuclear Magnetic Resonance
PBS	Phosphate buffered saline
ppm	Parts per million
q	Quartet
RNO	Reactive nitrogen species
r.t.	Room temperature
s	Singlet
t	Triplet
TLC	Thin layer chromatography
δ	Chemical shift
%	Percent
μM	Micromolar
μl	Microlitre
GPx	Glutathione Peroxidase
GSH	Glutathione (Reduced)
GSSG	Glutathione disulfide
GST	Glutathione-S-transferase
SOD	Superoxide Dismutase
QSAR	Quantitative structure-activity relationship
GI₅₀	50% growth inhibition

Table of contents

Abstract	i
Kurzdarstellung.....	ii
Abreviations.....	iii
Chapter I: Introduction.....	1
1.1. Reactive Oxygen Species and the Redox Balance	1
1.2. Assessment of Oxidative Stress	4
1.2.1. Dichlorofluorescein assay (DCF)	5
1.2.2. DHE assay	6
1.2.3. DTNB assay	7
1.3. Effect of Oxidative Stress on Cellular Morphology and Cytoskeleton.....	7
1.4. Oxidative Stress as a Mediator of Apoptosis.....	8
1.5. Connections between Oxidative Stress and Cell Cycle	9
1.6. Therapeutic Strategies against Cancer	10
1.6.1. Agents which Increase Intracellular ROS Concentrations	12
1.6.2. Agents that Inhibit Antioxidant Enzymes.....	12
1.6.3. Catalysts that Enhance the Toxicity of ROS.....	12
1.7. Synthesis of Redox Modulator Agents.....	17
1.7.1. Nucleophilic Substitution.....	18
1.7.2. Aminoalkylation.....	19
1.7.3. Amide Coupling.....	20
1.8. Multicomponent Reactions (MCRs).....	22
1.8.1. Isocyanides.....	24
1.8.2. History of isocyanides.....	24
1.8.3. Preparation of Isocyanides.....	24
1.8.4. The Passerini Reaction.....	26
1.8.5. The Ugi Reaction.....	28
The objectives of this project.....	30
Chapter II: Materials and Methods	31
2.1. Synthetic strategies	31
2.2. Chromatography	32

2.3. Synthesis of building blocks for multicomponent reactions.....	34
2.4. Cell culture	36
2.5. Bioassays	39
2.5.1. Dichlorofluorescein assay (DCF)	39
2.5.2. Dihydroethidium assay (DHE)	39
2.5.3. 5,5'-dithiobis(2-nitrobenzoate) assay (DTNB)	40
2.5.4. Thiophenol oxidation assay (PhSH assay).....	41
2.5.5. Thiobarbituric acid radical scavenging assay (TBA assay).....	42
2.5.6. Caspase activity assay.....	43
2.5.7. Cell cycle analysis.....	43
2.5.8. Apoptosis.....	44
2.5.9. Immunocytochemistry (ICC).....	44
2.5.10. Chemogenomic assay.....	45
2.5.11. Antifungal assay.....	47
2.5.12. Antibacterial assay.....	48
2.5.13. Lipophilicity measurements.....	49
Chapter III: Results	50
3.1. Synthetic avenues for multifunctional redox agents	50
3.1.1. Nucleophilic substitution	50
3.1.2. The Passerini three-component reaction	53
3.1.3. The Ugi four-component reaction	66
3.2. Cell culture and biological studies	82
3.2.1. Cytotoxicity.....	82
3.2.2. Immunocytochemistry (ICC).....	84
3.2.3. Assessment of intracellular levels of oxidative stress.....	85
3.2.4. Thiophenol oxidation assay (PhSH assay).....	90
3.2.5. Thiobarbituric acid radical scavenging assay (TBA assay).....	91
3.2.6. Cell cycle analysis.....	92
3.2.7. Caspase activity.....	95
3.2.8. Apoptosis.....	96
3.2.9. Chemogenomic assay.....	97
3.2.10. Microbiological assays.....	97

3.2.11. The partition coefficient ($\log P_{ow}$) measurements.....	100
Chapter IV: Discussion.....	101
4.1. Selection and Synthesis of Suitable Redox Agents.....	101
4.2. Cytotoxic Activity of Redox Compounds in Cancer and Healthy Cells.....	107
4.3. Induction of Oxidative Stress.....	110
4.4. Cell Cycle Delay.....	112
4.5. Phenotypical changes in Cellular Morphology and Cytoskeleton.....	113
4.6. Induction of apoptosis.....	113
4.7. Chemical Genetic Interaction Approach.....	114
4.8. Antimicrobial Activity.....	115
4.9. QSAR studies.....	116
Concluding Remarks and Future Perspectives.....	117
References.....	119
Appendix.....	127

Chapter I: Introduction

Therapeutic selectivity and drug resistance are two major issues in cancer chemotherapy. By targeting the genetic differences between normal and cancer cells, drugs like Gleevec and Herceptin show promising therapeutic activity and few side effects.¹ These gene-targeting strategies however, are still facing problems because of genetic instability of cancer cells and acquired drug resistance.² Recent studies suggest that targeting the particular biochemical changes in cancer cells might be a feasible approach to develop a cancer therapy that does not lead to the development of drug resistance.³ Many types of cancer cells exhibit a disturbed intracellular redox balance, making them different from their healthy counterparts. Some tumours, such as solid lung carcinoma, are hypoxic, *i.e.* their cells are more reducing than normal ones, while others, such as the cells of breast and prostate cancer are naturally under oxidative stress (OS), and when compared to healthy cells, their reactive oxygen species (ROS) levels are considerably closer to the critical redox threshold at which cell death is induced (Figure 1). These biochemical differences between healthy and malignant tissue are significant, and can be used to design selective, yet effective redox drugs.⁴

1.1. Reactive Oxygen Species and the Redox Balance

Free oxygen radicals or, more generally, ROS, are broadly defined as chemically reactive molecules that have specific physiological functions in living organisms. There are two types of ROS, those of free radicals, such as superoxide ($O_2^{\cdot-}$), nitric oxide and hydroxyl radicals (OH^{\cdot}), which contain one or more unpaired electrons in their outer molecular orbitals, and non-radical ROS, which do not have unpaired electrons, including hydrogen peroxide, ozone, and peroxyxynitrite.

Cells control ROS levels by ROS-scavenging systems which could either be enzymatic (*e.g.*, by catalase, glutathione peroxidase, superoxide dismutase) or nonenzymatic (*e.g.*, by glutathione, some vitamins and metals, or phytochemicals such as isoflavones, polyphenols, and flavanoids). ROS can be found either in the environment, as pollutants, tobacco smoke, iron salts and radiation, or they can be generated inside cells.

The most common intracellular forms of ROS are listed in Table 1, together with their main cellular sources and the relevant enzymatic antioxidant systems scavenging these ROS molecules. Normal cells produce ROS through multiple mechanisms.

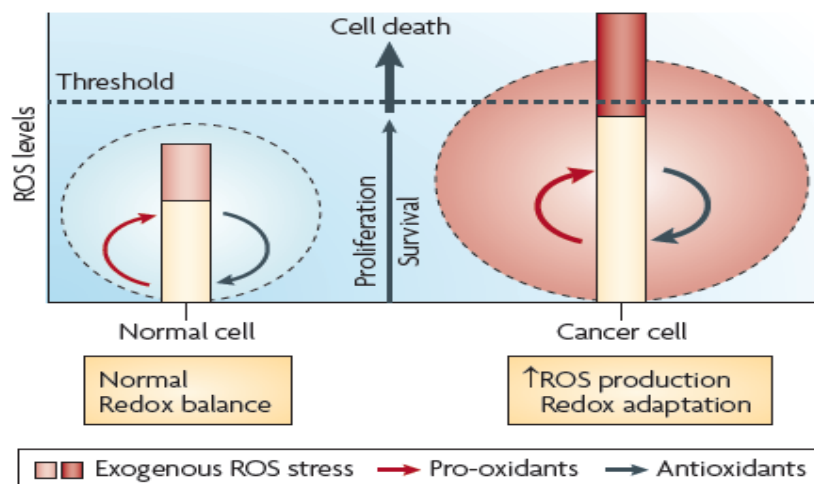


Figure 1. Cancer redox biology: a basis for therapeutic selectivity

Normal cells can tolerate a certain level of exogenous ROS stress owing to their 'reserve' antioxidant capacity, which can be mobilized to prevent the ROS level from reaching the cell-death threshold (horizontal dotted line in figure). In cancer cells, the increase in ROS generation may trigger a redox adaptation response, leading to an upregulation of antioxidant capacity and a shift of redox dynamics with high ROS generation and elimination to maintain the ROS levels below the toxic threshold. A further increase of ROS stress in cancer cells (red bar) using exogenous ROS-modulating agents is likely to cause elevation of ROS above the threshold level, leading to cell death.

(Nat. Rev. Drug Discov. 2009, 8, 579-591)

Mitochondrial respiration is considered to be the major source of ROS in the cell. Electrons leaking from the mitochondrial respiratory chain may react with molecular oxygen, resulting in the formation of superoxide, which can subsequently be converted to other ROS. The increase in ROS in some cancer cells has several causes. On the one hand, the increase of NADPH oxidase activity in malignant cells can lead to an increase in hydrogen peroxide concentrations. NADPH oxidase is regulated by the GTPase Rac1, which is itself downstream of the protooncogene Ras, linking cancer to ROS-production.⁵ Similarly, in most breast cancers, thymidine phosphorylase has been found to be overexpressed and its activity has been linked to increased ROS concentrations in tumour cells *in vitro*.⁶

This enzyme converts thymidine to thymine and 2-deoxy-D-ribose-1-phosphate. The latter is a highly reducing sugar able to glycosylate proteins and to generate oxygen radicals.

On the other hand, an increase in ROS can also occur because of the alteration in the activity of antioxidant enzymes.

Table 1. The major ROS molecules and their metabolism

ROS molecule	Main sources	Enzymatic defence systems	Products
Superoxide ($O_2^{\cdot-}$)	'Leakage' of electrons from the electron transport chain Activated phagocytes Xanthine oxidase Flavoenzymes	Superoxide dismutase (SOD)	$H_2O_2 + O_2$
Hydrogen peroxide (H_2O_2)	From $O_2^{\cdot-}$ via superoxide dismutase (SOD) NADPH-oxidase (neutrophils) Glucose oxidase Xanthine oxidase	Glutathione peroxidase Catalases Peroxiredoxins (Prx)	$H_2O + GSSG$ $H_2O + O_2$ $H_2O + GSSG$
Hydroxyl radical ($\cdot OH$)	From $O_2^{\cdot-}$ and H_2O_2 via transition metals (Fe or Cu) (Fenton's reaction) $Fe^{2+} + H_2O_2 \rightarrow Fe^{3+} + \cdot OH + OH^-$		
Nitric oxide (NO)	Nitric oxide synthases		GSNO

(Free Radical Biology and Medicine 2001, 31, 1287-1312)

ROS are well recognised for playing a dual role both as defender and destroyer species, they act as a double edged sword, *i.e.*, they can either be harmful or beneficial to living systems. Beneficial effects of ROS occur at low/moderate concentrations, for example in defence against infectious agents; as they are used by the immune system as a way to attack and kill pathogens, in the function of a number of cellular signalling systems, and in the induction of a mitogenic response. On the other hand, the overproduction of ROS on one side and a deficiency of enzymatic and/or non-enzymatic antioxidants on the other side, may cause potential biological damage, termed OS.

OS is considered to be a result of the disturbance in the equilibrium status of pro-oxidant/antioxidant reactions in living organisms. The excess ROS can damage cellular lipids, proteins, or DNA thus inhibiting their normal function.⁷

Because of this, OS has been implicated in a number of human ailments that are associated with a disturbed redox balance, among them various types of cancer, neurodegenerative diseases, and bacterial and viral infections, as well as disorders which occurs in the ageing process.⁸

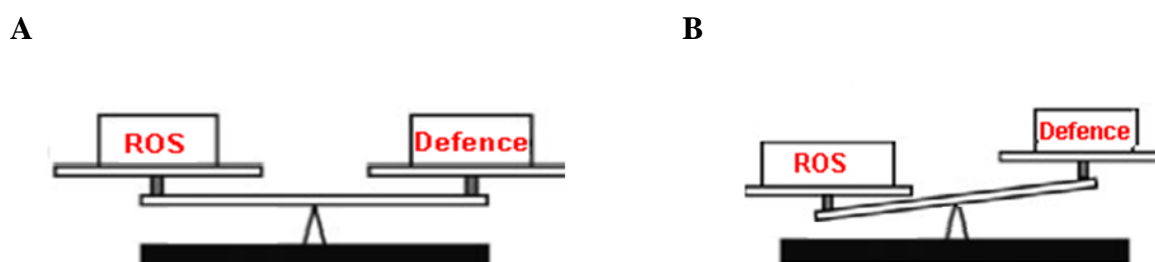


Figure 2. Redox balance and oxidative stress

- A) Under physiological conditions, normal cells maintain redox homeostasis with a low level of basal ROS by controlling the balance between ROS generation (pro-oxidants) and elimination (antioxidant capacity/defense).
- B) Oxidative stress could be found in biological systems when there is an overproduction of ROS on one side and a deficiency of enzymatic and non-enzymatic antioxidants on the other.

(J. Cell. Biochem. 2008, 104, 657-667)

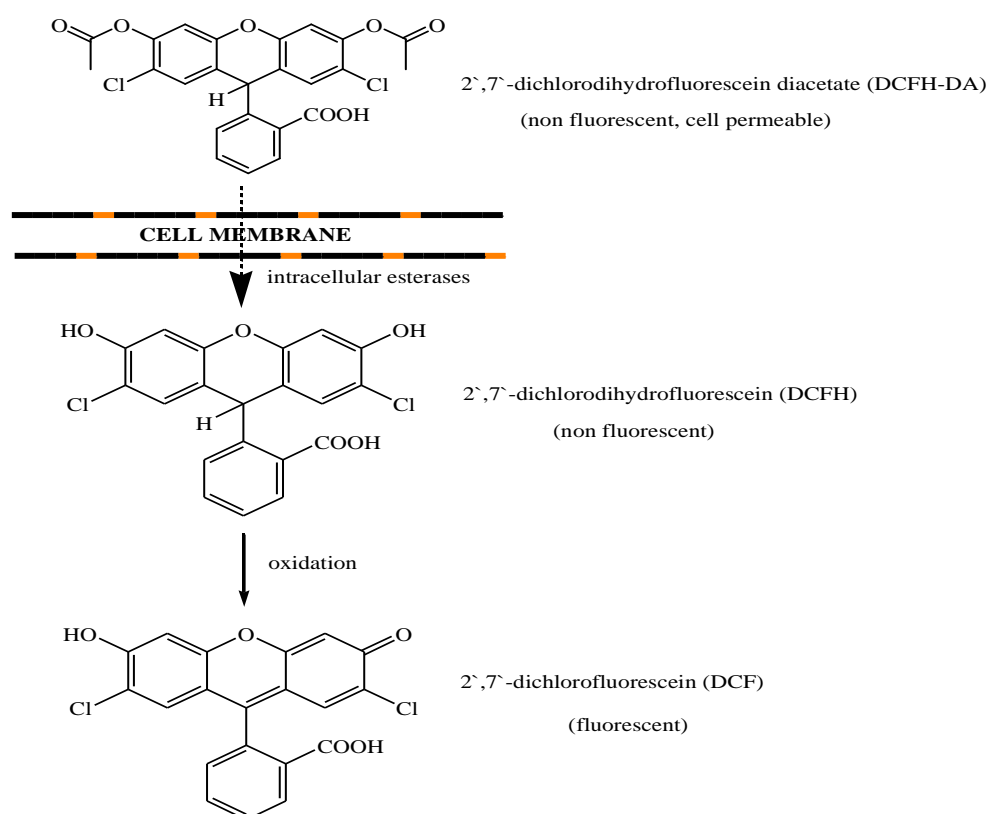
The fine balance between beneficial and harmful effects of free radicals is an important aspect in living organisms and is achieved by mechanisms called “redox regulation” (Figure 2). The process of “redox regulation” protects living organisms from various oxidative stresses and maintains “redox homeostasis” by controlling the redox status *in vivo*.⁹

1.2. Assessment of Oxidative Stress

Numerous methods have been used for estimating the oxidizing environment inside the cell. Among the most commonly used probes is 2',7'-dichloro(dihydro)fluorescein diacetate (DCFH-DA) and dihydroethidium (DHE) for the detection of intracellular ROS formation and 5,5'-dithiobis(2-nitrobenzoate) (DTNB) for the detection of intracellular reduced glutathione levels.¹⁰

a) Dichlorofluorescein assay (DCF)

DCF assay is considered to be a general indicator of ROS, reacting with H_2O_2 , ONOO^- , and lipid hydroperoxides.¹¹ It has been also used to implicate $\text{O}_2^{\cdot-}$ production, as H_2O_2 is considered a secondary product of $\text{O}_2^{\cdot-}$. DCFH-DA is cell permeable, and after uptake it is cleaved by intracellular esterases to the non-fluorescent 2',7'-dichlorodihydrofluorescein (DCFH). The latter is trapped within the cells and oxidized to the fluorescent 2',7'-dichlorofluorescein (DCF) by a variety of ROS (Figure 3).¹²

**Figure 3. Detection of ROS with the DCFH-DA probe**

DCFH-DA is cleaved by intracellular esterases to DCFH and oxidized by ROS to the highly fluorescent molecule DCF.

b) Dihydroethidium assay (DHE)

DHE is a lipophilic probe and diffuses readily across cell membranes. Once inside the cell, it is rapidly oxidized by superoxide to the red fluorescent 2-hydroxyethidium (2-OH-E⁺), which can be detected with a fluorescence detector using an excitation wavelength of 480 nm and an emission wavelength of 580 nm (Figure 4).¹⁰

Formerly, it was incorrectly thought that DHE reacts with O₂⁻ to form ethidium, a fluorescence probe which could be detected with a fluorescence detector using an excitation of 500-530 nm and an emission wavelength of 590-620 nm.¹⁰

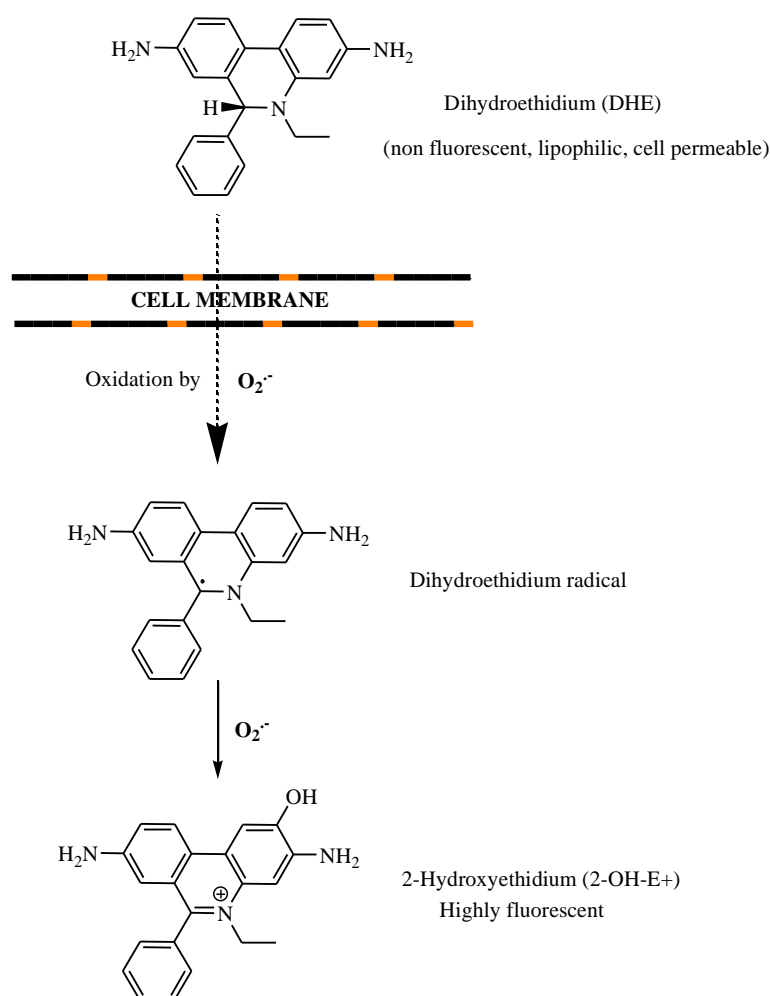


Figure 4. Detection of O₂⁻ by the DHE probe

The reaction of O₂⁻ with DHE produces 2-hydroxyethidium (2-OH-E⁺).

c) DTNB assay

Ellman's reagent or DTNB is a symmetrical aryl disulfide which readily undergoes the thiol-disulfide interchange reaction in the presence of a free thiol to give 2-nitro-5-thiobenzoic acid (NTB). The latter is ionized in water at neutral and alkaline pH to the yellow NTB^{2-} dianion which has a relatively intense absorbance at 412 nm. Because the stoichiometry of protein thiol to NTB formed is 1:1, NTB formation can be used to assess the number of thiols present (Figure 5).¹³

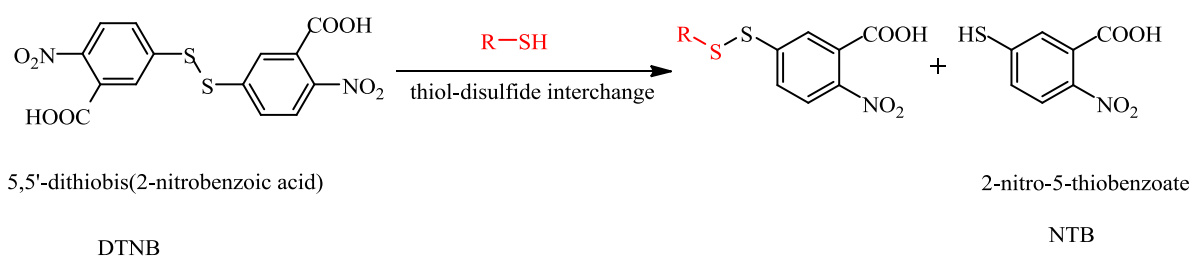


Figure 5. Detection of GSH by Ellman's reagent

The reaction of DTNB with a thiol to yield NTB.

1.3. Effect of Oxidative Stress on Cellular Morphology and Cytoskeleton

OS induces cellular injury by the production and accumulation of highly active free radicals, which may cause damage to all types of cellular biomolecules, including DNA, proteins, and lipids.¹⁴ In different mammalian cells, OS was reported to cause basically: free-thiol oxidation and appearance of oxidized proteins, disassembly of cytoskeleton, elevation of Ca^{2+} , increased plasma-membrane peroxidation and permeability, release of cytosolic components and breaking of DNA strands.^{15, 16} The eligible cellular targets of ROS are variable depending on many factors including: (i) cell-specific antioxidant pattern, (ii) intensity and nature of the stress imposed (*e.g.*, radical versus non-radical oxidant), and (iii) site of generation (*e.g.*, intra- versus extracellular).^{17, 18}

Due to its structure, the cytoskeleton may represent one of the preferential targets of ROS whatever OS is applied; indeed, cytoskeletal proteins are particularly abundant within the cells and several protein constituents of the cytoskeleton display highly reactive residues that can be oxidized easily.¹⁸

The actin cytoskeleton is considered to be an early target of cellular OS. The latter causes disruption of the normal organization of microfilaments, essentially due to oxidative modifications of specific methionine and cysteine sulfhydryls of actin.¹⁸

Although the interplay between the OS and endoplasmic reticulum (ER) stress is not clear, both of them have been implicated to participate in the pathogenesis of a wide variety of diseases such as neurodegenerative disorders, diabetes, and ischemia reperfusion heart disease.¹⁹

ER is an extensive intracellular membranous network involved in Ca^{2+} storage, Ca^{2+} signalling, glycosylation and trafficking of newly-synthesized membrane and secretory proteins. Perturbations of these processes cause a condition defined as ER stress.²⁰ It was reported that severe OS associated with accumulation of ROS and glutathione depletion may lead to a flux of calcium ions from the ER to the mitochondria and thereby to an activation of the ER stress-mediated apoptotic pathway.¹⁹

1.4. Oxidative Stress as a Mediator of Apoptosis

Cell death can follow two distinct pathways, apoptosis or necrosis. The early biochemical events that dictate the mode of cell death, however, are still unclear. On the one hand, necrosis appears to be the result of acute cellular dysfunction in response to severe stress conditions or after exposure to toxic agents, and is a relatively passive process associated with rapid cellular ATP depletion. Morphologically, necrosis is characterized by a dramatic increase in cell volume and rupture of the plasma membrane, with spilling of the cellular contents into the intercellular milieu.²¹

On the other hand, apoptosis is the process of programmed cell death (PCD) that may occur in multicellular organisms. Biochemical events lead to characteristic cell changes (morphology) and death. These changes include blebbing, loss of cell membrane integrity and attachment, cell shrinkage, nuclear fragmentation, chromatin condensation, and chromosomal DNA fragmentation. Several protease families are implicated in apoptosis, the most prominent being caspases. Caspases are cysteine-containing, aspartic acid-specific proteases which exist as zymogens in the soluble cytoplasm, mitochondrial intermembrane space, and nuclear matrix of virtually all cells.²¹

There are two types of apoptotic caspases: initiator and effector caspases. Initiator caspases (*e.g.*, CASP2, CASP8, CASP9, and CASP10) cleave inactive pro-forms of effector caspases, thereby activating them. Effector caspases (*e.g.*, CASP3, CASP6, and CASP7) in turn cleave other protein substrates within the cell, to trigger the apoptotic process. The initiation of this cascade reaction is regulated by caspase inhibitors.

Up to now, three predominant apoptotic pathways, namely death receptor-mediated extrinsic pathway, mitochondria-mediated intrinsic pathway, and endoplasmic reticulum (ER) stress-mediated apoptotic pathway have been elucidated.²²

It has been reported that ROS are able to activate both the ER stress-mediated apoptotic pathway (discussed in section 1.3) and the mitochondrial-mediated apoptotic pathway. The latter is activated by inducing loss of mitochondrial transmembrane potential, cytochrome *c* release and caspase cascade activation.¹⁹ Indeed, it has also been shown that the increase in the cytosolic free calcium concentration due to ER stress coordinates with the opening of the mitochondrial permeability transition pores, which is substantial in the induction of mitochondria-mediated intrinsic apoptotic pathway.²³

1.5. Connections between Oxidative Stress and Cell Cycle

In fact, the examination of the current literature on the effect of OS on the cell cycle reveals that increases in ROS-induced DNA damage are correlated with cell cycle arrest.²⁴ However, whether ROS-exposed cells undergo growth arrest or apoptosis may depend in part on where the cell resides in the cell cycle when insulted. For example, human fibroblasts treated with H₂O₂ underwent either cell cycle arrest or apoptosis. The majority of the apoptotic fibroblasts were in the S phase of the cell cycle, whereas growth-arrested cells were predominantly in the G₁ or the G₂/M phase.^{24, 25}

1.6. Therapeutic Strategies against Cancer

The role of OS in promoting cancer development and in causing oxidative damage provides two opposite therapeutic rationales against cancer.³ On the one hand, antioxidants could be used to increase reactive oxygen species (ROS) scavenging capacity, thereby nullifying ROS signalling and suppressing tumour growth.²⁶

On the other hand, an opposite approach is to treat cancer cells with pharmacological agents that have pro-oxidant properties, which increase ROS generation or abrogate the cellular antioxidant systems.²⁷

The use of antioxidants for cancer prevention has become popular since the 1980s. The function of antioxidants in physiological systems is to prevent ROS concentrations from reaching a damaging level within a cell and also to attenuate metastatic progress.²⁸ Although treating ROS-inducing tumours with antioxidants is reasonable, ironically, the mechanism underlying that many chemotherapeutic agents and ionizing radiation exert on tumour cell kill is not associated with the increase of antioxidants, but rather the production of more ROS leading to irreversible OS.

Recent studies have shown that supplementation with antioxidants, such as vitamin C or E, prevents some beneficial effects of exercise, such as adaptation to stress.²⁹ Moreover, several antioxidants used in clinical trials were associated with increased cancer incidence.³⁰ This undesired effect of antioxidants might be related to the prevention of oxidative damage in tumours and the inhibition of ROS mediated apoptosis. Antioxidants may therefore promote tumour-cell survival.

Several attempts have therefore been made during the last 10 years to use the naturally occurring OS to selectively kill cancer cells. In preclinical models, ROS-generating agents showed selective toxicity towards malignant cells under OS, raising their endogenous ROS levels over the threshold of toxicity as antioxidant systems become overwhelmed.^{4, 31} Within this context, currently explored ROS-inducing strategies can be divided into three main lines of investigation (Figure 6):

- a) Agents that directly increase ROS in cancer cells to lethal levels.
- b) Agents that inhibit antioxidant enzymes and hence raise ROS concentrations to lethal levels.
- c) Catalysts that enhance the toxicity of ROS.

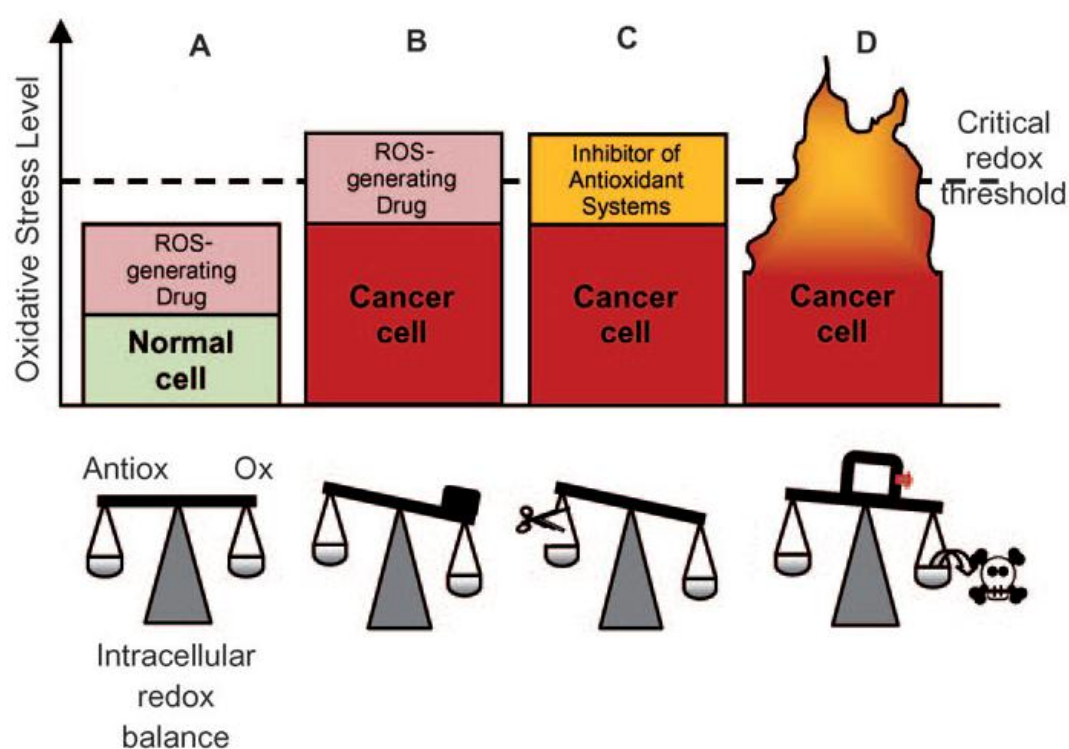


Figure 6. Redox modulation models

- A) Normal cells possess a redox homeostasis with a low level of basal ROS.
- B) ROS generating agents increase OS in cancer cells above the critical redox threshold and cause cell death.
- C) Agents inhibit the antioxidant enzymes, increase ROS concentrations by inhibiting ROS detoxification.
- D) Catalytic agents do not change the pre-existing redox balance or ROS composition, but facilitate the reaction of ROS with redox-sensitive pivotal proteins and enzymes. The rapid oxidation/modification of these potential enzymes subsequently triggers apoptotic processes in the cancer cells.

Please note that this is a preliminary model, and issues such as differences in redox thresholds between normal and cancer cells or antioxidant activities associated with certain compounds *in vitro* require further exploration.

(Antiox=antioxidants; Ox=oxidants.)

(Chemistry - A European Journal 2010, 16, 10920-10928)

1.6.1. Agents which Increase Intracellular ROS Concentrations

Agents investigated as a part of this strategy include arsenic trioxide, a compound able to increase superoxide levels by interfering with the mitochondrial respiratory chain; redox cycling quinones such as β -lapachone, emodin, daunorubicin and doxorubicin, compounds able to generate superoxide and hydrogen peroxide *via* a semiquinone intermediate; bortezomib, a proteasome inhibitor; as well as cisplatin and elesclomol (Figure 6, panel B and Figure 7).^{32, 33}

1.6.2. Agents that Inhibit Antioxidant Enzymes

The redox balance is maintained by various enzymes that readily neutralize many types of disease-causing free radicals and toxic oxidants, ridding the organism of their harmful effects. Superoxide dismutases (SOD) catalyze the conversion of $O_2^{\cdot-}$ to H_2O_2 , which can then be converted to water by catalase (CAT) or glutathione peroxidase (GPx). Antioxidant enzyme inhibitors lead to OS by inhibiting ROS detoxification. Such agents include chemically diverse compounds, such as 2-methoxyestradiol (a SOD inhibitor), aminotriazol (a CAT inhibitor), and mercaptosuccinic acid (a GPx inhibitor) (Figure 6, panel C and Figure 7).^{34, 35}

1.6.3. Catalysts that Enhance the Toxicity of ROS

ROS generators and inhibitors of antioxidant enzymes add an additional ROS burden without really discriminating directly between normal and sick cells (Figure 6, panel B and C). These previously mentioned strategies rely only on the pre-existing differences in ROS levels between cancer and normal cells. Furthermore, the dosage of such agents is a serious problem.^{4, 31, 36} These compounds are not catalytic, and therefore need to be administered in rather large quantities, which might lead to serious side effects.

Alternative approaches depending upon the usage of catalytic molecules that employ ROS as their substrates may not only raise ROS levels, but may also exhibit selectivity to cells rich in ROS, without exhibiting the same chemistry in normal cells (Figure 6, panel D). This delicate difference between ROS generators on one hand, and ROS users on the other, has significant implications for selective drug design. This leads to the area of sensor/effector agents and to metallo-organic, selenium, and tellurium chemistry. In principle, catalysts that enhance the toxicity of ROS could be divided into three classes.

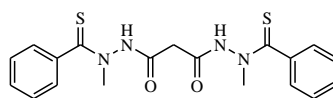
Agents able to generate oxidative stressors



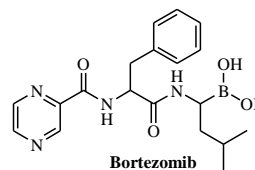
Arsenic trioxide



Cisplatin

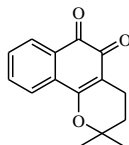


Elesclomol

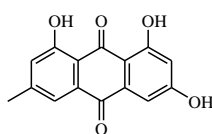


Bortezomib

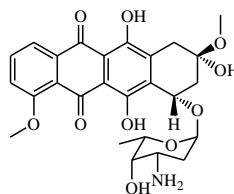
Redox cycler agents



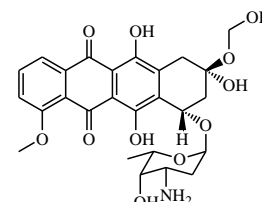
Beta-lapachone



Emodin

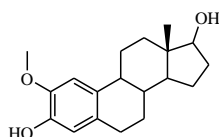
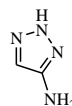
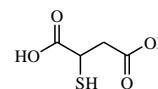


Daunorubicin

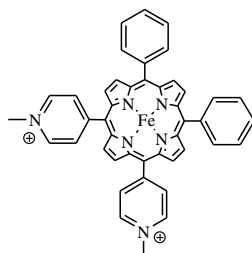
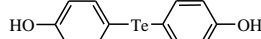


Doxorubicin

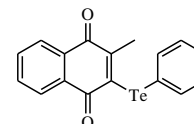
Agents inhibiting antioxidants enzymes

2-methoxyestradiol
SOD inhibitorAminotriazol
CAT inhibitorMercaptosuccinic acid
GPx inhibitor

Catalytic agents generating/enhancing the cytotoxicity of oxidative stressors

*cis*-FeMPy₂P₂P

4,4'-dihydroxydiphenyl telluride



2-(Phenyltelluryl)-3-methyl-(1,4)naphthoquinone

Figure 7. Chemical structures of compounds that enhance OS.

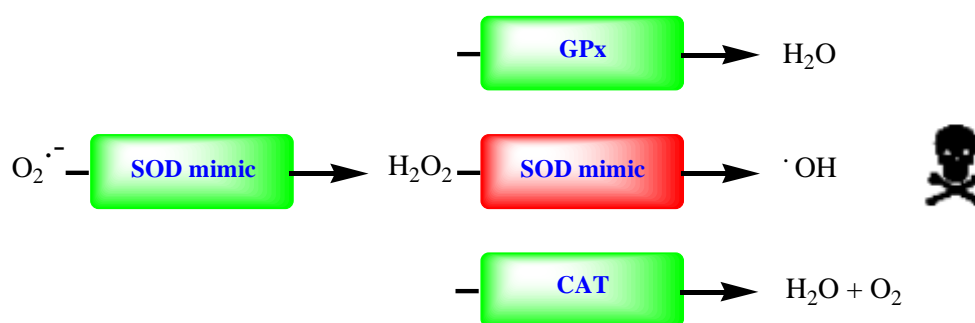
Agents are grouped according to their likely mode of action. Agents able to generate oxidative stressors (including redox-cycling quinones), agents inhibiting antioxidant enzymes and catalytic agents generating/enhancing the cytotoxicity of oxidative stressors.

The first class consists of compounds that are able to convert less reactive ROS to a cocktail of more damaging species. Such catalysts include various SOD mimics, which rely on pre-existing ROS in cancer cells and generate a different composition of ROS (Figure 8, panel A).

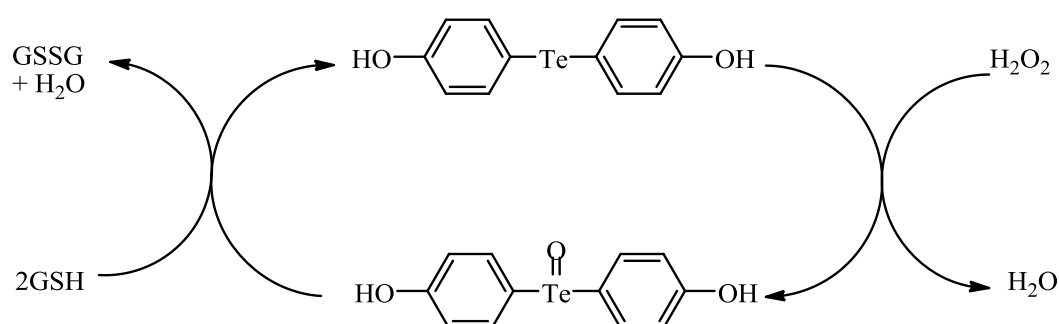
Kawakami *et al.*³⁷ have shown that an iron-based porphyrin complex (*cis*- or *trans*-FeMPy₂P₂P, Figure 7) with SOD activity is able to convert less reactive superoxide into a more reactive hydrogen peroxide and hydroxyl radical cocktail, since the latter is considerably more reactive towards proteins, DNA and membranes. Although metal-porphyrin complexes are highly specific for cancer cells, and do not exert a major effect on healthy cells, the use of such compounds has one major drawback. These complexes contain a metal ion that might dissociate from the complex during cellular metabolism.

The second class of ROS user consists of agents that are able to use ROS and speed up their reactions with redox-sensitive proteins and enzymes, ultimately causing malfunction and cell death. These compounds include organochalcogen-GPx mimics which do not generate any new ROS but rely on the pre-existing ROS in cancer cells.^{38, 39}

A



B



C

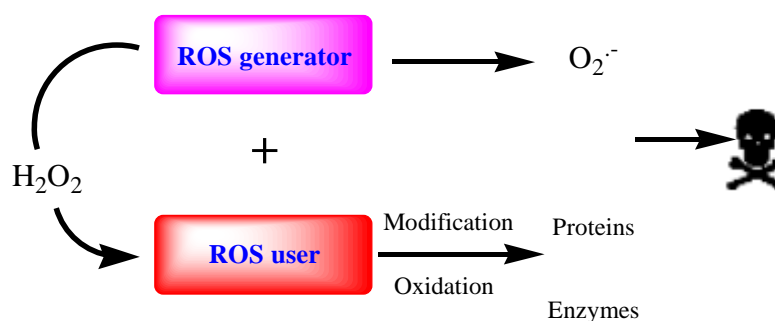


Figure 8. ROS enhancer catalyst models

- SOD mimics rely on pre-existing ROS in cancer cells; they are able to convert less reactive superoxide into a more reactive hydrogen peroxide and hydroxyl radicals leading to death of malignant cells.
- GPx mimics; 4,4'-dihydroxydiphenyltelluride catalyzes the oxidation of thiols in cells under (externally induced) H_2O_2 stress.
- Combinations of ROS-generating and ROS-using agents lead to the area of sensor/effector agents and to metallo-organic, selenium and tellurium chemistry, which could be a potent strategy to promote ROS accumulation in cells and enhance cytotoxicity against cancer cells.

Unlike iron, copper or manganese complexes, selenium (and tellurium) agents mimicking the activity of the selenium enzyme GPx are chemically and metabolically stable, the chalcogen being covalently attached to an alkyl or aryl group. A range of GPx mimics such as, 4,4'-dihydroxydiphenyltelluride (Figure 6), are known to exhibit some selectivity for cells under (externally induced) H₂O₂ stress. Such agents are able to catalyze the oxidation of thiols in the presence of hydrogen peroxide or peroxyxynitrite (Figure 8, panel B).⁴⁰

Since a disturbed redox balance is not just due to one chemical species but is the result of a combination of various ROS, reactive nitrogen species (RNS), metal ions and deficiencies in antioxidant defences, and to maximally exploit the ROS-mediated cell-death mechanism as a therapeutic strategy, it is possible to combine ROS-generating and ROS-using (GPx-mimic catalytic) agents.³¹ This approach has been adopted to increase the catalytic efficiency and might be particularly useful in cancer cells that have become adapted to stress and are therefore resistant to traditional anticancer agents.^{31,36}

Tailor-made compounds combining more than one redox centre in one molecule were expected to increase efficiency and selectivity (Figure 8, panel C). For example, 2-(phenyltelluryl)-3-methyl-(1,4)naphthoquinone (Figure 7), for the first time, could be employed effectively in sub-micromolar concentrations *i.e.*, at low concentration compared to the first generation of Se and Te GPx-like catalysts.⁴¹ The quinone redox system was chosen as ROS generator because of its known activity in bioreductive anticancer agents. Like the chalcogen centre, quinone agents utilise several mechanisms to exert a cytotoxic effect. Of special interest is their ability to perform redox cycling processes with triplet oxygen, forming superoxide and peroxide.³² This is especially advantageous as the peroxide formed as a result of redox cycling of the quinone moiety has the potential to activate the chalcogen moiety of the catalyst. Although bioreductive agents act *via* a different mechanism (the prodrug is activated by cellular reductase enzymes whose expression varies widely between cell lines), the sensitivity towards the status of the cellular redox environment makes quinone redox systems interesting to both approaches.

Quinones can undergo either one-electron or two-electron reductions. The first one might be mediated by microsomal NADPH P450 reductase, NADH cytochrome *b*₅ reductase or mitochondrial NADH-oxidoreductase to form the corresponding semiquinone radical.

Alternatively, a two electron reduction is mediated by NAD(P)H:quinone oxidoreductase (*nqo1*) (DT-diaphorase) to form the corresponding hydroquinone (Figure 9). The driving force is the formation of a fully aromatic system. Under aerobic conditions, the semiquinone radical and the hydroquinone can be oxidized to the parent quinone by molecular oxygen.⁴²

This process, the reduction by a reductase followed by auto-oxidation, yields the toxic superoxide anion radicals ($O_2^{\cdot-}$) and is known as “quinone redox cycling”. It is oxygen-dependent and continues until the system becomes anaerobic. In general, the redox cycling of quinones in cells would quickly lead to conditions of OS *via* the formation of ROS capable of inflicting damage. Therefore, the redox cycling of quinonoid drugs and other related compounds has been implicated widely as a mechanism for their cytotoxicity.³²

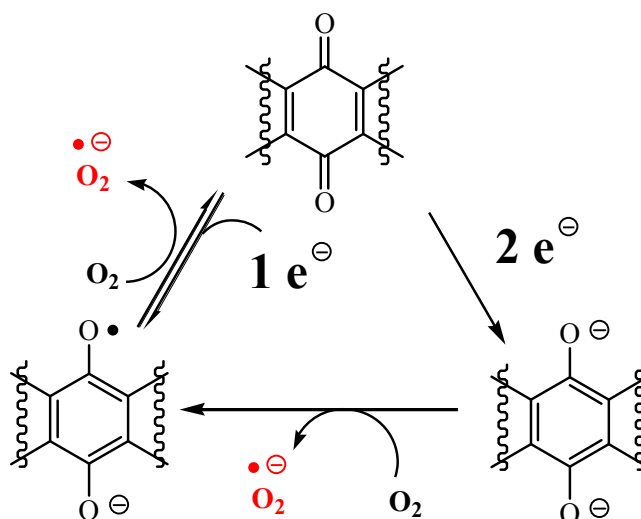


Figure 9. Redox cycling of quinones

Quinones can be bioreduced to semiquinones *via* a one-electron process. In the presence of oxygen the quinone can be regenerated, forming superoxide. Alternatively, a two-electron bioreduction of quinones leads to the hydroquinone anion.

(J. Am. Chem. Soc. 2010, 132, 5469-5478)

1.7. Synthesis of Redox Modulator Agents

The desire to increase the selectivity for cancer cells under OS has recently stimulated the synthesis of considerably more complicated multifunctional agents, which are tailored according to the biochemical redox signature of cancer cells and often combine two, three or even more functionalities (*e.g.* redox centres, metal binding sites) in one molecule.

Various synthetic avenues have been reported including: nucleophilic substitution, amino alkylation, and amide coupling. These avenues were used to generate a vast number of such multifunctional catalysts, which are chemically diverse and, depending on their structure, exhibit various interesting biological activities.⁴³

1.7.1. Nucleophilic Substitution by Redox Active Chalcogen Moiety at Quinone Core Structure

The direct attack of nucleophilic selenolate or tellurolate compounds at suitable bromoquinones was previously reported.^{44,45} This approach enables the generation of compounds combining two to four redox centres relevant to OS (Figure 10). While this one-step synthetic method is attractive because of its comparable simplicity, its scope appears to be limited by the chemical diversity, number of compounds achievable, and low yields especially in case of tellurium derivatives. In the case of compound **3n**, for instance, yields of just 9% have been obtained.^{36,39}

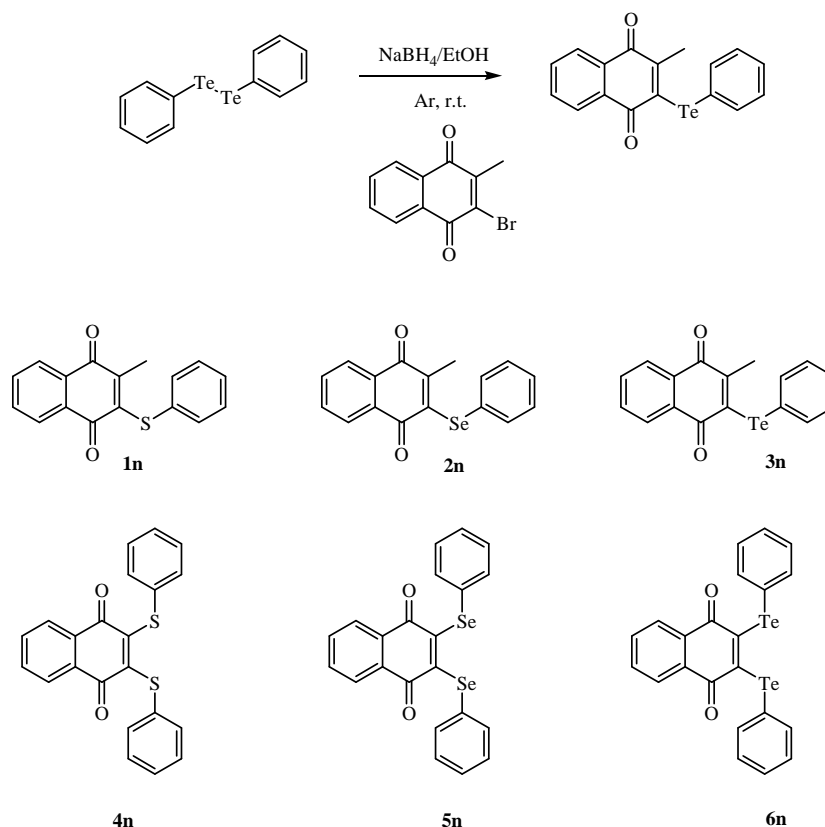


Figure 10. Schematic overview of the synthesis of redox modulators by nucleophilic substitution

NaBH₄ was added to a solution of the appropriate dichalcogenide in ethanol (the thiophenol was used in case of sulfur analogues, NaBH₄ was not required in this case) and the mixture was stirred until the solution turned colourless. A solution of the bromoquinone in ethanol was then added through the rubber septum and the reaction mixture was further stirred at room temperature and monitored *via* thin layer chromatography for completion.

1.7.2. Aminoalkylation

Aminoalkylation of the quinone by various chalcogen-containing amines was then explored to overcome the previous limitations.^{46, 47} This reaction proceeds *via* nucleophilic attack of the amine-based nucleophile at the quinone (Figure 11). Mechanistically it resembles the method described in section 1.7.1., with two significant differences: Firstly, aminoalkylation is a Michael addition reaction targeting quinones, and not bromoquinones. Secondly, the reactivity is controlled by the amine and not by the chalcogen (yet see below).

This method was employed successfully to synthesize compounds combining a naphthoquinone with one or two sulfur or selenium moieties in a yield of around 20 to 35%.

Although this method shows considerable promise for the synthesis of multifunctional sulfur and selenium agents, it could not (yet) be used for the synthesis of the corresponding tellurium analogues. One may speculate that the long reaction time of three days, combined with the oxidizing conditions required to re-oxidize the semi- or hydroquinone to quinone (*i.e.* presence of air), may adversely affect the tellurium moiety.⁴³

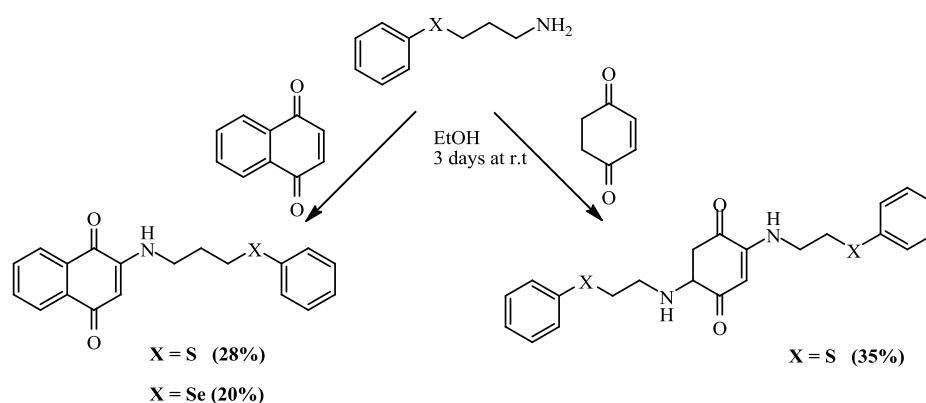


Figure 11. The aminoalkylation method

A solution of appropriate chalcogen-containing amine in ethanol was added dropwise to an ethanolic solution of quinone. The mixture was then stirred for three days on air and in the dark. The reaction was monitored *via* thin layer chromatography for completion. A selection of compounds synthesized according to this method is shown.

(Org. Biomol. Chem. 2009, 7, 4753-4762)

1.7.3. Amide Coupling

The amide coupling method is based on amide bond formation between acid and amine, a reaction used extensively in peptide synthesis and renowned for its wide applicability and mild conditions. This method is used to synthesize a range of compounds, some of which are shown in Figure 12.

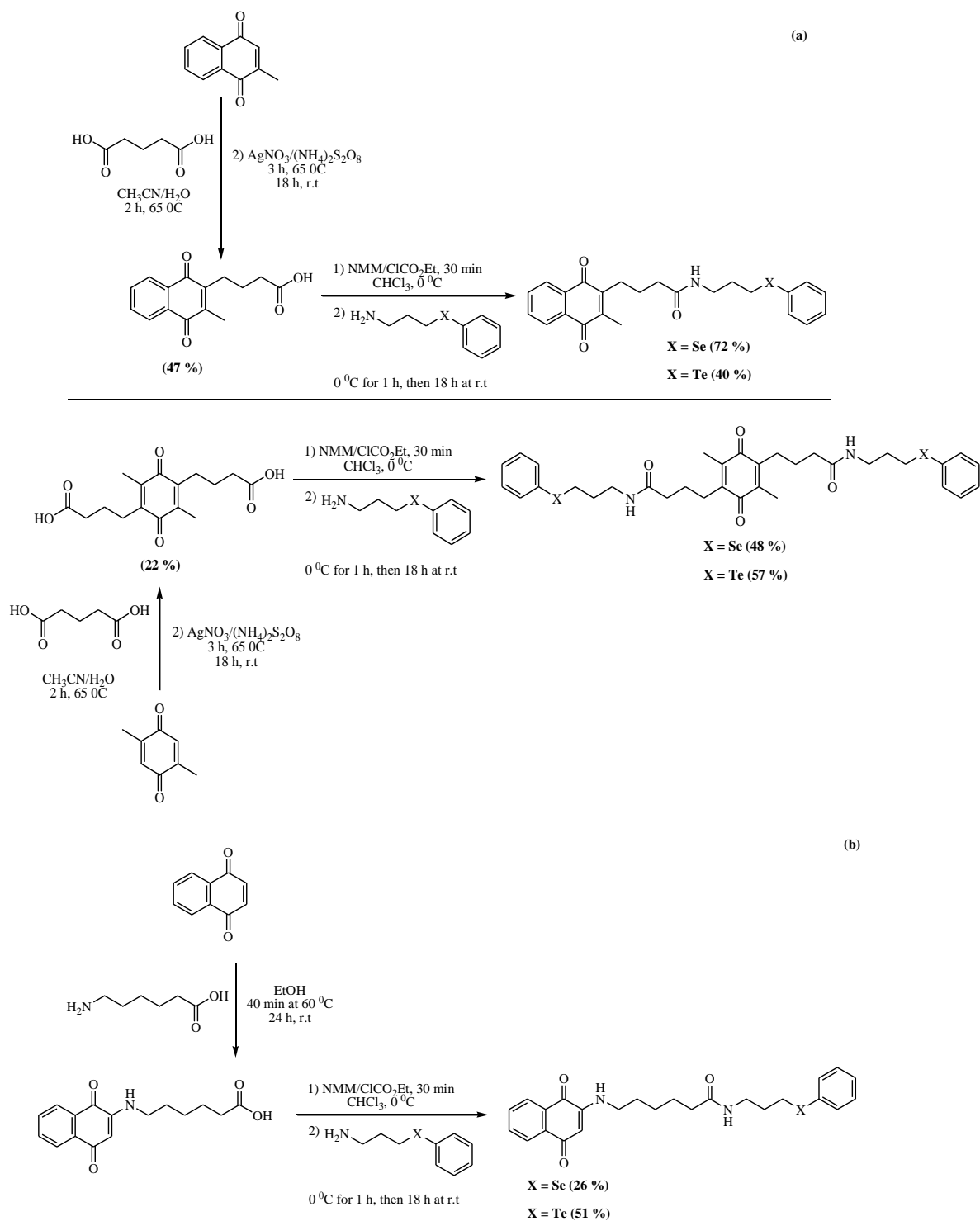


Figure 12. The amide coupling method

Individual components carrying different functional groups are synthesized first and then assembled in a final, straightforward step. This method employs ‘linkers’, which attach to the quinone *via* a carbon or nitrogen atom (panel a and b, respectively). A selection of compounds synthesized according to this method is shown.

(Org. Biomol. Chem. 2009, 7, 4753-4762)

In the first step, chalcogen-containing amines and quinone-containing carboxylic acid building blocks were obtained. It is possible, for instance, to attach a carbon chain to the quinone *via* oxidative decarboxylation of an acid, such as glutaric acid (Figure 12, panel a). Similarly, primary amines may be attached to quinones to form secondary amines (Figure 12, panel b).^{48,49}

Amide coupling works well for sulfur, selenium and tellurium providing compounds in rather good yields of around 50 to 60% (Figure 12). The preparation of the individual building blocks and the coupling reaction itself can be performed under rather mild conditions. It is also possible to ‘switch’ the acid and amine functions, *i.e.* to generate amine-bearing quinones and chalcogen-containing acids. This method is suitable for the creation of a small library of agents, but is limited by the number of building blocks which can be assembled at one time.⁴³

1.8. Multicomponent Reactions (MCRs)

Although amide coupling may be limited by the fact that just two building blocks (acid and amine) can be combined at a time, similar building blocks can be used in MCRs. MCRs are chemical transformations in which three or more reactants form a product derived from all of the inputs and they have been known for over 100 years. The development of MCRs is an efficient aspect in modern drug discovery for the preparation of so-called “substance libraries” from which pharmaceutical lead structures might be selected for the treatment of different diseases.

Although it would be difficult to identify the first example of a MCR, the Hantzsch dihydropyridine (DHP) synthesis was reported in 1882,⁵⁰ followed by the Biginelli 3CR in 1893.⁵¹ The first isocyanide-based MCRs were disclosed by Passerini (3CR) and Ugi (4CR) in 1921 and 1959, respectively (Figure 13).⁵² Many subsequent variants of the Passerini and Ugi reactions that capitalize on the unique reactivity of isocyanides have subsequently been described. During this time, MCRs have also found wide application in the synthesis of natural products and other targets of interest.⁵³

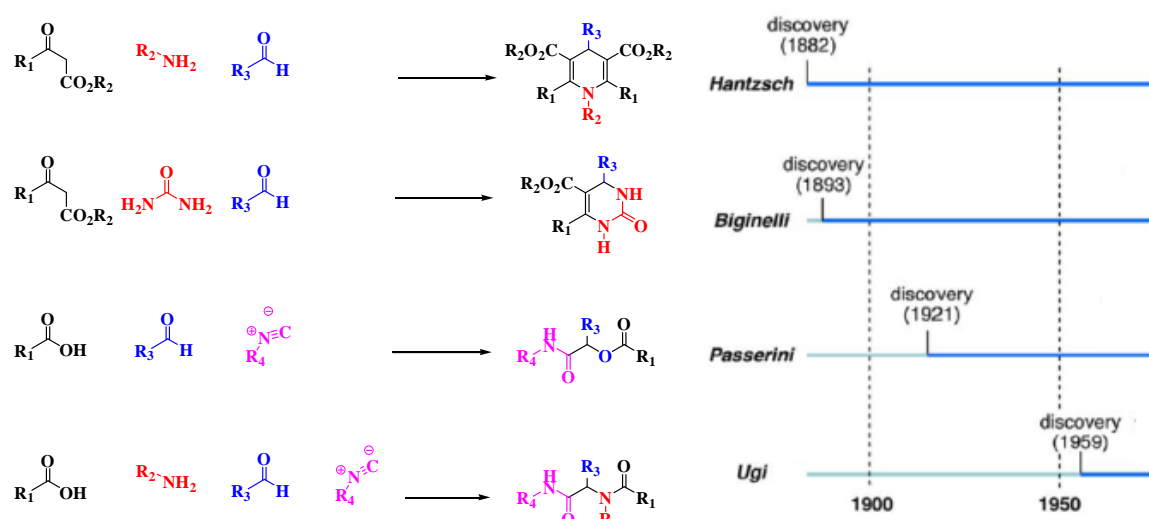


Figure 13. Timeline of discovery of multicomponent reactions (MCRs)

The Hantzsch dihydropyridine (DHP) synthesis was reported in 1882, followed by the Biginelli 3CR in 1893. The first isocyanide based MCRs were disclosed by Passerini (3CR) and Ugi (4CR) in 1921 and 1959, respectively.

(Curr. Opin. Chem. Biol. 2010, 14, 371-382)

Generally, there are different classification schemes of MCRs possible, *e.g.* according to the reaction mechanisms, the components involved, or their intrinsic variability.⁵⁴ Special subclasses are isocyanide based MCRs (IMCRs).⁵⁵ They are particularly interesting because they are more versatile and diverse than the remaining MCRs. The great potential of isocyanides for the development of multicomponent reactions lies in the diversity of bond forming processes available, their functional group tolerance, and the high levels of chemo-, regio-, and stereoselectivity often observed.⁵⁶

1.8.1. Isocyanides

Isocyanides, formerly known as isonitriles, are compounds, which contain a truly extraordinary functional group. They are the only class of organic compounds with a formally divalent carbon that could react with nucleophiles and electrophiles at the same atom, leading to the so-called α -adduct. In contrast other functional groups react typically at different atoms with either both nucleophiles or electrophiles.

Almost all commercially available isocyanides are volatile and carry a repulsive odor. Other liquid isocyanides do not smell and, in general, higher molecular weight isocyanides are often solid and odorless.

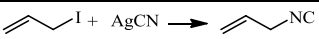
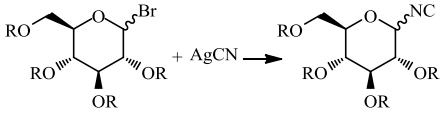
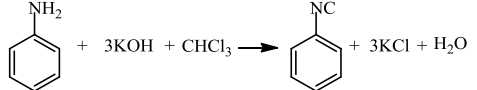
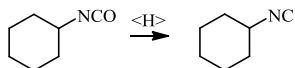
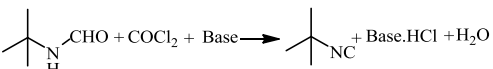
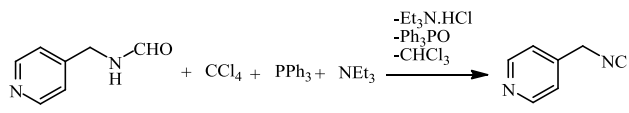
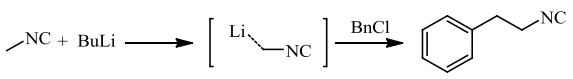
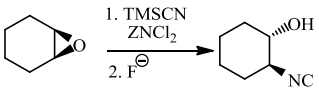
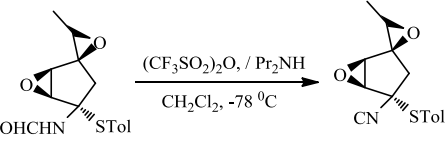
1.8.2. History of isocyanides

Isocyanides were first synthesized in 1859 by Lieke.⁵⁷ The classical syntheses were then developed in 1867 by Gautier⁵⁸ and Hoffmann.⁵⁹ For a whole century, the chemistry of isocyanides stood out because of their unpleasant smell, which forced the chemist to work in outdoors space. In this period, the most interesting reactions were Passerini's introduction and investigation of his three component conversions in 1921-1931.⁶⁰ The isocyanides became generally well available by 1958, and shortly after, Ugi *et al.*⁶¹ introduced the four-component reaction of the isocyanides, which is, since 1962, referred to as the Ugi reaction (U-4CR).

1.8.3. Preparation of Isocyanides

Isocyanides are relatively unavailable commercially and can be challenging to prepare. Even though dozens of methods for the preparation of isocyanides have been described,⁶² the most common method of isocyanide preparation is by dehydration of formamides, which is considered the method of choice regarding cost, yield, and execution in most cases.^{63, 64} Depending on which further functionalities are present, many alternative production methods can be drawn upon (Table 2).

Table 2. Important methods for the preparation of isocyanides.

Method	Example*	Reference
Lieke, 1859		57
Meyer, 1866		65
Hoffmann, 1867		59
Hoffmann, 1870		66
Ugi, 1958		67
Appel, 1972		68
Schöllkopf, 1971		69
Barton, 1988		70
Gassman, 1982		71
Baldwin, 1990		72
Kitano, 1998		73

* DABCO = 1,4-diazabicyclo[2.2.2]octane, TMS = Me₃Si, Tol = tolyl.

(Angew. Chem. Int. Ed Engl. 2000, 39, 3168-3210)

Today most MCR chemistry performed with isocyanides relates to the classical reactions of Passerini and Ugi. Indeed, the large number of different scaffolds now available are mostly built on these two MCRs and their combination with other types of reactions.

1.8.4. The Passerini Reaction

The Passerini reaction is a three-component condensation reaction of carboxylic acid, aldehyde and isocyanide with the concurrent generation of a stereogenic center to afford an α -acyloxyamide in a single step (Figure 14). This motif is present in the structures of many natural products, such as the pharmacologically active depsipeptides.⁷⁴ The P-3CR reaction can also lead to interesting and potentially bioactive peptidomimetic compounds and offers an inexpensive and rapid way to generate compound libraries. It is often a key step in the total synthesis of natural products.⁷⁵

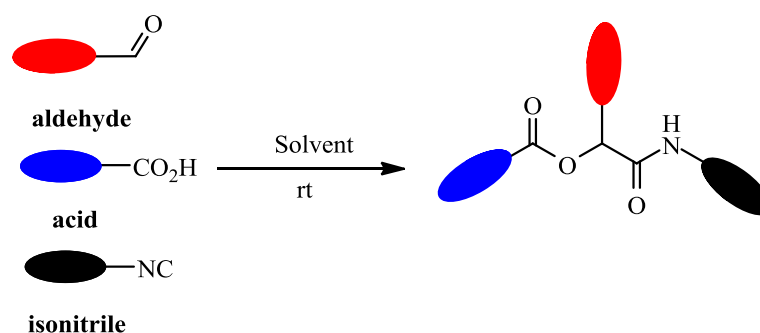


Figure 14. Passerini multicomponent reaction

This three-component reaction between a carboxylic acid, a carbonyl compound such as a ketone or aldehyde, and an isocyanide, offers direct access to α -acyloxyamides.

It was postulated that the reaction proceeds either *via* an ionic or *via* a concerted mechanism (Figure 15).⁵⁵ In polar solvents such as methanol or water, the reaction proceeds *via* an ionic mechanism *via* protonation of the carbonyl component followed by nucleophilic addition of the isocyanide and carboxylate residue, respectively. The resultant intermediate undergoes acyl group transfer and amide tautomerization to give the α -acyloxyamide. In non-polar solvents and at high concentrations a concerted mechanism is favorable: a trimolecular reaction between the isocyanide, the carboxylic acid, and the carbonyl in a sequence of nucleophilic additions has been proposed. The transition state [TS] is depicted as a 5-membered ring with partial covalent or double bonding. The last step includes the acyl migration to the neighbouring hydroxyl group to give the desired ester.

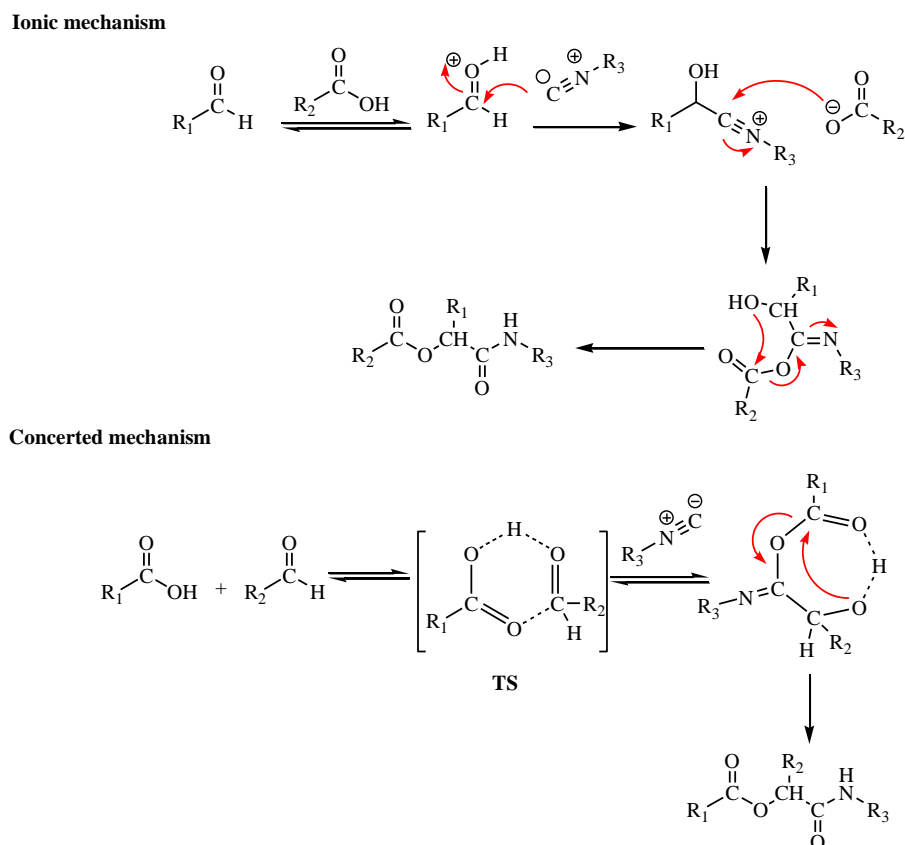


Figure 15. Mechanism of the Passerini reaction

Two different reaction pathways have been hypothesized:

- In polar solvents such as methanol or water, the reaction proceeds *via* an ionic mechanism.
- In non-polar solvents and at high concentrations a concerted mechanism is likely.

There is some support that the Passerini reaction proceeds *via* the concerted mechanism where the reaction kinetics depend on all three reactants and the reaction usually takes place in relatively non-polar solvents (in line with the transition state). There are three main factors, which have an influence on the rate of the Passerini reaction: acidity of the medium, concentration of the reagents and the polarity of the solvents. Thus, in the presence of strong mineral acids the reaction was complete in 1 min.⁷⁶ It was also established that the Passerini reaction is accelerated in aprotic solvents, supporting that the Passerini reaction proceeds *via* the concerted mechanism.⁷⁷

Another important factor is the concentration of reagents, because all MCRs including the Passerini reaction proceed better if the reactants are present in high concentration, that is 0.5-1 M.⁷⁶

1.8.5. The Ugi Reaction

The Ugi-4CR usually refers to the reaction between an amine (usually a primary amine; less often ammonia or a secondary amine), a carbonyl compound (aldehyde or ketone), an isocyanide and a carboxylic acid to give α -amido amides (Figure 16).⁵⁵ Thus, this reaction is an extension of the Passerini three- component reaction.

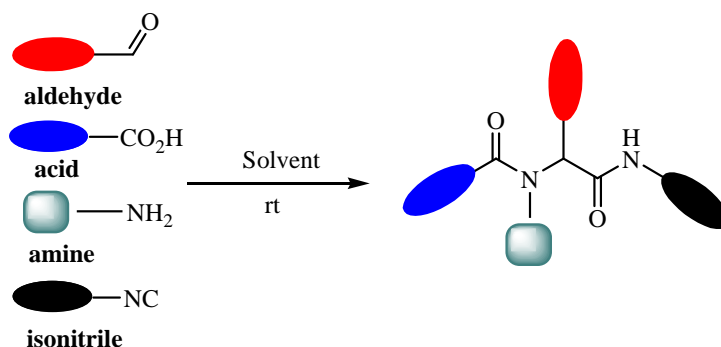


Figure 16. Ugi multicomponent reaction

This reaction involves a four-component condensation between an aldehyde, an amine, a carboxylic acid and an isocyanide which allows the rapid preparation of α -aminoacyl amide derivatives.

It was postulated that the reaction involves a sequence of four steps including: a) imine formation (step 1), b) protonation of the imine by acid, thus strongly increasing the electrophilicity of the C=N bond (step 2), c) α -addition of the electrophilic iminium cation and the nucleophilic carboxylate anion to isocyanide (step 3), and d) intramolecular acyl-transfer (step 4) (Figure 17). The Ugi reaction is known to work in polar aprotic solvents, like DMF. However, methanol and ethanol have also been used successfully.⁷⁸

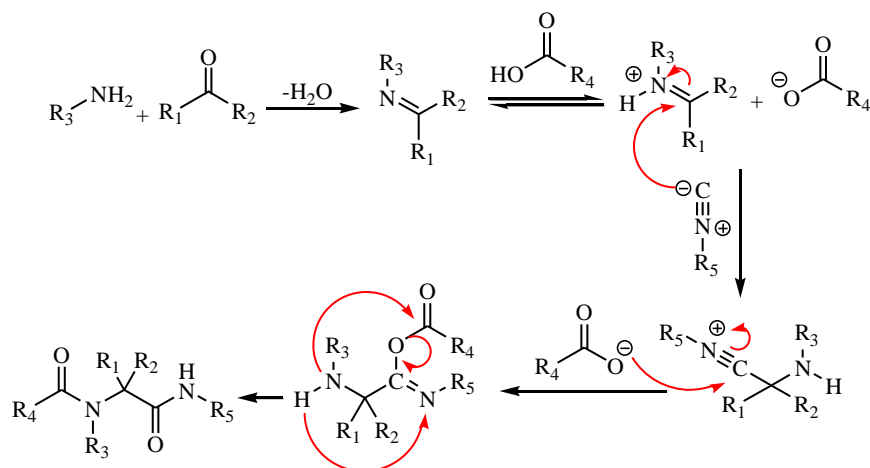


Figure 17. Mechanism of the Ugi reaction

The mechanism is believed to involve a prior formation of an iminium by condensation of the amine with the aldehyde, followed by addition of the carboxylic acid oxygen and the imino carbon across the isocyanide carbon; the resulting acylated isoamide rearranges by acyl transfer to generate the final product.

Recent research has shown that the Passerini and Ugi reactions are accelerated in water.⁷⁹ This acceleration has been attributed to many factors, such as the hydrophobic effect and enhanced hydrogen bonding in the transition state.^{80, 81}

The objectives of this project

Several attempts have been made to design and synthesize multifunctional agents able to recognize the *various* ingredients of OS in cells. Needless to say, the synthesis of such compounds encounters increasing difficulties when moving from just one or two to three or more redox sites, in particular if a rather complicated selenium and/or tellurium chemistry is involved.

The aim of this study is to discover suitable synthetic avenues that could be used to generate multi-functional agents. These agents are designed in order to represent di-, tri-, and even tetra-functional redox agents with multiple chalcogen and quinone redox sites.

The potency and selectivity of toxic compounds to inhibit cell proliferation is evaluated by using a range of cancer cell lines and healthy primary cells. Phenotypical changes, the induction of cell death, OS, cell cycle delay, and apoptosis are also intended to be explored as a part of this study.

Several techniques, such as immunostaining and fluorescence activated cell sorting (FACS) are applied for exploring the mode of action of these multifunctional compounds.

Chapter II: Materials and Methods

2.1. Synthetic strategies

While there is a strong demand for multifunctional redox agents containing sulfur, selenium or tellurium, synthetic avenues leading to such agents are often marred by difficulties and low yields. We have therefore explored three different methods for the synthesis of agents combining one, two, three or even four redox/metal binding sites in one molecule.

A. Method 1

This method relies on the direct attack of nucleophilic selenolate or tellurolate compounds at suitable bromoquinones. Several compounds combining two or three redox centres were generated by employing the heterogeneous solvent system (water and ethyl acetate (1:1)) and a phase transfer catalyst (PTC, tetrabutylammonium chloride).

Multicomponent reactions (MCRs)

Multicomponent reactions are convergent reactions, in which three or more starting materials react to form a product. This allows high synthetic efficiency, a minimization in the formation of by-products and simple synthetic procedures.

B. Method 2 (the Passerini three-component reaction (P-3CR))

This reaction type allows the synthesis of α -acyloxy carboxamides from a carboxylic acid, an aldehyde and an isocyanide.

C. Method 3 (the Ugi four component reaction (U-4CR))

This reaction type allows the synthesis of amide bonded α -aminoacyl amide structures from a carboxylic acid, an aldehyde, an amine and an isocyanide.

2.2. Chromatography

Thin layer chromatography (TLC)

Silica gel 60 F₂₅₄ (with fluorescent indicator) pre-coated sheets, 20 x 20 cm wide and 0.2 mm thick (Merck, Germany), were used for TLC analysis, during synthesis and isolation. The solvent systems used for TLC were mixtures of methanol and dichloromethane, or ethyl acetate and petroleum ether (40-65 °C) in different proportions.

Cerium Molybdate Stain (Hanessian's Stain) was applied to the TLC as a means to visualize compounds on the plate. For this stain, ammonium molybdate (12 g), ceric ammonium molybdate (0.5 g) and concentrated sulfuric acid (15 ml) were added to 235 ml of distilled water. This stain is a highly sensitive, multipurpose (multifunctional group) stain.

Column Chromatography (CC)

Silica gel 60 (0.063-0.200 mm) 70-230 mesh (Merck, Germany) was used as stationary phase for column chromatography. The solvent systems applied for the Silica gel column were mixtures of methanol and dichloromethane, or ethyl acetate and petroleum ether (40-65 °C) in different proportions.

Materials and analytical methods

Chemical reagents for the synthesis of compounds were purchased from Sigma-Aldrich-Fluka (Darmstadt, Germany) and used without further purification unless stated otherwise. CHCl₃ and CH₂Cl₂ were refluxed with phosphorus pentoxide (P₂O₅) and freshly distilled before use. THF was stored for two days over Na and then refluxed using benzophenone as indicator, and freshly distilled before use. Diethyl ether was stored over KOH, for two days refluxed using benzophenone as indicator and freshly distilled before use.

3-(Phenylselanyl)propanoic acid **2a**⁸², 3-(3-methyl-1,4-dioxo-1,4-dihydronaphthalen-2-ylthio)propanoic acid **2b**⁸³, 5-(4-carboxyphenyl)-10,15,20-triphenylporphyrin **2f**⁸⁴, 2-(phenylselanyl)acetaldehyde **1a**⁸⁵, 3-(phenyltellanyl)propan-1-amine⁸⁶, 3-(phenylselanyl)propan-1-amine⁸⁶, 3-(phenylthio)propan-1-amine⁸⁶, 1,2-bis(2,2-diethoxyethyl)diselane⁸⁵ and benzyl 6-isocyanohexanoate **3b** were synthesized according to the literature.⁸⁵ Reactions were carried out under argon (99.996%) using standard Schlenk techniques. Reaction progress was monitored by TLC on Alugram SIL G UV254 (Macherey-Nagel).

¹HNMR spectra were recorded at 500 MHz, and ¹³CNMR spectra at 125 MHz on a Bruker (Rheinstetten) DRX 500 or Avance 500 spectrometer. Chemical shifts are reported in δ (ppm), expressed relative to the solvent signal at 7.26 ppm (CDCl₃, ¹HNMR) and at 77.16 ppm (CDCl₃, ¹³CNMR), as well as 3.31 ppm (CD₃OD, ¹HNMR) and 49.00 ppm (CD₃OD, ¹³CNMR). Coupling constants (J) are given in Hz.

LC-MS/MS analysis was performed using a TSQ Quantum mass spectrometer equipped with an ESI source and a triple quadrupole mass detector (Thermo Finnigan, San Jose, CA). High-resolution mass spectrometry was performed on an Accela UHPLC-system (Thermo-Fisher) coupled to a linear trap- FT-Orbitrap combination (LTQ-Orbitrap), operating in positive ionization mode.

General synthetic procedure for Method 1

As a general procedure, the appropriate diselenide/ditelluride (0.6 mmol) was dissolved in a 1:1 mixture of water and ethylacetate (50 ml) along with the phase transfer catalyst (PTC) tricapyrylmethylammonium chloride (200 mg, 0.45 mmol) under nitrogen gas. NaBH₄ (60-100 mg) was added (as thiophenol was used in case of sulfur analogues, NaBH₄ was not required in this case). The mixture was stirred until the solution turned colourless (1-3 min) then acetaldehyde solution (2-3 ml) was added to destroy the remaining NaBH₄. The reaction mixture was stirred for further 5 min. A solution of bromoquinone (1 mmol) in ethylacetate (5 ml) was then added through the rubber septum without opening the reaction apparatus. The reaction mixture was stirred at room temperature and monitored *via* thin layer chromatography (TLC). Disappearance of the bromoquinone spot indicated that the reaction was complete (usually between 3 to 10 min).

Afterwards the solution was stirred for a further 30 min on air. The violet, dark red or orange coloured reaction mixture (depending upon the Te, Se or S counterpart of the product) was diluted with 50 ml of water and extracted with diethylether or ethylacetate.

The combined organic extracts were dried over Na_2SO_4 and the solvent was evaporated under reduced pressure. The crude product was purified by silica gel chromatography using a mixture of petrol ether (40-65 °C) and ethyl acetate as specified for each compound below. Yields between 76 and 94% were obtained by this method.

2.3. Synthesis of building blocks for multicomponent reactions

Several building blocks were synthesized according to literature methods. Some building blocks, however, have not been reported to date and were synthesized as follows:

Synthesis of the aldehyde building blocks **8n** and **7n**

Compound **8n** was synthesized *via* 2-(2,2-diethoxyethylselanyl)-3-methylnaphthalene-1,4-dione. The latter was synthesized from 1,2-bis(2,2-diethoxyethyl)diselane (237 μl , 0.6 mmol) dissolved in a 1:1 mixture of water and ethylacetate (50 ml) along with the phase transfer catalyst (PTC) tricarplylmethylammonium chloride (200 mg, 0.45 mmol) under nitrogen. NaBH_4 (76 mg, 2 mmol) was added and the mixture was stirred until the solution turned colorless. Acetaldehyde solution (2-3 ml) was added and the reaction stirred for a further 5 min. A solution of 3-bromo-2-methyl-1,4-naphthoquinone (250 mg, 1 mmol) in ethylacetate (5 ml) was added and the reaction mixture stirred at room temperature for 10 min under nitrogen and for a further 30 min on air. The orange coloured reaction mixture was diluted with 50 ml of water and extracted with diethylether. The combined organic extracts were dried over Na_2SO_4 and solvent was evaporated under reduced pressure. The resulting 2-(2,2-diethoxyethylselanyl)-3-methylnaphthalene-1,4-dione (**7n**) was purified by column chromatography on silica gel with petrol ether: ethyl acetate = 10:1.

Compound 8n was then synthesized in a two-phase system consisting of a solution of **7n** (386 μ l, 1 mmol) in 500 ml of ether and 500 ml of 1 M HCl. The reaction mixture was vigorously stirred for 24 h. After separation of the phases, the aqueous layer was re-extracted with ether (2x) and the organic layers were washed with water (2x) and brine (1x). The combined organic extracts were dried over Na₂SO₄ and the solvent was evaporated under reduced pressure. **8n** was purified by column chromatography on silica gel with petrol ether: ethyl acetate = 7:1.

General procedure for the preparation of chalcogen containing isocyanide building blocks

For the Ugi and Passerini reactions, chalcogen bearing isocyanide building blocks suitable for multicomponent chemistry were devised, including the sulfur, selenium and tellurium containing isocyanides.

A mixture of 1 g of appropriate amine, 1.0-1.2 equivalents of formic acid and 1.5-2.0 equivalents of acetic anhydride were mixed and heated for 2h. The progress of the reaction was monitored by TLC, and after the starting material had disappeared, the solvent was evaporated from the reaction mixture to give the crude *N*-formyl compound, essentially as an oily product which could be purified by chromatography on silica gel, usually with dichloromethane: methanol (10: 1).

The *N*-formyl compound (6.05 g, 50.0 mmol) and diisopropylamine (DIPA) (19 ml, 0.14 mol) were dissolved in CH₂Cl₂ (50 ml) and cooled to 0 °C. POCl₃ (5.0 ml, 55 mmol) was added slowly and stirring was continued at 0 °C for another 30 min. Sodium carbonate (10 g) in H₂O (50 ml) was added at room temperature in a rate so that the temperature was maintained between 25 and 35 °C. The mixture was stirred for 90 min at room temperature. H₂O and CH₂Cl₂ (25 ml each) were added. The organic layer was separated, washed with H₂O (3x 25 ml), dried over MgSO₄ and purified by chromatography on silica gel, with petrol ether: ethyl acetate (8: 1) as eluent.

General procedure for the preparation of α -acyloxy amide via the three-component Passerini reaction (Method 2)

As a general procedure, a mixture of aldehyde (1 mmol), carboxylic acid (1.2 mmol) and isocyanide (1.5 mmol) in 5 ml solvent (H_2O was used in most cases) was stirred at room temperature overnight. Upon completion (monitored by TLC), 10 ml CH_2Cl_2 were added to dissolve the sticky product.

The water layer was extracted three times with CH_2Cl_2 , the organic layers were combined, dried over Na_2SO_4 and concentrated to yield a sticky product which was purified by chromatography on silica gel, with petrol ether: ethyl acetate (4: 1) as eluent.

General procedure for the preparation of α -aminoacyl amide via the four-component Ugi reaction (Method 3)

As a general procedure, a mixture of aldehyde (1 mmol), amine (1 mmol), carboxylic acid (1.2 mmol), and isocyanide (1.5 mmol) in 5 ml solvent (H_2O was used in most cases) was stirred at room temperature overnight. Upon completion (monitored by TLC), 10 ml CH_2Cl_2 were added to dissolve the sticky product. The water layer was extracted three times with CH_2Cl_2 , the organic layers were combined, dried over Na_2SO_4 and concentrated to yield a sticky product which was purified by chromatography on silica gel, with petrol ether: ethyl acetate (5: 2).

The synthesis of individual products, including building blocks, yields and analytical data are provided in the Results section.

2.4. Cell culture

The effects of the tested compounds on cell proliferation were initially assayed *in vitro* with different mammalian cancer cell lines, *i.e.* MCF-7 (human breast adenocarcinoma), A-498 (human kidney carcinoma), A-431 (human epidermoid carcinoma), A-549 (human lung carcinoma), SW-480 (human colon adenocarcinoma) and L-929 (mouse fibroblasts). The primary human fibroblasts (HF) and human umbilical vein endothelial cells (HUVEC) were used as normal controls. The metabolic activity at different incubation times was measured by means of an MTT cell survival colorimetric assay.

Furthermore, one-dose and five-dose screens were performed independently by the National Cancer Institute (Bethesda, MD, USA). 58 tumour cell lines representing leukemia, non-small cell lung cancer, colon cancer, cancer of the central nervous system, melanoma, ovarian cancer, renal cancer, prostate cancer and breast cancer were used to estimate selectivity and to identify possible cancer targets.

Solutions and media used

- **Phosphate buffered saline (PBS)**

PBS solution (pH=7.45) was prepared by dissolving one PBS tablet (Gibco, U.K.) in 500 ml distilled water.

- **Isopropanol/HCl**

0.4 ml of concentrated HCl was added to 100 ml isopropanol.

- **[3-(4,5-dimethylthiazol-2-yl)2,5-diphenyltetrazolium bromide] (MTT) solution**

1 g of MTT (98%, Sigma Aldrich) powder was dissolved in 200 ml of PBS and used directly without dilution. This solution was stored below 4°C, in the dark and was used within two weeks.

Apparatus used for cell culture experiments

Apparatus	Details
Incubator	CO ₂ -Auto-Zero, Thermo Scientific
Sterile Workbench	Heraeus LaminAir Instruments, HBB 2472 S
Centrifuge	Eppendorf Centrifuge 5810 R
Microscope	Axiovert 35, Zeiss, Germany
Multi-plate reader	Wallac, 1420 Victor Multilabel Counter
Autoclave	Autoklavi Spa, Fedegari (Italien)
Vortex	Heidolph, REAX 1 R, Germany
Digital multichannel Pipette	Matrix Technologies Corp, Thermo Scientific
Pipette controller	Pipetus, Hirschmann
Pipettes	Cellstar, Greiner bio-One
Falcon Flasks	Falcon, Becton Dickinson, USA
96 well plates	Falcon, Becton Dickinson, USA
Scraper	Nalge nunc international, nunc, USA
Reservoir	Carl Roth, Germany

Cell culture

Cell lines were purchased from DSMZ (Braunschweig, Germany) and grown at 37°C and 10% CO₂ in the following media: MCF-7 cells in DMEM supplemented with 1% L-glutamine and 1% non essential amino acids, A-498 cells in MEM (Lonza), A-431 cells in RPMI 1640 (Gibco), L-929 cells in DMEM medium (lonza), A-549 cells in DMEM medium (lonza), SW-480 cells in McCoy's medium (Gibco), HUVEC cells in EBM-2 (Lonza) and HF cells in MEM (Gibco) supplemented with 1% L-glutamine.

All media were supplemented with 10 % fetal calf serum (Lonza or Gibco). In all experiments, exponentially growing cells were used.

MTT dye was used to measure the metabolic activity of cells which are capable of reducing it by dehydrogenases to a violet formazan product. Briefly, 120 µl aliquots of a cell suspension (50,000 cells/ml) in 96-well microplates were incubated at 37°C and 10% CO₂ and allowed to grow for two days.

Then 60 μ l of serial dilutions of the test compounds were added and incubated for further 24h. After 24h incubation at 37°C and 10% CO₂, 20 μ l MTT in PBS were added to a final concentration of 0.5 mg/ml. After 2 h the precipitate of formazan crystals was centrifuged, and the supernatant discarded.

The precipitate was washed two times with 100 μ l PBS and dissolved in 100 μ l isopropanol containing 0.4% hydrochloric acid. The resulting colour was measured at 590 nm using an ELISA plate reader.

In another experiment, 60 μ l of serial dilutions of the test compounds were added to 120 μ l aliquots of a cell suspension (50,000/ml) in 96-well microplates. After 5 days incubation at 37°C and 10% CO₂, the MTT assay was performed as described before.

All investigations were carried out in two parallel experiments. The IC₅₀ values were determined as the concentrations of tested compounds, at which cell samples developed 50% of the absorbance of untreated control cells as estimated from the dose–response curves.

2.5. Bioassays

2.5.1. DCF assay

One of the most commonly used methods for the detection of intracellular ROS formation. This assay is based on the oxidation of non fluorescent DCFH probe to the highly fluorescent DCF. Also it is considered as a general indicator of ROS, since this it reacts with H₂O₂, ONOO⁻, lipid hydroperoxides, and, to a lesser extent, O₂⁻.

2',7'-dichlorodihydrofluorescein diacetate stock solution (DCFH-DA)

30 mM DCFH-DA stock solution was prepared by dissolving 2',7'-dichlorodihydrofluorescein diacetate (50 mg, 97%, Sigma Aldrich) in 3.4 ml DMSO.

Assay procedure

A-431/HUVECs were seeded in a black-walled 96-well plate at a density of 10^5 cells per well in RPMI 1640/ EBM-2 medium and treated with different concentrations of test compounds for 1 h. The cells were then stained with DCFH-DA (20 μ l, 10 μ M) and allowed to incubate for 30 min in the dark. The intensity of fluorescence was read immediately in a spectrofluorophotometer (DCF, λ_{ex} = 485 \pm 20 nm; λ_{em} = 528 \pm 20 nm). Results were expressed as arbitrary units of fluorescence (Au) per 10^5 cells.

2.5.2. DHE assay

The intracellular ROS levels could also be assayed further spectrofluorimetrically by oxidation of the DHE probe. This assay is as close to being a “gold standard” for detecting only $O_2^{\cdot-}$ in intact tissues or cells in the presence of other ROS.

DHE stock solution

30 mM stock DHE solution was prepared by dissolving DHE (10 mg, 95%, Sigma Aldrich) in 1 ml DMSO.

Assay procedure

A-431/HUVECs were seeded in a black-walled 96-well plate at a density of 10^5 cells per well in RPMI 1640/ EBM-2 medium and treated with different concentrations of test compounds for 1 h. The cells were then stained with DHE (20 μ l, 10 μ M) and allowed to incubate for 30 min in the dark. The intensity of fluorescence was immediately read in a spectrofluorophotometer (DHE, λ_{ex} = 540 \pm 25nm; λ_{em} = 600 \pm 40 nm). Results were expressed as arbitrary units of fluorescence (Au) per 10^5 cells.

2.5.3. 5,5'-dithiobis(2-nitrobenzoate) assay (DTNB)

Ellman's reagent (DTNB, 98%, Sigma Aldrich) was used to estimate the intracellular levels of thiols (primarily glutathione).

Preparation of stock solutions

- Miller Phosphate buffer solution

NaH₂PO₄ solution (5.3 ml, 0.2 M) and Na₂HPO₄ solution (94.7 ml, 0.2 M) were mixed together. The resulting buffer was then diluted to 0.1 M (pH=8) by adding an equal volume of distilled H₂O (~ 100 ml).

- L-Glutathione stock solution (GSH)

A 10 mM stock solution of GSH was prepared by dissolving L-glutathione (50 mg, 98%, Sigma Aldrich) in 16 ml DMSO.

- DTNB stock solution

A 0.04 mM stock solution of DTNB was prepared by dissolving 5,5'-dithiobis(2-nitrobenzoate) (50 mg, 98%, Sigma Aldrich) in 3 ml DMSO.

Assay procedure

MCF-7 cells (10⁶ cell/well) were treated with different concentrations of test compounds for 1 h at 37 °C. The cells were removed by mild trypsinization, centrifuged at 800 rpm for 5 min, washed twice with cold PBS and lysed using 5% w/v chilled metaphosphoric acid at 4 °C for 2 h to extract cellular GSH.

The suspension was then centrifuged at 13,000 rpm for 5 min and GSH was determined by the following method: The supernatant was mixed with 0.2 M sodium phosphate buffer (pH 8.0) and 0.04 mM DTNB and kept at room temperature for 10 min.

The absorbance of the samples was recorded against reagent blank at $\lambda=412$ nm in an UV-Vis double beam spectrophotometer (Shimadzu-1640). The GSH levels were determined by comparison with a standard curve prepared with known concentrations of GSH under similar conditions.

2.5.4. Thiophenol oxidation assay (PhSH assay)

The GPx-like catalytic activity of the compounds was measured by monitoring the formation of PhSSPh formed during thiophenol oxidation in presence of H₂O₂.

Reagents

Ebselen and hydrogen peroxide (H₂O₂ 35% in water) were purchased from Acros Organic (Germany). Thiophenol (PhSH) was purchased from Fluka (Germany).

All solvents were used dried and Millipore Direct-Q® 3 UV water was used. Spectra were recorded on a CARY 50Bio UV-Visible spectrophotometer (Varian).

Assay procedure

To 890 μL methanolic solution of PhSH (1 mM) containing Et_3N (0,05 mM) was added 10 μL of compound (100 μM) in DMSO. The reaction was initiated by adding 100 μL H_2O_2 (2 mM) and monitored at 305 nm for 30 min at 25 °C. Negative control included compounds in the presence of H_2O_2 and compounds in the presence of PhSH. Ebselen was used as positive control in this assay.

2.5.5. Thiobarbituric acid radical scavenging assay (TBA assay)

The thiobarbituric acid (TBA) assay was performed by measuring at 532 nm the formation of the adduct between malonaldehyde (MA) and TBA (MA-TBA). MA is produced by lipid oxidation.

Reagents

TBA, 2,6-di-*tert*-butyl-4-methylphenol (BHT), vitamin C, were purchased from Acros Organic (Germany). Sodium dodecyl sulphate (SDS) and glycine were purchased from Roth (Germany). Arachidonic acid was obtained from Sigma-Aldrich (Germany) and $\text{FeCl}_3 \cdot 6\text{H}_2\text{O}$ from Fluka (Germany).

Assay procedure

1.5 mL aqueous solution of TBA/SDS, 1.5 mL glycine-hydrochloric acid buffer (pH 2.5), 0.1 mL ethanolic solution of BHT, 0.1 mL aqueous solution of $\text{FeCl}_3 \cdot 6\text{H}_2\text{O}$, 0.1 mL of sample in DMSO (0.3 mM) and 10 μL arachidonic acid in DMSO (0.5 mM) were mixed in a glass vial and heated in a water bath for 15 min. A pink colour developed. After cooling, 1 mL of acetic acid and 2 mL of CHCl_3 were added, the mixture was centrifuged and the absorbance of the supernatant was measured using a spectrophotometer at 532 nm. Vitamin C was used as positive control and benchmark antioxidant in this assay.

2.5.6. Caspase activity assay

The caspase-3 and -7 activities were assessed using the homogeneous, luminescent caspase-Glo 3/7 kit (Promega, Germany).

Assay procedure

A-431 cells seeded in white-walled 384 well plates at a density of 20,000 cells per well were treated with 2.8 μM of different test compounds and allowed to incubate for 1, 2, 4, 6, 12 and 24 h at 37 $^{\circ}\text{C}$, in 5% CO_2 and 95% air in the dark. Caspase-Glo 3/7 reagent was then added and the cells were incubated at room temperature for further 30 min in the dark. The luminescence was measured in a plate-reading Multi-plate luminometer (1420 Victor Multilabel Counter, Wallac).

2.5.7. Cell cycle analysis

The cell cycle distribution was evaluated by flow cytometric analysis of MCF-7 cells stained with propidium iodide (PI).

Reagents and stock solutions

- PI staining solution
PI (2 mg, 95%, Sigma Aldrich) dissolved in 1 ml PBS.
- RNase A stock solution
RNase (50 mg, Worthington Biochemicals) dissolved in 1 ml deionized H_2O .
- Ice-cold 70% ethanol
Ethanol/ H_2O (70%) was prepared and stored in the freezer at -20 $^{\circ}\text{C}$.
- Saponin washing buffer (PBS-S)
Saponin (1 mg, Sigma Aldrich) was dissolved in 10 ml PBS.

Assay procedure

MCF-7 cells (10^6 /experiment) were treated with different test compounds at their respective IC_{50} values for 24 h. They were subsequently fixed with ice-cold ethanol/ H_2O (70%) and kept at 4 $^{\circ}\text{C}$ for one day. Cells were then washed with PBS-S wash buffer.

A mixture of propidium iodide (500 μ l, 20 μ g/ml) and RNase (1 mg/ml) were used for staining and after 30 min, samples were analyzed by FacScan.

2.5.8. Apoptosis

Apoptosis were assessed by flow cytometric analysis of A-431 cells treated for 12 h with different concentrations of test compounds using the FITC Annexin V Apoptosis Detection Kit II (BD Pharmingen).

Assay procedure

A-431 cells (10^6 /experiment) were treated with different concentrations (0, 8, 11 and 13 μ M) of test compounds for 12 h. They were suspended in 1 ml binding buffer. 100 μ l of the solution were stained with a mixture of 5 μ l FITC Annexin V and 5 μ l PI. After 15 min of incubation, 400 μ l of binding buffer was added and the samples were analyzed after further 30 min by FacScan.

2.5.9. Immunocytochemistry (ICC)

The phenotypical changes of cell shape and adhesion were investigated by the technique of immunofluorescence. Actin filaments, microtubules and the endoplasmic reticulum (ER) were investigated upon treatment of the potoroo cells (PtK2) cells with/without test compounds.

Reagents

- Fixation solutions
- Ice cold MeOH/acetone (50:50)
- Paraformaldehyde (3.7 %)
- PBS
- Triton X-100 (0.1 %)
- 4',6-diamidino-2-phenylindole stain (DAPI)
- Anti-fade solution
- Primary and secondary antibodies

Assay procedure

PtK2 cells were grown on cover slips in 4-well plates. Test compounds were added after the cells became semi-confluent and incubated for 24 h. Cells were then fixed with 3.7% paraformaldehyde or cold methanol /acetone (50:50) for 10 min and washed with phosphate-buffered saline (PBS). Primary antibodies were added and incubated for 45 min and washed with PBS. Secondary antibodies were then added to the cells and incubated for further 45 min.

After washing with PBS, DAPI was added and incubated at room temperature for 5 min. Cover slips were mounted in anti fade mounting medium. Images were taken with a CCD camera attached to a fluorescence microscope. The following antibodies were used: anti-GRP94, anti- α -tubulin, anti-mouse Alexa Fluor 488 and anti-rat Alexa Fluor 488. The actin filaments were stained with phalloidin Alexa Fluor 594

2.5.10. Chemogenomic assay

A chemical Genetic Interaction Approach (CGI) has proven to be a powerful means to study and predict the mode of action of bioactive compounds. Chemogenomic assays using mutant libraries of *Saccharomyces cerevisiae* rely on comparing the growth of each gene deletion strain to the wild type strain in the presence and absence of the test compounds. The growth inhibition of deletion strains upon exposure to compounds allows the establishment of a chemical-genetic interaction profile. Analyzing such profiles provides valuable information about the possible pathways and targets of new compounds which are not revealed that easy by conventional methods.

Apparatus and materials used for establishment of chemical-genetic interaction profiles

Apparatus and Materials	Details
<i>S. cerevisiae</i> mutants	COMP-SET1-A (haploid MATa), EUROSCARF
Automated pipetting system	EpMotion 5070, Eppendorf
Sterile Workbench	Heraeus LaminAir Instruments, HBB 2472 S
Multi-plate reader	Wallac, 1420 Victor Multilabel Counter
Autoclave	Autoklavi Spa, Fedegari (Italien)
96 well plates	Falcon, Becton Dickinson, USA
384 well plates	Falcon, Becton Dickinson, USA
Reservoir	Carl Roth, Germany
Incubator	30 °C, Memmert, Germany
Spectrophotometer	UV-vis. recording spectrophotometer, 2401PC Shimadzu

Reagents

- Yeast growth medium

YPD bRoth (65 g, Sigma Aldrich) was dissolved in 1 l deionized H₂O. This solution was sterilized by autoclaving and stored below 4°C.

- Yeast agar medium 90

A mixture of malt extract (30 g, BD), bacto peptone (3 g, BD) and bacto agar (18 g, BD) suspended in 1 l deionized H₂O. The pH of the mixture was adjusted to 5.6 by adding 10 % acetic acid. The mixture was then sterilized by autoclaving and stored below 4°C.

Assay procedure

- **Agar diffusion assay**

Mutants of *S. cerevisiae* generated by the European Archive for functional Analysis (EUROSCARF) were grown on standard YPD medium and seeded into liquid agar medium 90 to a final optical density of 0.1 AU. Paper discs of 6 mm diameter soaked with 20 µl of methanolic solution of the test compounds (1mg/ml) were added to the agar plates and incubated at 30°C. The yeast growth was observed after 1 and 2 days. The diameter of the resulting inhibition zones is given as a measure of antimicrobial activity.

- **Minimal inhibitory concentration assay (MIC)**

MIC values were determined with serial dilutions of the compounds that were added to the suspended mutants in liquid media using 96-well microtiter plates. The concentration range of tested compounds was 0.36-50 µg/ml in methanol. The seeded plates were incubated at 30 °C for 24 h, and then the optical density at 620 nm was recorded on a VICTOR 1420 micro plate reader. MIC was defined as the compound concentration that induces 90% inhibition of growth compared to control.

- **High-throughput screening (HTS)**

A mutant library of *S. cerevisiae* consisting of 4,800 deletion mutants were used to screen for chemical-genetic interactions. 5 µl of each mutant was seeded into wells of 384-well plates with 40 µl/well YPD medium to which 5 µl of compound was added. Liquid handling was done by means of an automated pipetting system. The seeded plates were incubated at 30 °C for 24 h, and then the optical density of each well was recorded on a VICTOR 1420 micro plate reader at $\lambda = 620$ nm.

2.5.11. Antifungal assay

The potential antifungal activity of the test compounds was assayed against *Saccharomyces cerevisiae*, *Candida albicans* and *Aspergillus niger* by means of an agar diffusion assay.

Reagents

- **Yeast growth medium**

YPD bRoth (65 g, Sigma Aldrich) was dissolved in 1 l deionized H₂O. This solution was sterilized by autoclaving and stored below 4°C.

- **Yeast agar medium 90**

A mixture of malt extract (30 g, BD), bacto peptone (3 g, BD) and bacto agar (18 g, BD) was suspended in 1 l deionized H₂O. The pH of the mixture was adjusted to 5.6 by adding 10 % acetic acid. The mixture was then sterilized by autoclaving and stored below 4°C.

Assay procedure

The fungi were grown on standard YPD medium and seeded into liquid agar medium 90 to a final optical density of 0.1 AU. Paper discs of 6 mm diameter soaked with 20 μ l of methanolic solution of the test compounds (1mg/ml) were added to the agar plates and incubated at 30°C. The fungi growth was observed after 1 and 2 days. The diameter of the resulting inhibition zones is given as a measure of antifungal activity.

2.5.12. Antibacterial assay

The potential antibacterial activity of the test compounds was assayed against *Mycobacterium phlei*, *Micrococcus luteus*, *Pseudomonas aeruginosa*, *Staphylococcus aureus*, *Klebsiella pneumonia* and *E. coli tolC* by means of an agar diffusion assay.

Reagents

▪ Bacteria growth medium

A mixture of proteose peptone (8 g, Roth), bacto peptone (5 g, BD), dry meat extract (1 g, Merck), HEPES buffer (10 g, Roth) and bacto yeast extract (1 g, BD) were suspended in 1 l deionized H₂O. The pH was adjusted to 7 and the mixture was then sterilized by autoclaving and stored below 4°C.

▪ Bacteria agar medium

A mixture of proteose peptone (8 g, Roth), bacto peptone (5 g, BD), dry meat extract (1 g, Merck), HEPES buffer (10 g, Roth), bacto yeast extract (1 g, BD) and bacto agar (17 g, BD) were suspended in 1 l deionized H₂O. The pH was adjusted to 7 and the mixture was then sterilized by autoclaving and stored below 4°C.

Assay procedure

The bacteria were grown on standard bacteria growth medium and seeded into liquid agar medium to a final optical density of 0.01AU. Paper discs of 6 mm diameter soaked with 20 μ l of methanolic solution of the test compounds (1mg/ml) were added to the agar plates and incubated at 30°C. The bacteria growth was observed after 1 and 2 days. The diameter of the resulting inhibition zones is given as a measure for antibacterial activity.

2.5.13. Lipophilicity measurements

Lipophilicity is one of the properties which influences the partition of a substance in (biological) media. It is also an essential parameter in the development of the QSARs. High performance liquid chromatography (HPLC) was used as a rapid method for the determination of lipophilicity. In order to correlate the measured HPLC data of a compound with its P value, a calibration graph of $\log P$ versus chromatographic data using at least six reference points has to be established.

Equipments and Procedure

The retention times (t_R), of the compounds were determined using a Hewlett Packard series 1090 HPLC fitted with a diode array detector and UV detection with maximum absorbance at $\lambda=230$ and $\lambda=245$ nm. Chromatographic conditions were as follows: column EC 125/2 mm and precolumn, Nucleosil 120-5-C₁₈; flow rate 0.5 ml/min. Isocratic elution was performed with water/methanol at a volume ratio of (3:1) as the mobile phase. The dead time (t_0) of the system was determined using thiourea (as unretained substance) with a t_0 value of 0.728 min.

Evaluation of Experimental Data

The retention factors under isocratic conditions, k , were calculated according to the equation $k = (t_R - t_0)/t_0$. The calibration lines for the RP-HPLC retention factors ($Y = A + B \cdot X$, with $Y = \log k$ and $X = \log P_{ow}$) were established by linear regression with the reference data.

Chapter III: Results

3.1. Synthetic avenues for multifunctional redox agents containing sulfur, selenium and tellurium

Several attempts have been made to design and synthesize multifunctional agents able to recognize the *various* ingredients of OS in cells. Unfortunately, the synthesis of such agents is far from trivial. This chemistry is frequently marred by decomposition of products, difficult purification processes and low yields. Furthermore, the synthesis of such compounds encounters increasing difficulties when moving from just one or two to three or more redox sites - in particular if a rather complicated selenium and/or tellurium chemistry is involved. In order to resolve this obstacle posed by synthetic chemistry, we describe here the use of three different methods for the synthesis of the multifunctional agents.

3.1.1. Method 1

Nucleophilic substitution by direct attack of a redox-active chalcogen moiety at a haloquinone core structure leads to the synthesis of seven multifunctional redox compounds (**1n-8n**) (Figure 18). Modifying the original method by employing a heterogeneous solvent system (water and ethyl acetate) and a phase transfer catalyst (PTC) significantly improved the yield. In the case of compound **3n**, for instance, yields of 79% have been obtained with the two-phase-system, compared to a yield of just 9% in the original method.

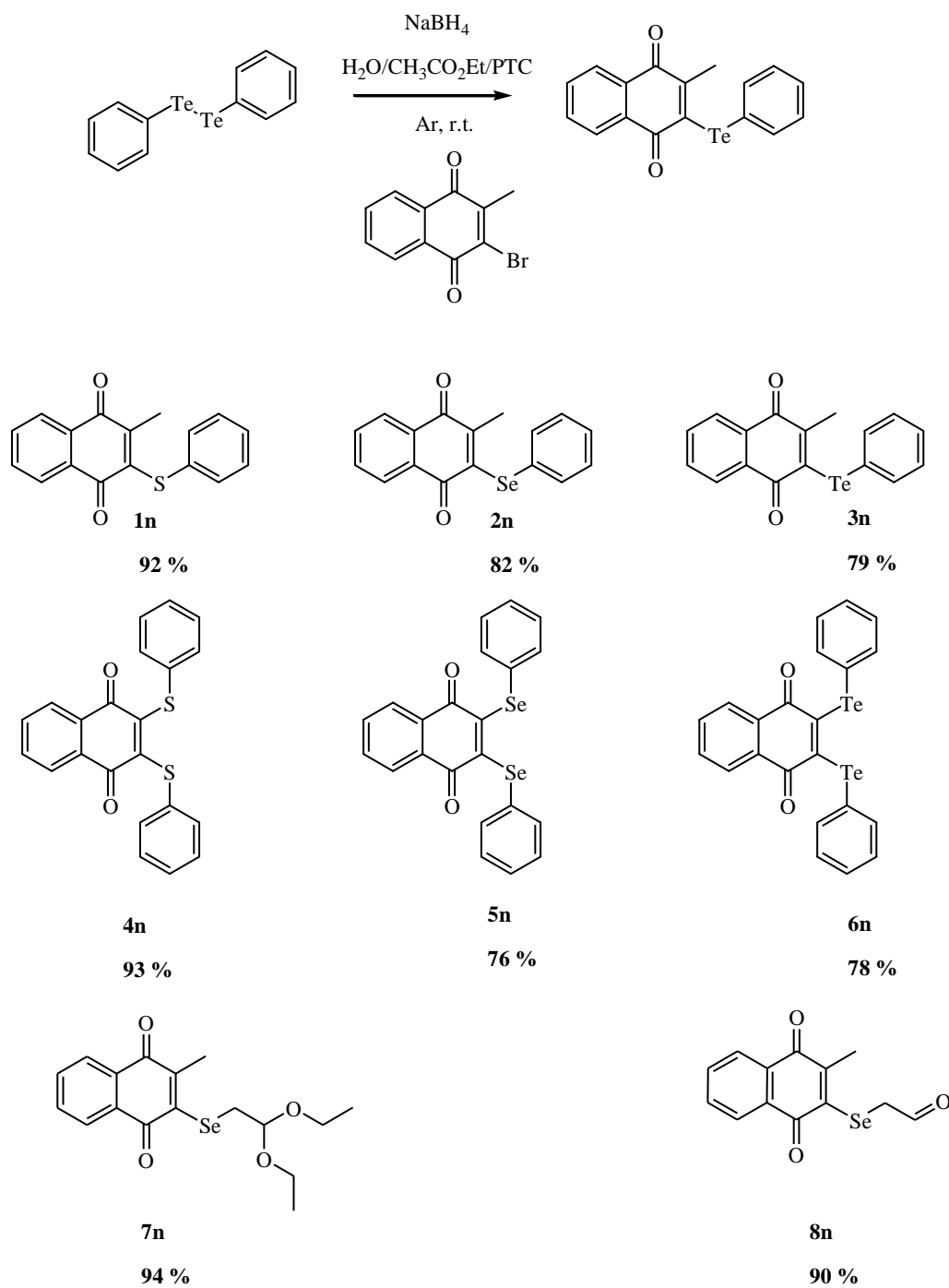


Figure 18. The nucleophilic substitution reaction.

The nucleophilic substitution reaction was used for the synthesis of mono- and di-chalcogenoquinone redox agents **1n** – **8n** containing quinone and sulfur, selenium, or tellurium chalcogen redox sites.

The synthesis of compounds **1n** to **6n** has previously been reported in the literature.³⁶ These compounds were synthesized according to a more general procedure for yield improvement purpose. The synthesis of mono- and di-substituted chalcogenoquinone compounds was developed as part of this study and also applied for the synthesis of hitherto unknown compounds **7n** and **8n**.

Compound 7n: 2-(2,2-diethoxyethylselanyl)-3-methylnaphthalene-1,4-dione

The compound was purified by column chromatography on silica gel with petrol ether: ethyl acetate = 10:1. It was obtained as a yellow solid. Yield = 94 %.

TLC (petroleum ether: ethyl acetate 9:1), $R_f = 0.75$.

$^1\text{H-NMR}$ (CDCl_3 , 500 MHz): 8.02 – 7.98 (m, 2H), 7.63 – 7.58 (m, 2H), 4.72 – 4.70 (t, 1H), 3.63 – 3.56 (m, 2H), 3.48 – 2.42 (m, 2H), 3.28 (d, 2H), 2.30 (s, 3H), 1.08 (s, 3H), 1.05 (s, 3H) ppm.

$^{13}\text{C-NMR}$ (CDCl_3 , 75.5 MHz): 181.6 (s), 181.4 (s), 148.0 (s), 146.8 (s), 133.5 (d), 133.2 (d), 132.9 (s), 131.9 (s), 126.9 (d), 126.6 (d), 102.8 (d), 62.2 (t, 2C), 30.9 (t), 17.3 (q), 15.2 (q, 2C) ppm.

Compound 8n: 2-(1,4-dihydro-2-methyl-1,4-dioxonaphthalen-3-ylselanyl)acetaldehyde

The compound was purified by column chromatography on silica gel with petrol ether: ethyl acetate = 7:1. It was obtained as yellow solid. Yield = 90 %.

TLC (petroleum ether: ethyl acetate 9:1), $R_f = 0.55$.

$^1\text{H-NMR}$ (CDCl_3 , 500 MHz): 8.02 – 7.98 (m, 2H), 7.63–7.58 (m, 2H), 3.28(d, 2H), 2.30 (s, 3H) ppm.

$^{13}\text{C-NMR}$ (CDCl_3 , 75.5 MHz): 181.9 (d), 181.6 (s), 181.2 (s), 148.0 (s), 146.8 (s), 133.5 (d), 133.2 (d), 132.9 (s), 131.9 (s), 126.9 (d), 126.6 (d), 30.9 (t), 17.3 (q) ppm.

LC-MS (ESI): m/z calc. 293.98, $R_t = 7.01$ min, m/z found 295.79 $[\text{M}+\text{H}]^+$.

HRMS: $[\text{M}+\text{H}]$ calc. 294.9873, $[\text{M}+\text{H}]$ found 294.9868.

Multicomponent reactions

Multicomponent reactions enable the efficient synthesis of a vast number of redox-active multifunctional sulfur, selenium and tellurium compounds, of which some exhibit interesting biological activities.

3.1.2. Method 2 (the Passerini three-component reaction)

A Passerini-type reaction has been employed for the synthesis of 15 representative sulfur and selenium multifunctional redox agents.

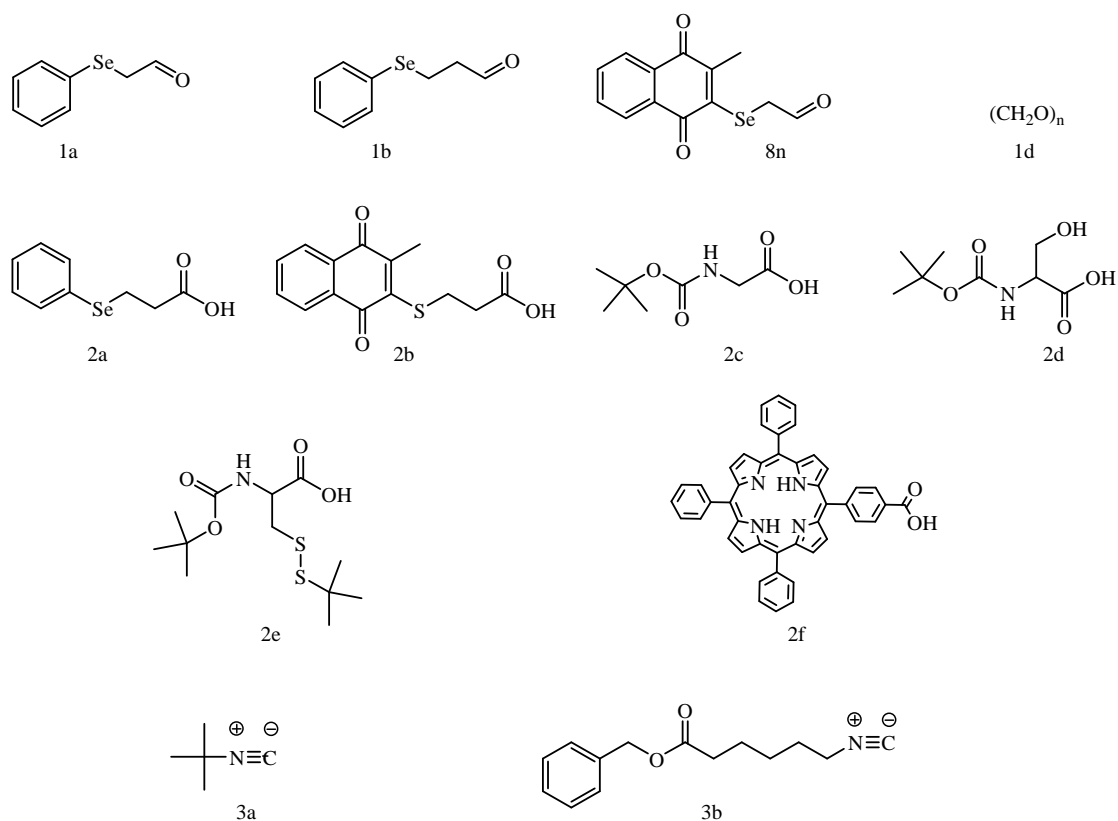


Figure 19. Building blocks used to synthesize multifunctional redox agents.

Acid, aldehyde and isocyanide building blocks used in P-3CR were synthesized following literature procedures or, in case of hitherto unknown agents, could be synthesized in sufficient yield.

The Passerini reaction described here has required a range of building blocks, which needed to be designed and synthesized first (Figure 19). Figures 20, 21 and 22 show the synthesis of the aldehyde, carboxylic acid and isocyanide building blocks used as part of P-3CR. Details regarding the synthesis of these compounds are provided in the Materials and Methods section.

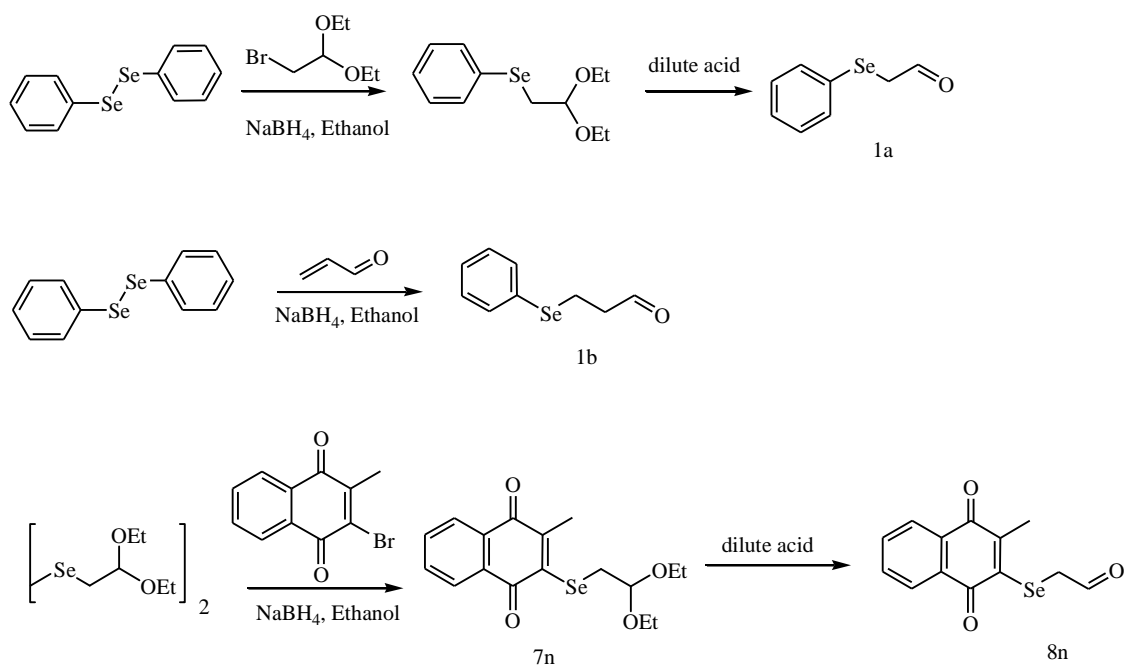


Figure 20. Synthesis of aldehyde building blocks required for the P-3CR.

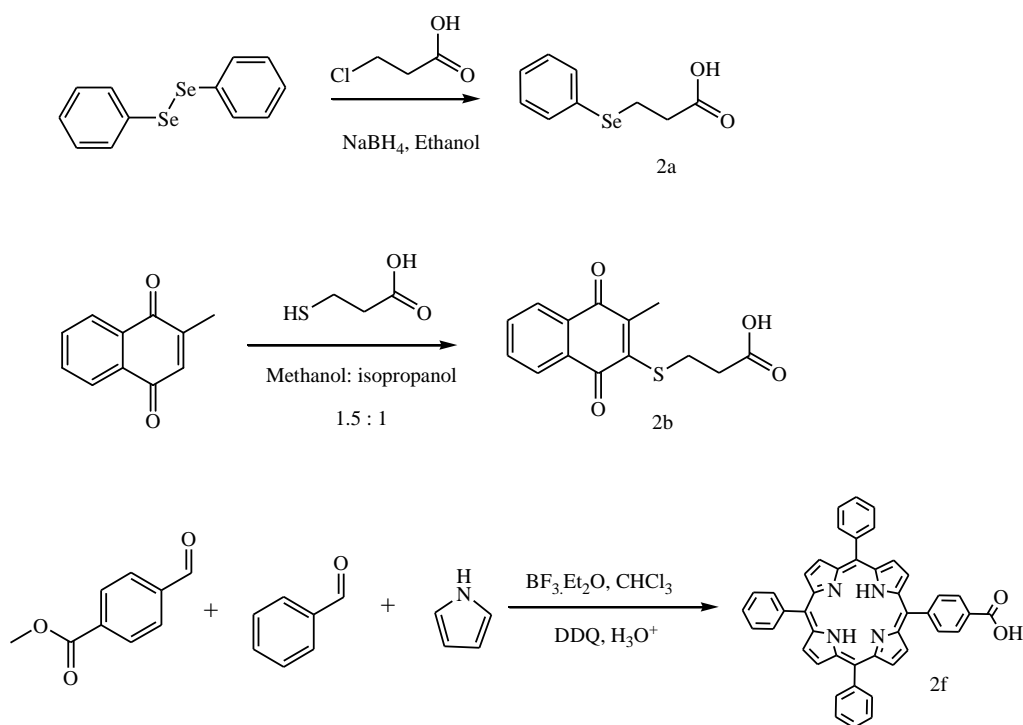


Figure 21. Synthesis of carboxylic acid building blocks required for the P-3CR.

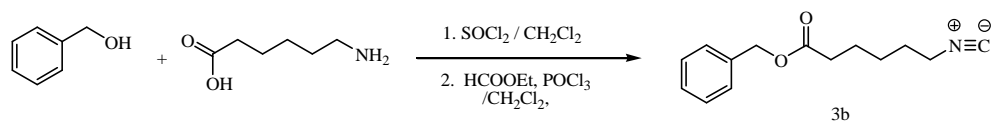
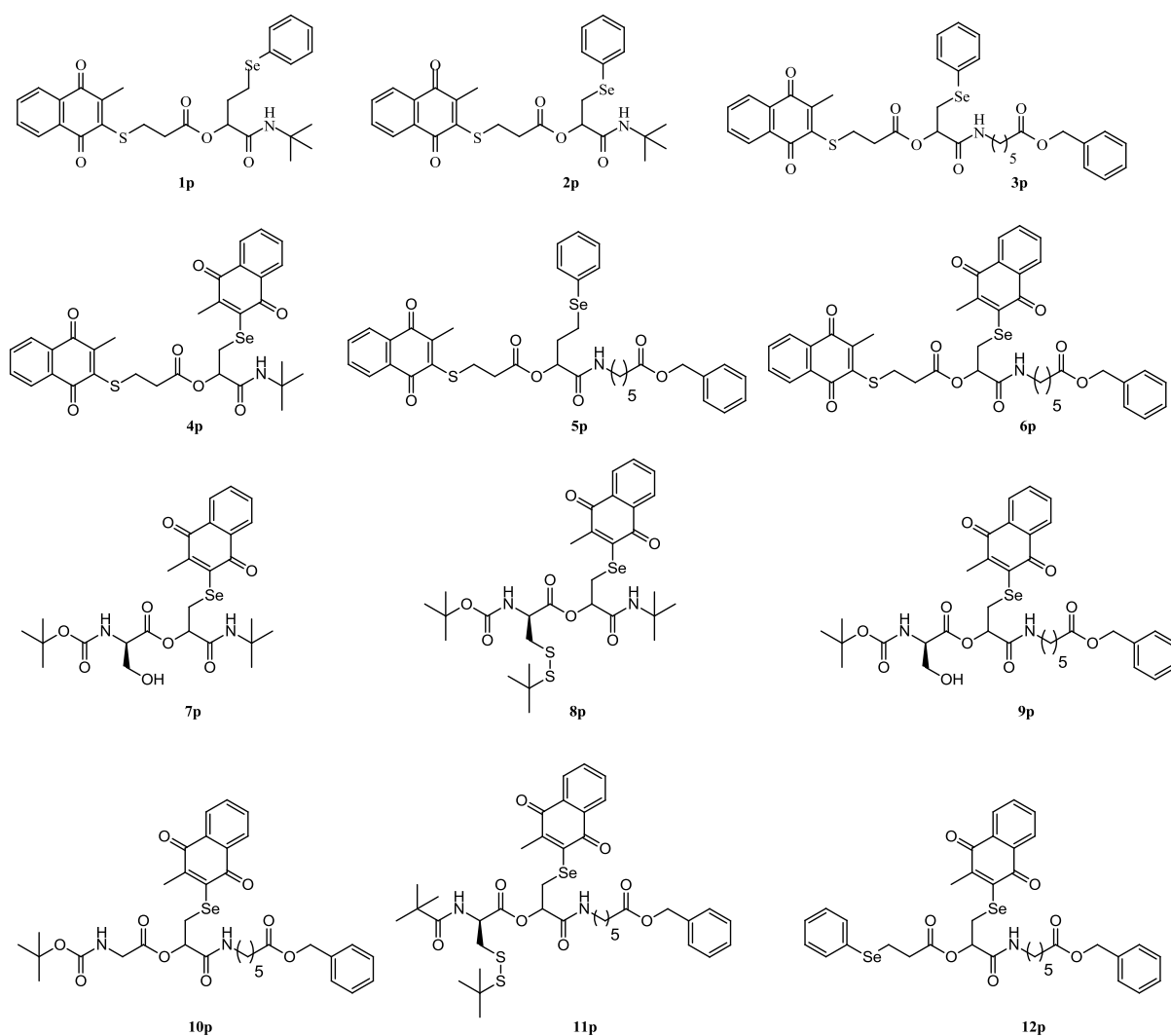


Figure 22. Synthesis of benzyl 6-isocyano-hexanoate.

Figure 23 provide an overview of the chemical structures of the multifunctional compounds synthesized *via* P-3CR. For details regarding the synthesis of these compounds see the Materials and Methods section as well as Table 3.



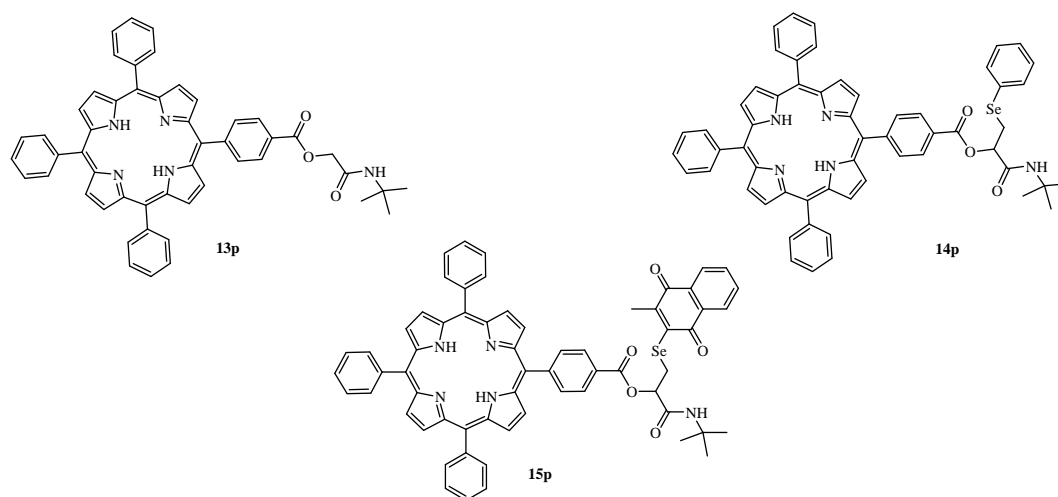


Figure 23. Chemical structures of the multifunctional compounds synthesized *via* the P-3CR.

Table 3. Building blocks, solvents, and yields of the synthesized compounds 1p-15p.

Cpd.	Building blocks	Solvent	Yield [%]	Redox centres	Cpd.	Building blocks	Solvent	Yield [%]	Redox centres
1p	1b, 2b, 3a	H ₂ O	62	3	9p	8n, 2d, 3b	H ₂ O	75	2
2p	1a, 2b, 3a	H ₂ O	68	3	10p	8n, 2c, 3b	H ₂ O	66	2
3p	1a, 2b, 3b	H ₂ O	71	3	11p	8n, 2e, 3b	H ₂ O	85	3
4p	8n, 2b, 3a	H ₂ O	76	4	12p	8n, 2a, 3b	H ₂ O	79	3
5p	1b, 2b, 3b	H ₂ O	75	3	13p	1d, 2f, 3a	CHCl ₃	93	1
6p	8n, 2b, 3b	H ₂ O	73	4	14p	1a, 2f, 3a	CHCl ₃	89	2
7p	8n, 2d, 3a	H ₂ O	76	2	15p	8n, 2f, 3a	CHCl ₃	86	3
8p	8n, 2e, 3a	H ₂ O	54	3					

Building blocks were designed to carry one or two relevant redox or metal binding sites, which could be combined to larger, highly functionalized molecules with four or more biologically interesting sites. The reaction was performed mostly in water at high concentrations and under mild condition.

Sulfur and selenium multifunctional redox compounds provided by P-3CR were synthesized as follows:

Compound 1p: *1-(tert-butylcarbamoyl)-3-(phenylselanyl)propyl3-(1,4-dihydro-2-methyl-1,4-dioxonaphthalen-3-ylthio)propanoate*

The compound was purified by column chromatography on silica gel with petrol ether: ethyl acetate = 5:1. It was obtained as yellow oil. Yield = 62 %.

TLC (petroleum ether: ethyl acetate 4:1), $R_f = 0.63$.

$^1\text{H-NMR}$ (CDCl_3 , 500 MHz): 8.03-7.97 (m, 2H), 7.66-7.61 (m, 2H), 7.41-7.38 (m, 2H), 7.17-7.14 (m, 3H), 5.84 (br s, 1H), 5.08-5.06 (t, $J = 5.4, 11.8$ Hz, 1H), 3.37-3.34 (t, $J = 7.3, 13.9$ Hz, 2H), 2.86-2.83 (t, $J = 7.9, 15.5$ Hz, 2H), 2.74-2.71 (m, 2H), 2.27 (s, 3H), 2.18-2.12 (m, 2H), 1.27 (s, 9H) ppm.

$^{13}\text{C-NMR}$ (CDCl_3 , 125.79Hz): 182.0 (s), 181.3 (s), 170.2 (s), 167.7 (s), 147.5 (s), 145.3 (s), 133.8 (d), 133.5 (d), 132.7 (d, 2C), 132.6 (s), 131.9 (s), 129.6 (s), 129.1 (d, 2C), 127.1 (d), 126.8 (d), 126.7 (d), 74.2 (d), 51.5 (s), 35.6 (t), 32.5 (t), 29.1 (t), 28.6 (q, 3C), 22.5 (t), 15.4 (q) ppm.

LC-MS (ESI): m/z calc. 573.21, $R_t = 14.76$ min, m/z found 574.15 $[\text{M}+\text{H}]^+$.

HRMS: $[\text{M}+\text{H}]$ calc. 574.1141, $[\text{M}+\text{H}]$ found 574.1161, $[\text{M}+\text{Na}]$ calc. 596.0130 $[\text{M}+\text{Na}]$ found 596.0980. Isotopic pattern of selenium: m/z (relative abundance %) 574.1161 (100), 575.1194 (30), 576.1163 (18), 577.1196 (7).

Compound 2p: *1-(tert-butylcarbamoyl)-2-(phenylselanyl)ethyl3-(1,4-dihydro-2-methyl-1,4-dioxonaphthalen-3-ylthio)propanoate*

The compound was purified by column chromatography on silica gel with petrol ether: ethyl acetate = 5:1. It was obtained as yellow oil. Yield = 68 %.

TLC (petroleum ether: ethyl acetate 5:1), $R_f = 0.67$.

$^1\text{H-NMR}$ (CDCl_3 , 500 MHz): 8.03-7.98 (m, 2H), 7.66-7.62 (m, 2H), 7.45-7.52 (m, 2H), 7.18-7.12 (m, 3H), 5.98 (br s, 1H), 5.25-5.22, (dd, $J = 5.1, 7.0$ Hz, 1H), 3.38-3.34 (m, 1H), 3.30-3.20 (m, 3H), 2.58-2.52 (m, 1H), 2.49-2.43 (m, 1H), 2.27 (s, 3H), 1.29 (s, 9H) ppm.

$^{13}\text{C-NMR}$ (CDCl_3 , 125.79Hz): 182.0 (s), 181.2 (s), 169.6 (s), 167.0 (s), 147.5 (s), 145.4 (s), 133.8 (d), 133.5 (d), 132.9 (d, 2C), 132.7 (s), 131.9 (s), 129.6 (s), 129.2 (d, 2C), 127.3

(d), 126.8 (d), 126.7 (d), 73.9 (d), 51.7 (s), 35.3 (t), 29.0 (t), 28.9 (t), 28.6 (q, 3C), 15.4 (q) ppm.

LC-MS (ESI) m/z calc. 559.09, R_t = 14.33 min, m/z found 560.08 [M+H]⁺.

HRMS: [M+H] calc. 560.1009, [M+H] found 560.1004, [M+Na] calc. 582.0829 [M+Na] found 582.0824. Isotopic pattern of Se: m/z (relative abundance %) 554.1064 (2), 556.1031(20), 558.1012 (48), 560.1004 (100), 561.1038 (31), 562.1006 (21), 563.1040 (6).

Compound 3p: *1-(benzyl hexanoatecarbamoyl)-2-(phenylselanyl)ethyl 3-(1,4-dihydro-2-methyl-1,4-dioxonaphthalen-3-ylthio)propanoate*

The compound was purified by column chromatography on silica gel with petrol ether: ethyl acetate = 3:1. It was obtained as yellow oil. Yield = 71 %.

TLC (petroleum ether: ethyl acetate 4:1), R_f = 0.35.

¹H-NMR (CDCl₃, 500 MHz): 8.02-7.97 (m, 2H), 7.65-7.61 (m, 2H), 7.45-7.41(m, 2H), 7.29-7.21 (m, 5H), 7.17-7.12 (m, 3H), 6.41 (br t, 1H), 5.37-5.33 (dd, J = 4.4, 5.8 Hz, 1H), 5.00 (s, 2H), 3.41-3.37 (dd, J = 4.4, 13.5 Hz, 1H), 3.28-3.11 (m, 5H), 2.56-2.50 (m, 1H), 2.46-2.40 (m, 1H), 2.27-2.41 (m, 5H), 1.59-1.53 (m, 2H), 1.48-1.42(m, 2H), 1.31-1.25(m, 2H) ppm.

¹³C-NMR (CDCl₃, 125.79Hz): 182.3 (s), 181.5 (s), 173.5 (s), 170.2 (s), 168.2 (s), 148.3 (s), 145.5 (s), 136.3 (s), 134.1 (d), 133.7 (d), 133.1 (d, 2C), 132.9 (s), 132.2 (s), 129.8 (s), 129.4 (d, 2C), 128.8 (d, 2C), 128.4 (d), 128.3 (d, 2C), 127,5 (d), 127.6 (d), 126.9 (d), 73.9 (d), 66.4 (t), 39.5 (t), 35.4 (t), 34.2 (t), 29.3 (t, 2C), 29.1 (t), 26.5 (t), 24.6 (t), 15.7 (q) ppm.

LC-MS (ESI): m/z calc. 707.146, R_t = 15.16 min, m/z found 708.08 [M+H]⁺.

HRMS: [M+H] calc. 708.1456, [M+H] found 708.1529, [M+Na] calc. 730.1456 [M+Na] found 730.1348. Isotopic pattern of selenium: m/z (relative abundance %) 708.1529 (100), 709.1562 (40), 710.1530 (20), 711.1564 (5), 730.1348 (100), 731.1382 (38), 732.1350 (20), 733.1383 (5).

Compound 4p: *1-(tert-butylcarbamoyl)-2-(1,4-dihydro-2-methyl-1,4-dioxonaphthalen-3-ylselanyl)ethyl3-(1,4-dihydro-2-methyl-1,4-dioxonaphthalen-3-ylthio)propanoate*

The compound was purified by column chromatography on silica gel with petrol ether: ethyl acetate = 3:1. It was obtained as yellow oil. Yield = 76 %.

TLC (petroleum ether: ethyl acetate 2.5:1), R_f = 0.57.

¹H-NMR (CDCl₃, 500 MHz): 8.01-7.96 (m, 4H), 7.65-7.58 (m, 4H), 6.01 (br s, 1H), 5.37-5.35 (dd, J = 5.2, 7.1 Hz, 1H), 3.69-3.65 (dd, J = 5.2, 13.2 Hz, 1H), 3.46-3.42 (dd, J

= 6.6, 13.2 Hz, 1H), 3.31-3.28 (t, $J = 6.6, 13.2$ Hz, 2H), 2.69-2.66 (m, 2H), 2.30 (s, 3H), 2.24 (s, 3H), 1.28 (s, 9H) ppm.

^{13}C -NMR (CDCl_3 , 125.79 Hz): 182.1 (s), 181.7 (s), 181.3 (s), 181.2 (s), 170.1 (s), 166.8 (s), 148.7 (s), 147.4 (s), 145.6 (s), 145.5 (s), 133.8 (d), 133.7 (d), 133.5 (d), 133.4 (d), 132.7 (s, 2C), 132.0 (s), 131.8 (s), 126.9 (d), 126.8 (d), 126.7 (d), 126.6 (d), 74.4 (d), 51.7 (s), 35.6 (t), 29.1 (t), 28.9 (t), 28.6 (q, 3C), 17.4 (q), 15.3 (q) ppm.

LC-MS (ESI): m/z calc. 653.09, $R_t = 14.68$ min, m/z found 654.20 $[\text{M}+\text{H}]^+$.

HRMS: $[\text{M}+\text{H}]$ calc. 654.1064, $[\text{M}+\text{H}]$ found 654.1059, $[\text{M}+\text{Na}]$ calc. 676.0884 $[\text{M}+\text{Na}]$ found 676.0879. Isotopic pattern of Se: m/z (relative abundance %) 648.1119 (2), 650.1086 (20), 652.1067 (47), 654.1079 (100), 655.1093 (35), 656.1061 (18), 657.1095 (7).

Compound 5p: *1-(benzyl hexanoatecarbamoyl)-3-(phenylselanyl)propyl 3-(1,4-dihydro-2-methyl-1,4-dioxonaphthalen-3-ylthio)propanoate*

The compound was purified by column chromatography on silica gel with petrol ether: ethyl acetate = 2.5:1. It was obtained as yellow oil. Yield = 75 %.

TLC (petroleum ether: ethyl acetate 4:1), $R_f = 0.33$.

^1H -NMR (CDCl_3 , 500 MHz): 7.99-7.93 (m, 2H), 7.63-7.57 (m, 2H), 7.39-7.35 (m, 2H), 7.27-7.20 (m, 5H), 7.16-7.12 (m, 3H), 6.33 (br s, 1H), 5.19-5.16 (m, 1H), 4.96 (s, 2H), 3.71-3.69 (t, $J = 5.4, 12.1$ Hz, 2H), 3.34-3.30 (t, $J = 5.7, 12.4$ Hz, 2H), 2.86-2.81 (t, $J = 8.0, 15.9$ Hz, 2H), 2.76-2.65 (m, 2H), 2.29-2.24 (m, 5H), 2.15-2.09 (m, 2H), 1.56-1.50 (q, $J = 7.2, 15.25$ Hz, 2H), 1.44-1.38 (q, $J = 7.2, 14.8$ Hz, 2H), 1.26-1.19 (m, 2H) ppm.

^{13}C -NMR (CDCl_3 , 125.79 Hz): 181.9 (s), 181.3 (s), 173.2 (s), 170.1 (s), 168.6 (s), 147.9 (s), 145.2 (s), 135.9 (s), 133.8 (d), 133.4 (d), 132.7 (d, 2C), 132.5 (s), 132.1 (s), 129.5 (s), 129.1 (d, 2C), 128.4 (d, 2C), 128.1 (d), 128.0 (d, 2C), 127.0 (d), 127.7 (d), 126.6 (d), 73.9 (d), 66.0 (t), 39.0 (t), 35.4 (t), 33.9 (t), 32.5 (t), 29.2 (t), 29.0 (t), 26.1 (t), 24.3 (t), 22.5 (t), 15.3 (q) ppm.

LC-MS (ESI): m/z calc. 721.16, $R_t = 15.10$ min, m/z found 721.94 $[\text{M}+\text{H}]^+$.

HRMS: $[\text{M}+\text{H}]$ calc. 722.1556, $[\text{M}+\text{H}]$ found 722.1685, $[\text{M}+\text{Na}]$ calc. 744.1456 $[\text{M}+\text{Na}]$ found 744.1505. Isotopic pattern of selenium: m/z (relative abundance %) 722.1685 (100), 723.1719 (39), 724.1687 (18), 725.1721 (6), 744.1505 (100), 745.1538 (36), 746.1506 (16), 747.1540 (5).

Compound 6p: *1-(benzyl hexanoatecarbamoyl)-2-(1,4-dihydro-2-methyl-1,4-dioxonaphthalen-3-ylselanyl)ethyl-3-(1,4-dihydro-2-methyl-1,4-dioxonaphthalen-3-ylthio)propanoate*

The compound was purified by column chromatography on silica gel with petrol ether: ethyl acetate = 2.5:1. It was obtained as yellow oil. Yield = 73 %.

TLC (petroleum ether: ethyl acetate 4:1), $R_f = 0.30$.

$^1\text{H-NMR}$ (CDCl_3 , 500 MHz): 8.02-7.95 (m, 4H), 7.66-7.56 (m, 4H), 7.30-7.21 (m, 5H), 6.48 (br s, 1H), 5.49-5.46 (m, 1H), 5.01 (s, 2H), 3.69-3.65 (dd, $J = 4.5, 13.0$ Hz, 1H), 3.50-3.46 (dd, $J = 6.2, 13.0$ Hz 1H), 3.31-3.23 (m, 2H), 3.19-3.15 (dt, $J = 6.7, 13.0$ Hz, 2H), 2.67-2.64 (t, $J = 6.2, 13.0$ Hz, 2H), 2.29-2.24 (m, 8H), 1.58-1.52 (m, 2H), 1.48-1.42 (m, 2H), 1.30-1.18 (m, 2H) ppm.

$^{13}\text{C-NMR}$ (CDCl_3 , 125.79Hz): 182.0 (s), 181.6 (s), 181.3 (s), 181.2 (s), 173.3 (s), 170.0 (s), 167.7 (s), 148.9 (s), 148.0 (s), 145.5 (s), 145.2 (s), 135.9 (s), 133.8 (d), 133.7 (d), 133.5 (d), 133.4 (d), 132.7 (s), 132.6 (s), 131.9 (s), 131.8 (s), 128.5 (d, 2C), 128.2 (d), 128.1 (d, 2C), 127.0 (d), 126.7 (d), 126.6 (d, 2C), 74.1 (d), 66.1 (t), 39.2 (t), 35.4 (t), 34.0 (t), 29.1 (t), 29.0 (t), 28.8 (t), 26.3 (t), 24.4 (t), 17.5 (q), 15.4 (q) ppm.

LC-MS (ESI): m/z calc. 801.151, $R_t = 17.44$ min, m/z found 823.89 $[\text{M}+\text{Na}]^+$.

HRMS: $[\text{M}+\text{H}]$ calc. 802.1576, $[\text{M}+\text{H}]$ found 802.1584, $[\text{M}+\text{Na}]$ calc. 824.1406 $[\text{M}+\text{Na}]$ found 824.1403. Isotopic pattern of selenium: m/z (relative abundance %) 802.1584 (100), 803.1617 (43), 804.1585 (17), 805.1619 (7), 808.1610 (2), 824.1403 (100), 825.1437 (41), 826.1405 (5), 827.1438 (3).

Compound 7p: *tert-butyl(R)-1-((1-(tert-butylcarbamoyl)-2-(1,4-dihydro-2-methyl-1,4-dioxonaphthalen-3-ylselanyl)ethoxy)carbonyl)-2-hydroxyethylcarbamate*

The compound was purified by column chromatography on silica gel with petrol ether: ethyl acetate = 2.5:1. It was obtained as yellow oil. Yield = 76 %.

TLC (petroleum ether: ethyl acetate 4:1), $R_f = 0.54$.

$^1\text{H-NMR}$ (CDCl_3 , 500 MHz): 8.05-8.02 (m, 1H), 7.99-7.97 (m, 1H), 7.68-7.62 (m, 2H), 6.64 (br s, 1H), 5.37-5.30 (m, 2H), 4.28 (br d, 1H), 4.16 (br s, 1H), 3.74-3.66 (m, 2H), 3.50 (br t, 1H), 3.31-3.26 (dd, $J = 8.3, 13.5$ Hz, 1H), 2.29 (s, 3H), 1.37 (s, 9H), 1.29 (s, 9H) ppm.

^{13}C -NMR (CDCl_3 , 125.79Hz): 182.6 (s), 181.2 (s), 170.3 (s), 167.5 (s), 148.9 (s), 144.8 (s), 134.0 (d), 133.5 (d), 132.6 (s), 132.0 (s), 126.9 (d), 126.8 (d), 80.3 (s), 63.7 (t), 56.1 (s), 52.0 (s), 75.3 (d), 77.3 (d), 28.9 (t), 28.6 (q, 3C), 28.3 (q, 3C), 17.3 (q) ppm.

LC-MS (ESI): m/z calc. 582.148, R_t = 12.58 min, m/z found 583.04 $[\text{M}+\text{H}]^+$.

HRMS: $[\text{M}+\text{H}]$ calc. 583.1523, $[\text{M}+\text{H}]$ found 583.1553, $[\text{M}+\text{Na}]$ calc. 605.1306 $[\text{M}+\text{Na}]$ found 605.1373. Isotopic pattern of selenium: m/z (relative abundance %) 583.1553 (100), 584.1587 (34), 585.1555 (20), 586.1588 (4), 605.1373 (100), 606.1406 (26), 607.1374 (16), 608.1408 (4).

Compound 8p: *tert-butyl(S)-1-((1-(tert-butylcarbamoyl)-2-(1,4-dihydro-2-methyl-1,4-dioxonaphthalen-3-ylselanyl)ethoxy)carbonyl)-2-(2-tert-butylsulfonyl)ethylcarbamate*

The compound was purified by column chromatography on silica gel with petrol ether: ethyl acetate = 3:1. It was obtained as yellow oil. Yield = 54 %.

TLC (petroleum ether: ethyl acetate 3:1), R_f = 0.45.

^1H -NMR (CDCl_3 , 500 MHz): 8.02-7.99 (m, 2H), 7.65-7.60 (m, 2H), 6.54-6.47 (br s, 1H), 5.41-5.11 (m, 1H), 4.45-4.25 (m, 1H), 3.75-3.65 (m, 1H), 3.55-3.45 (m, 1H), 3.13-2.90 (m, 2H), 2.29 (s, 3H), 1.38 (s, 9H), 1.28 (s, 9H), 1.26 (s, 9H) ppm.

^{13}C -NMR (CDCl_3 , 125.79Hz): 181.6 (s), 181.3 (s), 170.1 (s), 169.8 (s), 166.7 (s), 148.6 (s), 133.6 (d), 132.8 (s), 131.9 (s), 127.0 (d), 126.8 (d), 126.7 (d), 75.1 (d), 53.9 (d), 53.8 (s), 48.8 (s), 41.1 (t), 29.8 (q, 3C), 29.7 (s), 29.1 (t), 28.6 (q, 3C), 28.3 (s), 28.2 (q, 3C), 17.5 (q) ppm.

LC-MS (ESI): m/z calc. 686.16, R_t = 15.87 min, m/z found 687.02 $[\text{M}+\text{H}]^+$.

HRMS: $[\text{M}+\text{H}]$ calc. 687.1676, $[\text{M}+\text{H}]$ found 687.1671, $[\text{M}+\text{Na}]$ calc. 709.1496 $[\text{M}+\text{Na}]$ found 709.1491. Isotopic pattern of selenium: m/z (relative abundance %) 687.1671 (100), 688.1705 (32), 689.1673 (18), 690.1707 (8), 698.1732 (2).

Compound 9p: *tert-butyl (R)-1-((1-(benzyl hexanoatecarbamoyl)-2-(1,4-dihydro-2-methyl-1,4-dioxonaphthalen-3-ylselanyl)ethoxy)carbonyl)-2-hydroxyethylcarbamate*

The compound was purified by column chromatography on silica gel with petrol ether: ethyl acetate = 2:1. It was obtained as yellow oil. Yield = 75 %.

TLC (petroleum ether: ethyl acetate 2.5:1), R_f = 0.18.

^1H -NMR (CDCl_3 , 500 MHz): 8.02-7.99 (m, 2H), 7.65-7.60 (m, 2H), 7.29-7.24 (m, 5H), 7.15 (br s, 1H), 5.50-5.45 (m, 2H), 5.05 (s, 2H), 4.25-4.15 (m, 1H), 4.05-3.95 (m, 1H), 3.85-3.65

(m, 2H), 3.45-3.40 (m, 1H), 3.25- 3.15 (m, 2H), 2.31-2.38 (m, 5H), 1.57-1.39 (m, 4H), 1.35 (s, 9H), 1.27-1.21 (m, 2H) ppm.

¹³C-NMR (CDCl₃, 125.79Hz): 182.1 (s), 181.3 (s), 174.3 (s), 169.9 (s), 168.1 (s), 153.7 (s), 145.0 (s), 133.8 (d), 133.5 (d), 132.6 (s), 132.0 (s), 130.8 (s), 128.8 (s), 128.6 (d, 2C), 128.3 (d), 128.2 (d, 2C), 127.1 (d), 126.8 (d), 80.4 (s), 74.5 (d), 66.5 (t), 63.7 (t), 56.1 (d), 39.2 (t), 33.9 (t), 28.8 (t), 28.5 (t), 28.3 (q, 3C), 26.0 (t), 24.2 (t), 17.5 (q) ppm.

LC-MS (ESI): m/z calc. 730.20, R_t = 13.53 min, m/z found 730.96 [M+H]⁺.

HRMS: [M+H] calc. 731.2097, [M+H] found 731.2077, [M+Na] calc. 753.1807 [M+Na] found 753.1897. Isotopic pattern of selenium: m/z (relative abundance %) 731.2077 (100), 732.2111 (37), 733.2079 (21), 734.2113 (4), 753.1897 (100), 754.1930 (28), 755.1899 (15), 756.1932 (4).

Compound 10p: *tert-butyl ((1-(benzyl hexanoatecarbamoyl)-2-(1,4-dihydro-2-methyl-1,4-dioxonaphthalen-3-ylselanyl)ethoxy)carbonyl)methylcarbamate*

The compound was purified by column chromatography on silica gel with petrol ether: ethyl acetate = 2:1. It was obtained as yellow oil. Yield = 66 %.

TLC (petroleum ether: ethyl acetate 2.5:1), R_f = 0.54.

¹H-NMR (CDCl₃, 500 MHz): 8.03-8.00 (m, 2H), 7.66-7.60 (m, 2H), 7.30-7.23 (m, 5H), 6.79 (br s, 1H), 5.53-5.51 (m, 1H), 5.03 (s, 2H), 4.79 (br t, 1H), 3.80-3.63 (m, 3H), 3.50-3.46 (dd, J = 6.9, 13.8 Hz, 1H), 3.21-3.07 (m, 2H), 2.30-2.28 (m, 5H), 1.61-1.55 (m, 2H), 1.50-1.44 (m, 2H), 1.35 (s, 9H), 1.30-1.24 (m, 2H) ppm.

¹³C-NMR (CDCl₃, 125.79Hz): 181.6 (s), 181.3 (s), 173.3 (s), 168.8 (s), 167.6 (s), 156.5 (s), 148.9 (s), 136.4 (s), 133.7 (d), 133.5 (d, 2C), 132.7 (s), 131.9 (s), 128.5 (d, 2C), 128.2 (d, 2C), 126.9 (d), 126.8 (d), 80.6 (s), 74.4 (d), 66.1 (t), 42.3 (t), 39.3 (t), 34.1 (t), 28.9 (t), 28.8 (t), 28.2 (q, 3C), 26.2 (t), 24.4 (t), 17.5 (q) ppm.

LC-MS (ESI): m/z calc. 700.19, R_t = 13.83 min, m/z found 701.15 [M+H]⁺.

HRMS: [M+H] calc. 701.1976, [M+H] found 701.1972, [M+Na] calc. 723.1707 [M+Na] found 723.1791. Isotopic pattern of selenium: m/z (relative abundance %) 701.1972 (100), 702.2005 (36), 703.1974 (19), 704.2007 (2), 723.1791 (100), 724.1825 (39), 725.1825 (20), 726.1827 (2).

Compound 11p: (2*S*)-1-(benzyl hexanoatecarbamoyl)-2-(1,4-dihydro-2-methyl-1,4-dioxonaphthalen-3-ylselanyl)ethyl 3-(2-*tert*-butyldisulfanyl)-2-(pivalamido)propanoate

The compound was purified by column chromatography on silica gel with petrol ether: ethyl acetate = 2:1. It was obtained as yellow oil. Yield = 85 %.

TLC (petroleum ether: ethyl acetate 2.5:1), $R_f = 0.18$.

$^1\text{H-NMR}$ (CDCl_3 , 500 MHz): 8.03-7.99 (m, 2H), 7.65-7.61 (m, 2H), 7.30-7.22 (m, 5H), 7.04 (br s, 1H), 5.48-5.48 (m, 1H), 5.23 (s, 2H), 5.03 (s, 2H), 3.14-3.02 (m, 3H), 2.30-2.26 (m, 6H), 1.60-1.54 (m, 2H), 1.50-1.43 (m, 3H), 1.37 (s, 3H), 1.33 (s, 9H), 1.24 (s, 9H) ppm.

$^{13}\text{C-NMR}$ (CDCl_3 , 125.79Hz): 181.46 (s), 181.3 (s), 170.1(s), 169.6 (s), 167.6 (s), 148.7 (s), 136.1 (s), 133.7 (d), 133.5 (d), 133.6 (d), 132.8 (s), 132.7 (s), 131.9 (s), 128.5 (d, 2C), 128.2 (d, 2C), 126.9 (d), 126.7 (d), 74.8 (d), 74.5 (d), 66.5 (t), 53.9 (s), 53.4 (s), 48.6 (s), 39.4 (t), 33.3 (t), 34.1 (t), 29.8 (q, 3C), 28.9 (t), 28.3 (q, 3C), 26.3 (t), 24.5 (t, 2C), 17.5 (q) ppm.

LC-MS (ESI): m/z calc. 818.20, $R_t = 16.13$ min, m/z found 835.02 $[\text{M}+\text{NH}_4]^+$.

HRMS: $[\text{M}+\text{H}]$ calc. 818.1196, $[\text{M}+\text{H}]$ found 835.2196, $[\text{M}+\text{NH}_4]$ calc. 857.2017 $[\text{M}+\text{K}]$ found 857.2015. Isotopic pattern of selenium: m/z (relative abundance %) 835.2196 (100), 836.2229 (47), 837.2197 (20), 840.2189(2).

Compound 12p: 1-(benzyl hexanoatecarbamoyl)-2-(1,4-dihydro-2-methyl-1,4-dioxonaphthalen-3-ylselanyl)ethyl 3-(phenylselanyl)propanoate

The compound was purified by column chromatography on silica gel with petrol ether: ethyl acetate = 5:1. It was obtained as yellow oil. Yield = 79 %.

TLC (petroleum ether: ethyl acetate 2.5:1), $R_f = 0.43$.

$^1\text{H-NMR}$ (CDCl_3 , 500 MHz): 8.02-7.97 (m, 2H), 7.65-7.61 (m, 2H), 7.45-7.41(m, 2H), 7.29-7.21 (m, 5H), 7.17-7.12 (m, 3H), 6.41 (br s, 1H), 5.37-5.33 (dd, $J = 4.4, 5.8$ Hz, 1H), 5.03 (s, 2H), 3.31-3.23 (m, 2H), 3.19-3.15 (t, $J = 6.2, 13.0$ Hz, 2H), 3.01-2.95 (m, 2H), 2.66-2.64 (t, $J = 7.1, 14.0$ Hz, 2H), 2.46- 2.30 (m, 5H), 1.61-1.55 (m, 2H), 1.50-1.44 (m, 2H), 1.30-1.24 (m, 2H) ppm.

$^{13}\text{C-NMR}$ (CDCl_3 , 125.79Hz): 182.3 (s), 181.5 (s), 173.5 (s), 170.2 (s), 168.2 (s), 148.3 (s), 145.5 (s), 136.3 (s), 134.1 (d), 133.7 (d), 133.1 (d, 2C), 132.9 (s), 132.2 (s), 129.8 (s), 129.4 (d, 2C), 128.8 (d, 2C), 128.4 (d), 128.3 (d, 2C), 127.6 (d), 127.5 (d), 126.9 (d), 73.9 (d), 66.4 (t), 39.5 (t), 35.4 (t), 34.2 (t), 32.5 (t), 29.1 (t), 26.5 (t), 24.6 (t), 22.5 (t), 15.7 (q).

HRMS: [M+H] calc. 756.0978, [M+H] found 756.0973. Isotopic pattern of Se: m/z (relative abundance %) 746.1060 (1.5), 749.1034 (5), 750.1008 (20), 752.1000 (40), 756.0973 (100), 757.1007 (41), 759.1009 (15), 760.0977 (7).

Compound 13p: 21H,23H-Porphine, 5-(4- ((*tert*-butylcarbamoyl)methyl formate)phenyl)-10,15,20-triphenyl

The compound was purified by column chromatography on silica gel with petrol ether: ethyl acetate = 5:2. It was obtained as yellow oil. Yield = 93 %.

TLC (petroleum ether: ethyl acetate 4:1), R_f = 0.39.

$^1\text{H-NMR}$ (DMSO- d^6 , 500 MHz): 8.90-8.88 (m, 6H), 8.80-8.75 (m, 2H), 8.53-8.49 (m, 2H), 8.39-8.25 (m, 2H), 8.24-8.19 (m, 6H), 7.79-7.71 (m, 9H), 6.12 (s, 1H), 4.92 (s, 2H), 1.50 (s, 9H), -2.75 (s, 2H) ppm.

$^{13}\text{C-NMR}$ (DMSO- d^6 , 125.79 Hz): 167.44 (s), 166.0 (s), 149.60 (s), 148.19 (s), 145.72 (s), 142.25 (s, 8C), 134.81 (d), 134.53 (d, 10C), 128.02 (d, 2C), 127.87 (d, 2C), 126.73 (d, 10C), 120.99 (s), 120.70 (s, 4C), 118.17 (s), 77.02 (d, 2C), 52.08 (s), 29.36 (t), 28.79 (q, 3C) ppm.

LC-MS (ESI): m/z calc. 771.32, R_t = 16.99 min, m/z found 772.18 [M+H] $^+$.

HRMS: [M+H] calc. 772.3377, [M+H] found 772.3265.

Compound 14p: 21H,23H-Porphine, 5-(4- (1-(*tert*-butylcarbamoyl)-2-(phenylselanyl)ethyl formate)phenyl)-10,15,20-triphenyl

The compound was purified by column chromatography on silica gel with petrol ether: ethyl acetate = 5:2. It was obtained as yellow oil. Yield = 89 %.

TLC (petroleum ether: ethyl acetate 4:1), R_f = 0.51.

$^1\text{H-NMR}$ (DMSO- d^6 , 500 MHz): 8.98-8.90 (m, 6H), 8.85-8.75 (m, 2H), 8.20-8.35 (m, 10H), 7.82-7.75 (m, 10H), 7.68-7.60 (m, 2H), 7.29-7.35 (m, 2H), 6.15 (s, 1H), 5.75 (t, J = 5.7, 12.4 Hz, 1H), 3.75-3.40 (m, 2H), 1.45 (s, 9H), -2.85 (s, 2H) ppm.

$^{13}\text{C-NMR}$ (CDCl₃, 125.79 Hz): 167.43 (s), 165.35 (s), 165.30 (s), 147.80 (s), 142.01 (s, 10C), 134.66 (d, 4C), 134.53 (d, 10C), 132.99 (d, 2C), 129.74 (s), 129.29 (d, 6C), 128.02 (d), 127.82 (d), 127.32 (s), 126.73 (d, 8C), 120.71 (s, 2C), 120.45 (s, 2C), 74.4 (d), 51.81 (s), 29.08 (t), 28.79 (q, 3C) ppm.

LC-MS (ESI): m/z calc. 941.28, R_t = 18.40 min, m/z found 942.43 [M+H] $^+$.

HRMS: [M+H] calc. 942.2937, [M+H] found 942.2917. Isotopic pattern of Se: m/z (relative abundance %) 942.2917 (100), 943.2950 (63), 944.2984 (20), 945.2952 (12).

Compound 15p: 21H,23H-Porphine, 5-(4-(1-(tert-butylcarbamoyl)-2-(1,4-dihydro-2-methyl-1,4-dioxonaphthalen-3-ylselanyl)ethylformate)phenyl)-10,15,20-triphenyl

The compound was purified by column chromatography on silica gel with petrol ether: ethyl acetate = 5:2. It was obtained as yellow solid. Yield = 86 %.

TLC (petroleum ether: ethyl acetate 4:1), $R_f = 0.45$.

$^1\text{H-NMR}$ (DMSO- d^6 , 500 MHz): 8.90-8.88 (d, $J = 5.27$ Hz, 2H), 8.85 (s, 3H), 8.73-8.72 (d, $J = 4.52$ Hz, 2H), 8.82-8.20 (m, 8H), 8.14-8.13 (m, 2H), 8.07-8.05 (m, 1H), 7.94-7.92 (m, 1H), 7.78-7.73 (m, 8H), 7.57-7.54 (m, 1H), 7.41-7.38 (m, 1H), 6.28 (s, 1H), 5.85-5.83 (q, $J = 4.35$, 6.40, 10.92 Hz, 1H), 4.03-3.83 (m, 3H), 2.44 (s, 3H), 1.47 (s, 9H), -2.8 (s, 2H) ppm.

$^{13}\text{C-NMR}$ (DMSO- d^6 , 125.79 Hz): 181.89 (s), 181.57 (s), 167.44 (s), 149.60 (s), 148.19 (s), 145.72 (s), 142.25 (s, 8C), 135.03 (d, 2C), 134.79 (d, 10C), 133.87 (d), 133.59 (d), 132.95 (s), 132.05 (s), 128.18 (s), 128.07 (d, 2C), 128.03 (d, 2C), 127.22 (d), 126.99 (d, 8C), 126.96 (d, 2C), 126.91 (d, 2C), 120.99 (s), 120.70 (s, 4C), 118.17 (s, 2C), 75.37 (d), 60.61 (s), 52.08 (s), 29.36 (t), 29.03 (q, 3C), 17.99 (q) ppm.

LC-MS (ESI): m/z calc. 1035.00, $R_t = 18.27$ min, m/z found 1035.91 $[\text{M}+\text{H}]^+$.

HRMS: $[\text{M}+\text{H}]$ calc. 1036.2977, $[\text{M}+\text{H}]$ found 1036.2972. Isotopic pattern of Se: m/z (relative abundance %) 1030.3031 (3), 1032.2999 (19), 1034.2980 (49), 1036.2972 (100), 1037.3005 (69.5), 1038.3039 (24), 1039.3007 (13).

3.1.3. Method 3 (the Ugi four-component reaction)

An Ugi-type reaction has been employed for the synthesis of 15 representative sulfur, selenium and for the first time, (up to our knowledge), tellurium redox compounds. The Ugi reaction described here has required a range of building blocks, which needed to be designed and synthesized first (Figure 24).

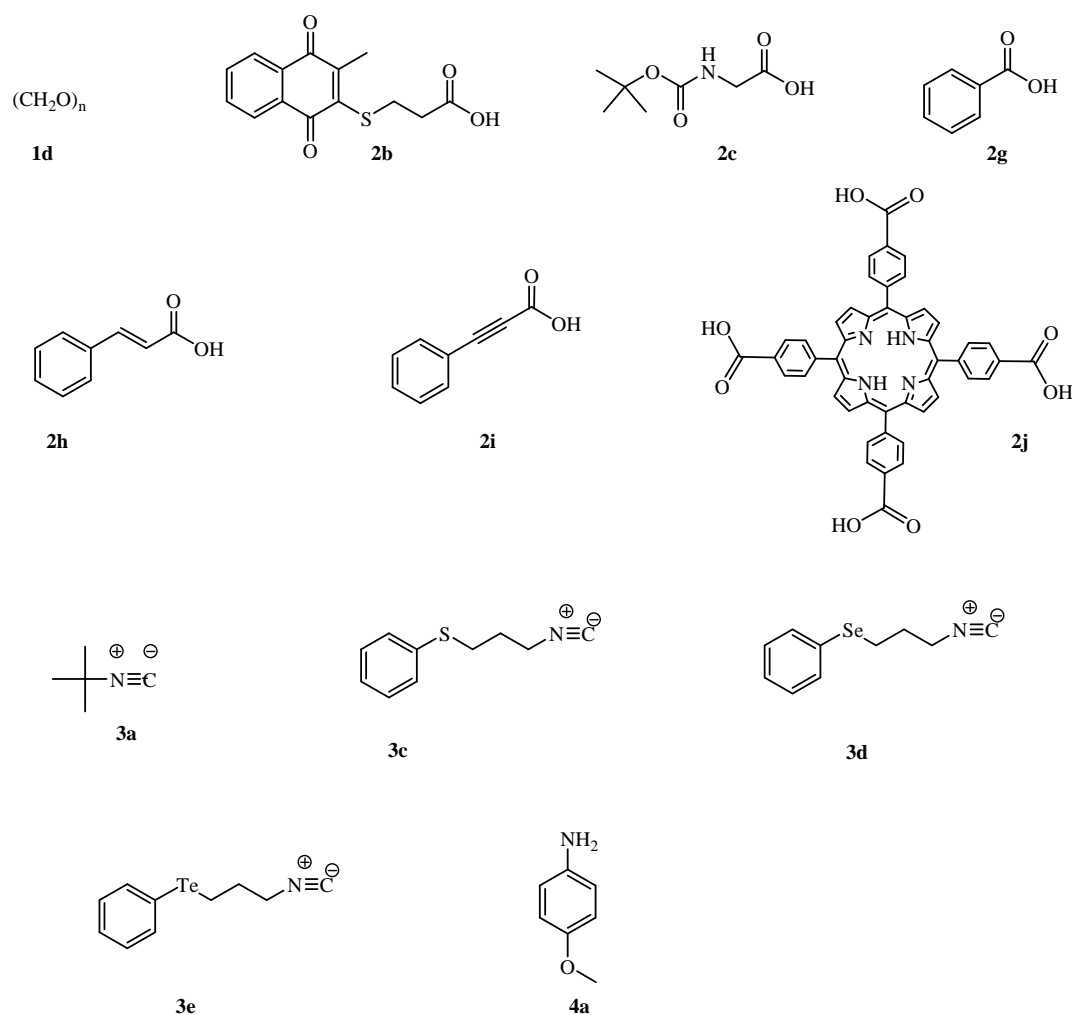


Figure 24. Building blocks used to synthesize multifunctional redox agents.

Acid, aldehyde, isocyanide, and amine building blocks used in U-4CR reaction were synthesized following literature procedures or, in case of hitherto unknown agents, could be synthesized in sufficient yield.

Figures 25 and 26 show the synthesis of the carboxylic acid and isocyanide building blocks used as part of U-4CR. Details regarding the synthesis of these compounds are provided in the Materials and Methods section.

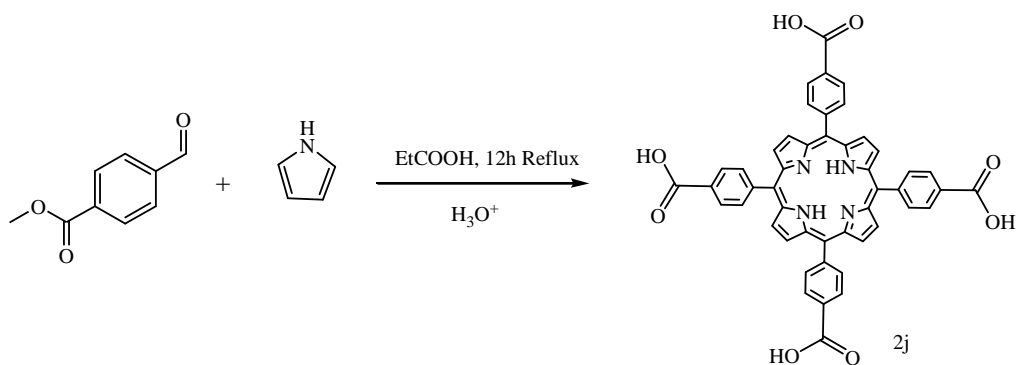


Figure 25. Synthesis of tetracarboxytertaphenyl porphyrin.

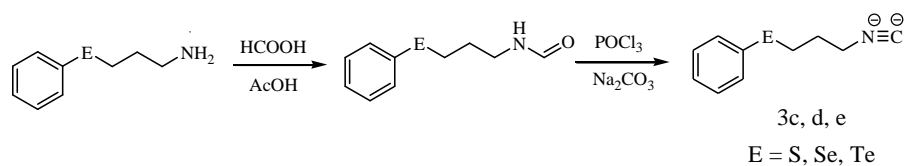


Figure 26. Synthesis of sulfur, selenium, and tellurium isocyanides.

Figure 27 provides an overview of the chemical structures of the redox compounds synthesized *via* U-4CR. For details regarding the synthesis of these compounds see the Materials and Methods section as well as Table 4.

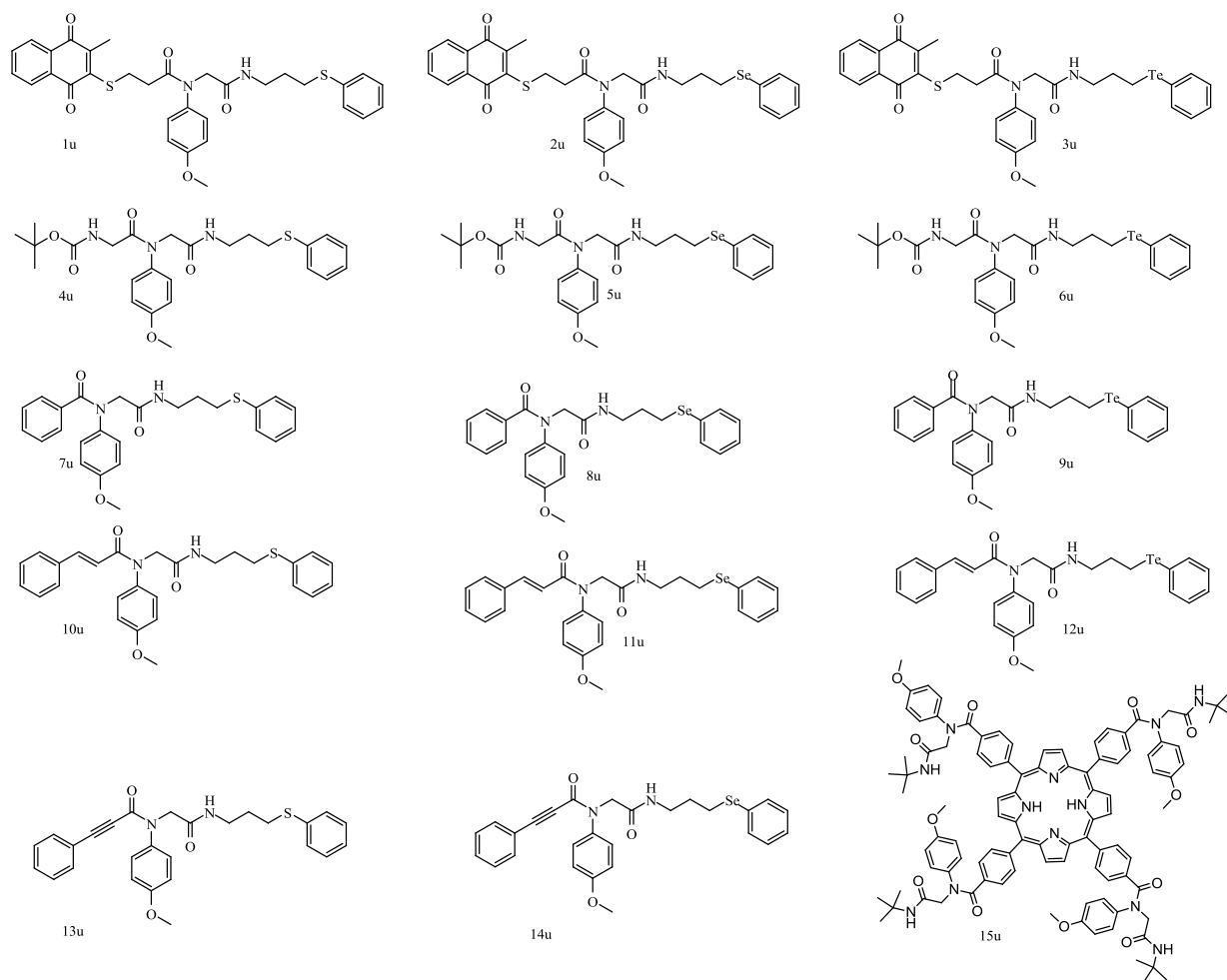


Figure 27: Chemical structures of the multifunctional compounds synthesized *via* U-4CR.

Table 4. Building blocks, solvents, and yields of the synthesized compounds 1u-15u.

Cpd.	Building Blocks	Solvent	Yield [%]	Redox centres	Cpd.	Building Blocks	Solvent	Yield %	Redox centres
1u	1d, 2b, 3c, 4a	H ₂ O	88	3	9u	1d, 2g, 3e, 4a	CHCl ₃	69	1
2u	1d, 2b, 3d, 4a	H ₂ O	94	3	10u	1d, 2h, 3c, 4a	H ₂ O	87	1
3u	1d, 2b, 3e, 4a	CHCl ₃	81	3	11u	1d, 2h, 3d, 4a	H ₂ O	92	1
4u	1d, 2c, 3c, 4a	H ₂ O	77	1	12u	1d, 2h, 3e, 4a	CHCl ₃	77	1
5u	1d, 2c, 3d, 4a	H ₂ O	86	1	13u	1d, 2i, 3c, 4a	H ₂ O	86	1
6u	1d, 2c, 3e, 4a	CHCl ₃	70	1	14u	1d, 2i, 3d, 4a	H ₂ O	90	1
7u	1d, 2g, 3c, 4a	H ₂ O	75	1	15u	1d, 2j, 3a, 4a	CHCl ₃	85	1
8u	1d, 2g, 3d, 4a	H ₂ O	79	1					

Building blocks were designed to carry one or two relevant redox or metal binding sites, which could be combined to larger, highly functionalized molecules with four or more biologically interesting sites. Reaction was mostly performed in water at high concentrations and under mild conditions.

Taking advantage of the novel tellurium isocyanide, Passerini tellurium containing redox compounds were for the first time, up to our knowledge, also synthesized (Figure 28). For details regarding the synthesis of these compounds see the Materials and Methods section as well as Table 5.

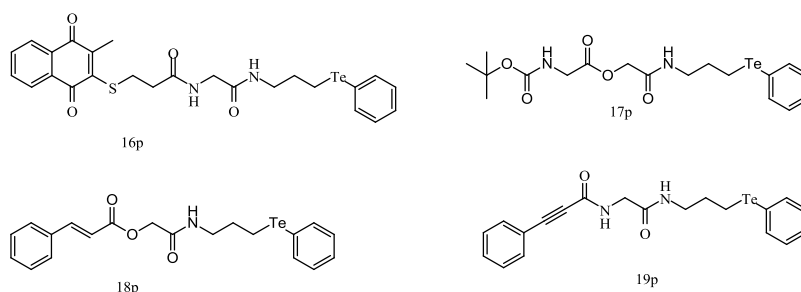
**Figure 28. Chemical structures of the telluro compounds synthesized via P-3CR.**

Table 5: Building blocks, solvents, and yields of the synthesized compounds of 16-19p.

Cpd. Nr.	Building Blocks	Solvent	Yield %	Redox centres
16p	1d, 2b, 3e	CHCl ₃	96	3
17p	1d, 2c, 3e	CHCl ₃	83	1
18p	1d, 2h, 3e	CHCl ₃	90	1
19p	1d, 2i, 3e	CHCl ₃	86	1

Compound 3c: (3-isocyanopropyl)(phenyl)sulfane

The compound was purified by column chromatography on silica gel with petrol ether: ethyl acetate = 5:1. It was obtained as colorless oil. Yield = 77 %.

TLC (petroleum ether: ethyl acetate 8:1), $R_f = 0.69$.

¹H-NMR (CDCl₃, 500 MHz): 7.30-7.28 (m, 2H), 7.25-7.22 (m, 2H), 7.17-7.13 (m, 1H), 3.44-3.41 (m, 2H), 2.98-2.95 (t, $J = 6.83, 13.66$ Hz, 2H), 1.89-1.83 (m, 2H) ppm.

¹³C-NMR (CDCl₃, 125.79 Hz): 156.65 (s), 134.68 (s), 129.45 (d, 2C), 128.76 (d, 2C), 126.22 (d), 39.74 (t), 29.94 (t), 28.01 (t) ppm.

LC-MS (ESI): m/z calc. 177.26, $R_t = 15.26$ min, m/z found 178.15 [M+H]⁺.

HRMS: [M+H] calc. 178.0690, [M+H] found 178.0685.

Compound 3d: (3-isocyanopropyl)(phenyl)selane

The compound was purified by column chromatography on silica gel with petrol ether: ethyl acetate = 5:1. It was obtained as colorless oil. Yield = 82 %.

TLC (petroleum ether: ethyl acetate 8:1), $R_f = 0.66$.

¹H-NMR (CDCl₃, 500 MHz): 7.51-7.49 (m, 2H), 7.30-7.28 (m, 3H), 3.48-3.46 (m, 2H), 2.95-2.90 (m, 2H), 1.98-1.90 (m, 2H) ppm.

^{13}C -NMR (CDCl_3 , 125.79 Hz): 156.65 (s), 134.68 (s), 130.00 (d, 2C), 129.10 (d, 2C), 127.76 (d), 40.74 (t), 29.94 (t), 19.20 (t) ppm.

LC-MS (ESI), m/z calc. 225.16, $R_t = 1.65$ min, m/z found 226.18 $[\text{M}+\text{H}]^+$.

HRMS: $[\text{M}+\text{H}+\text{O}]$ calc. 242.0134, $[\text{M}+\text{H}+\text{O}]$ found 242.0243. Isotopic pattern of Se: m/z (relative abundance %) 244.0235 (100), 246.0237 (30), 247.0270 (10).

Compound 3e: (3-isocyanopropyl)(phenyl)tellane

The compound was purified by column chromatography on silica gel with petrol ether: ethyl acetate = 5:1. It was obtained as colorless oil. Yield = 62 %.

TLC (petroleum ether: ethyl acetate 10:1), $R_f = 0.41$.

^1H -NMR (CDCl_3 , 500 MHz): 7.76-7.74 (m, 2H), 7.34-7.30 (m, 1H), 7.27-7.22 (m, 2H), 3.49-3.45 (m, 2H), 2.97-1.98 (t, $J = 7.18$, 14.67 Hz, 2H), 2.13-2.05 (m, 2H) ppm.

^{13}C -NMR (CDCl_3 , 125.79Hz): 156.73 (s), 138.68 (d, 2C), 129.43 (d, 2C), 128.11 (d), 110.69 (s), 43.25 (t), 31.00 (t), 3.64 (t) ppm.

LC-MS (ESI): m/z calc. 274.99, $R_t = 1.33$ min, m/z found 276.1 $[\text{M}+\text{H}]^+$.

HRMS: $[\text{M}+\text{H}+\text{O}]$ calc. 291.9981, $[\text{M}+\text{H}+\text{O}]$ found 291.9976. Isotopic pattern of Te: m/z (relative abundance %) 281.9954 (1), 283.9944 (8), 285.9942 (14.5), 286.9958 (21), 287.9946 (55.5), 289.9958 (93.5), 291.9976 (100), 293.0009 (11), 294.0043 (05).

Sulfur and selenium and tellurium redox compounds provided by U-4CR and P-3CR were synthesized as follows:

Compound 1u: *N*-((3-(phenylthio)propylcarbonyl)methyl)-3-(1,4-dihydro-2-methyl-1,4-dioxonaphthalen-3-ylthio)-*N*-(4-methoxyphenyl)propanamide

The compound was purified by column chromatography on silica gel with petrol ether: ethyl acetate = 5:1. It was obtained as yellow oil. Yield = 88 %.

TLC (petroleum ether: ethyl acetate 4:1), $R_f = 0.51$.

^1H -NMR (CDCl_3 , 500 MHz): 8.16-7.90 (m, 2H), 7.75-7.50 (m, 2H), 7.29-7.26 (m, 4H), 7.14-7.00 (m, 2H), 6.77-6.70 (m, 2H), 6.56 (br s, 1H), 4.18 (s, 2H), 3.71 (s, 3H), 3.41-3.32 (t, $J =$

5.86, 12.48 Hz, 2H), 3.27-3.25 (t, $J = 6.28, 10.47$ Hz, 2H), 2.80-2.76 (t, $J = 6.43, 12.28$ Hz, 2H), 2.50-2.46 (t, $J = 6.87, 11.00$ Hz, 2H), 2.28 (s, 3H), 1.88-1.82 (m, 2H) ppm.

^{13}C -NMR (CDCl_3 , 125.79 Hz): 182.14 (s), 181.20 (s), 172.15 (s), 168.77 (s), 159.32 (s), 147.06 (s), 146.40 (s), 136.12 (s), 134.92 (s), 133.62 (d), 133.32 (d), 132.73 (s), 131.96 (s), 129.20 (d, 2C), 128.92 (d, 2C), 128.64 (d, 2C), 126.72 (d), 126.53 (d), 126.02 (d), 114.99 (d, 2C), 55.41 (q), 54.48 (t), 38.45 (t), 35.04 (t), 31.07 (t), 30.02 (t), 28.84 (t), 15.29 (q) ppm.

LC-MS (ESI): m/z calc. 588.18, $R_t = 1.85$ min, m/z found 589.85 $[\text{M}+\text{H}]^+$.

HRMS: $[\text{M}+\text{H}]$ calc. 589.1830, $[\text{M}+\text{H}]$ found 589.1825, $[\text{M}+\text{Na}]$ calc. 611.1650 $[\text{M}+\text{Na}]$ found 611.1645. Isotopic pattern of S: m/z (relative abundance %) 589.1825 (100), 590.1859 (37), 591.1783 (10), 593.1850 (0.6).

Compound 2u: *N*-((3-(phenylselanyl)propylcarbonyl)methyl)-3-(1,4-dihydro-2-methyl-1,4-dioxonaphthalen-3-ylthio)-*N*-(4-methoxyphenyl)propanamide

The compound was purified by column chromatography on silica gel with petrol ether: ethyl acetate = 5:1. It was obtained as yellow oil. Yield = 94 %.

TLC (petroleum ether: ethyl acetate 4:1), $R_f = 0.52$.

^1H -NMR (CDCl_3 , 500 MHz): 8.05-7.98 (m, 1H), 7.97-7.91 (m, 1H), 7.69-7.59 (m, 2H), 7.45-7.37 (m, 2H), 7.20-7.10 (m, 3H), 7.09-7.02 (m, 2H), 6.71-6.68 (m, 2H), 6.48 (br s, 1H), 4.20 (s, 2H), 3.70 (s, 3H), 3.29-3.26 (m, 4H), 2.80-2.75 (t, $J = 7.30, 14.59$ Hz, 2H), 2.50-2.45 (t, $J = 6.78, 13.37$ Hz, 2H), 2.20 (s, 3H), 1.98-1.76 (m, 2H) ppm.

^{13}C -NMR (CDCl_3 , 125.79 Hz): 182.09 (s), 181.16 (s), 172.08 (s), 168.69 (s), 159.28 (s), 155.16 (s), 153.19 (s), 146.98 (s), 146.39 (s), 134.91 (s), 133.59 (d), 133.29 (d), 132.55 (d), 131.93 (s), 129.06 (d, 2C), 128.64 (d, 2C), 126.86 (d), 126.69 (d), 126.50 (d), 114.95 (d, 2C), 114.30 (d), 55.39 (q), 54.39 (t), 39.29 (t), 35.02 (t), 29.98 (t), 29.87 (t), 24.81 (t), 15.29 (q) ppm.

LC-MS (ESI): m/z calc. 636.12, $R_t = 17.74$ min, m/z found 637.10 $[\text{M}+\text{H}]^+$.

HRMS: $[\text{M}+\text{H}]$ calc. 637.1275, $[\text{M}+\text{H}]$ found 637.1270, $[\text{M}+\text{Na}]$ calc. 659.1094 $[\text{M}+\text{Na}]$ found 659.1089. Isotopic pattern of Se: m/z (relative abundance %) 631.1329 (2), 633.1297 (20), 635.1278 (49), 637.1270 (100), 638.1303 (36), 639.1272 (19), 640.1305 (9).

Compound 3u: *N*-((3-(phenyltellanyl)propylcarbonyl)methyl)-3-(1,4-dihydro-2-methyl-1,4-dioxonaphthalen-3-ylthio)-*N*-(4-methoxyphenyl)propanamide

The compound was purified by column chromatography on silica gel with petrol ether: ethyl acetate = 5:1. It was obtained as yellow oil. Yield = 81 %.

TLC (petroleum ether: ethyl acetate 5:2), $R_f = 0.54$.

$^1\text{H-NMR}$ (CDCl_3 , 500 MHz): 8.00-7.98 (m, 1H), 7.93-7.92 (m, 1H), 7.64-7.60 (m, 5H), 7.12-7.09 (m, 2H), 7.03-7.01 (m, 2H), 6.71-6.69 (m, 2H), 6.39 (br s, 1H), 4.11 (s, 2H), 3.65 (s, 3H), 3.29-3.24 (m, 4H), 2.80-2.77 (t, $J = 7.43, 15.04$ Hz, 2H), 2.44-2.41 (t, $J = 6.49, 12.98$ Hz, 2H), 2.23 (s, 3H), 1.96-1.90 (m, 2H) ppm.

$^{13}\text{C-NMR}$ (CDCl_3 , 125.79 Hz): 182.14 (s), 181.21 (s), 172.12 (s), 170.80 (s), 168.72 (s), 159.32 (s), 147.03 (s), 146.43 (s), 138.43 (d, 2C), 134.93 (s), 133.64 (d), 133.33 (d), 132.74 (s), 131.98 (s), 129.23 (d, 2C), 128.67 (d), 127.69 (d, 2C), 126.74 (d), 126.55 (d), 114.99 (d, 2C), 55.43 (q), 54.45 (t), 41.18 (t), 35.05 (t), 31.56 (t), 30.03 (t), 15.33 (q), 4.80 (t) ppm.

LC-MS (ESI): m/z calc. 686.11, $R_t = 1.63$ min, m/z found 687.11 $[\text{M}+\text{H}]^+$.

HRMS: $[\text{M}+\text{H}]$ calc. 687.1172, $[\text{M}+\text{H}]$ found 687.1167, $[\text{M}+\text{H}+\text{O}]$ calc. 703.1121 $[\text{M}+\text{H}+\text{O}]$ found 703.1116. Isotopic pattern of Te: m/z (relative abundance %) 695.1084 (8), 698.1098 (24), 699.1087 (57), 702 (94), 703.1116 (100), 704.1150 (36), 705.1183 (6).

Compound 4u: *tert-butyl ((2-(N-(4-methoxyphenyl)-N-amino)-N-(3-(phenylthio)propyl)acetamide)carbonyl)methylcarbamate*

The compound was purified by column chromatography on silica gel with petrol ether: ethyl acetate = 5:1. It was obtained as colorless oil. Yield = 77 %.

TLC (petroleum ether: ethyl acetate 4:1), $R_f = 0.63$.

$^1\text{H-NMR}$ (CDCl_3 , 500 MHz): 7.31-7.24 (m, 6H), 7.17-7.14 (m, 1H), 6.99 (br s, 1H), 6.88-6.86 (d, $J = 8.90$ Hz, 2H), 5.48 (s, 1H), 4.26 (s, 2H), 3.78 (s, 3H), 3.66-3.64 (d, $J = 5.07$ Hz, 2H), 3.37-3.33 (q, $J = 6.82, 13.00, 19.77$ Hz, 2H), 2.92-2.89 (t, $J = 7.24, 14.49$ Hz, 2H), 1.86-1.81 (p, $J = 7.24, 13.96, 21.11, 28.00$ Hz, 2H), 1.49 (s, 9H) ppm.

$^{13}\text{C-NMR}$ (CDCl_3 , 125.79Hz): 170.13 (s), 168.18 (s), 159.39 (s), 155.84 (s), 136.00 (s), 133.46 (s), 128.82 (d, 2C), 128.69 (d, 2C), 128.54 (d), 125.71 (d, 2C), 114.94 (d, 2C), 79.44 (s), 55.25 (q), 53.71 (t), 42.80 (t), 38.22 (t), 30.70 (t), 28.61 (t), 28.08 (q, 3C) ppm.

LC-MS (ESI): m/z calc. 487.21, $R_t = 1.61$ min, m/z found 488.2 $[\text{M}+ 1]^+$.

HRMS: [M+Na] calc. 510.2039, found 510.2033 [M+Na]. Isotopic pattern of S: m/z (relative abundance %) 488.2214 (100), 489.2247 (25), 490.2172 (5), 510.2033 (100), 511.2067 (25), 512.1991 (5).

Compound 5u: *tert-butyl ((2-(N-(4-methoxyphenyl)-N-amino)-N-(3-(phenylselanyl)propyl)acetamide)carbonyl)methylcarbamate*

The compound was purified by column chromatography on silica gel with petrol ether: ethyl acetate = 5:1. It was obtained as colorless oil. Yield = 86 %.

TLC (petroleum ether: ethyl acetate 4:1), R_f = 0.45.

$^1\text{H-NMR}$ (CDCl_3 , 500 MHz): 7.49-7.46 (m, 2H), 7.27-7.21 (m, 5H), 6.89-6.87 (d, J = 8.92 Hz, 2H), 6.77 (br s, 1H), 5.40 (br s, 1H), 4.24 (s, 2H), 3.79 (s, 3H), 3.66-3.64 (d, J = 5 Hz, 2H), 3.37-3.33 (q, J = 6.71, 12.71, 19.56 Hz, 2H), 2.89-2.87 (t, J = 7.37, 14.35 Hz, 2H), 1.93-1.87 (p, J = 7.00, 13.73, 21.00, 27.95 Hz, 2H), 1.41 (s, 9H) ppm.

$^{13}\text{C-NMR}$ (CDCl_3 , 125.79Hz): 170.18 (s), 168.20 (s), 159.52 (s), 155.88 (s), 133.52 (s), 132.39 (d, 2C), 129.89 (s), 128.95 (d, 2C), 128.61 (d), 126.73 (d, 2C), 115.07 (d, 2C), 79.59 (s), 55.37 (q), 53.91 (t), 42.90 (t), 39.21 (t), 29.69 (t), 28.18 (q, 3C), 24.68 (t) ppm.

LC-MS (ESI): m/z calc. 535.16, R_t = 1.73 min, m/z found 558.10 [M+ Na] $^+$.

HRMS: [M+H] calc. 536.1585, [M+H] found 536.1658, [M+Na] calc. 558.1478 [M+Na] found 559.1511. Isotopic pattern of Se: m/z (relative abundance %) 536.1658 (100), 537.1692 (26), 538.1660 (15), 539.1694 (5).

Compound 6u: *tert-butyl ((2-(N-(4-methoxyphenyl)-N-amino)-N-(3-(phenyltellanyl)propyl)acetamide)carbonyl)methylcarbamate*

The compound was purified by column chromatography on silica gel with petrol ether: ethyl acetate = 5:1. It was obtained as colorless oil. Yield = 70 %.

TLC (petroleum ether: ethyl acetate 4:1), R_f = 0.37.

$^1\text{H-NMR}$ (CDCl_3 , 500 MHz): 7.66-7.64 (m, 2H), 7.19 (s, 1H), 7.14-7.10 (m, 4H), 6.82-6.79 (d, J = 8.9 Hz, 2H), 6.32 (br s, 1H), 5.20 (br s, 1H), 4.13 (s, 2H), 3.73 (s, 3H), 3.58-3.57 (d, J = 5.28 Hz, 2H), 3.28-3.24 (q, J = 6.55, 13.41, 19.32 Hz, 2H), 2.80-2.77 (t, J = 7.66, 15.15 Hz, 2H), 1.97-1.91 (p, J = 6.95, 14.24, 21.66, 28.65 Hz, 2H), 1.43 (s, 9H) ppm.

$^{13}\text{C-NMR}$ (CDCl_3 , 125.79Hz): 170.25 (s), 168.30 (s), 159.72 (s), 155.92 (s), 138.45 (d, 2C), 133.58 (s), 129.23 (d, 2C), 128.68 (d, 2C), 127.70 (d), 115.26 (d, 2C), 111.46 (s), 79.80 (s), 55.25 (q), 54.22 (t), 43.05 (t), 41.22 (t), 31.52 (t), 28.30 (q, 3C), 4.75 (t) ppm.

LC-MS (ESI): m/z calc. 585.15, $R_t = 1.54$ min, m/z found 608.15 $[M+Na]^+$.

HRMS: $[M+H]$ calc. 586.1482, $[M+H]$ found 586.1555, $[M+H+O]$ calc. 602.1431 $[M+H+O]$ found 602.1504, $[M+Na]$ calc. 608.1380 $[M+Na]$ found 608.1656. Isotopic pattern of Te: m/z (relative abundance %) 586.1555 (100), 587.1589 (29), 588.1622 (5), 602.1504 (100), 603.1538 (26), 604.1571 (5), 608.1656 (1).

Compound 7u: *N-((3-(phenylthio)propylcarbamoyl)methyl)-N-(4-methoxyphenyl)benzamide*

The compound was purified by column chromatography on silica gel with petrol ether: ethyl acetate = 5:1. It was obtained as colorless oil. Yield = 75 %.

TLC (petroleum ether: ethyl acetate 4:1), $R_f = 0.56$.

1H -NMR ($CDCl_3$, 500 MHz): 7.25-7.22 (m, 4H), 7.19-7.17 (m, 2H), 7.11-7.07 (m, 3H), 6.94-6.91 (m, 2H), 6.64-6.61 (m, 3H), 4.38 (s, 2H), 3.63 (s, 3H), 3.36-3.32 (q, $J = 6.48, 12.34, 19.75$ Hz, 2H), 2.87-2.84 (t, $J = 7.35, 18.85$ Hz, 2H), 1.82-1.76 (p, $J = 6.98, 13.85, 20.83, 27.92$ Hz, 2H) ppm.

^{13}C -NMR ($CDCl_3$, 125.79Hz): 171.49 (s), 168.18 (s), 158.52 (s), 136.70 (s), 136.30 (s), 135.09 (s), 130.26 (d), 129.52 (d, 2C), 129.38 (d), 129.15 (d), 129.06 (d, 2C), 128.52 (d, 2C), 128.04 (d, 2C), 126.28 (d), 114.70 (d, 2C), 55.57 (q), 38.62 (t), 31.32 (t), 29.06 (t) ppm.

LC-MS (ESI): m/z calc. 434.17, $R_t = 15.69$ min, m/z found 435.2 $[M+H]^+$.

HRMS: $[M+H]$ calc. 435.1764, $[M+H]$ found 435.1737, $[M+Na]$ calc. 457.1562 $[M+Na]$ found 457.1556. Isotopic pattern of S: m/z (relative abundance %) 435.1737 (100), 436.1770 (29), 437.1695 (5), 457.1556 (100), 458.1590 (25), 459.1514 (5).

Compound 8u: *N-((3-(phenylselanyl)propylcarbamoyl)methyl)-N-(4-methoxyphenyl)benzamide*

The compound was purified by column chromatography on silica gel with petrol ether: ethyl acetate = 5:1. It was obtained as colorless oil. Yield = 79 %.

TLC (petroleum ether: ethyl acetate 4:1), $R_f = 0.43$.

1H -NMR ($CDCl_3$, 500 MHz): 7.40-7.38 (m, 2H), 7.24-7.22 (m, 2H), 7.16-7.14 (m, 4H), 7.11-7.07 (m, 2H), 6.94-6.91 (m, 2H), 6.64-6.61 (m, 2H), 4.36 (s, 2H), 3.63 (s, 3H), 3.33-3.29 (q, $J = 6.57, 13.14, 19.41$ Hz, 2H), 2.83-2.81 (t, $J = 7.06, 14.52$ Hz, 2H), 1.86-1.81 (p, $J = 6.98, 13.96, 21.31, 28.29$ Hz, 2H) ppm.

^{13}C -NMR (CDCl_3 , 125.79Hz): 171.22 (s), 168.88 (s), 158.26 (s), 136.44 (s), 134.84 (s), 132.60 (d, 2C), 130.00 (d), 129.86 (s), 129.06 (d, 2C), 128.79 (d, 2C), 128.27 (d, 2C), 127.79 (d, 2C), 126.89 (d), 114.44 (d, 2C), 55.31 (q), 55.28 (t), 39.23 (t), 29.78 (t), 24.78 ppm.

HRMS: $[\text{M}+\text{H}]$ calc. 483.1109, $[\text{M}+\text{H}]$ found 483.1181, $[\text{M}+\text{Na}]$ calc. 505.1007 $[\text{M}+\text{Na}]$ found 505.1001. Isotopic pattern of Se: m/z (relative abundance %) 483.1181 (100), 484.1215 (30), 485.1183 (20), 486.1217 (8), 505.1001 (100), 506.1034 (30), 507.1003 (20), 508.1036 (5).

Compound 9u: *N-((3-(phenyltellanyl)propylcarbamoyl)methyl)-N-(4-methoxyphenyl)benzamide*

The compound was purified by column chromatography on silica gel with petrol ether: ethyl acetate = 5:1. It was obtained as colorless oil. Yield = 69 %.

TLC (petroleum ether: ethyl acetate 4:1), $R_f = 0.31$.

^1H -NMR (CDCl_3 , 500 MHz): 7.78-7.75 (m, 2H), 7.38-7.30 (m, 5H), 7.24-7.22 (m, 3H), 7.06-7.04 (m, 2H), 6.77-6.75 (m, 2H), 4.49 (s, 2H), 3.78 (s, 3H), 3.43-3.38 (p, $J = 6.68$, 13.09, 19.56, 25.44 Hz, 2H), 2.93-2.90 (t, $J = 7.52$, 15.16 Hz, 2H), 2.08-2.03 (p, $J = 6.84$, 14.37, 21.49, 28.74 Hz, 2H) ppm.

^{13}C -NMR (CDCl_3 , 125.79Hz): 171.24 (s), 170.80 (s), 168.90 (s), 158.30 (s), 138.48 (d, 2C), 136.46 (s), 134.85 (s), 130.04 (d), 129.22 (d, 2C), 128.82 (d, 2C), 128.27 (d, 2C), 127.82 (d, 2C), 127.69 (d), 114.47 (d, 2C), 55.36 (t), 55.35 (q), 41.11 (t), 31.52 (t), 4.67 ppm.

LC-MS (ESI): m/z calc. 532.10, $R_t = 1.54$ min, m/z found 533.0 $[\text{M}+\text{H}]^+$.

HRMS: $[\text{M}+\text{H}+\text{O}]$ calc. 549.1006, $[\text{M}+\text{H}+\text{O}]$ found 549.1028. Isotopic pattern of Te: m/z (relative abundance %) 549.1028 (100), 550.1061 (30), 551.1095 (6).

Compound 10u: *(E)-N-((3-(phenylthio)propylcarbamoyl)methyl)-N-(4-methoxyphenyl)cinnamamide*

The compound was purified by column chromatography on silica gel with petrol ether: ethyl acetate = 5:1. It was obtained as colorless oil. Yield = 87 %.

TLC (petroleum ether: ethyl acetate 4:1), $R_f = 0.48$.

^1H -NMR (CDCl_3 , 500 MHz): 7.61-7.58 (m, 1H), 7.24-7.04 (m, 11H), 6.88-6.71 (m, 3H), 6.30-6.27 (m, 1H), 4.28 (s, 2H), 3.73 (s, 3H), 3.33-3.29 (q, $J = 6.73$, 12.95, 19.68 Hz, 2H), 2.87-2.84 (t, $J = 7.16$, 14.50 Hz, 2H), 1.81-1.75 (p, $J = 6.94$, 13.99, 21.04, 27.98 Hz, 2H) ppm.

^{13}C -NMR (CDCl_3 , 125.79Hz): 169.02 (s), 167.10 (s), 159.11 (s), 142.92 (d), 136.08 (s), 134.87 (s), 134.73 (s), 129.78 (d), 129.13 (d, 2C), 128.82 (d, 2C), 128.75(d, 2C), 128.64 (d, 2C), 127.90 (d, 2C), 125.90 (d), 117.71 (d), 114.83 (d, 2C), 55.42 (q), 54.71 (t), 38.33 (t), 30.99 (t), 28.82 (t) ppm.

LC-MS (ESI): m/z calc. 460.18, R_t = 14.10 min, m/z found 461.2 $[\text{M}+\text{H}]^+$.

HRMS: $[\text{M}+\text{H}]$ calc. 461.1821, $[\text{M}+\text{H}]$ found 461.1893. Isotopic pattern of Se: m/z (relative abundance %) 461.1893 (100), 462.1927 (30), 463.1851 (5), 464.1885 (2).

Compound 11u: *(E)-N-((3-(phenylselanyl)propylcarbamoyl)methyl)-N-(4-methoxyphenyl)cinnamamide*

The compound was purified by column chromatography on silica gel with petrol ether: ethyl acetate = 5:1. It was obtained as colorless oil. Yield = 92 %.

TLC (petroleum ether: ethyl acetate 4:1), R_f = 0.39.

^1H -NMR (CDCl_3 , 500 MHz): 7.62-7.59 (m, 1H), 7.39-7.37 (m, 2H), 7.24-7.08 (m, 9 H), 6.88-6.64 (m, 3H), 6.30-6.27 (m, 1H), 4.27 (s, 2H), 3.75 (s, 3H), 3.31-3.27 (q, J = 7.10, 13.37, 20.20 Hz, 2H), 2.83-2.80 (t, J = 7.25, 14.87 Hz, 2H), 1.86-1.81 (p, J = 6.96, 14.21, 21.31, 28.42 Hz, 2H) ppm.

^{13}C -NMR (CDCl_3 , 125.79Hz): 169.03 (s), 167.14 (s), 159.15 (s), 142.96 (d), 134.88 (s), 134.76 (s), 132.56 (d, 2C), 129.91 (s), 129.81 (d), 129.02(d, 2C), 128.76 (d, 2C), 128.67 (d, 2C), 127.93 (d, 2C), 126.82 (d), 117.71 (d), 114.83 (d, 2C), 55.46 (q), 54.78 (t), 39.22 (t), 29.82 (t), 24.78 (t) ppm.

LC-MS (ESI): m/z calc. 508.13, R_t = 1.71 min, m/z found 509.10 $[\text{M}+\text{H}]^+$.

HRMS: $[\text{M}+\text{H}]$ calc 509.1265, $[\text{M}+\text{H}]$ found 509.1338. Isotopic pattern of Se: m/z (relative abundance %) 509.1338 (100), 510.1371 (30), 511.1340 (17), 512.1373 (7), 513.1407 (2).

Compound 12u: *(E)-N-((3-(phenyltellanyl)propylcarbamoyl)methyl)-N-(4-methoxyphenyl)cinnamamide*

The compound was purified by column chromatography on silica gel with petrol ether: ethyl acetate = 5:1. It was obtained as colorless oil. Yield = 77 %.

TLC (petroleum ether: ethyl acetate 4:1), R_f = 0.33.

^1H -NMR (CDCl_3 , 500 MHz): 7.64-7.61 (m, 3H), 7.40-7.3 (m, 5H), 7.25-7.2 (m, 3H), 6.71-7.02 (m, 3H), 6.75 (br s, 1H), 6.30-6.27 (m, 1H), 4.26 (s, 2H), 3.76 (s, 3H), 3.28-3.24 (q, J =

6.42, 12.84, 19.69 Hz, 2H), 2.80-2.77 (t, $J = 7.59, 15.19$ Hz, 2H), 1.96-1.91 (p, $J = 6.94, 14.52, 21.47, 28.88$ Hz, 2H) ppm.

^{13}C -NMR (CDCl_3 , 125.79Hz): 169.30 (s), 167.42 (s), 159.43 (s), 143.25 (d), 138.64 (d, 2C), 135.13 (s), 135.03 (s), 130.10 (d), 129.42 (d, 2C), 129.02 (d, 2C), 128.95 (d, 2C), 128.21 (d, 2C), 127.87 (d), 117.97 (d), 115.15 (d, 2C), 111.66 (s), 55.74 (q), 55.06 (t), 41.33 (t), 31.78 (t), 4.95 (t) ppm.

LC-MS (ESI): m/z calc. 558.12, $R_t = 17.19$ min, m/z found 558.80 $[\text{M} + \text{H}]$, 582.1, $[\text{M} + \text{Na}]$. HRMS: $[\text{M} + \text{H} + \text{O}]$ calc. 575.1162, $[\text{M} + \text{H} + \text{O}]$ found 575.1184. Isotopic pattern of Te: m/z (relative abundance %) 575.1184 (100), 576.1218 (30), 577.1251 (5), 578.1285 (2).

Compound 13u: *N*-((3-(phenylthio)propylcarbamoyl)methyl)-*N*-(4-methoxyphenyl)-3-phenylpropiolamide

The compound was purified by column chromatography on silica gel with petrol ether: ethyl acetate = 5:1. It was obtained as colorless oil. Yield = 86 %.

TLC (petroleum ether: ethyl acetate 4:1), $R_f = 0.55$.

^1H -NMR (CDCl_3 , 500 MHz): 7.29-7.24 (m, 4H), 7.19-7.16 (m, 5H), 7.10-7.06 (m, 3H), 6.84-6.81 (m, 2H), 6.47 (br s, 1H), 4.27 (s, 2H), 3.74 (s, 3H), 3.35-3.31 (q, $J = 6.77, 12.89, 19.49$ Hz, 2H), 2.88-2.85 (t, $J = 7.09, 14.34$ Hz, 2H), 1.83-1.77 (p, $J = 7.09, 13.86, 20.94, 27.71$ Hz, 2H) ppm.

^{13}C -NMR (CDCl_3 , 125.79Hz): 168.15 (s), 159.44 (s), 155.33 (s), 136.02 (s), 134.81 (s), 132.51 (d), 130.20 (d, 2C), 129.29 (d, 2C), 128.98 (d, 2C), 128.92 (d, 2C), 128.35 (d, 2C), 126.03 (d), 120.03 (s), 114.39 (d, 2C), 92.68 (s), 81.96 (s), 55.53 (q), 53.62 (t), 38.51 (t), 31.08 (t), 28.79 (t) ppm.

LC-MS (ESI): m/z calc. 458.17, $R_t = 1.56$ min, m/z found 459.2 $[\text{M} + \text{H}]^+$.

HRMS: $[\text{M} + \text{H}]$ calc. 459.1664, $[\text{M} + \text{H}]$ found 459.1734, $[\text{M} + \text{Na}]$ calc. 482.1590 $[\text{M} + \text{Na}]$ found 481.1556. Isotopic pattern of S: m/z (relative abundance %) 459.1734 (100), 460.1770 (30), 461.1695 (4), 481.1556 (100), 482.1590 (30), 483.1514 (5).

Compound 14u: *N*-((3-(phenylselanyl)propylcarbamoyl)methyl)-*N*-(4-methoxyphenyl)-3-phenylpropiolamide

The compound was purified by column chromatography on silica gel with petrol ether: ethyl acetate = 5:1. It was obtained as colorless oil. Yield = 90 %.

TLC (petroleum ether: ethyl acetate 4:1), $R_f = 0.46$.

¹H-NMR (CDCl₃, 500 MHz): 7.42-7.39 (m, 2H), 7.27-7.22 (m, 3H), 7.18-7.13 (m, 5H), 7.11-7.07 (m, 2H), 6.84-6.82 (m, 2H), 6.46 (br s, 1H), 4.26 (s, 2H), 3.74 (s, 3H), 3.32-3.28 (q, J = 6.94, 13.23, 19.84 Hz, 2H), 2.84-2.80 (t, J = 7.07, 14.40 Hz, 2H), 1.87-1.81 (p, J = 6.91, 13.92, 20.72, 27.74 Hz, 2H) ppm.

¹³C-NMR (CDCl₃, 125.79Hz): 168.08 (s), 159.40 (s), 155.28 (s), 134.79 (s), 132.61 (s), 132.48 (d, 2C), 130.18 (d, 2C), 129.87 (d), 128.06 (d, 2C), 128.98 (d, 2C), 128.33 (d, 2C), 126.86 (d), 120.01 (s), 114.36 (d, 2C), 92.62 (s), 81.97 (s), 55.51 (q), 53.54 (t), 39.34 (t), 29.76 (t), 24.77 (t) ppm.

LC-MS (ESI): m/z calc. 506.11, R_t = 11.45 min, m/z found 507.54 [M+H]⁺.

HRMS: [M+H] calc. 507.1109, [M+H] found 507.1181. Isotopic pattern of Se: m/z (relative abundance %) 507.1181 (100), 508.1215 (33), 509.1183 (18), 510.1217 (7), 511.1250 (1).

Compound 15u: 4,4',4'',4'''-(Porphine-5,10,15,20-tetrayl)tetrakis(((tert-butylcarbamoyl)methyl)(4-methoxyphenyl)carbamic chloride)

The compound was purified by column chromatography on silica gel with petrol ether: ethyl acetate = 5:2. It was obtained as colorless oil. Yield = 85 %.

TLC (petroleum ether: ethyl acetate 4:1), R_f = 0.38.

¹H-NMR (DMSO-*d*⁶, 500 MHz): 8.50 (s, 7H), 8.00-7.85 (m, 8H), 7.70-6.65 (m, 8H), 7.20-7.30 (m, 9H), 7.80-7.75 (m, 9H), 6.30 (s, 4H), 4.50 (s, 8H), 3.75 (s, 12H), 1.45 (s, 35H), -3.10 (s, 2H) ppm.

¹³C-NMR (DMSO-*d*⁶, 125.79 Hz): 171.21 (s, 4C), 167.90 (s, 4C), 158.70 (s, 6C), 143.60 (s, 4C), 136.74 (s, 6C), 135.91 (s, 6C), 133.78 (d, 10C), 128.71 (d, 8C), 127.07 (d, 10C), 117.57 (d, 2C), 119.24 (s, 6C), 116.98 (s, 4C), 114.56 (d, 10C), 55.57 (q, 4C), 56.36 (t, 4C), 28.88 (q, 12C) ppm.

HRMS: [M+H] calc. 1663.77, [M+H] found 1663.7784.

Compound 16p: N-((3-(phenyltellanyl)propylcarbamoyl)methyl)-3-(1,4-dihydro-2-methyl-1,4-dioxonaphthalen-3-ylthio)propanamide

The compound was purified by column chromatography on silica gel with petrol ether: ethyl acetate = 5:1. It was obtained as yellow oil. Yield = 96 %.

TLC (petroleum ether: ethyl acetate 4:1), R_f = 0.62.

$^1\text{H-NMR}$ (CDCl_3 , 500 MHz): 8.02-7.97 (m, 2H), 7.65-7.62 (m, 2H), 7.15-7.10 (m, 1H), 7.09-7.04 (m, 2H), 6.79-6.70 (m, 2H), 6.5 (br s, 1H), 4.25 (s, 2H), 3.75-3.73 (m, 2H), 3.45-3.25 (m, 2H), 2.95-2.80 (m, 2H), 2.50-2.48 (m, 2H), 2.27 (s, 3H), 1.85-1.75 (m, 2H) ppm.

$^{13}\text{C-NMR}$ (CDCl_3 , 125.79 Hz): 182.04 (s), 181.40 (s), 169.96 (s), 166.81 (s), 148.25 (s), 145.18 (s), 138.33 (d, 2C), 133.86 (d), 133.52 (d), 132.54 (s), 131.92 (s), 129.19 (d, 2C), 127.69 (d), 126.79 (d), 126.67 (d), 111.35 (s), 63.14 (t), 40.82 (t), 35.29 (t), 31.39 (t), 29.22 (t), 15.43 (q), 4.64 (t) ppm.

LC-MS (ESI): m/z calc. 580.07, $R_t = 1.60$ min, m/z found 581.12 $[\text{M}+\text{H}]^+$.

HRMS: $[\text{M}+\text{H}]$ calc. 580.0712, $[\text{M}+\text{H}]$ found 582.0588, $[\text{M}+\text{H}+\text{O}]$ calc. 598.0543 $[\text{M}+\text{H}+\text{O}]$ found 598.0538. Isotopic pattern of Te: m/z (relative abundance %) 590.0506 (8), 593.0520 (23), 594.0508 (58), 596 (93), 598.0538 (100), 599.0571 (29), 600.0496 (6).

Compound 17p: *tert-butyl* (((3-(phenyltellanyl)propylcarbamoyl)methoxy)carbonyl)methylcarbamate

The compound was purified by column chromatography on silica gel with petrol ether: ethyl acetate = 5:1. It was obtained as colorless oil. Yield = 83 %.

TLC (petroleum ether: ethyl acetate 4:1), $R_f = 0.54$.

$^1\text{H-NMR}$ (CDCl_3 , 500 MHz): 7.66-7.63 (m, 2H), 7.23-7.20 (m, 1H), 7.15-7.11 (m, 2H), 6.70 (br s, 1H), 5.05 (br s, 1H), 4.56 (s, 2H), 3.83-3.82 (d, 2H), 3.30-3.26 (q, $J = 6.68, 12.91, 19.81$ Hz, 2H), 2.81-2.78 (t, $J = 7.50, 15.11$ Hz, 2H), 1.99-1.93 (p, $J = 7.26, 14.53, 21.55, 29.05$ Hz, 2H), 1.37 (s, 9H) ppm.

$^{13}\text{C-NMR}$ (CDCl_3 , 125.79Hz): 168.99 (s), 166.87 (s), 156.48 (s), 138.42 (d, 2C), 129.21 (d, 2C), 127.68 (d), 111.50 (s), 80.79 (s), 63.13 (t), 42.88 (t), 40.96 (t), 31.44 (t), 28.30 (q, 3C), 4.70 (t) ppm.

LC-MS (ESI): m/z calc. 480.09, $R_t = 7.21$ min, m/z found 497.59 $[\text{M}+\text{H}+\text{O}]$, 497.44 $[\text{M}+\text{H}+\text{O}]^+$.

HRMS: $[\text{M}+\text{H}+\text{O}]$ calc. 497.0849, $[\text{M}+\text{H}+\text{O}]$ found 497.0926, $[\text{M}+\text{Na}]$ calc. 503.0904, $[\text{M}+\text{Na}]$ found 503.1078. Isotopic pattern of Te: m/z (relative abundance %) 495.0908 (93), 497.0926 (100), 498.0959 (22), 499.0993 (7), 503.1078 (2).

Compound 18p: *(E)*-(3-(phenyltellanyl)propylcarbamoyl)methyl cinnamate

The compound was purified by column chromatography on silica gel with petrol ether: ethyl acetate = 5:1. It was obtained as colorless oil. Yield = 90 %.

TLC (petroleum ether: ethyl acetate 4:1), $R_f = 0.37$.

$^1\text{H-NMR}$ (CDCl_3 , 500 MHz): 7.73-7.64 (m, 3H), 7.57-7.45 (m, 2H), 7.37-7.33 (m, 2H), 7.22-7.18 (m, 2H), 7.11-7.15 (m, 2H), 6.50-6.35 (m, 1H), 6.12 (br s, 1H), 4.60 (s, 2H), 3.35-3.31 (q, $J = 6.63, 13.07, 19.96$ Hz, 2H), 2.82-2.79 (t, $J = 7.28, 14.82$ Hz, 2H), 2.00-1.95 (p, $J = 7.09, 14.27, 21.45, 28.81$ Hz, 2H) ppm.

$^{13}\text{C-NMR}$ (CDCl_3 , 125.79Hz): 167.23 (s), 165.42 (s), 146.79 (d), 138.51 (d, 2C), 133.96 (d), 130.87 (s), 129.28 (d, 2C), 129.02 (d, 2C), 128.28 (d, 2C), 127.81 (d), 116.38 (d), 111.33 (s), 63.07 (t), 40.80 (t), 31.47 (t), 4.60 (t) ppm.

LC-MS (ESI): m/z calc. 453.06, $R_t = 9.01$ min, m/z found 469.85 $[\text{M}+\text{O}]^+$.

HRMS: $[\text{M}+\text{H}+\text{O}]$ calc. 470.0584, $[\text{M}+\text{H}+\text{O}]$ found 470.0606. Isotopic pattern of Te: m/z (relative abundance %) 470.0606 (100), 471.0639 (23), 472.0673 (4).

Compound 19p: *N-((3-(phenyltellanyl)propylcarbamoyl)methyl)-3-phenylpropiolamide*

The compound was purified by column chromatography on silica gel with petrol ether: ethyl acetate = 5:1. It was obtained as colorless oil. Yield = 86 %.

TLC (petroleum ether: ethyl acetate 4:1), $R_f = 0.58$.

$^1\text{H-NMR}$ (CDCl_3 , 500 MHz): 7.70-7.65 (m, 2H), 7.55-7.51 (m, 2H), 7.36-7.31 (m, 3H), 7.22-7.21 (m, 1H), 7.15-7.10 (m, 2H), 6.60 (br s, 1H), 4.65 (s, 1H), 4.60 (s, 2H), 3.64-3.61 (m, 2H), 2.75-2.72 (m, 2H), 1.72-1.67 (m, 2H) ppm.

$^{13}\text{C-NMR}$ (CDCl_3 , 125.79Hz): 167.40 (s), 166.55 (s), 152.53 (s), 133.43 (d, 2C), 133.37 (d), 131.44 (d), 131.39 (d, 2C), 128.97 (d), 128.93 (d, 2C), 126.85 (d), 119.28 (s), 88.87 (s), 79.81 (s), 63.97 (t), 43.75 (t), 36.63 (t), 32.89 (t) ppm.

HRMS: $[\text{M}+\text{O}]$ calc. 466.0427, $[\text{M}+\text{O}]$ found 466.0449. Isotopic pattern of Te: m/z (relative abundance %) 468.0449 (100), 469.0483 (21), 470.0516 (5).

3.2. Cell culture and biological studies

3.2.1. Cytotoxicity

The cytotoxic activity was assayed with MCF-7 (human breast adenocarcinoma), A-498 (human kidney carcinoma), A-431 (human epidermoid carcinoma), L-929¹ (mouse fibroblasts), A-549¹ (human lung carcinoma), and SW-480¹ (human colon adenocarcinoma), cancer cell lines as well as primary human fibroblasts (HF) and endothelium cells (HUVEC) by means of an MTT assay at different incubation times¹ (Table 6).

Furthermore, one-dose and five-dose screens of compounds **2p**, **4p**, **6p**, **7p**, **8p**, **9p**, **11p**, **12p**, **15p**, **16p**, **3u**, **6u**, and **9u** with 58 tumour cell lines were performed at the National Cancer Institute (see Appendix for details).

¹ The results shown here are only after one-day incubation with the multifunctional compounds. Results obtained after five-days incubation time as well as the IC₅₀ values in case of L-929, A-549, and SW-480 cell lines are shown in the Appendix section.

Table 6. Influence of multifunctional redox compounds on the viability of human cancer and primary cell lines.

Cpd.	MCF-7	A-498	A-431	HUVEC	HF	Cpd.	MCF-7	A-498	A-431	HUVEC	HF
1p	26	>100	>100	13	11	18p	1	52	6	7	11
2p	14	>100	7	34	26	19p	1	63	7	10	7
3p	10	>100	>100	23	50	1u	16	>100	17	24	26
4p	3	3	1	1	n.d.	2u	8	>100	17	21	24
5p	19	>100	>100	17	21	3u	7	7	1	6	4
6p	10	5	6	7	5	4u	>100	>100	>100	>100	>100
7p	3	5	2	3	7	5u	>100	>100	>100	>100	>100
8p	3	5	2	2	4	6u		>100	5	6	25
9p	5	5	4	35	27	7u	>100	>100	>100	>100	>100
10p	4	7	5	36	6	8u	>100	>100	>100	>100	>100
11p	8	13	4	10	4	9u		2	5	5	7.5
12p	9	4	4	3	6	10u	>100	>100	>100	>100	>100
13p	>100	>100	>100	>100	>100	11u	>100	>100	>100	>100	>100
14p	>100	>100	>100	>100	>100	12u	2	9	6	4.5	5
15p	>100	>100	>100	>100	>100	13u	>100	>100	>100	>100	>100
16p	12	1	1	4	13	14u	>100	>100	>100	>100	>100
17p		5	0	2.5	19	15u	>100	>100	>100	>100	>100

The metabolic activity of the cells was measured after one day of incubation with different concentrations of the test compounds by means of an MTT assay. The IC₅₀ was determined from the dose-response curves as the mean of two parallel experiments.

3.2.2. Immunocytochemistry (ICC)

Phenotypical changes in the cytoskeleton architecture, nucleus, and the morphology of the endoplasmic reticulum were monitored in potoroo cells (PtK2) treated with different multifunctional compounds (see Appendix for more results).

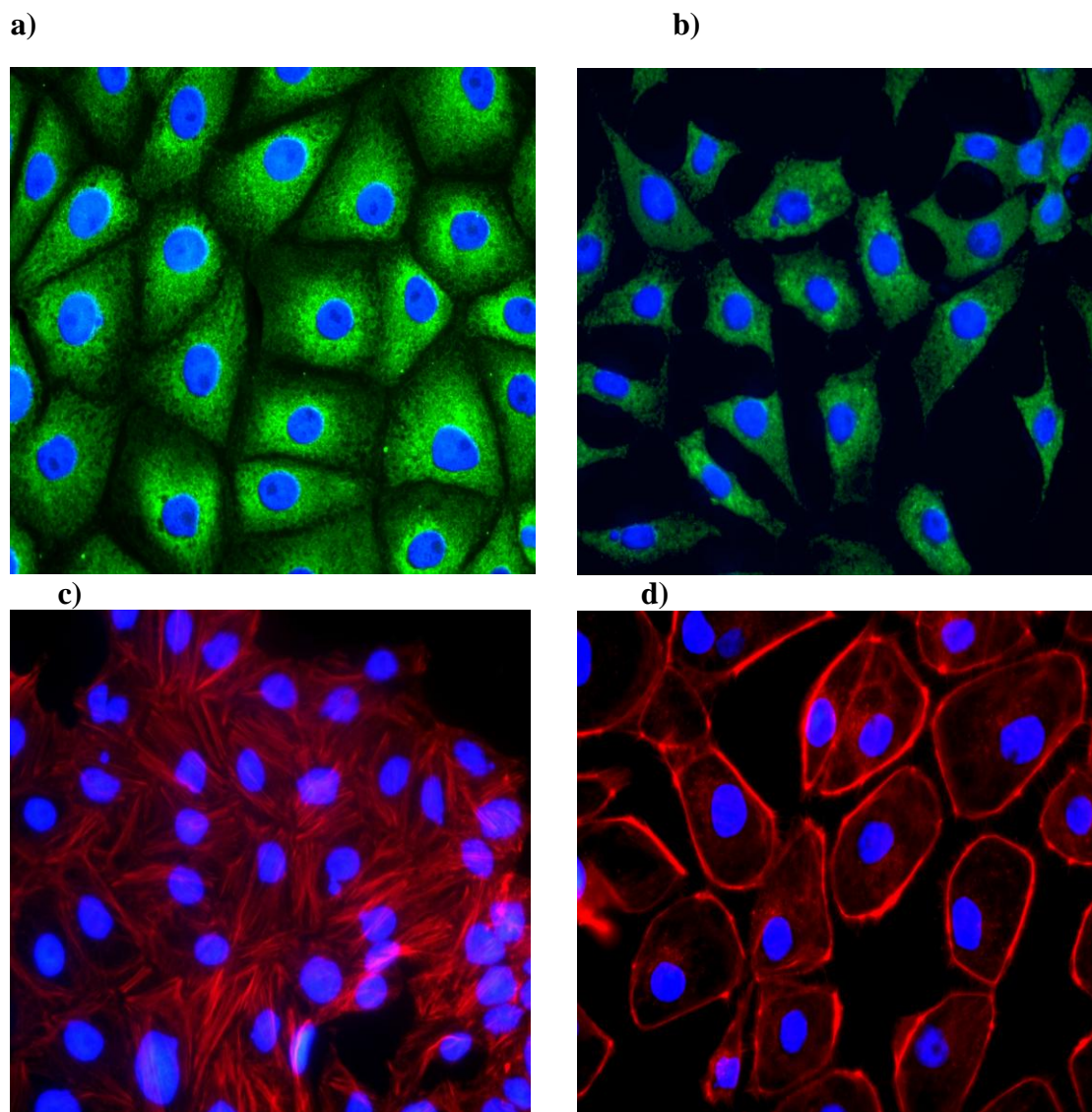


Figure 29. Immunofluorescence investigations of the ER (panel a and b) and the actin cytoskeleton (panel c and d) of PtK2 cells.

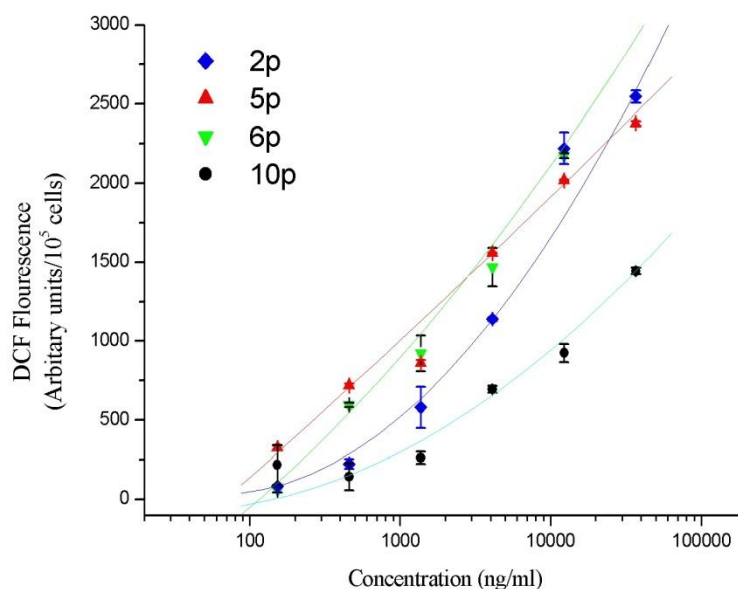
PtK2 cells were incubated with **7p** and **6p**, respectively, in comparison with control cells. Treated cells show holes in the ER (panel b) and reduced Actin stress fibers (panel d). Cells are rounded and detached from each other.

Figure 29 shows that the ER structure is affected and the cell morphology in general is altered; cells are rounded and detached from each other. The adhesion of the cells seems to be reduced and actin stress fibers are barely detectable. On the other hand, no phenotypical changes were noticed in case of the microtubular network.

3.2.3. Assessment of intracellular levels of oxidative stress

Compounds possessing chalcogen(s) and quinone(s) redox centres were able to significantly increase the ROS levels in A-431 melanoma cells in a concentration dependent manner over 1 h treatment in both DCF (Figure 13, panel a) and DHE assays (Figure 30, panel b).

a)



b)

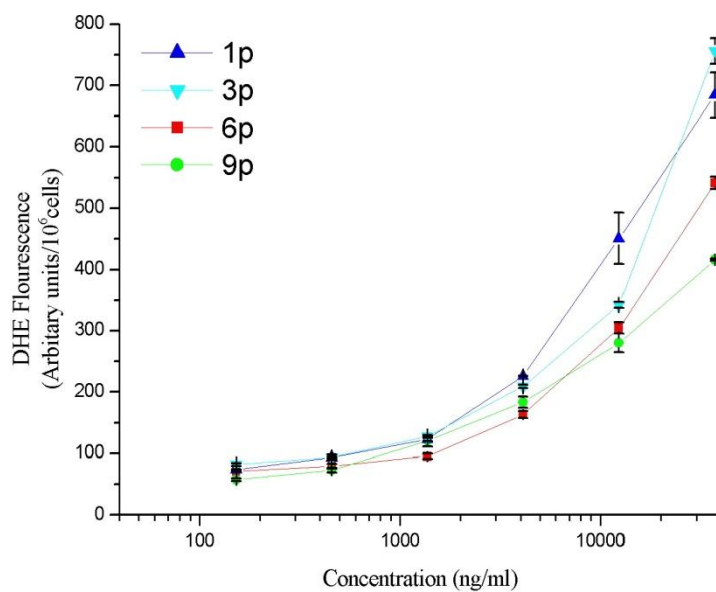


Figure 30. ROS levels were measured in A-431 using two different methods after 1 h of treatment with different concentrations of multifunctional compounds.

- a) A DCF assay was run after incubation with **2p**, **5p**, **6p**, and **10p**
- b) A DHE assay was performed after incubation with **1p**, **3p**, **6p**, and **9p**.

On the other hand, compounds with one redox centre (sulfur and selenium) were not able to disturb the ROS levels in A-431 melanoma cells over a 1 h treatment in the tested concentration range in the DCF assay (Figure 31).

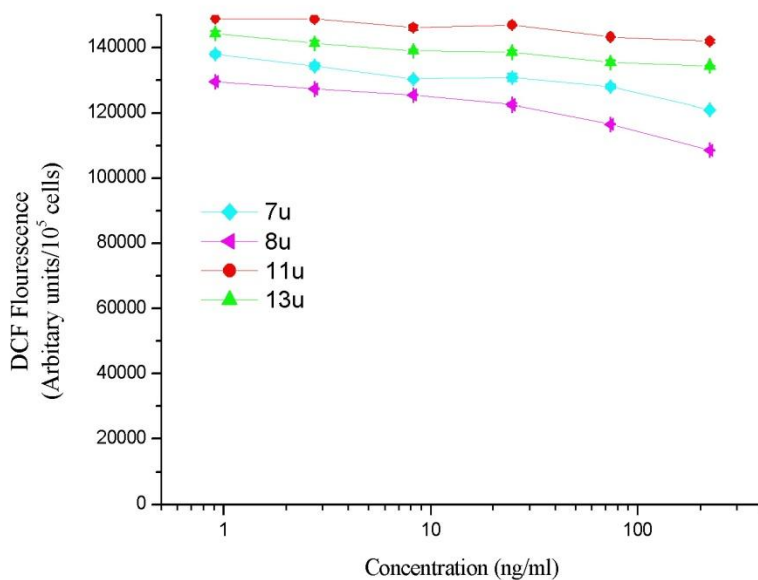


Figure 31. ROS levels were measured in A-431 using the DCF assay after 1 h of treatment with different concentrations of 7u, 8u, 11u, and 13u.

Interestingly, compounds with tellurium redox centres (only one redox centre) were able to decrease the ROS levels to some extent in A-431 melanoma cells in a concentration dependent manner over 1 h treatment in the DCF assay (Figure 32).

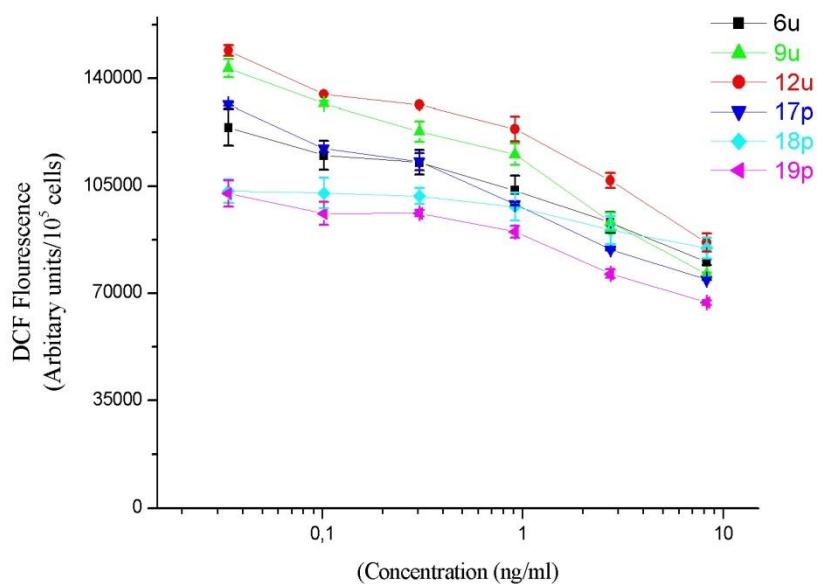


Figure 32. ROS levels were measured in A-431 using the DCF assay after 1 h of treatment with different concentrations of tellurium containing compounds 6u, 9u, 12u, 17p, 18p, and 19u.

Figure 33 (panel a and b) shows the levels of ROS monitored in both, A-431 melanoma cancer cells and primary HUVECs.

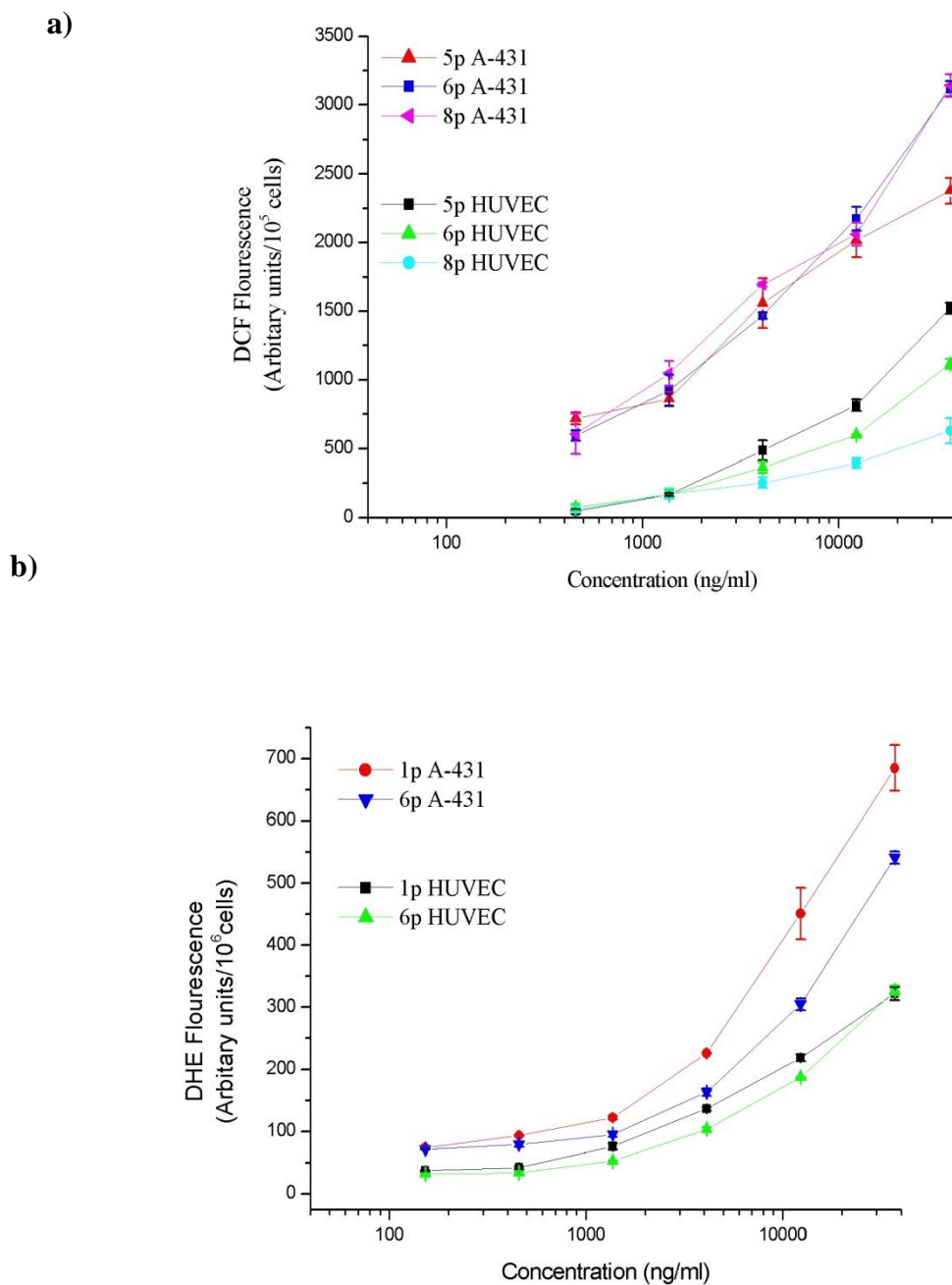


Figure 33. Assessment of oxidative stress in melanoma and normal human umbilical vein endothelial cells.

Using two different methods ROS levels were measured in A-431 in comparison with HUVECs after 1 h of treatment with different concentrations of multifunctional compounds.

- a) A DCF assay was run after incubation with **5p**, **6p**, and **8p**
b) A DHE assay was performed after incubation with **1p** and **6p**.

The intracellular levels of reduced glutathione after a 1 h treatment of exponentially growing MCF-7 cells with different concentrations of test compounds were then estimated by the DTNB assay. A concentration of 5 μM of compounds **7p**, **8p**, **10p**, and **12p** causes a decrease of the intracellular GSH level in the breast cancer cell line up to 46%, 59%, 62%, and 76%, respectively (Figure 34).

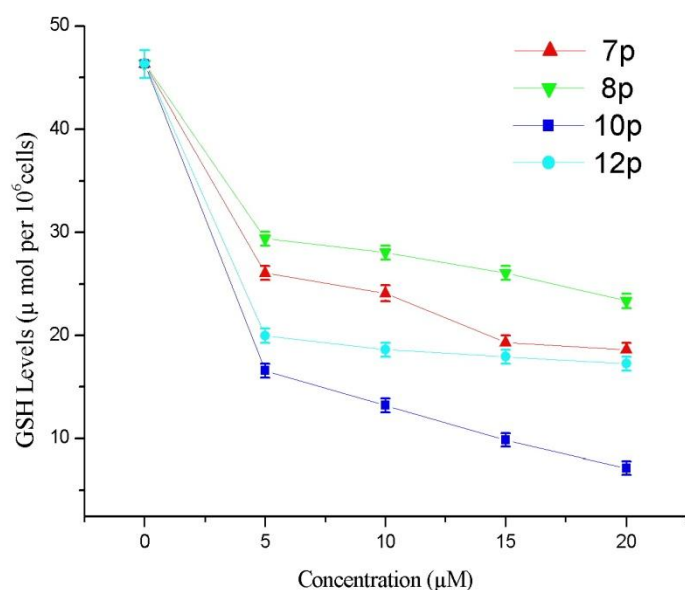


Figure 34. Assessment of the intracellular levels of reduced glutathione in breast cancer cells.

Depletion of the intracellular levels of reduced GSH in MCF-7 cells treated with compounds **7p**, **8p**, **10p**, and **12p** for 1 h were assessed employing the DTNB assay. This assay is not entirely specific for GSH, but DTNB reacts also with other thiols, including proteins and enzymes.

3.2.4. Thiophenol oxidation assay (PhSH assay)

This assay was used as a predictor of activity in cell culture. The results shown in Table 7 confirm that all compounds enhance the oxidation of thiols in the presence of H_2O_2 . Several compounds are even considerably more active than the benchmark compound ebselen (1.5-fold increase vs. DMSO), with tellurium compounds **16p** and **3u** being the most active.

Table 7. The thiophenol (PhSH) assay (normalized for DMSO).

Product	PhSH- Assay
ebsele n	1.5
2p	1.32
4p	1.81
8p	2.09
15p	1.95
16p	5.09
3u	4.73
2u	1.23
1u	1.14

3.2.5. Thiobarbituric acid radical scavenging assay (TBA assay)

Most of the compounds were not particularly active in this assay. Only the tellurium compounds **16p** and **3u** showed some activity, probably due to the higher reducing power of tellurides compared to selenides. In contrast, most of the other (selenium) compounds were not active (Figure 35).

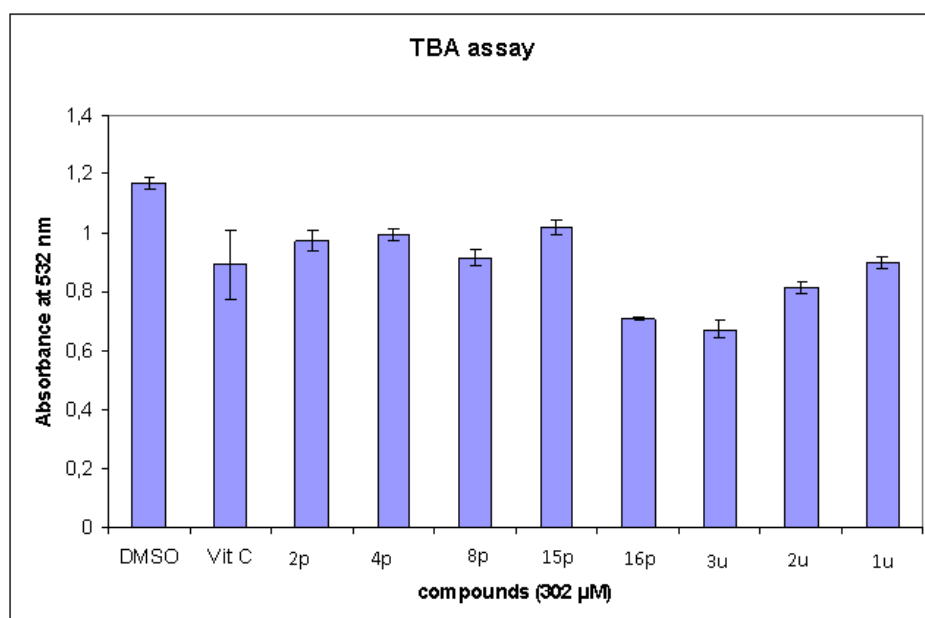


Figure 35. Thiobarbituric acid radical scavenging assay

3.2.6. Cell cycle analysis

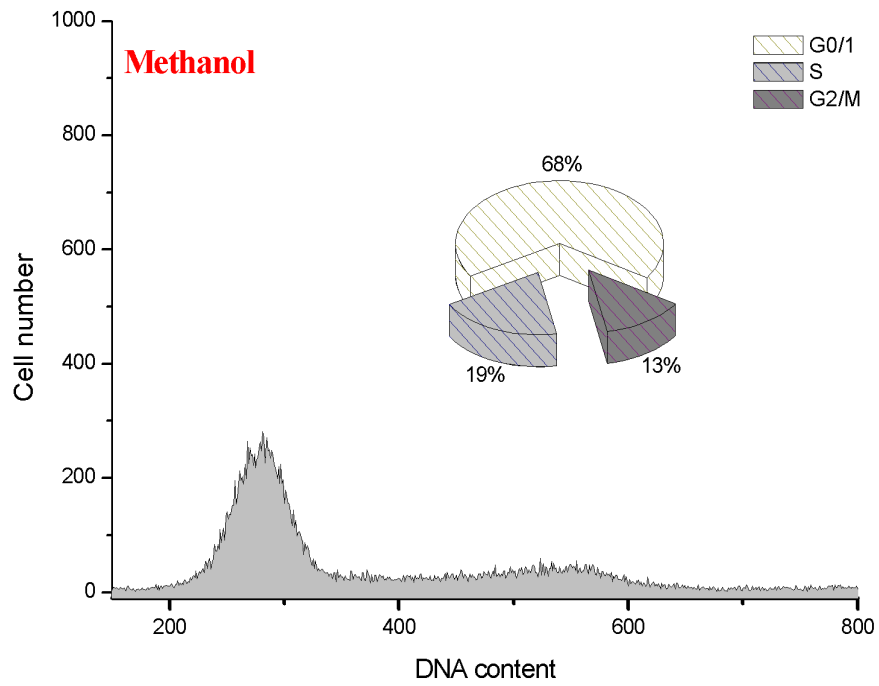
Flow cytometric analysis of MCF-7 cells treated with **7p**, **8p**, **12p**, **17p**, **9u**, and **3u** at their respective IC_{50} s for 24 h revealed a significant delay in cell cycle progression.

Figure 36 and Table 8 show a clear increase in the G_0/G_1 phase and reduction in G_2/M phase compared to vehicle control (See Appendix for more results).

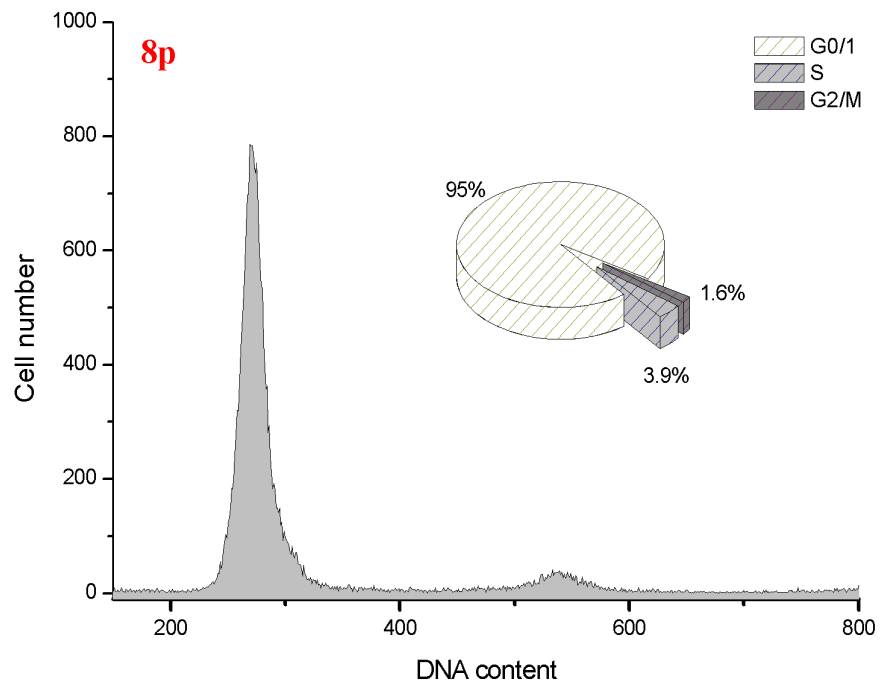
Table 8. The distribution percentage of cell cycle phases with different multifunctional compounds compared to vehicle treated methanol

	Cell cycle Phase		
	G_0/G_1	% S	G_2/M
Methanol (negative control)	68	19	1.6
7p	80	7.7	12
8p	95	3.9	1.6
12p	87	6.8	6
17p	92	6.2	8.8
3u	89	5.5	5.8
9u	85	6.2	8.8

a)



b)



c)

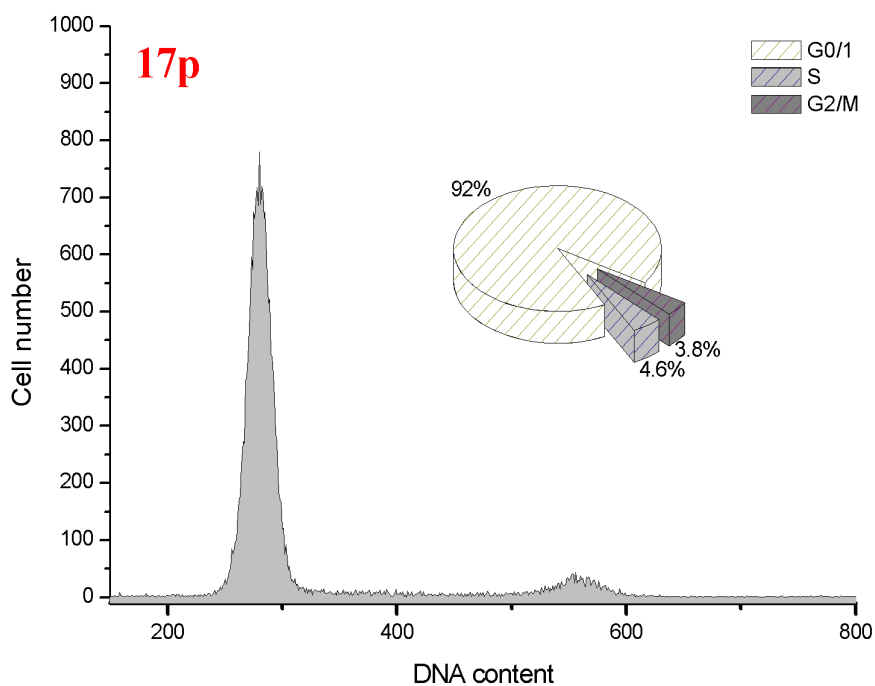


Figure 36. Cell cycle analysis of MCF-7 breast cancer cells.

MCF-7 cells were treated with methanol (vehicle control; panel a), or with **8p** (panel b), and **17p** (panel c) at their respective IC_{50} s for 24 h. The diagrams show the distribution of the cells according to their DNA content. The inserts give the percentages of cells in different cell cycle phases.

3.2.7. Caspase activity

The caspase-3/7 activity in A-431 cells was assessed in cells treated with **12p** for 24 hours employing the homogeneous, luminescent caspase-Glo 3/7 kit.

Figure 37 shows that caspase-3/7 activity increased significantly in a time dependent manner in case of the multifunctional compounds **12p** with three redox centres (one quinone and two selenium atoms).

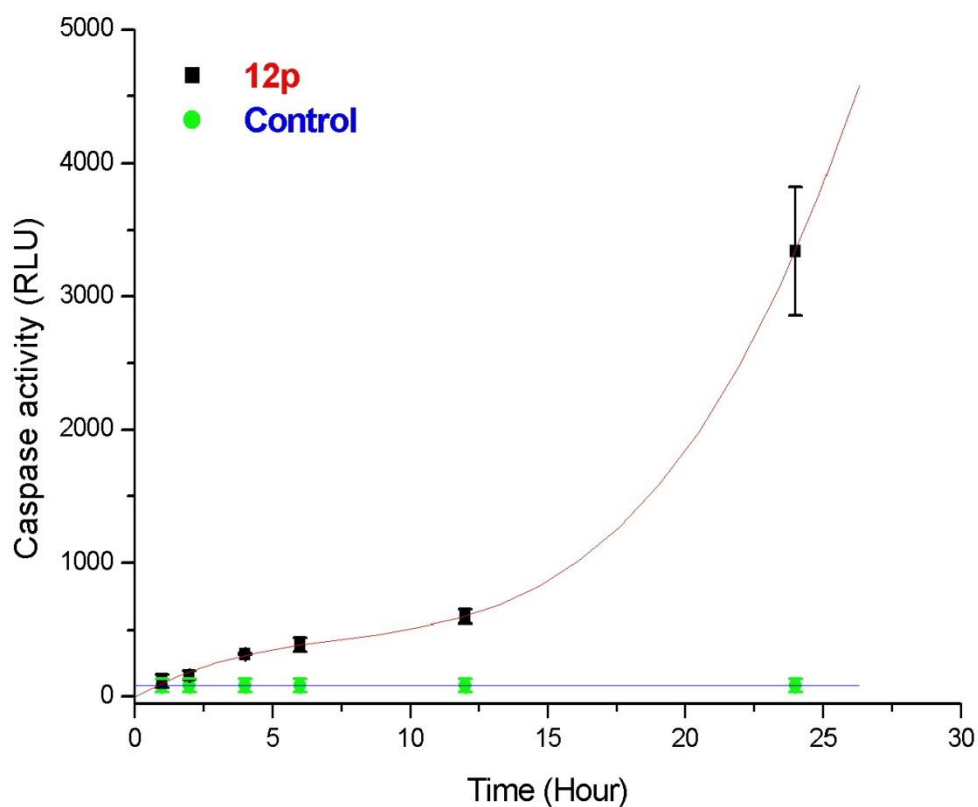


Figure 37. The activity of caspase-3 and -7 in A-431 melanoma cells.

A-431 cells were treated with compound **12p** was monitored employing a homogeneous, luminescent caspase-3/7 assay.

On the other hand, there was no significant change in caspase-3/7 activity after 24 hr treatment with compounds possessing one redox centre (sulfur, selenium or even tellurium).

3.2.8. Apoptosis

Flow cytometric analysis of FITC Annexin V labeled A-431 cells treated with different concentrations (0, 8, 11 and 13 μM) of **12p** for 12 h indicated a concentration dependent increase of apoptotic cells (Figure 38).

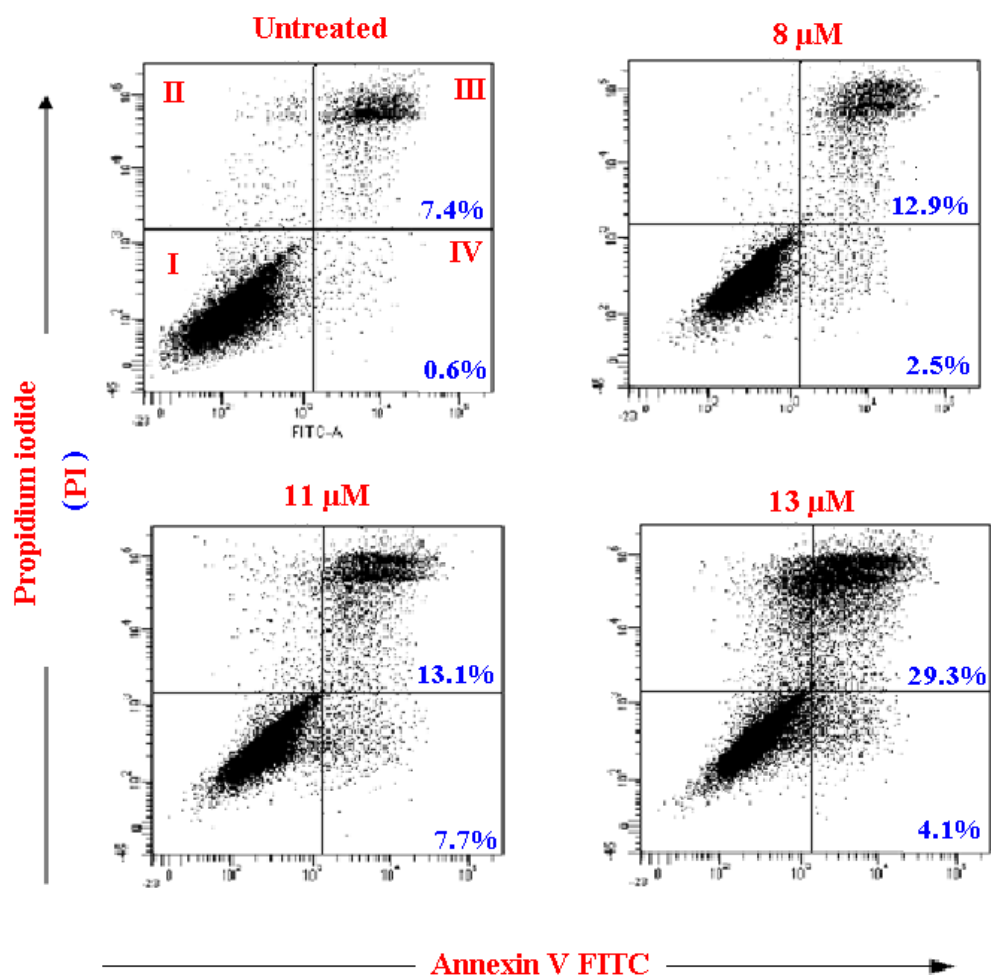


Figure 38. Flow cytometric analysis of apoptosis.

A-431 melanoma cells were treated with 0, 8, 11, and 13 μM of compound **12p** for 12 h, and stained with FITC Annexin V and propidium iodide. Quadrant I contains the percentage of viable cells (stained neither with PI nor with FITC Annexin V); quadrant III shows the percentage of late apoptotic cells (stained with both PI and FITC Annexin V), and quadrant IV the percentage of early apoptotic cells (stained with FITC Annexin V only).

3.2.9. Chemogenomic assay

The compounds activity against *S. cerevisiae* wild type and other mutant strains was determined using agar diffusion assays. Diameters [mm] of inhibition zones of agar diffusion assays are given in Table 9.

Table 9. Activity of the multifunctional compounds against *S. cerevisiae* wild type and mutant strains. Diameters [mm] of inhibition zones of agar diffusion assays are given.

	BY4741	YJR104	CYHR008	CYDR032	CYHL028	WYLL060	CYPL188	WYGL158	WYOL049	WYLL009	CYDL190C
Wild type	SOD1	SOD2	PST2	WSC4	GTT2	POS5	RCK1	GSH2	COX17	UFD2	
1p	0	10	0	12	11	0	0	0	0	10	10
2p	0	15	12	12	11	12	9	9	9	0	0
3p	0	18	13	12	12	0	0	0	0	0	0
5p	0	13	12	11	11	17	0	0	0	0	0
6p	0	16	15	11	16	12	10	10	10	11	0
7p	0	22	19	11	19	21	11	18	18	13	13
8p	0	21	18	11	20	20	11	14	14	14	0
9p	0	17	11	15	0	12	0	0	0	0	0
10p	0	20	25	11	14	18	0	0	0	0	0
11p	0	12	0	11	14	12	0	0	0	0	0
12p	0	14	19	16	26	25	17	15	15	15	15

Diameters (mm) of inhibition zones of an agar diffusion assay are given. In each case 6-mm disks with 20 µg of the test compounds were incubated.

3.2.10. Microbiological assays

The antifungal activity of was evaluated against *Saccharomyces cerevisiae*, *Candida albicans* and *Aspergillus niger*, and the antibacterial activity against *Mycobacterium phlei*, *Micrococcus luteus*, *Staphylococcus aureus*, *Klebsiella pneumonia*, *Pseudomonas aeruginosa* and *Escherichia coli tolC* using agar diffusion assays. Diameters [mm] of inhibition zones of agar diffusion assays are given in Table 10.

Table 10. Diameters [mm] of inhibition zones of agar diffusion assays against a variety of fungi and bacteria, the fungal growth was observed after 1 and 2 days.

	<i>S. cerevisiae</i>	<i>C. albicans</i>	<i>As. niger</i>	<i>M. phlei</i>	<i>M. Luteus</i>	<i>S. aureus</i>	<i>K. pneumonia</i>	<i>P. aeruginosa</i>	<i>E. coli</i> <i>tolC</i>
1p	0	0	0	0	0	0	0	0	0
3p	0	0	0	0	0	0	0	0	0
5p	0	0	0	0	0	0	0	0	9
6p	0	0	0	9	9	0	0	9	11
7p	0	0	18	19	18	0	0	15	16
8p	0	0	10	10	10	0	0	12	10
9p	0	0	0	9	9	0	0	13	11
10p	0	0	0	0	7	0	0	10	9
11p	0	0	0	0	0	0	0	10	9
12p	0	0	0	0	7	0	0	10	0
16p	0	0	19	16	11	13	13	12	11
1u	0	0	0	0	0	0	0	0	0
2u	0	0	0	0	7	0	0	0	0
3u	0	0	0	15	8	11	12	0	12
13p	0	0	0	0	0	0	0	0	0
14p	0	0	0	0	0	0	0	0	0
15p	0	0	0	0	0	0	0	0	0
15u	0	0	0	0	0	0	0	0	0

Table 10: continued.....

	<i>S. cerevisiae</i>	<i>C. albicans</i>	<i>As. niger</i>	<i>M. phlei</i>	<i>M. Luteus</i>	<i>S. aureus</i>	<i>K. pneumonia</i>	<i>P. aeruginosa</i>	<i>E. coli</i> <i>tolC</i>
4u	0	0	0	0	0	0	0	0	0
5u	0	0	0	0	0	0	0	0	0
6u	0	0	0	12	7	10	12	10	12
7u	0	0	0	0	0	0	0	0	0
8u	0	0	18	0	0	0	0	0	0
9u	0	0	10	17	13	12	12	9	11
10u	0	0	0	15	0	0	0	0	0
11u	0	0	0	0	0	0	0	0	0
12u	0	0	0	12	8	11	13	9	11
13u	0	0	0	0	0	0	0	0	0
14u	0	0	19	0	0	0	0	0	0
17p	0	0	0	14	7	16	15	0	12
18p	0	0	0	0	7	0	0	0	0
19p	0	0	0	15	9	0	0	0	0

Diameters (mm) of inhibition zones of an agar diffusion assay are given. In each case 6-mm disks with 20 µg of the test compounds were incubated.

3.2.11. The partition coefficient ($\log P_{ow}$) measurements

The experimental partition coefficient values ($\log P_{ow}$) of the compounds in the octanol-water system were measured by the high performance liquid chromatography (HPLC) technique (Table 11) to check the compliance with Lipinski's rule.

Table 11: Retention times, $\log K$ and $\log P_{ow}$ values for compounds and several reference standards.

Cpd.	Retention time 75% MeOH	$\log K$	$\log P_{ow}$	Cpd.	Retention time 75% MeOH	$\log K$	$\log P_{ow}$
Thiourea	0.728	-----	----	7u	1.407	-0.03	3.10
Acetanilide	0.811	-0.94	1	8u	1.412	-0.03	3.10
Benzene	0.941	-0.53	2.1	9u	0.890	-0.65	1.72
Toluene	1.508	0.03	2.7	10u	2.514	0.39	4.00
Thymol	1.285	-0.12	3.3	11u	2.088	0.27	3.70
Naphthalene	1.894	0.20	3.6	12u	0.834	-0.84	1.31
Phenanthrene	3.615	0.60	4.5	13u	1.698	0.12	3.40
1u	2.940	0.48	4.20	14u	1.134	-0.25	2.60
2u	3.297	0.55	4.23	16p	0,928	-0.56	1.92
3u	0.938	-0.54	1.97	17p	2.247	0.32	3.83
4u	2.170	0.3	3.80	18p	1.356	-0.06	3.01
5u	1.434	-0.01	3.12	19p	0.794	-1.04	0.90
6u	1.548	0.05	3.30				

In essence, these values point towards a lipophilicity which is in compliance with Lipinski's rule requiring a $\log P_{ow}$ value of below 5 (and above -0.4).

Chapter IV: Discussion

As introduced before, the aim of this study was to serve three major, interdependent, purposes; namely the synthesis of multifunctional catalytic agents potentially able to recognize the biochemical signature of OS in cancer cells, the subsequent evaluation of this potential in both primary and malignant cells, and the characterisation of the underlying mode of action(s) by which these agents exert their activity.

4.1. Selection and Synthesis of Suitable Redox Agents

The synthesis of multifunctional redox agents encounters many challenges by moving from just one or two to three or even more redox centres- in particular if a rather complicated selenium and/or tellurium chemistry is involved.⁴³ Many synthetic avenues have been described for the synthesis of multifunctional redox agents. Such avenues, however, have often been marred by low yields, decomposition of the products, and difficulties to generate compounds in sufficient quantities and purities.^{36, 39}

Although the most basic ‘nucleophilic substitution’ approach appears to be a simple one-step procedure (Figure 10), it is ultimately limited in scope, mainly, by the low yield. Indeed, the attraction of one-step synthesis is lost once rather complex starting materials have to be synthesized first.

Furthermore, the aminoalkylation method, which works rather well in case of sulfur and selenium compounds (Figure 11), seems to be unsuccessful in case of the corresponding tellurium analogues. Even more, the yields obtained are usually only up to 35%, which is still considered low, in principle.

The amide coupling approach is capable of overcoming the previous difficulties. It allows the successful synthesis of *various* selenium and tellurium compounds (Figure 12) in rather good yield (50-60 %). Higher functionalized or more diverse compounds, however, may become difficult. This is due to the fact that generally just two building blocks are assembled *via* amide coupling, and additional groups would have to be introduced *via* more complex building blocks. Ultimately, the issue of generating highly functionalized molecules would simply shift from the synthesis of the final product to the synthesis of the individual building blocks. All these obstacles in addition to the strong demand for multifunctional redox agents

compelled me to look for and develop new synthetic avenues that are able to overcome the previous mentioned drawbacks and to generate a wide range of tailor-made multi-functional agents.

In 2005, Fry *et al.*³⁶ have shown that compounds integrating two redox sites, *i.e.* a redox active quinone and a chalcogen moiety, are able to discriminate between oxidatively stressed and unstressed cells in culture. The potential selective anticancer activities of such agents were also established to occur at submicromolar and low micromolar concentrations. At that time, the ability of such catalysts to effectively and selectively kill cells under OS was only demonstrated for rat PC12, human Jurkat and human Daudi cells.^{39, 41} Moreover, the precise redox behaviour and mode of action of these compounds were not fully explored.

From the perspective of synthetic chemistry, the synthesis of such compounds provides interesting challenges since they were prepared in quite low yield, for instance, in case of compound **3n**, yields of just 9% have been obtained, emphasising the urgent need to develop more efficient methods for the preparation.

The synthesis of 2-methyl-3-(phenyltellanyl)naphthalene-1,4-dione (**3n**) has already been described in literature with dramatic variation in the yield.³⁶ Sodium borohydride (NaBH_4) was used for the reduction of the corresponding ditelluride employing ethanol as the solvent.

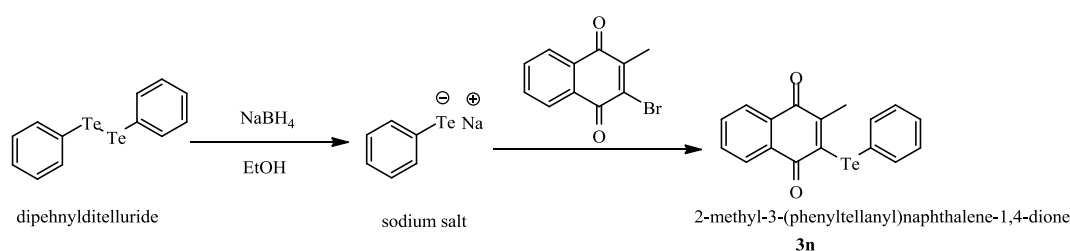


Figure 39. Reaction mechanism for the synthesis of quinone-chalcogen compounds by nucleophilic substitution.

In order to increase the yield, other procedures (metal-catalyzed), quoted from literature, have been explored including; samarium (II) iodide (SmI_2), indium (I) iodide (InI), triphenylphosphine (C_6H_5)₃P, and tributylphosphine [$\text{CH}_3(\text{CH}_2)_3$]₃P based reactions.^{45, 87-89}

Unfortunately, such strategies turn out to be low yielding or ineffective with our starting materials.

This impelled us to reconsider the reaction employing NaBH_4 as it is a cheap and shelf chemical reagent. During the initial studies we observed that: The ethanolic, colourless, solution of ditelluride/ NaBH_4 turns to a deep violet colour upon adding the bromoquinone. This colour disappears immediately. We thought that the violet colour is due to the product formation *i.e.* violet crystals, and the disappearance is due to the reduction by excess NaBH_4 , which is always used in excess (2-5 equivalents). The excess NaBH_4 was then reduced either by decreasing the amount of NaBH_4 to 1 equivalent, or by adding acetaldehyde to the reaction mixture. As the preliminary trials showed little improvement in the yield, we looked for other possible strategies. Back *et al.* reported a method for the preparation of sodium diselenide (Na_2Se_2) in 'water' from selenium and NaBH_4 .⁹⁰

This directed us to think of using mixed organic-aqueous solvent systems, since some of the starting materials are not soluble in water or organic solvents.

Theoretically, a two phase system and phase transfer catalyst (PTC) would be appropriate for this type of reaction. The sodium salt (resulting from the reduction of the ditelluride by NaBH_4) would be soluble in water, and the bromoquinone would be soluble in organic solvent (*e.g.* ethyl acetate). The role of the PTC is to facilitate the migration of the salt from the aqueous phase into the ethyl acetate phase, where the reaction ultimately takes place. Owing to the fact that the reactant in this case is anionic, the quaternary ammonium salt 'tricaprylmethylammonium chloride' was used as the PTC.

This coupling method enabled the synthesis of a range of mono- and di-substituted quinones in a simple one-step synthetic method. Good yields, for instance, in the case of compound **3n** yields of 79%, have been obtained with the two-phase-system, compared to a yield of just 9% for **3n** by the original method. Nonetheless, this method is ultimately limited by the number of achievable compounds, chemical diversity, and the availability of suitable quinones and chalcogen-derivatives. It is also questionable if higher substitutions, such as three- or four-substituted quinones, may be accessible by this method or stable in aqueous media, especially in the case of tellurium.^{43, 91}

A bolder approach has therefore been investigated. The use of a simple Passerini three component reaction has elegantly cleared the way for tri- and even tetra-functional redox agents containing multiple chalcogen and quinone redox sites. Apart from being able to deliver the complicated multifunctional redox catalysts, the Passerini reaction employed here is characterized by the utilization of the same building blocks which were used previously as part of the less sophisticated synthetic avenues (namely aminoalkylation and amide coupling).

Initial experiments showed that the classical volatile organic solvents usually used for the Passerini reaction, such as CH_2Cl_2 and CHCl_3 , were associated with several disadvantages such as long reaction times, low yields, undesired side reactions and the formation of by-products (monitored by TLC). A significant enhancement of reaction rate and yields has been achieved upon using water as solvent instead of the classical organic solvents. This acceleration could be attributed to many factors, including the hydrophobic effect and enhanced hydrogen bonding in the transition state. As described above, not only does the use of water as solvent permit the reaction to be conducted rapidly, the products are often insoluble, facilitating their ready isolation as precipitates.

Since the last 10 to 15 years have seen an increased interest in both, quinone and chalcogen chemistry, a wide range of building blocks for the Passerini reaction are now available and can be synthesized with comparable ease following well-established literature methods (see Materials and Methods section).[†] The bifunctionalized quinone-selenium bearing an aldehyde (**8n**) and the quinone-sulfur bearing an acid (**2b**) are of particular importance since they were used for the construction of three- and four-functional molecules. Other building blocks were chosen to incorporate the amino acid residues of glycine, L-serine, and cysteine to the product backbone for biological and pharmacological purposes (**2c-2e**). In case of the isocyanide building blocks, **3b** was used in addition to the commercially available, frequently used, but expensive *tert*-butyl isocyanide (**3a**). In most cases **3b** offers superior reactivity compared to the **3a**.

[†] A range of such compounds have now been reported by us in the literature.^{43, 91}

Furthermore, **3b** adducts could be used for further derivatization. According to the design criteria ‘mix and match’ compounds were synthesized in order to combine diverse redox centres. For example, if one building block were to carry just one function, three- to four-functional molecules may become accessible.

The Passerini reaction described here has been employed to synthesize a total of 15 compounds (**1p-15p**), whose chemical structures are shown in Figure 23. These compounds contain different number of redox centres: A) compounds possess two redox centres of which one is quinone and the other is selenium (**7p, 9p, 10p**); B) compounds with three redox centres, either with one quinone, one selenium and one sulfur (**1p, 2p, 3p, 5p**); with one quinone and two selenium (**12p**); or with one quinone, one selenium and one disulfide (**8p, 11p**); and even C) compounds containing four redox centres with two quinones, one selenium, and one sulfur as the redox centres (**4p, 6p**).^{43, 91}

Furthermore, SOD mimics (containing a porphyrin metal binding centre) with/without chalcogen and quinone redox sites were also synthesized. These compounds contain: A) only a metal binding porphyrin centre (**13p**); B) a metal binding porphyrin centre and a selenium redox centre (**14p**); and C) a metal binding porphyrin centre, one quinone and selenium redox centre (**15p**).⁹¹

The Passerini chemistry described here is rather straightforward: It can be carried out under mild conditions in solvents such as water, and yields are high when compared to the other methods evaluated in this study. Furthermore, it could also be used to generate molecules bearing four redox sites in one molecule. Nevertheless, the Passerini reaction may not always be the method of choice. The reasons for this are associated with the fact that a Passerini reaction introduces a low degree of diversity, since three components are only available to mix and match. Finally, the Passerini reaction leads to an α -acyloxy amide, *i.e.* a compound containing an ester bond, which is not particularly stable and may be cleaved chemically or enzymatically. It is possible that such compounds are readily modified *in vivo*, either for the benefit of activation or, less desirable, in conjunction with a loss of activity.

A versatile version of multicomponent reaction was therefore employed for the next generation of multifunctional redox agents. The utilization of the Ugi reaction, in general, offers superior advantages over the Passerini reaction.

Owing to the fact that the Ugi reaction is an extension of the Passerini three-component reaction, both of them share almost the same building blocks. Furthermore, a four-component condensation (Ugi reaction) introduces a higher degree of diversity than a three-component one (Passerini reaction). Finally, the two amide bonds which link the components of the Ugi adduct are more stable and also suitable for the synthesis of peptidomimetics than the combination of one ester and one amide bond produced in the Passerini reaction.

While the Ugi reaction is an excellent tool for a library synthesis of this core structure, it also suffers from a lack of commercially available isocyanides. Unlike the other three readily available components, fewer than two dozen isocyanides can be purchased. One possible solution is the creation of a sub-library of isocyanides as input into the Ugi four component condensations (Ugi-4CC) library. The isocyanides are the most difficult building blocks to functionalise, since they are typically not simple to prepare, volatile, and have quite offensive odours. This smell has been described by Hofmann and Gautier as ‘highly specific, almost overpowering’, ‘horrible’, and ‘extremely distressing’. In order to turn this apparent limitation of the isocyanide building blocks into an advantage, we have devised chalcogen bearing isocyanides suitable for multicomponent chemistry, including the tellurium containing isocyanide. This is considered the first example where tellurium participates in both Passerini and Ugi IMCRs, according to the best of our knowledge.⁹¹

The most effective reported isocyanide preparation method is based on the dehydration of formamides with the dangerous reagent phosgene. While some alternative syntheses have been reported, they are not considered a general method of preparation. In our case, the dehydration of the formamide was carried out using the less dangerous phosphoryl chloride (POCl₃) within only 2 hours in a good yield (up to 82 %). The newly synthesized isocyanides allowed the synthesis of a total of 19 compounds (**1u-15u** and **16p-19p**).⁹¹

In general, this approach has two major benefits. Firstly, we are now able to generate selenium and tellurium containing molecules, which combine two, three or even four redox sites in one molecule at will. Secondly, the synthetically more accessible acid, aldehyde, and amine building blocks remain variable and can be used to contribute further functionalities to the multicomponent reaction products.

To conclude, the reaction conditions not only place the Passerini and Ugi reactions within the realm of ‘green’ chemistry, but also enable the use of a wide range of sensitive building blocks, which may decompose otherwise (*e.g.* at elevated temperatures) - ultimately allowing the employment of a range of redox active aldehydes, acids and isocyanides containing quinones, selenium and similar redox centres. The individual building blocks required can now be synthesized with comparable ease (including functionalized isocyanides) and one may ‘mix and match’ them according to individual design criteria. Multicomponent chemistry ultimately was used to generate molecules bearing one, two, three, or even four redox and/or metal binding sites in one molecule. Analytical data for these compounds ($^1\text{H-NMR}$, $^{13}\text{C-NMR}$, LC-MS) were in accordance with the calculated/predicted values.

4.2. Cytotoxic Activity of Redox Compounds in Cancer and Healthy Cells

Initial screens for antiproliferative activity against different cancer cell lines revealed two distinct groups, separating multifunctional agents into toxic and non-toxic compounds. On the one hand, compounds possessing only one redox centre (sulfur or selenium) **4u**, **5u**, **7u**, **8u**, **10u**, **11u**, **13u**, and **14u** were not able to reduce the cell survival of cancer cells. The same behaviour was also noticed in case of porphyrin containing compounds, **13p**, **14p**, **15p**, and **15u**, regardless if these compounds were combined with one additional redox centre (such as the selenium in the case of compound **14p**) or with two redox centres (for example compound **15p** which contains a selenium and quinone redox sites) besides the porphyrin moiety.[‡]

[‡] Since this group of compounds was not toxic against cancer cell lines, the compounds were considered of less importance to us, and will be less considered thereafter.

On the other hand, compounds with tellurium comprising one redox centre, such as compounds **6u**, **9u**, **12u**, **17p**, **18p**, and **19p**, exhibited a significant toxic effect, compared to the sulfur and selenium analogues, against the same cancer cell lines. Indeed, compounds incorporating two, three, and four redox centres (with sulfur, selenium, and /or tellurium besides the quinone moiety) were also able to inhibit the proliferation of different cancer cell lines, as expected, in a moderate to high toxicity range. A closer look at the synthesized compounds revealed a certain correlation between chemical structure and toxic activity. Including, but not limited to: Tellurium compounds, in general, show higher toxic effects than the other synthesized agents (sulfur and selenium analogues). Moreover, compounds **4p** and **6p** with four redox centres were more cytotoxic than their homologues with three redox centres (**1p**, **2p**, **3p**, and **12p**) as was expected. Nevertheless, there were exceptions: Compounds **7p**, **9p**, and **10p** with just two redox centres were among the most toxic compounds, while compound **11p** with four redox centres showed only modest toxicity.

These observations were in excellent agreement with the one- and five-dose screens performed as a part of this study at the National Cancer Institute (Bethesda, MD, USA) for compounds **2p**, **4p**, **6p**, **7p**, **8p**, **9p**, **11p**, **12p**, **15p**, **16p**, **3u**, **6u**, and **9u**.[§] Their corresponding GI₅₀ (50% growth inhibition) values were in the low to sub-micromolar range (see Appendix for details).

[§] These compounds were selected by the National Cancer Institute according to their defined guidelines.

COMPARE analyses were performed using the correlation coefficient method. The compounds' pattern of activities correlates with cisplatin, which is used to treat various types of cancers, including sarcomas, lymphomas, and germ cell tumours. It also correlates with redox-activated methyl mitomycin C, which has an antitumour antibiotic activity against breast cancer, and last but not least, with anthracycline-based redox compounds such as menogaril, doxydoxorubicin, and MX₂ HCl, which are used in the treatment of prostate cancer and leukemia (see Appendix for details).

Interestingly, when incubated with primary human fibroblasts (HF) and human umbilical vascular endothelial cells (HUVEC), some of the test compounds showed low toxicity (Table 6). Compound **9p** clearly showed five to seven times lower cytotoxicity against primary cells than against the cancer cells. The same holds true for **10p** with the exception that it was also toxic to primary fibroblasts. Compound **6u** was five times more toxic to breast and epidermoid cancer cells (but not against the kidney cancer cells), than in case of the primary fibroblasts. In case of **16p**, a toxic effect was only noticed in case of kidney and epidermoid cancer cells and not against the breast cancer cells. The IC₅₀ value of **16p** in killing cancer cells were thirteen fold lower than the one measured for the primary fibroblasts.

Importantly, compounds **3p**, **18p**, and **19p** point to a different type of selectivity. These compounds were only toxic to breast cancer cells (and not toxic to kidney and epidermoid cancer cells). Even though one can only speculate about the compounds' mode(s) of action, the various redox sites in these molecules point towards a modulation of the intracellular redox state. Quinones are known to increase ROS production in cells, while chalcogen compounds may 'use' ROS to oxidize and hence impair redox-sensitive proteins and enzymes.

It is likely that a combination of a 'ROS generator' and a 'ROS user' will be effective in increasing levels and severity of OS in cells and, in the case of cancer cells, push them over the critical ROS threshold. In contrast, normal cells with comparably low intrinsic levels of OS may be less affected.

4.3. Induction of Oxidative Stress

Mounting evidence suggests that, compared to their normal counterparts, many types of cancer cells have increased levels of ROS.^{3, 31, 32} In turn, ROS are considered to be responsible for the maintenance of the cancer phenotype. The enhanced ROS generation is described in several *in vitro* and *in vivo* cancer models. For instance, cell lines from melanoma, colon, and pancreatic carcinoma, breast and ovarian cancer, and neuroblastoma produce more H₂O₂ than normal, non-transformed cells. Likewise, chronic lymphocytic leukemia cells obtained from patients show an increased ROS production when compared to normal lymphocytes. Furthermore, elevated oxidative modifications in DNA, proteins, and lipids have been detected in *various* primary cancer tissues including renal cell carcinoma, mammary invasive ductal carcinoma, and colorectal adenocarcinomas, further suggesting that cancer cells are inherently under OS.⁹²

The disparities in ROS generation in cancer versus normal cells may provide a biochemical basis for the development of new therapeutic strategies to selectively kill the malignant cells. Our studies have demonstrated that it may be possible to take advantage of this biochemical difference between cancer cells and normal cells to preferentially increase ROS to a toxic level in cancer cells, consequently leading to death of the malignant cells.

According to our results, multifunctional redox agents are able to enhance the ROS levels (in a concentration-dependent manner) in melanoma cells (Figure 30) assessed by DCF and DHE assays (see Materials and Methods for more details). This effect is likely to be the result of quinone redox cycling (Figure 9). Quinones are able to perform a redox cyclization process with triplet oxygen, to yield semiquinone and hydroquinone, which readily auto-oxidize back to the parent quinone, with concomitant production of O₂^{•-}, which could be detected by DHE and DCF assays. The O₂^{•-} formed is then rapidly metabolised by superoxide dismutase enzymes to dioxygen and H₂O₂, which is detected by the DCF assay.

The physiological impact of H₂O₂ is thereafter enhanced by the peroxidation catalysis process which takes place at the chalcogen redox sites. Chalcogens are able, for instance, to catalyze the oxidation of thiols such as GSH (Figure 8, panel B) as well as cysteine residues in proteins and enzymes.

Primary cells have a low basal level of ROS compared to cancer cells and can tolerate exogenous ROS stress to a certain degree owing to their antioxidative ‘reserve’ capacity,

which can be mobilized to prevent the ROS levels from reaching the cell-death threshold. In order to determine if any of the synthesized compounds may be useful for further biological investigations, the ROS levels in A-431 melanoma and HUVECs were monitored. The results obtained clearly show that:

- A) HUVECs have lower basal intracellular ROS levels compared to melanoma cells. This is considered a further support for our hypothesis.
- B) Multifunctional agents were able to significantly increase ROS levels in melanoma cells to higher level compared to HUVECs. This may be due to the fact that primary cells have full antioxidant capacity that renders them less vulnerable to the kind of ROS stress that is induced by multifunctional redox agents.

Although it is too early to speculate about possible uses of such catalytic, multifunctional redox agents in therapy, their rather high activity and selective toxicity against selected cancer cells encourages further *in vivo* investigations of such agents as potential anticancer drugs. Furthermore, it had previously been reported that the ROS-mediated cytotoxicity induced by *various* drugs also caused a depletion of endogenous levels of GSH.^{12, 13} To determine whether a similar phenomenon occurred in cells treated with the multifunctional agents used as part of this study, levels of reduced glutathione were estimated in these cells by the DTNB assay. The intracellular GSH is the most important biomolecule in protecting cells against chemically induced cytotoxicity. It acts by removal of free radicals by direct quenching, by hydroperoxide reduction or by elimination of reactive intermediates *via* conjugation.

Upregulation of glutathione levels is an important factor in the protection against apoptosis and it is associated with resistance development in cancer therapy. Consequently, low glutathione levels are sometimes linked to mitochondrial dysfunction and induction of apoptosis, thus decreasing the chemoresistance of cancer cells. Figure 34 points towards a rapid decline in levels of endogenous, cellular GSH upon treatment of MCF-7 cells with different doses of redox agents, confirming the induction of OS. These results were consistent with a recent report, in which the anticancer-based redox drugs anthracycline, juglone, plumbagin, and menadione were shown to cause OS in various malignant cells *via* depletion of GSH.¹²

In order to rule out any major antioxidant activity (which may be counter-productive), the thiobarbituric acid (TBA) assay has also been performed (see Results for more details). This assay measures the ability of compounds to sequester oxygen-based radicals. Most of the compounds studied here were not particularly active in this assay (Figure 35).

Only the tellurium compounds **3u** and **16p** showed some activity, probably due to the higher reducing power of tellurides compared to selenides. These results confirm that tellurides (and some) selenides can scavenge oxygen-based radicals - likely by forming telluroxides and selenoxides, respectively. Interestingly, HRMS also gave signals for telluroxides, but not for selenoxides, pointing towards ready oxidation of the tellurium compounds to telluroxides.

The comparably straightforward synthesis of such multifunctional agents does not, of course, address the question whether such rather complex agents are at all useful in cancer therapy. We have therefore performed the thiophenol assay, which measures catalytic activity of compounds in the presence of thiols and H₂O₂. This assay has been used as a predictor of activity in cell culture. The results shown in Table 7 confirm that the multifunctional compounds were able to enhance the oxidation of thiols in the presence of H₂O₂. Several compounds are even considerably more active than the benchmark compound ebselen (1.5-fold increase vs. DMSO), with tellurium compounds **3u** and **16p** being the most active ones. These findings are in excellent agreement with previous studies emphasizing the activity of tellurium agents in this assay. In cell culture, this apparent ‘antioxidant’ reactivity is dominated by the catalytic activity demonstrated by the PhSH assay.

4.4. Cell Cycle Delay

Upadhyay *et al.*²⁵ recently reported that a sublethal dose of H₂O₂ prevents progression of cell cycle by causing delay in the G₀/G₁ phase. We observed that multifunctional redox agents **7p**, **8p**, **12p**, and **3u** manifested the same behaviour (Figure 36). For example, cell cycle analysis of MCF-7 cells treated with **8p** for 24h revealed 95 % cells were in G₀/G₁, with 3.9 % in S, and 1.6 % in G₂/M, compared to methanol treated cells with 68 % in G₀/G₁, 19 % in S, and 13 % in G₂/M phase (see Appendix for more details).

Interestingly, the same results were also obtained with the tellurium compounds **9u** and **17p**. These compounds were able to induce cell cycle delay in G0/G1 phase (85 % and 92 %, respectively). These results were consistent with a recent report from the patent literature, showing that the tellurium immunomodulating compound ammoniumtrichloro[1,2-ethanediolato-*O,O'*]-tellurate (AS101) is able to cause G0/G1 cell cycle delay.⁹³

4.5. Phenotypical changes in Cellular Morphology and Cytoskeleton

As shown in the results section, alterations of cell morphology and the microfilament network were also observed, upon treatment with the redox compounds together with the perturbation of the ER. The cause was obviously OS. Previous reports have shown that such OS can cause damage to all types of biological molecules, including DNA, proteins, and lipids. The primary cellular target of OS can vary depending on the cell type, the nature of stress imposed (e.g., radical *vs.* non-radical oxidants), its site of generation (e.g., intra- *vs.* extracellular), the proximity of the oxidant to a specific cellular substrate, and how severe the stress is.⁹⁴

Cytoskeletal proteins are particularly abundant within the cell and several protein constituents of the cytoskeleton display highly reactive residues that can be oxidized easily. Owing to this reason, the cytoskeleton may represent one of the preferential targets of ROS whatever kind of OS is applied.

4.6. Induction of apoptosis

Overwhelming evidence shows that the production of ROS is an early event that initiates mitochondria-mediated apoptotic pathways by triggering mitochondrial permeability transition pore opening, release of proapoptotic factors and activation of the caspase cascade.⁹⁵ On the other hand, the role of ER stress in ROS-induced apoptosis has seldom been reported in cancer cells. A recent report from Seung-Ki Min *et al.*⁹⁴ suggests that ER stress-mediated apoptosis occurs in human immortalized and malignant oral keratinocytes treated with H₂O₂. In general, most apoptosis pathways depend on the activation of caspases, in particular effector caspase 3 and 7, for the final execution of apoptosis. Therefore, it might be reasonable to first investigate these two caspases as a sign of apoptosis.

Our findings confirm the activation of caspase-3 / 7 in a time dependent manner after A-431 cells were treated with compound **12p** for 24h. This result is considered to be a first proof that these compounds act as inducers of apoptosis.

The apoptosis induction was further investigated by flow cytometry after staining the cells with Annexin V and PI. Externalization of phosphatidylserine (PS) from the inner leaflet to the outer one of the plasma membrane is a hallmark of early apoptosis.

FITC labelled Annexin V binds to PS in the presence of calcium ions, resulting in green fluorescence of apoptotic cells. In later stages of apoptosis, PI enters the cells and binds to cellular DNA, resulting in red fluorescence. As shown in the Figure 38, treatment of A-431 cells with **12p** for 12 h resulted in an increase in FITC Annexin V (+) (lower right quadrant) and PI (+) (upper right quadrant) fluorescence also indicating that apoptosis is induced. The appearance of late apoptotic cells was predominantly (12.9- 29.3 %) seen at the higher concentrations (13 μ M) of **12p**. These results were similar to the findings of Kalyanaraman *et al.*⁹⁵ where adriamycin (an anthracycline drug used in cancer chemotherapy) induced cell death by induction of apoptosis.

4.7. Chemical Genetic Interaction Approach

Chemogenomic assays using a mutant library of *S. cerevisiae* have proven to be a powerful means to study and predict the mode of action of bioactive compounds. These assays rely on comparing the growth of each gene deletion strain to the wild type strain in the absence and presence of test compounds.

The growth inhibition of deletion strains upon exposure to compounds is resulting in a chemical-genetic interaction profile. Analyzing such profiles provides information about the targets and pathways that are affected by compounds. Such information cannot be obtained easily by conventional methods⁹⁶. We have applied a five-step strategy to possibly link the multifunctional compounds used in this study to their target pathways:

- i. We screened all the multifunctional compounds using an agar diffusion assay against *S. cerevisiae* wild type (BY4741) and four mutants (YJR104C, YHR008C, YHR106W and YLR011W), which were chosen based on a literature survey because the genes knocked out might be important to counterbalance OS.

ii. The IC₅₀ values of compounds **7p** and **12p** (the most active compounds) were determined using a serial-dilution assay against the sensitive mutants YJR104C and YHR008C.

iii. Compounds **7p** and **12p** were then screened against a set of ~ 4,800 viable *S. cerevisiae* deletion strains using the IC₅₀ concentration found in step (ii).

iv. We identified a set of mutants which were sensitive in two chemical-genetic interaction screening procedures (step iii).

v. The results from the chemical-genetic interaction profiling were evaluated and confirmed using an agar diffusion assay in a second round of analysis.

At the concentrations applied the compounds under investigation had no effect on the wild type strain, BY4741, but striking effects were observed with 10 mutants (Table 3). Superoxide dismutase (mitochondrial and cytosolic copper-zinc SOD), glutathione synthetase (GSH2) and transferase (GTT2), and cytochrome *c* oxidase (COX17) deficient strains were among the mutants most sensitive to the test compounds.

These enzymes play a major role in the antioxidant defence system and are pivotal for the removal of toxic oxidants. Deletion of the respective genes therefore might cause an OS sensitive phenotype of the mutant. These observations are in excellent agreement with the other cell-based assays performed as a part of this study, all of which unambiguously point towards a link between the redox compounds and a redox modulated cellular mode of action.

4.8. Antimicrobial Activity

The antimicrobial activity of the synthesized compounds was evaluated against three fungal strains namely *Saccharomyces cerevisiae*, *Candida albicans* and *Aspergillus niger* and six bacterial strains including *Mycobacterium phlei*, *Micrococcus luteus*, *Staphylococcus aureus*, *Klebsiella pneumonia*, *Pseudomonas aeruginosa* and *Escherichia coli* tol C using agar diffusion assays (Table 10).

In general, almost all the compounds were nontoxic against *S. cerevisiae*, *C. albicans* and *A. niger*. Interestingly, compounds **7p** and **16p** showed a striking toxic effect against *A. niger* (the inhibition zone diameter was 18 and 19 mm, respectively).

On the other hand, most of the compounds show low to moderate toxicity against *Mycobacterium phlei* and *Micrococcus luteus*. Tellurium compounds were rather toxic to *Staphylococcus aureus* and *Klebsiella pneumonia*, while the quinone-containing compounds were not. The reverse effect was noticed in case of *Pseudomonas aeruginosa* and *Escherichia coli* *tol C*. Finally, compounds with one redox centre (sulfur and selenium) were not toxic at all to the tested organisms.

4.9. QSAR studies

Computer simulation techniques potentially offer further means to probe inhibition mechanisms. The quantitative structure–activity relationships (QSAR) represent one of the most effective computational approaches in drug design. While QSAR is largely used to predict activities and to define pharmacophore models, it was not useful or reliable in our case due to the small number of compounds available and the potential diversity of cellular targets involved (see Appendix for details)

Concluding Remarks and Future Perspectives

This study has developed a promising synthetic avenue able to generate, with comparable ease, a wide range of tailor-made multi-functional catalysts designed to target cancer cells under OS. The use of a simple, straight forward, yet effective multi-component reactions have elegantly cleared the way for the synthesis of tri- and tetra-functional redox agents containing multiple chalcogen, porphyrin metal binding and quinone redox sites. In addition, the implementation of all combinations of P-3CR and U-4CR even with rather flexible building blocks supports the great potential of this concept towards the diversity-oriented synthesis of multifunctional agents.

In cancer cells, such agents inhibit proliferation and induce cell death *via* multifactorial mechanisms such as induction of OS, cell cycle delay, and apoptosis. Although one can only speculate about the exact mode(s) of biochemical action of these compounds, the presence of several redox sites in these molecules points towards a modulation of the intracellular redox state in these cells. Quinones are known to increase ROS production in cells, while chalcogen compounds may ‘use’ ROS to oxidize and hence impair or inhibit proteins and enzymes. It is therefore likely that a combination of a ‘ROS generator’ and a ‘ROS user’ will be effective in increasing levels and severity of OS in cells and, in the case of cancer cells, push them over the critical ROS threshold. In contrast, normal cells with comparably low intrinsic levels of OS may be less affected. Interestingly, some of the compounds studied here showed no apparent reduction in cell survival when incubated with normal healthy cells, and it is possible that such compounds may have a selective anticancer activity.

As far as synthetic chemistry is concerned, future studies may refine and expand the method proposed here, building upon more -and more diverse- building blocks, most of which will be easily accessible. At the same time, there is a need for more chemically diverse catalytic compounds. Here, the development of such multifunctional catalysts is not just dictated by an interest in anticancer drugs. It also poses a real challenge to synthetic organic chemistry, which needs to employ a sophisticated arsenal of modern synthesis to deal with the relevant quinone and chalcogen chemistry. The synthesis of organoselenium and organotellurium compounds has never been an easy task, and this area of research provides ample opportunities for further development and expansion.

This opens the door to a range of follow-up studies in the area of synthetic chemistry, redox chemistry, biochemistry and, ultimately, drug development.

Preliminary cell based studies point towards a reasonably selective activity of some of these compounds, which needs to be investigated further by using a considerably wider arsenal of cells. Furthermore, in order to establish the complete picture of redox catalysts as possible therapeutics, this line of investigation will then need to move on to studies in animal models.

In any case, there is plenty of scope for further, multi-disciplinary studies involving chemistry, biochemistry, cell biology, and pharmacology in order to develop a strategy to treat cancer by applying redox active compounds.

References

1. Fischer, O. M.; Streit, S.; Hart, S.; Ullrich, A. Beyond Herceptin and Gleevec. *Curr. Opin. Chem. Biol.* **2003**, *7*, 490-495.
2. Stegmeier, F.; Warmuth, M.; Sellers, W. R.; Dorsch, M. Targeted cancer therapies in the twenty-first century: Lessons from imatinib. *Clin. Pharmacol. Ther.* **2010**, *87*, 543-552.
3. Trachootham, D.; Alexandre, J.; Huang, P. Targeting cancer cells by ROS-mediated mechanisms: a radical therapeutic approach? *Nat. Rev. Drug Discov.* **2009**, *8*, 579-591.
4. Fry, F. H.; Jacob, C. Sensor/effector drug design with potential relevance to cancer. *Curr. Pharm. Des.* **2006**, *12*, 4479-4499.
5. Sundaresan, M.; Yu, Z.; Ferrans, V. J.; Sulciner, D. J.; Gutkind, J. S.; Irani, K.; Goldschmidt-Clermont, P. J.; Finkel, T. Regulation of reactive-oxygen-species generation in fibroblasts by Rac1. *Biochem. J.* **1996**, *318*, 379-382.
6. Brown, N. S.; Bicknell, R. Oxidative stress: Its effects on the growth, metastatic potential and response to therapy of breast cancer. *Breast Canc. Res.* **2001**, *3*, 323-327.
7. Perry, G.; Raina, A. K.; Nunomura, A.; Wataya, T.; Sayre, L. M.; Smith, M. A. How important is oxidative damage? Lessons from Alzheimer's disease. *Free Radic. Biol. Med.* **2000**, *28*, 831-834.
8. Toyokuni, S.; Okamoto, K.; Yodoi, J.; Hiai, H. Persistent oxidative stress in cancer. *FEBS Lett.* **1995**, *358*, 1-3.
9. Jones, D. P.; Go, Y. -. Redox compartmentalization and cellular stress. *Diabetes, Obesity and Metabolism.* **2010**, *12*, 116-125.
10. Dikalov, S.; Griendling, K. K.; Harrison, D. G. Measurement of reactive oxygen species in cardiovascular studies. *Hypertension.* **2007**, *49*, 717-727.
11. Karlsson, M.; Kurz, T.; Brunk, U. T.; Nilsson, S. E.; Frennesson, C. I. What does the commonly used DCF test for oxidative stress really show? *Biochem. J.* **2010**, *428*, 183-190.
12. Wang, C. C.; Chiang, Y. M.; Sung, S. C.; Hsu, Y. L.; Chang, J. K.; Kuo, P. L. Plumbagin induces cell cycle arrest and apoptosis through reactive oxygen species/c-Jun N-terminal kinase pathways in human melanoma A375.S2 cells. *Canc. Lett.* **2008**, *259*, 82-98.

13. Kumar, M. R.; Aithal, K.; Rao, B. N.; Udupa, N.; Rao, B. S. Cytotoxic, genotoxic and oxidative stress induced by 1,4-naphthoquinone in B16F1 melanoma tumor cells. *Toxicol. In Vitro*. **2009**, *23*, 242-250.
14. Fruehauf, J. P.; Meyskens, F. L., Jr Reactive oxygen species: a breath of life or death? *Clin. Canc. Res.* **2007**, *13*, 789-794.
15. Dalle-Donne, I.; Rossi, R.; Milzani, A.; Di Simplicio, P.; Colombo, R. The actin cytoskeleton response to oxidants: from small heat shock protein phosphorylation to changes in the redox state of actin itself. *Free Radic. Biol.Med.* **2001**, *31*, 1624-1632.
16. Eşrefolu, M. Cell injury and death: Oxidative stress and antioxidant defense system: Review. *Turkiye Klinikleri Journal of Medical Sciences.* **2009**, *29*, 1660-1676.
17. Vigilanza, P.; Aquilano, K.; Rotilio, G.; Ciriolo, M. R. Transient cytoskeletal alterations after SOD1 depletion in neuroblastoma cells. *Cell. Molec. Life Sci.* **2008**, *65*, 991-1004.
18. Dalle-Donne, I.; Rossi, R.; Milzani, A.; Di Simplicio, P.; Colombo, R. The actin cytoskeleton response to oxidants: From small heat shock protein phosphorylation to changes in the redox state of actin itself. *Free Rad. Biol. Med.* **2001**, *31*, 1624-1632.
19. Guo, R.; Ma, H.; Gao, F.; Zhong, L.; Ren, J. Metallothionein alleviates oxidative stress-induced endoplasmic reticulum stress and myocardial dysfunction. *J. Mol. Cell. Cardiol.* **2009**, *47*, 228-237.
20. Xu, C.; Bailly-Maitre, B.; Reed, J. C. Endoplasmic reticulum stress: Cell life and death decisions. *J. Clin. Invest.* **2005**, *115*, 2656-2664.
21. Debbasch, C.; Pisella, P. -.; De Saint Jean, M.; Rat, P.; Warnet, J. -.; Baudouin, C. Mitochondrial activity and glutathione injury in apoptosis induced by unpreserved and preserved β -blockers on chang conjunctival cells. *Invest. Ophthalmol. Visual Sci.* **2001**, *42*, 2525-2533.
22. Baumgartner, H. K.; Gerasimenko, J. V.; Thorne, C.; Ashurst, L. H.; Barrow, S. L.; Chvanov, M. A.; Gillies, S.; Criddle, D. N.; Tepikin, A. V.; Petersen, O. H.; Sutton, R.; Watson, A. J. M.; Gerasimenko, O. V. Caspase-8-mediated apoptosis induced by oxidative stress is independent of the intrinsic pathway and dependent on cathepsins. *Am. J. Phys. Gast. Liver Phys.* **2007**, *293*, .
23. Ozben, T. Oxidative stress and apoptosis: Impact on cancer therapy. *J. Pharm. Sci.* **2007**, *96*, 2181-2196.

24. Melchheier, I.; Von Montfort, C.; Stuhlmann, D.; Sies, H.; Klotz, L. Quinone-induced Cdc25A inhibition causes ERK-dependent connexin phosphorylation. *Biochem. Biophys. Res. Commun.* **2005**, *327*, 1016-1023.
25. Upadhyay, D.; Chang, W.; Wei, K.; Gao, M.; Rosen, G. D. Fibroblast growth factor-10 prevents H₂O₂-induced cell cycle arrest by regulation of G1 cyclins and cyclin dependent kinases. *FEBS Lett.* **2007**, *581*, 248-252.
26. Bruckdorfer, K. R. Antioxidants and CVD. *Proc. Nutr. Soc.* **2008**, *67*, 214-222.
27. Wang, J.; Yi, J. Cancer cell killing via ROS: to increase or decrease, that is the question. *Cancer. Biol. Ther.* **2008**, *7*, 1875-1884.
28. Ferraro, D.; Corso, S.; Fasano, E.; Panieri, E.; Santangelo, R.; Borrello, S.; Giordano, S.; Pani, G.; Galeotti, T. Pro-metastatic signaling by c-Met through RAC-1 and reactive oxygen species (ROS). *Oncogene.* **2006**, *25*, 3689-3698.
29. Halliwell, B. The antioxidant paradox. *Lancet.* **2000**, *355*, 1179-1180.
30. Bjelakovic, G.; Nikolova, D.; Gluud, L. L.; Simonetti, R. G.; Gluud, C. Mortality in randomized trials of antioxidant supplements for primary and secondary prevention: Systematic review and meta-analysis. *J. Am. Med. Assoc.* **2007**, *297*, 842-857.
31. Jamier, V.; Ba, L. A.; Jacob, C. Selenium- and tellurium-containing multifunctional redox agents as biochemical redox modulators with selective cytotoxicity. *Chem. A Eur. J.* **2010**, *16*, 10920-10928.
32. Bair, J. S.; Palchadhuri, R.; Hergenrother, P. J. Chemistry and biology of deoxyxyboquinone, a potent inducer of cancer cell death. *J. Am. Chem. Soc.* **2010**, *132*, 5469-5478.
33. Leu, L.; Mohassel, L. Arsenic trioxide as first-line treatment for acute promyelocytic leukemia. *Am. J. Heal. Sys. Phar.* **2009**, *66*, 1913-1918.
34. Huang, P.; Feng, L.; Oldham, E. A.; Keating, M. J.; Plunkett, W. Superoxide dismutase as a target for the selective killing of cancer cells. *Nature.* **2000**, *407*, 390-395.
35. Hileman, E. O.; Liu, J.; Albitar, M.; Keating, M. J.; Huang, P. Intrinsic oxidative stress in cancer cells: A biochemical basis for therapeutic selectivity. *Canc. Chemother. Pharmacol.* **2004**, *53*, 209-219.

36. Fry, F. H.; Holme, A. L.; Giles, N. M.; Giles, G. I.; Collins, C.; Holt, K.; Pariagh, S.; Gelbrich, T.; Hursthouse, M. B.; Gutowski, N. J.; Jacob, C. Multifunctional redox catalysts as selective enhancers of oxidative stress. *Org. Biomol. Chem.* **2005**, *3*, 2579-2587.
37. Ohse, T.; Nagaoka, S.; Arakawa, Y.; Kawakami, H.; Nakamura, K. Cell death by reactive oxygen species generated from water-soluble cationic metalloporphyrins as superoxide dismutase mimics. *J. Inorg. Biochem.* **2001**, *85*, 201-208.
38. Fry, F. H.; Holme, A. L.; Giles, N. M.; Giles, G. I.; Collins, C.; Holt, K.; Pariagh, S.; Gelbrich, T.; Hursthouse, M. B.; Gutowski, N. J.; Jacob, C. Multifunctional redox catalysts as selective enhancers of oxidative stress. *Org. Biomol. Chem.* **2005**, *3*, 2579-2587.
39. Giles, N. M.; Gutowski, N. J.; Giles, G. I.; Jacob, C. Redox catalysts as sensitisers towards oxidative stress. *FEBS Lett.* **2003**, *535*, 179-182.
40. Giles, N. M.; Gutowski, N. J.; Giles, G. I.; Jacob, C.; Celis, J. Redox catalysts as sensitisers towards oxidative stress. *FEBS Lett.* **2003**, *535*, 179-182.
41. Fry, F. H.; Holme, A. L.; Giles, N. M.; Giles, G. I.; Collins, C.; Holt, K.; Pariagh, S.; Gelbrich, T.; Hursthouse, M. B.; Gutowski, N. J.; Jacob, C. Multifunctional redox catalysts as selective enhancers of oxidative stress. *Org. Biomol. Chem.* **2005**, *3*, 2579-2587.
42. Fernandez Villamil, S.; Stoppani, A. O.; Dubin, M. Redox cycling of beta-lapachone and structural analogues in microsomal and cytosol liver preparations. *Meth. Enzymol.* **2004**, *378*, 67-87.
43. Mecklenburg, S.; Shaaban, S.; Ba, L. A.; Burkholz, T.; Schneider, T.; Diesel, B.; Kiemer, A. K.; Roseler, A.; Becker, K.; Reichrath, J.; Stark, A.; Tilgen, W.; Abbas, M.; Wessjohann, L. A.; Sasse, F.; Jacob, C. Exploring synthetic avenues for the effective synthesis of selenium- and tellurium-containing multifunctional redox agents. *Org. Biomol. Chem.* **2009**, *7*, 4753-4762.
44. Fieser, L. F.; Brown, R. H. Synthesis of naphthoquinones for studies of the inhibition of enzyme systems. *J. Am. Chem. Soc.* **1949**, *71*, 3609-3614.
45. Sakakibara, M.; Watanabe, Y.; Toru, T.; Ueno, Y. New selenenylation method. Synthesis of selenonaphthoquinones and selenoquinolinequinones mediated by phenyl selenide ion. *J. Chem. Soc. Perk. Trans. 1.* **1991**, 1231-1234.
46. Salmon-Chemin, L.; Buisine, E.; Yardley, V.; Kohler, S.; Debreu, M. -.; Landry, V.; Sergheraert, C.; Croft, S. L.; Krauth-Siegel, R. L.; Davioud-Charvet, E. 2- and 3-substituted

- 1,4-naphthoquinone derivatives as subversive substrates of trypanothione reductase and lipoamide dehydrogenase from *Trypanosoma cruzi*: Synthesis and correlation between redox cycling activities and in vitro cytotoxicity. *J. Med. Chem.* **2001**, *44*, 548-565.
47. Bittner, S.; Gorohovsky, S.; Paz-Tal Levi, O.; Becker, J. Y. Synthesis, electrochemical and spectral properties of some ω -N-quinonyl amino acids. *Amino Acids.* **2002**, *22*, 71-93.
48. Baldwin, J. E.; Adlington, R. M.; Robertson, J. Carbocyclic ring expansion reaction VIA radical chain processes. *Tetrahedron* **1989**, *45*, 909-922.
49. Andersen, J. M.; Kochi, J. K. Silver(I)-catalyzed oxidative decarboxylation of acids by peroxydisulfate. The role of silver (II). *J. Am. Chem. Soc.* **1970**, *92*, 1651-1659.
50. Simon, C.; Constantieux, T.; Rodriguez, J. Utilisation of 1,3-dicarbonyl derivatives in multicomponent reactions. *Eur. J. Org. Chem.* **2004**, 4957-4980.
51. Kappe, C. O. Recent advances in the Biginelli dihydropyrimidine synthesis. New tricks from an old dog. *Acc. Chem. Res.* **2000**, *33*, 879-888.
52. Biggs-Houck, J. E.; Younai, A.; Shaw, J. T. Recent advances in multicomponent reactions for diversity-oriented synthesis. *Curr. Opin. Chem. Biol.* **2010**, *14*, 371-382.
53. Sani, M.; Fossati, G.; Huguenot, F.; Zanda, M. Total synthesis of tubulysins U and V. *Ang. Chem. Int.l Ed.* **2007**, *46*, 3526-3529.
54. Ugi, I.; Dömling, A.; Hörl, W. Multicomponent reactions in organic chemistry. *Endeavour* **1994**, *18*, 115-122.
55. Domling, A.; Ugi, I. I. Multicomponent Reactions with Isocyanides. *Angew. Chem. Int. Ed Engl.* **2000**, *39*, 3168-3210.
56. Domling, A. Recent developments in isocyanide based multicomponent reactions in applied chemistry. *Chem. Rev.* **2006**, *106*, 17-89.
57. Lieke, W. Ueber das Cyanallyl. *Jus. Lieb. Ann. Chem.* **1859**, *112*, 316-321.
58. Gautier, A. Ueber die Einwirkung des Chlorwasserstoffs u. a. auf das Aethyl- und Methylcyanür. *Jus. Lieb. Ann. Chem.* **1867**, *142*, 289-294.
59. Hofmann, A. W. Ueber eine neue Reihe von Homologen der Cyanwasserstoffsäure. *Jus. Lieb. Ann. Chem.* **1867**, *144*, 114-120.
60. Banfi, L.; Riva, R. The Passerini Reaction. *Org. React.* **2004**, *65*: 1-140.
61. Ugi, I.; Lohberger, S.; Karl, R. The Passerini and Ugi Reactions. *In Comprehensive Organic Synthesis; Barry M. Trost, Ian Fleming, Eds.; Pergamon: Oxford, 1991*; 1083-1109.

62. Lentz, D. Fluorierte Isocyanide - mehr als Liganden mit ungewöhnlichen Eigenschaften. *Ang. Chem.* **1994**, *106*, 1377-1393.
63. Skorna, G.; Ugi, I. Isocyanid-Synthese mit Diphosgen. *Ang. Chem.* **1977**, *9*, 267-268.
64. Eckert, H.; Forster, B. Triphosgen, ein kristalliner Phosgen-Ersatz. *Ang. Chem.* **1987**, *99*, 922-923.
65. Meyer, G.; Ferres-Torres, R.; Feo, J. J. Quantitative analysis of the effects of visual stimulation and deprivation on the development of dendrite spines of various telencephalic centers. *Verh. Anat. Ges.* **1977**, 147-150.
66. Hofmann, A. W. Reaction auf Chloroform. *Zeit. Anal. Chem.* **1871**, *10*, 225.
67. Ugi, I.; Meyr, R. Neue Darstellungsmethode für Isonitrile. *Ang. Chem.* **1958**, *70*, 702-703.
68. Appel, R.; Kleinstück, R.; Ziehn, K. Neues Verfahren zur Darstellung von Isocyaniden. *Ang. Chem.* **1971**, *83*, 143-143.
69. - Schöllkopf, U. Neuere Anwendungen η -metallierter Isocyanide in der organischen Synthese. *Ang. Chem.* **1977**, *89*, 351-360.
70. Barton, D. H. R.; Bowles, T.; Husinec, S.; Forbes, J. E.; Llobera, A.; Porter, A. E. A.; Zard, S. Z. Reductive formylation of oximes; an approach to the synthesis of vinyl isonitriles. *Tet. Lett.* **1988**, *29*, 3343-3346.
71. Gassman, P. G.; Guggenheim, T. L. Opening of epoxides with trimethylsilyl cyanide to produce β -hydroxy isonitriles. A general synthesis of oxazolines and β -amino alcohols. *J. Am. Chem. Soc.* **1982**, *104*, 5849-5850.
72. Baldwin, J. E.; Bradley, M. Isopenicillin N synthase: Mechanistic studies. *Chem. Rev.* **1990**, *90*, 1079-1088.
73. Kitano, Y.; Chiba, K.; Tada, M. A direct conversion of alcohols to isocyanides. *Tet. Lett.* **1998**, *39*, 1911-1912.
74. Berłożecki, S.; Szymanski, W.; Ostaszewski, R. α -Amino acids as acid components in the Passerini reaction: influence of N-protection on the yield and stereoselectivity. *Tetrahedron.* **2008**, *64*, 9780-9783.
75. Faure, S.; Hjelmgaard, T.; Roche, S. P.; Aitken, D. J. Passerini reaction-amine deprotection-acyl migration peptide assembly: Efficient formal synthesis of cyclotheonamide c. *Org. Lett.* **2009**, *11*, 1167-1170.

76. Mironov, M. A.; Ivantsova, M. N.; Tokareva, M. I.; Mokrushin, V. S. Acceleration of the Passerini reaction in the presence of nucleophilic additives. *Tet. Lett.* **2005**, *46*, 3957-3960.
77. Paravidino, M.; Scheffelaar, R.; Schmitz, R. F.; De Kanter, F. J. J.; Groen, M. B.; Ruijter, E.; Orru, R. V. A. A flexible six-component reaction to access constrained depsipeptides based on a dihydropyridinone core. *J. Org. Chem.* **2007**, *72*, 10239-10242.
78. Denmark, S. E.; Fan, Y. Catalytic, enantioselective α -additions of isocyanides: Lewis base catalyzed Passerini-type reactions. *J. Org. Chem.* **2005**, *70*, 9667-9676.
79. Pirrung, M. C.; Das Sarma, K. Multicomponent Reactions Are Accelerated in Water. *J. Am. Chem. Soc.* **2004**, *126*, 444-445.
80. Breslow, R. Hydrophobic effects on simple organic reactions in water. *Acc. Chem. Res.* **1991**, *24*, .
81. Chandrasekhar, J.; Shariffskul, S.; Jorgensen, W. L. QM/MM simulations for Diels-Alder reactions in water: Contribution of enhanced hydrogen bonding at the transition state to the solvent effect. *J. Phys. Chem. B.* **2002**, *106*, 8078-8085.
82. Bhalla, A.; Sharma, S.; Bhasin, K. K.; Bari, S. S. Convenient preparation of benzylseleno- and phenylselenoalkanoic acids: Reagents for synthesis of organoselenium compounds. *Syn. Comm.* **2007**, *37*, 783-793.
83. Chen, C.; Liu, Y. -.; Shia, K. -.; Tseng, H. -. Synthesis and anticancer evaluation of vitamin K₃ analogues. *Bioorg. Med. Chem. Lett.* **2002**, *12*, 2729-2732.
84. Jiang, M. Y.; Dolphin, D. Site-specific prodrug release using visible light. *J. Am. Chem. Soc.* **2008**, *130*, 4236-4237.
85. Abbas, M.; Bethke, J.; Wessjohann, L. A. One pot synthesis of selenocysteine containing peptoid libraries by Ugi multicomponent reactions in water. *Chem. Comm.* **2006**, 541-543.
86. Amosova, S. V.; Makhaeva, N. A.; Martynov, A. V.; Potapov, V. A.; Steele, B. R.; Kostas, I. D. Terminal organylchalcogenoethyl- and -propylamines and their Schiff base derivatives. *Synthesis* **2005**, 1641-1648.
87. Ranu, B. C.; Mandal, T. Indium(I) iodide-promoted cleavage of diaryl diselenides and disulfides and subsequent condensation with alkyl or acyl halides. One-pot efficient synthesis of diorganyl selenides, sulfides, selenoesters, and thioesters. *J. Org. Chem.* **2004**, *69*, 5793-5795.

88. Zhong, W.; Zhang, Y. Synthesis of 2H-1,4-benzothiazin-3(4H)-ones and 2H-1,4-benzoselenazin-3(4H)-ones with the aid of samarium(II) iodide. *Tet. Lett.* **2001**, *42*, 3125-3127.
89. Shin-ichi Fukuzawa, ; k Yasuhiko Niimoto, Tatsuo Fujinami, and Shizuyoshi Sakai Samarium (II) diiodide-induced reductive cleavage of SeSe and TeTe bond in diphenyl diselenide and ditelluride leading to a samarium phenylselenolate and tellurolate: Preparation of unsymmetrical alkylphenyl selenides and tellurides. *Heteroatom Chem.* **1990**, *1*, 491-495.
90. Back, T. G.; Moussa, Z. Diselenides and Allyl Selenides as Glutathione Peroxidase Mimetics. Remarkable Activity of Cyclic Seleninates Produced in Situ by the Oxidation of Allyl ω -Hydroxyalkyl Selenides. *J. Am. Chem. Soc.* **2003**, *125*, 13455-13460.
91. Shabaan, S.; Ba, L. A.; Abbas, M.; Burkholz, T.; Denkert, A.; Gohr, A.; Wessjohann, L. A.; Sasse, F.; Weber, W.; Jacob, C. Multicomponent reactions for the synthesis of multifunctional agents with activity against cancer cells. *Chem. Commun.* **2009**, (31), 4702-4704.
92. Pelicano, H.; Carney, D.; Huang, P. ROS stress in cancer cells and therapeutic implications. *Drug Resis. Upd.* **2004**, *7*, 97-110.
93. Sredni, B.; Kfar-Saba; Michael Albeck; Ramat-Gan Use of tellurium containing compounds as nerve protecting agents. *US Patent Publication Dec. 8, 2009*, US 7,629,382, B2, .
94. Min, S. -.; Lee, S. -.; Park, J. -.; Lee, J.; Paeng, J. -.; Lee, S. -.; Lee, H. -.; Kim, Y.; Pae, H. -.; Lee, S. -.; Kim, E. -. Endoplasmic reticulum stress is involved in hydrogen peroxide induced apoptosis in immortalized and malignant human oral keratinocytes. *J. Oral Path. Med.* **2008**, *37*, 490-498.
95. Kalyanaraman, B.; Joseph, J.; Kalivendi, S.; Wang, S.; Konorev, E.; Kotamraju, S. Doxorubicin-induced apoptosis: Implications in cardiotoxicity. *Mol. Cell. Biochem.* **2002**, *234-235*, 119-124.
96. Lopez, A.; Parsons, A. B.; Nislow, C.; Giaever, G.; Boone, C. Chemical-genetic approaches for exploring the mode of action of natural products. *Prog.s Drug Res.* **2008**, *66*, 237-271.

Appendix

Appendix 1. Influence of different multifunctional redox compounds on the viability and proliferation of different cell lines. The IC₅₀ [µg/ml] was measured in two different sets of experiments using an MTT reduction assay after five days.

Cpd. Nr.	L-929	A-549	SW-480	MCF-7	A-431	A-498
1p	7	22	11	4	8	22
2p	6	10	10	8	6	28
3p	10	>100	8	5	8	23
4p	22	1	1	1	1	1
5p	8	>100	9	5	9	>100
6p	8	3	6	5	5	4
7p	1	1	1	1	1	2
8p	1	1	1	1	1	1
9p	15	4	>100	5	2	2
10p	8	2	11	4	5	2
11p	6	2	3	1	2	1
12p	1	1	1	1	1	1
13p	>100	>100	>100	>100	65	>100
14p	>100	>100	>100	>100	>100	>100
15p	>100	>100	>100	>100	>100	>100

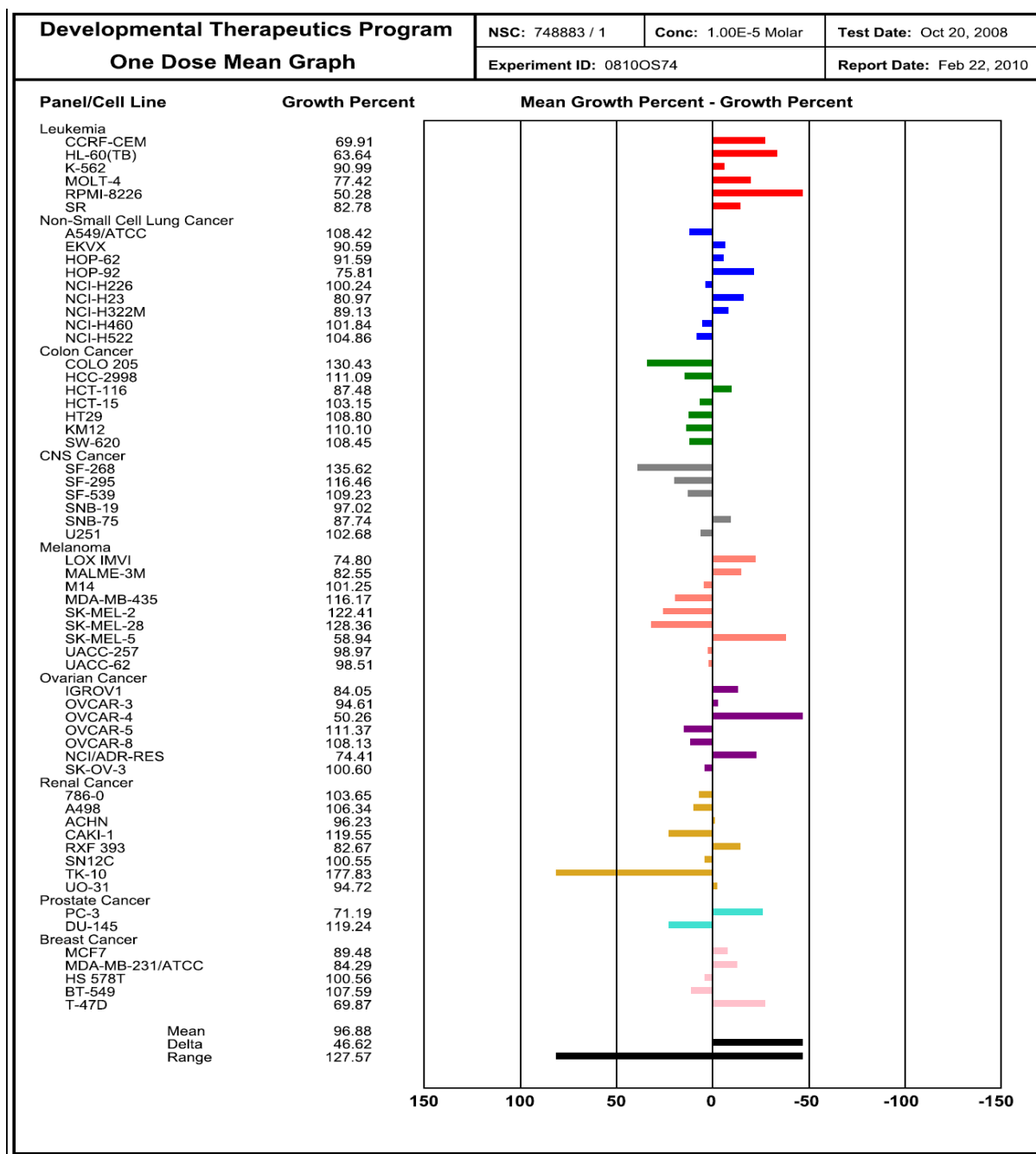
Appendix 1 :continued.....

Cpd. Nr.	L-929	A-549	SW-480	MCF-7	A-431	A-498
17p	1	1	1	1	2	1
18p	3		1	1		
19p	8		4	1		
1u	7	35	>100	6		19
2u	8	>100	>100	3	14	
3u	1	1	1	1	1	
4u	>100	>100	3	18	>100	10
5u	>100	10	>100	31	>100	>100
6u	29	2	2	3	3	6
7u	>100	>100	28	>100		46
8u	1	>100		15	70	12
9u	3	1	2	1	4	2
10u	>100	>100	>100		17	9
11u	>100	>100	>100		>100	>100
12u	4	1	2	1	5	4
13u		>100	>100	3	5	>100
14u	6	14				
15u	>100	>100	>100	>100	>100	>100

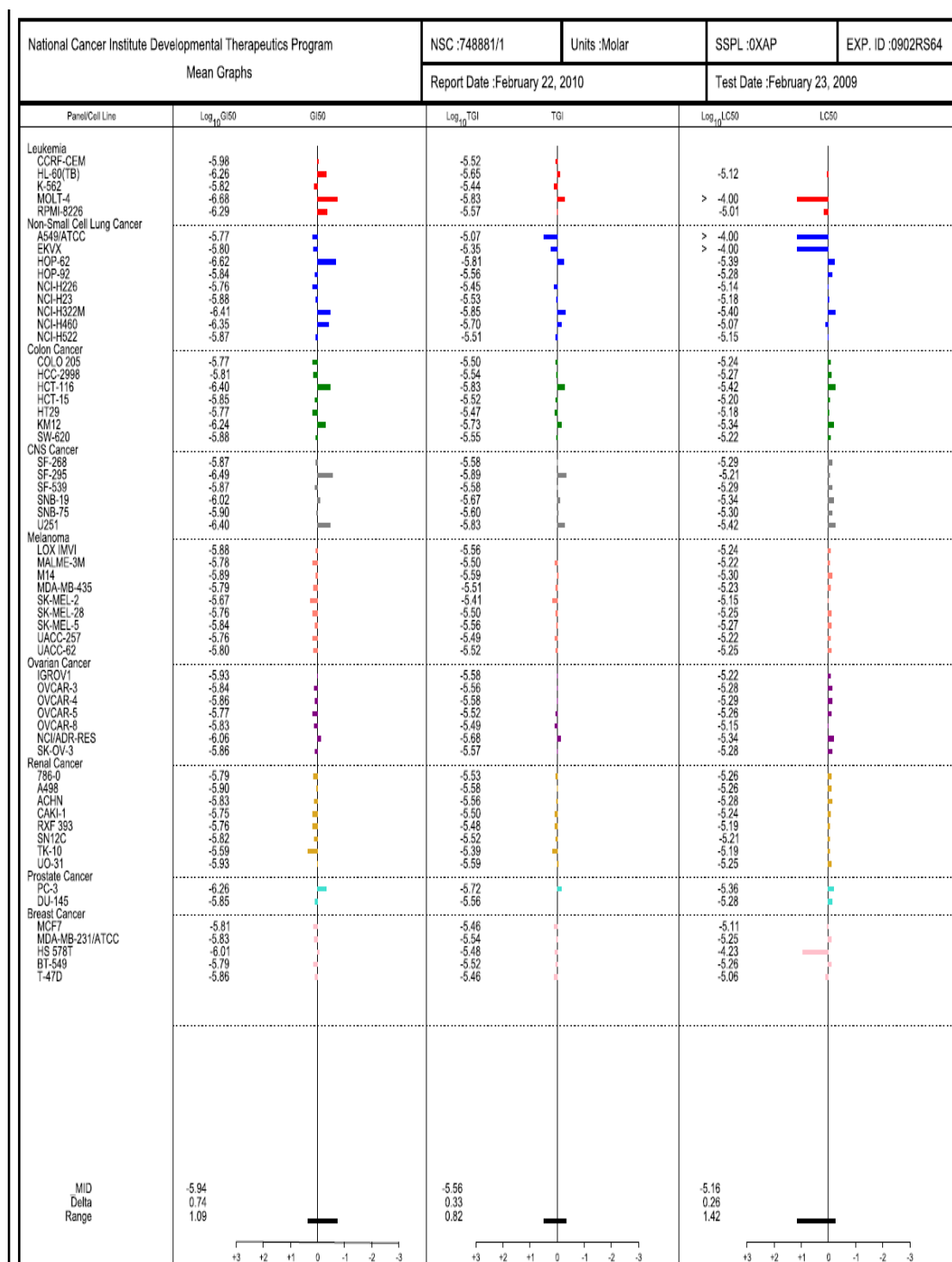
58 CANCER CELL LINE SCREEN

The 58 cancer cell line screen for was performed at the National Cancer Institute (NCI) at the NIH (US). These single dose tests (at 10 μ M) were performed for cell lines clustered in cells representing leukemia, non-small cell lung cancer, colon cancer, cancer of the central nervous system, melanoma, ovarian cancer, renal cancer, prostate cancer and breast cancer. All compounds were selected for 5-dose testing. All tests follow a standard protocol for cytotoxicity screens, details of which can be obtained from the NCI website at <http://dtp.nci.nih.gov>.

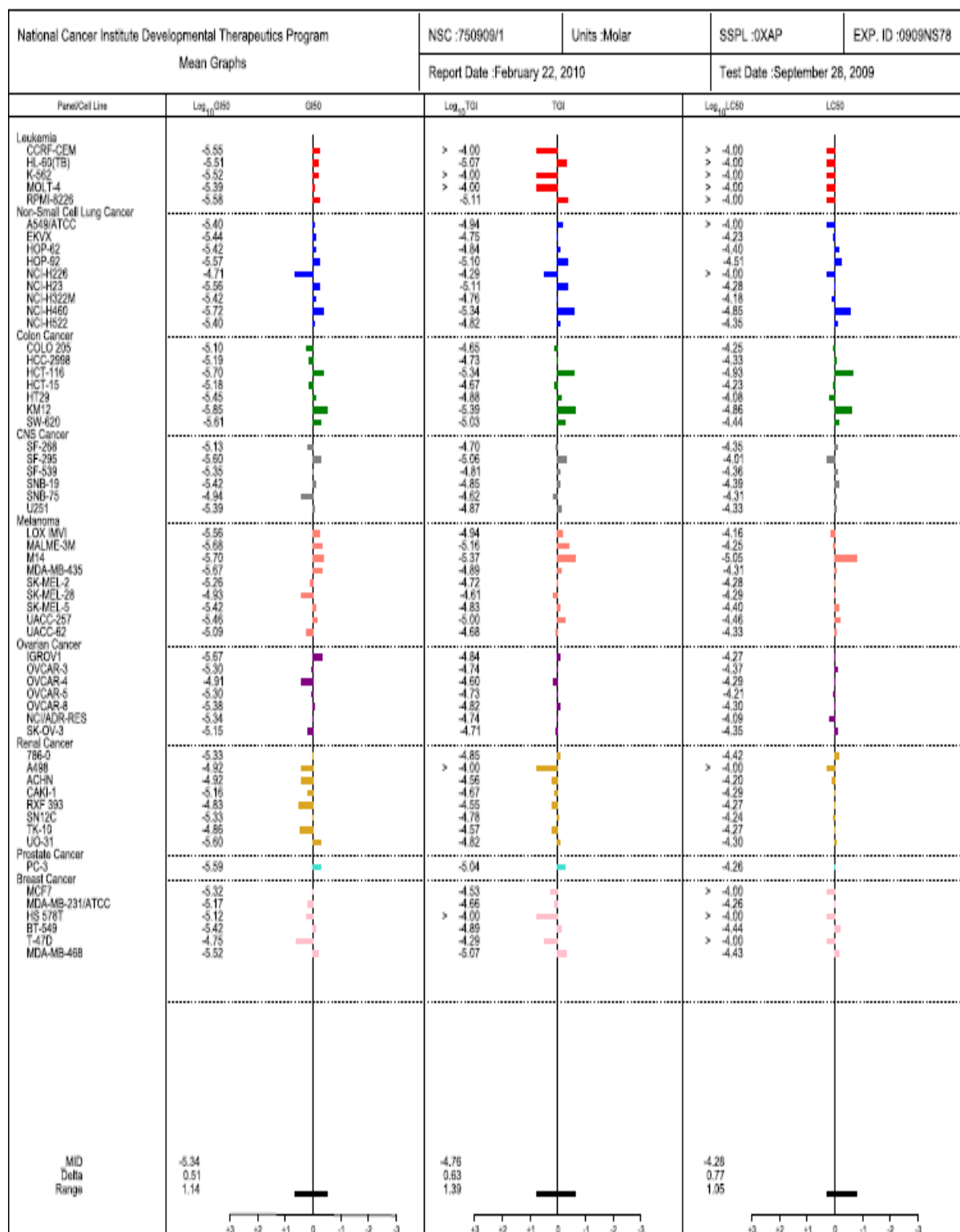
Appendix 2. Assay data obtained for compound 2p in different cancer cell lines.



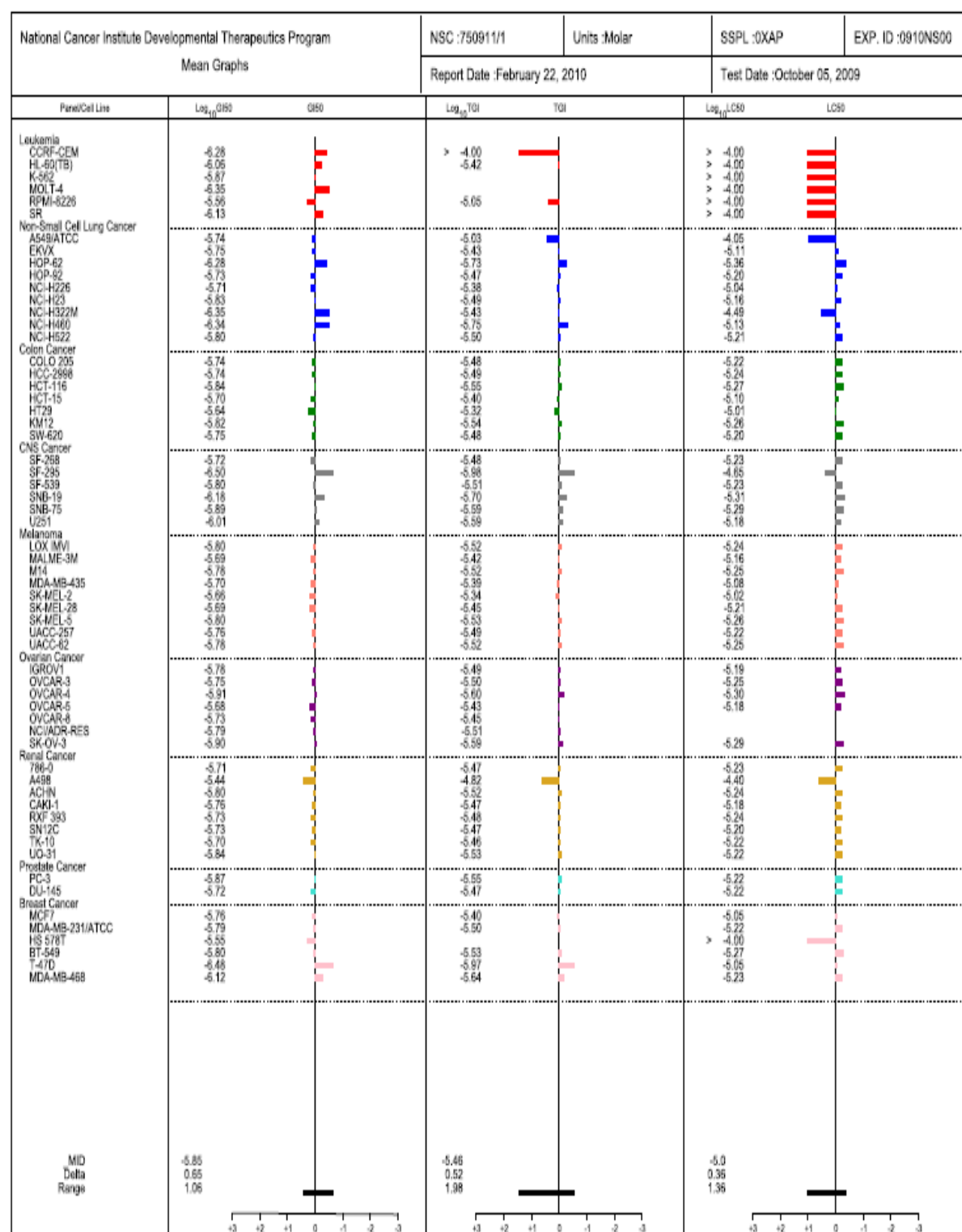
Appendix 3. Assay data obtained for compound 4p in different cancer cell lines.



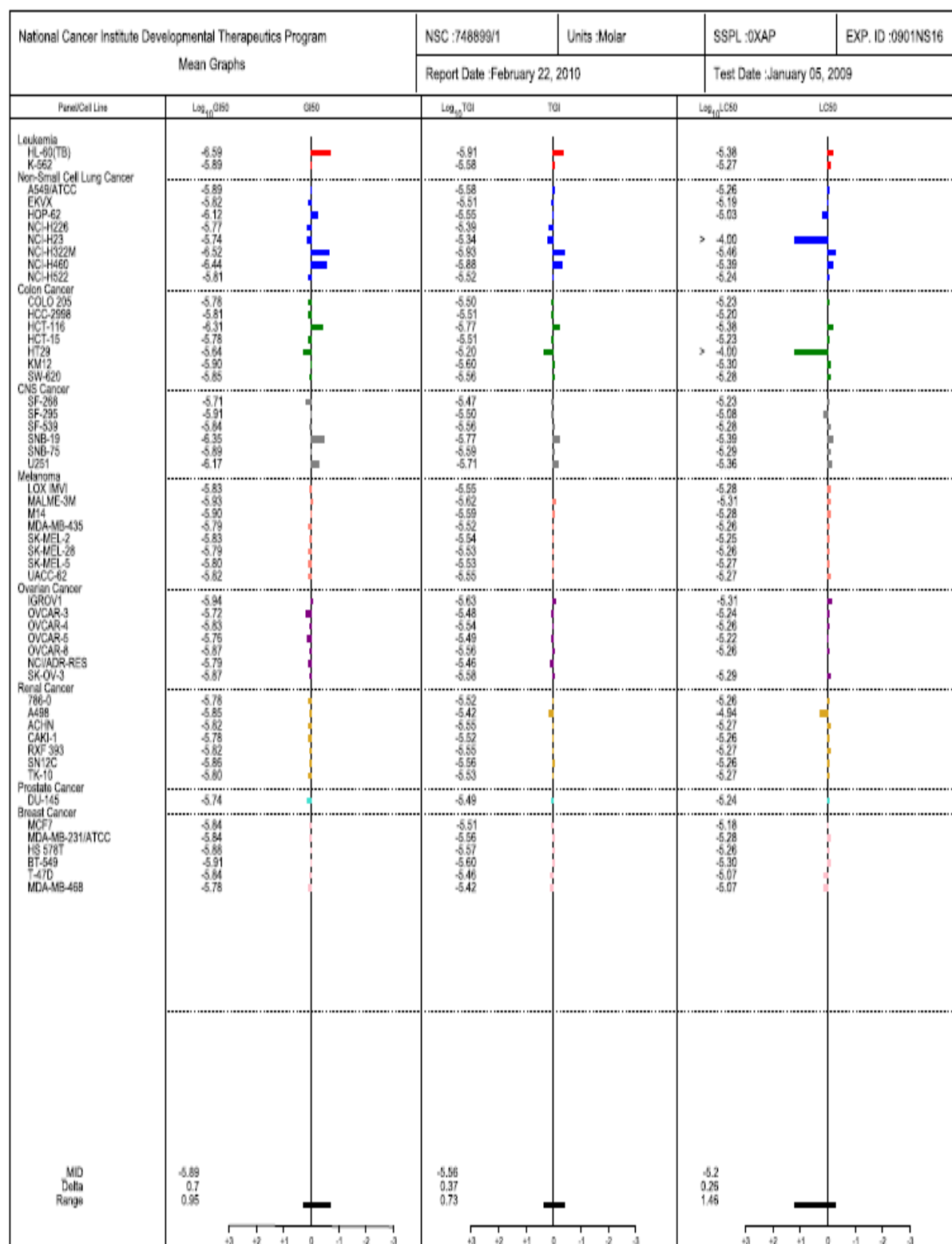
Appendix 4. Assay data obtained for compound 6p in different cancer cell lines.



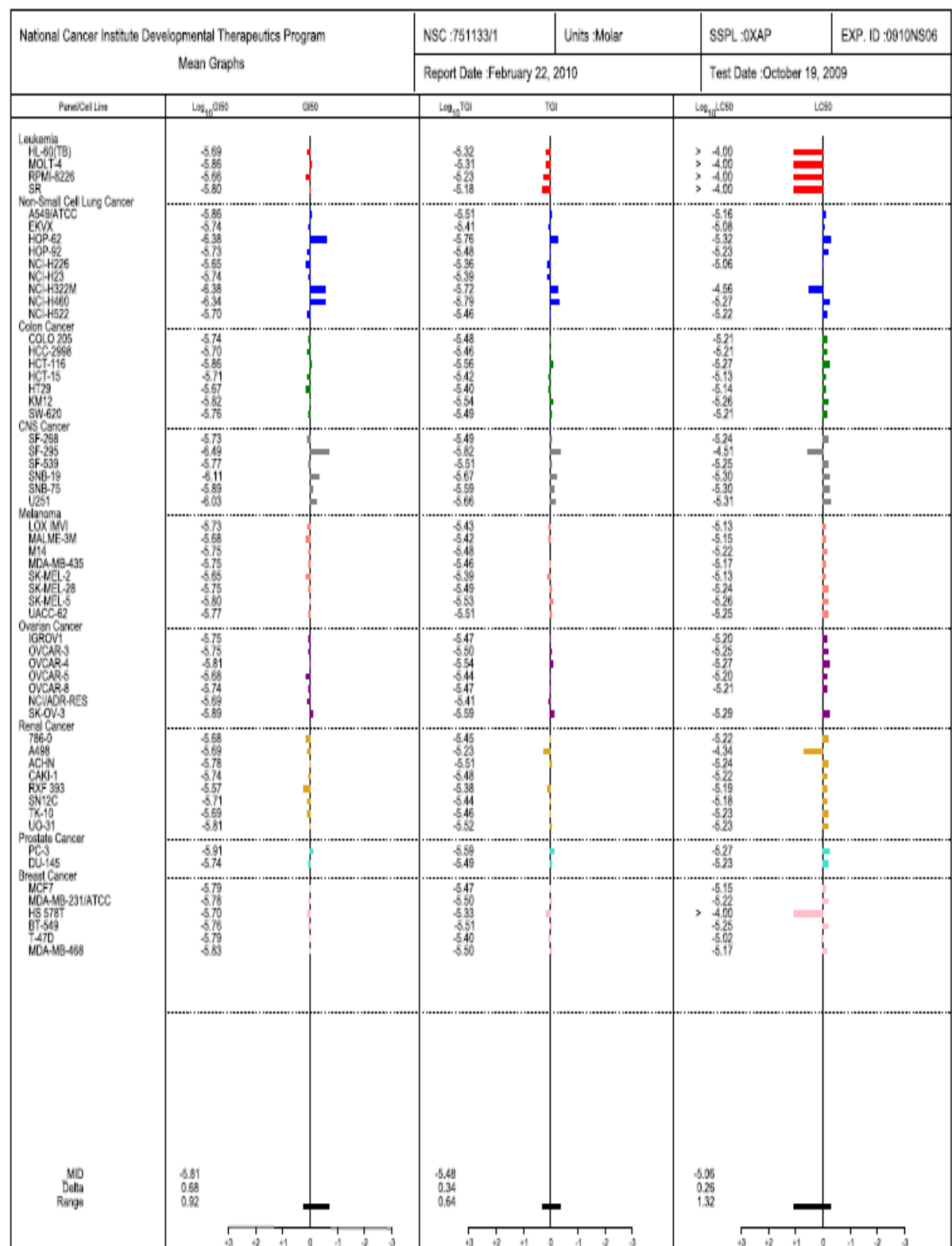
Appendix 5. Assay data obtained for compound 7p in different cancer cell lines.



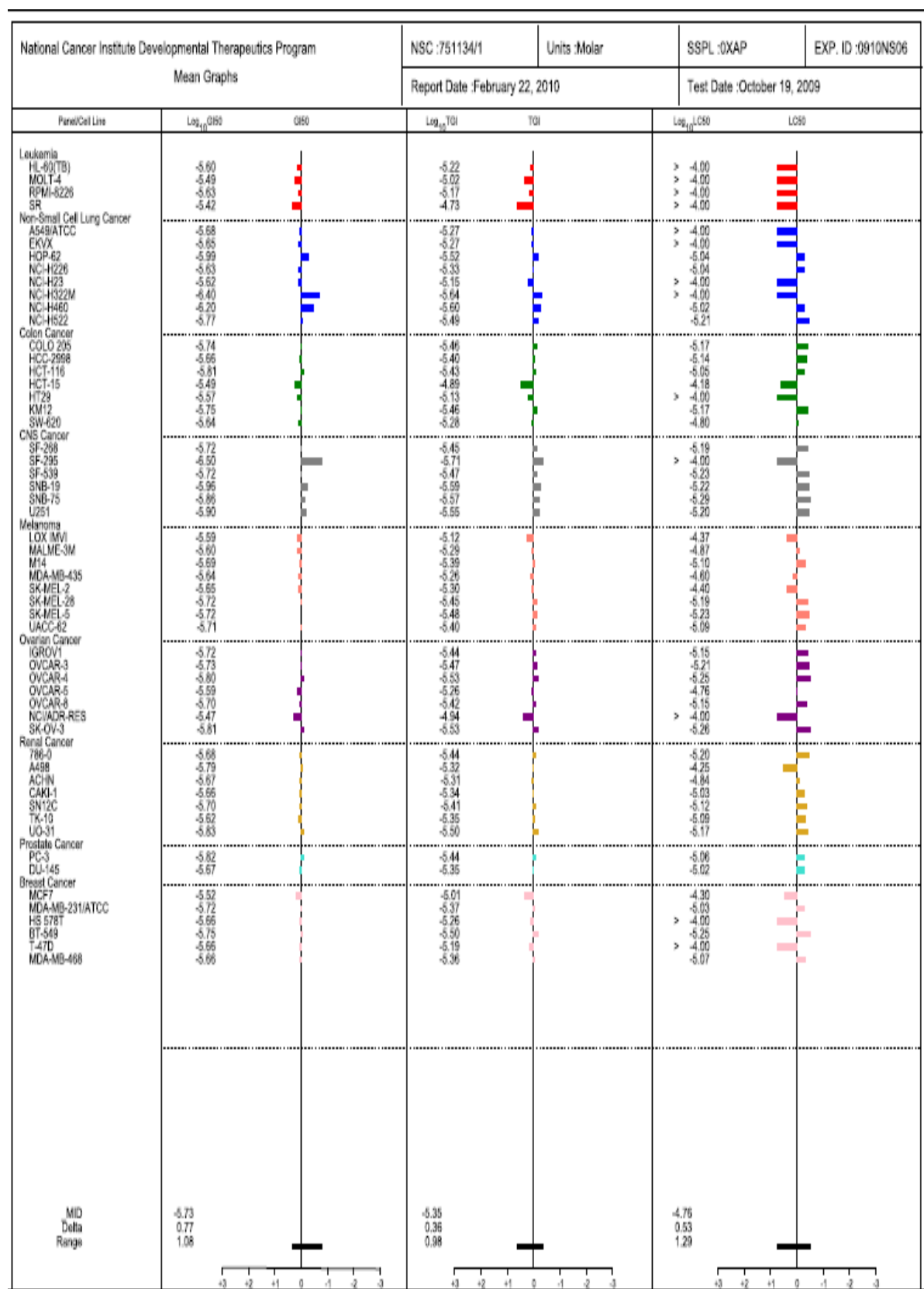
Appendix 6. Assay data obtained for compound 8p in different cancer cell lines.



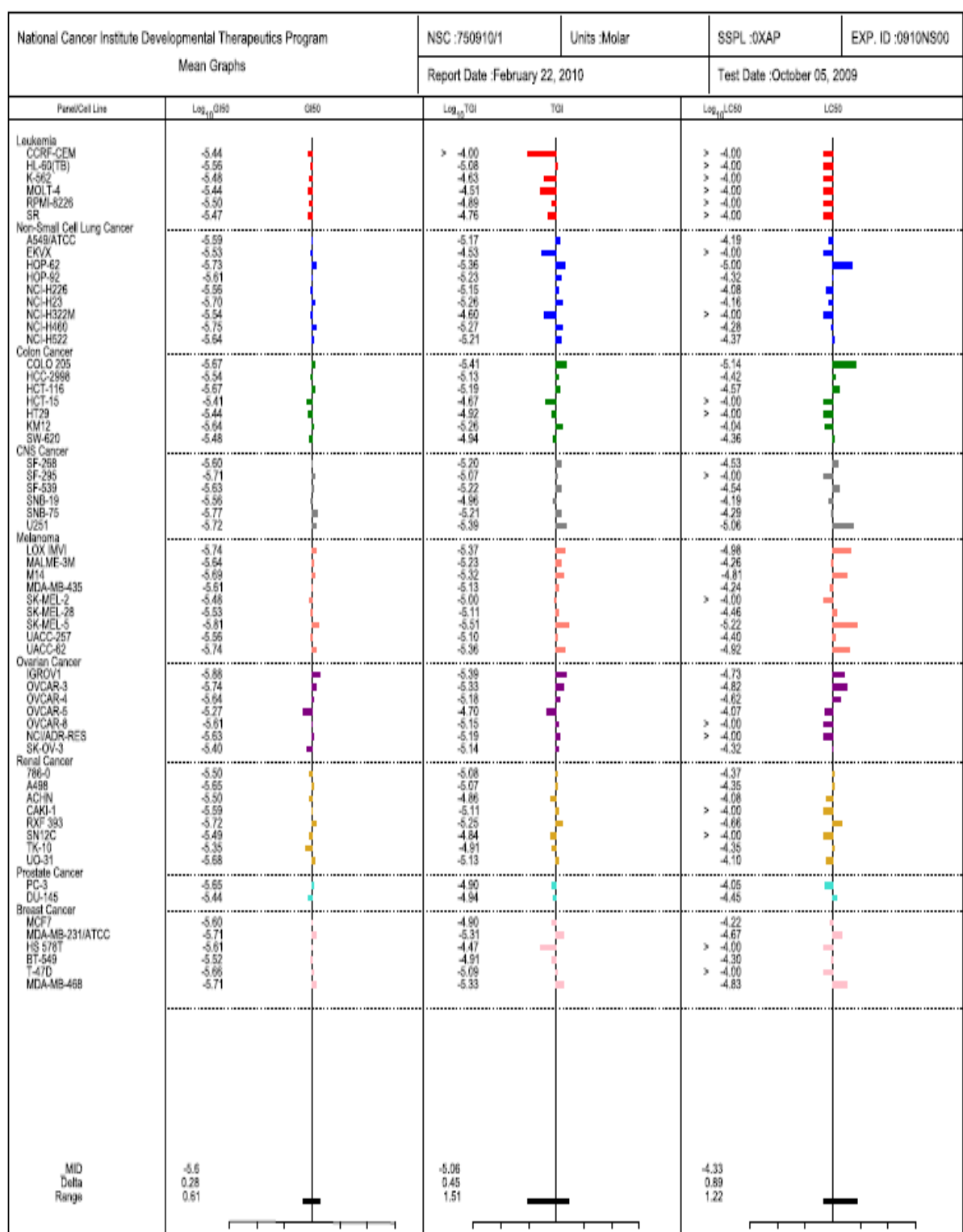
Appendix 7. Assay data obtained for compound 9p in different cancer cell lines.



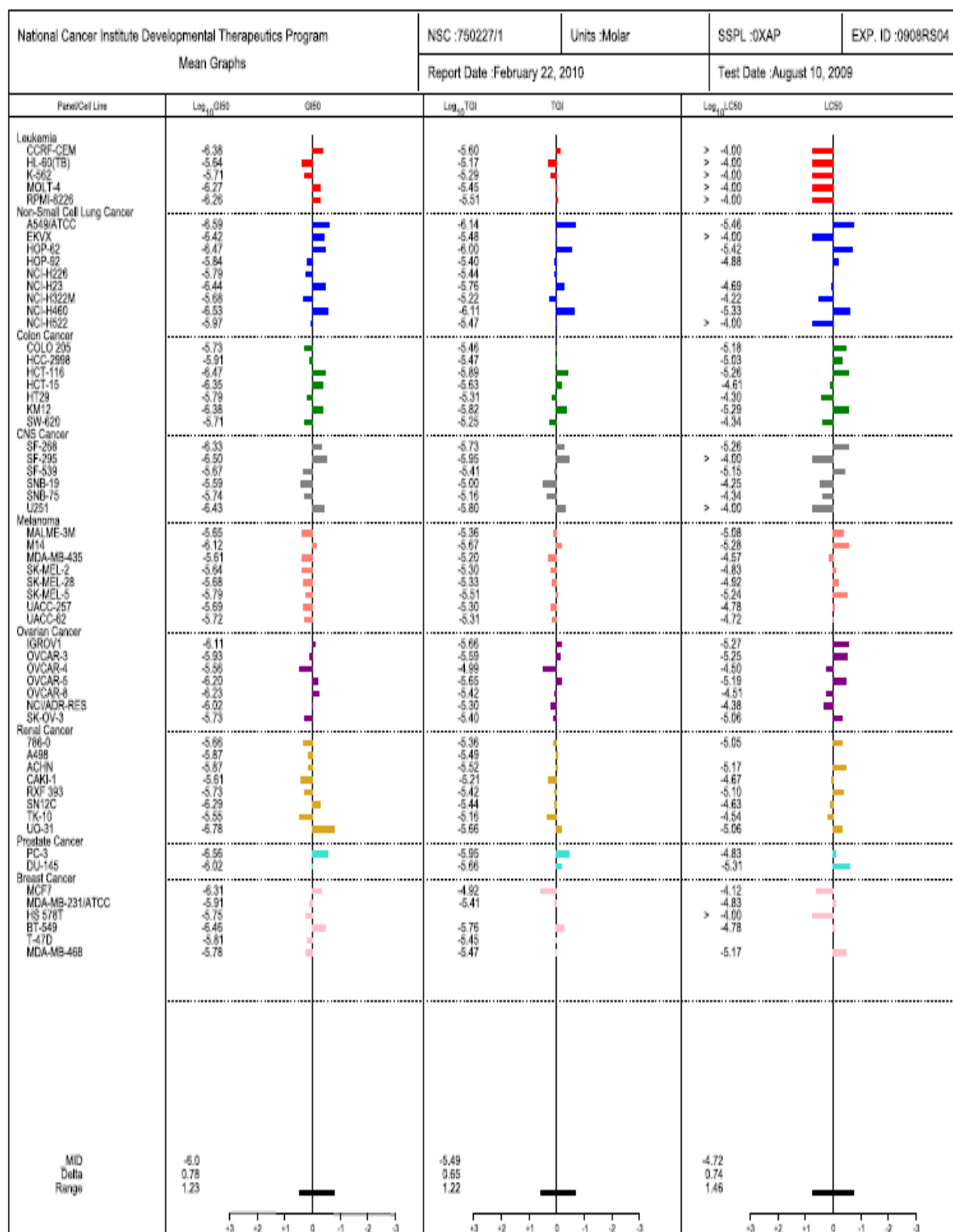
Appendix 8. Assay data obtained for compound 11p in different cancer cell lines.



Appendix 9. Assay data obtained for compound 12p in different cancer cell lines.



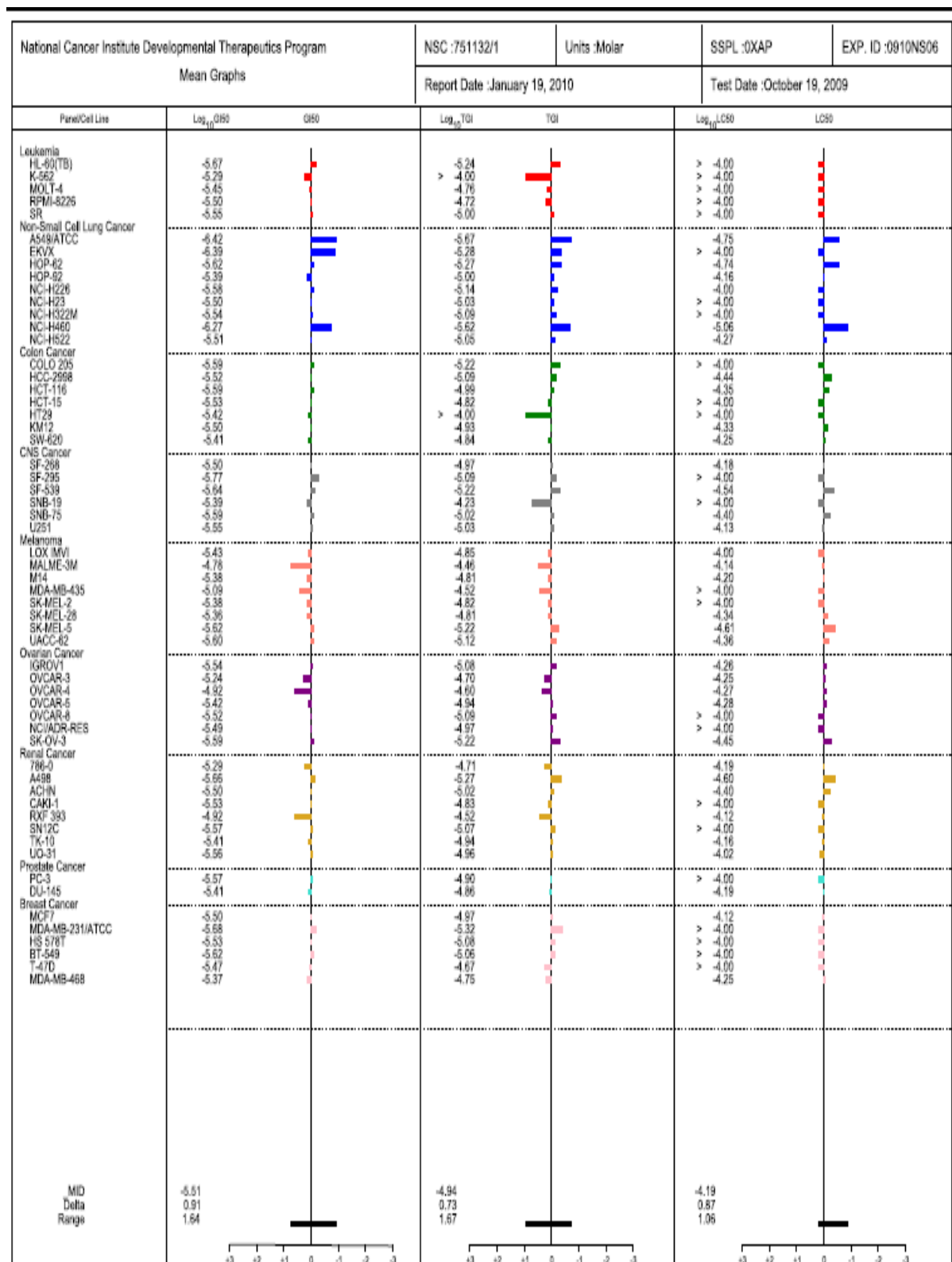
Appendix 10. Assay data obtained for compound 3u in different cancer cell lines.



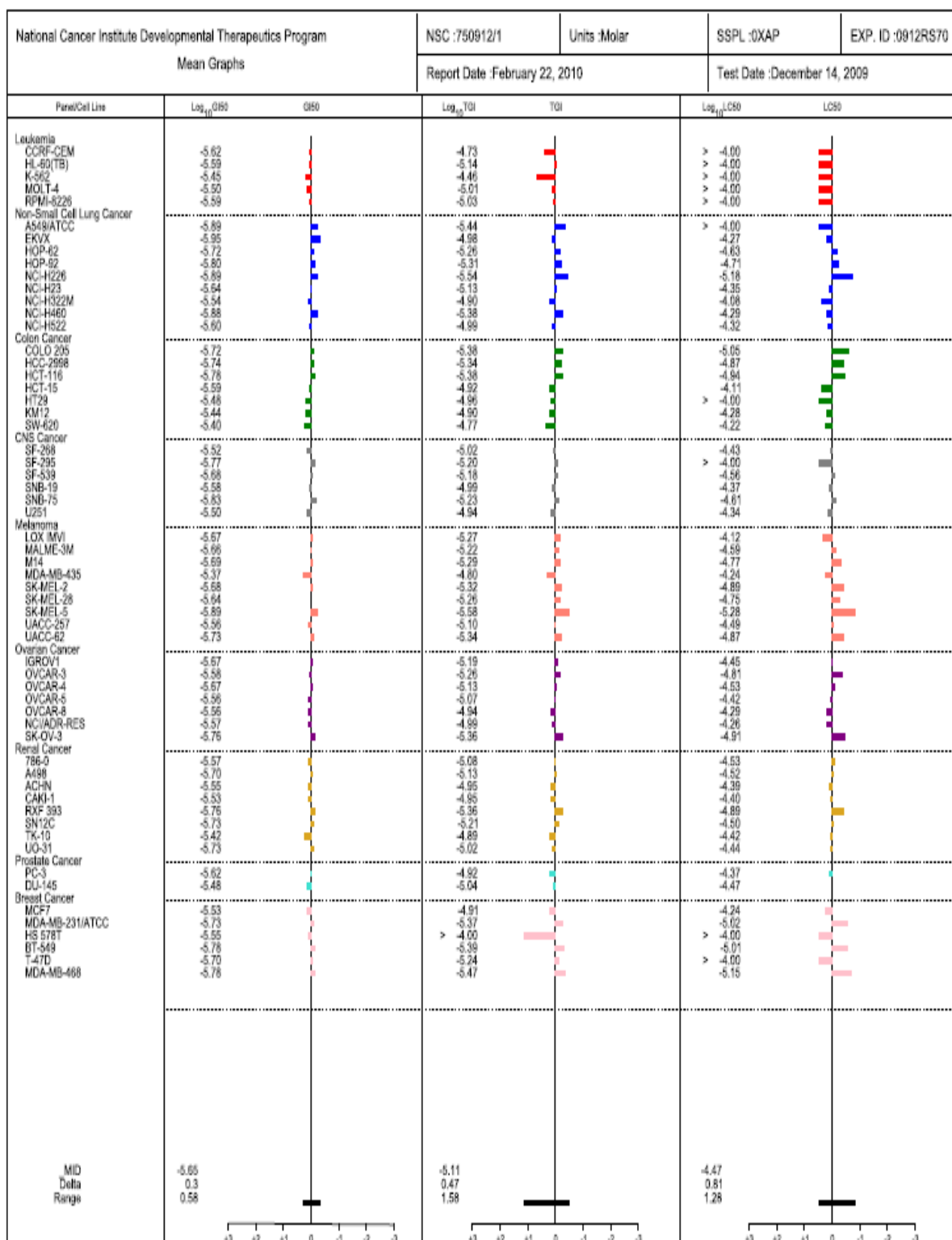
Appendix 11. Assay data obtained for compound 6u in different cancer cell lines.

National Cancer Institute Developmental Therapeutics Program		NSC :751131/1		Units :Molar		SSPL :0XAP		EXP. ID :0910NS06	
Mean Graphs		Report Date :January 19, 2010				Test Date :October 19, 2009			
Panel/Cell Line	Log ₁₀ GI50	GI50	Log ₁₀ TGI	TGI	Log ₁₀ LC50	LC50			
Leukemia									
HL-60(TB)	-5.68		-5.25		> -4.00				
K-562	-5.25		> -4.00		> -4.00				
MOLT-4	-5.51		-5.00		> -4.00				
RPMI-8226	-5.52		-5.14		> -4.00				
SR	-5.78		-5.11		> -4.00				
Non-Small Cell Lung Cancer									
A549(ATCC)	-6.28		-5.66		-5.17				
EKVX	-4.46		-5.63		> -4.00				
HOP-62	-5.66		-5.33		-4.96				
HOP-92	-5.63		-5.31		-4.18				
NCH-H226	-5.64		-5.27		-4.10				
NCH-H23	-5.60		-5.18		> -4.00				
NCH-H322M	-5.64		-5.18		> -4.00				
NCH-H460	-6.35		-5.73		-5.13				
NCH-H522	-5.59		-4.98		-4.25				
Colon Cancer									
COLO 205	-5.70		-5.42		-5.14				
HCC-2998	-5.59		-5.18		-4.56				
HCT-116	-5.68		-5.19		-4.31				
HCT-15	-5.50		-4.93		-4.03				
HT29	-5.42		-4.86		> -4.00				
KM12	-5.48		-4.94		-4.36				
SW-620	-5.46		-4.84		> -4.00				
CNS Cancer									
SF-298	-5.57		-5.12		-4.09				
SF-295	-5.89		-5.35		> -4.00				
SF-539	-5.67		-5.32		-4.60				
SNB-19	-5.05		-5.02		> -4.00				
SNB-75	-5.68		-5.13		-4.44				
U251	-5.52		-5.19		-4.31				
Melanoma									
LOX IMVI	-5.63		-5.24		-4.46				
MALME-3M	-4.80		-4.48		-4.16				
M14	-5.45		-4.97		-4.34				
MDA-MB-435	-5.48		-4.87		-4.29				
SK-MEL-2	-5.52		-5.17		> -4.00				
SK-MEL-28	-5.51		-5.00		-4.44				
SK-MEL-5	-5.50		-5.04		-4.46				
UACC-257	-5.07		-4.62		-4.21				
UACC-62	-5.78		-5.42		-5.06				
Ovarian Cancer									
IGROV1	-5.55		-5.27		-4.59				
OVCAR-3	-5.52		-5.10		-4.03				
OVCAR-4	-4.85		> -4.00		> -4.00				
OVCAR-6	-5.52		-5.13		-4.41				
OVCAR-8	-5.52		-5.16		> -4.00				
NCIADR-RES	-5.54		-5.14		> -4.00				
SK-OV-3	-5.63		-5.32		-5.00				
Renal Cancer									
786-O	-5.43		-4.89		-4.25				
A498	-5.64		-5.27		-4.47				
ACHN	-5.51		-5.05		> -4.00				
CAKI-1	-5.66		-5.25		> -4.00				
SN12C	-5.69		-5.30		> -4.00				
TK-10	-5.41		-4.97		-4.08				
UO-31	-5.52		-5.04		> -4.00				
Prostate Cancer									
PC-3	-5.77		-5.00		> -4.00				
DU-145	-5.54		-5.12		-4.51				
Breast Cancer									
MCF7	-5.59		-5.12		-4.43				
MDA-MB-231(ATCC)	-5.72		-5.41		> -4.00				
HS 578T	-5.56		-5.14		> -4.00				
BT-549	-5.77		-5.31		> -4.00				
T-47D	-4.96		-4.39		> -4.00				
MDA-MB-468	-5.50		-4.96		-4.22				
MID	-5.59		-5.09		-4.27				
Delta	0.87		0.64		0.9				
Range	1.81		1.73		1.17				

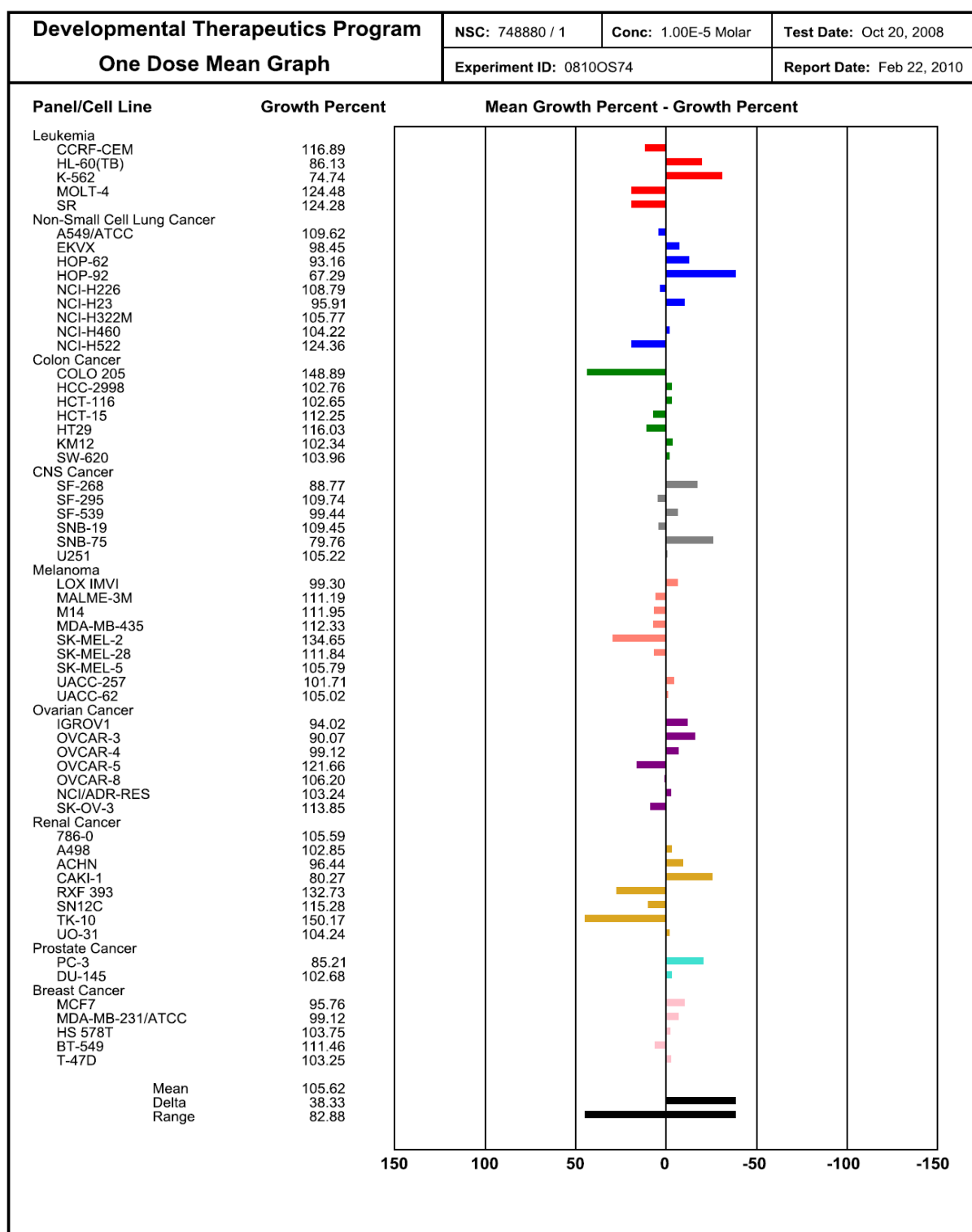
Appendix 12. Assay data obtained for compound 9u in different cancer cell lines.



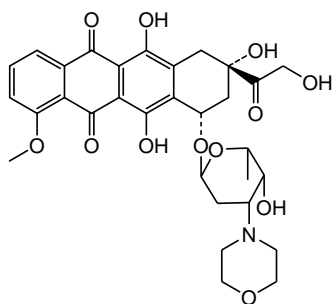
Appendix 13. Assay data obtained for compound 16p in different cancer cell lines.



Appendix 14. Assay data obtained for compound 15p in different cancer cell lines.

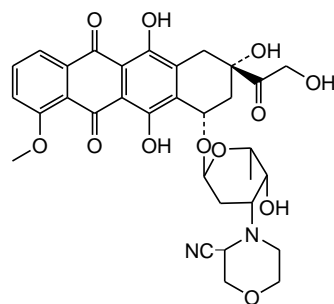


Appendix 15. COMPARE analysis for compound 2p.



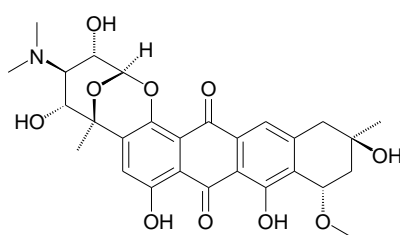
Morpholino-ADR

R = 0.322



Cyanomorpholino-ADR

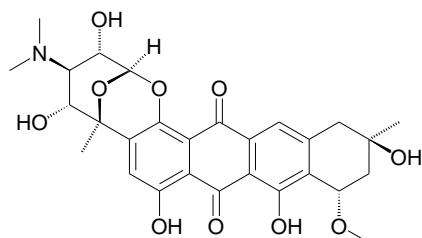
R = 0.316



Menogaril

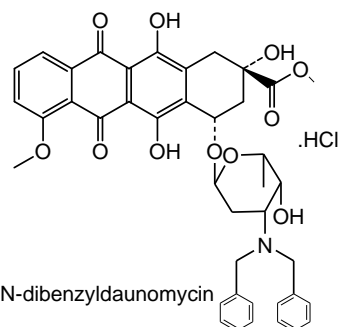
R = 0.234

Appendix 16. COMPARE analysis for compound 4p.



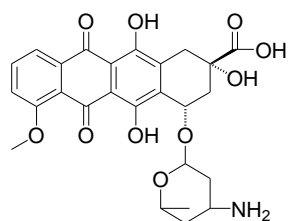
Menogaril

R = 0.51



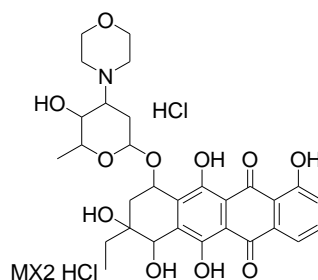
N,N-dibenzyl-daunomycin

R = 0.427



Deoxydoxorubicin

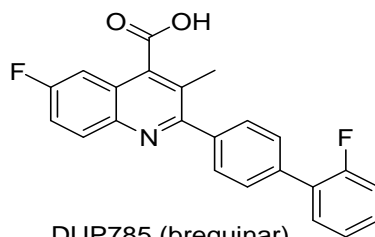
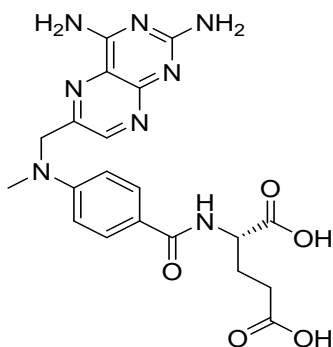
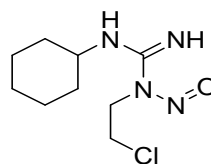
R = 0.391



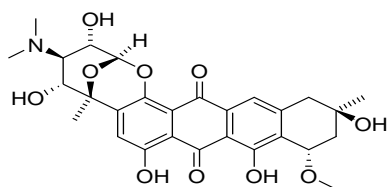
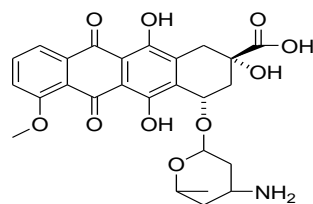
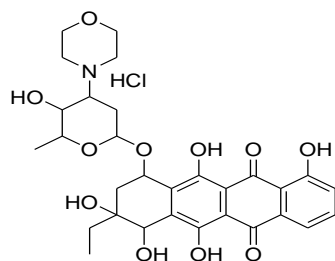
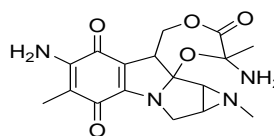
MX2 HCl

R = 0.385

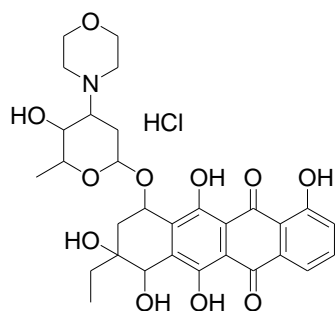
Appendix 17. COMPARE analysis for compound 6p.

Trimetrexate
R= 0.596DUP785 (brequinar)
R= 0.477Methotrexate
R= 0.567Lomustine
R= 0.463

Appendix 18. COMPARE analysis for compound 7p.

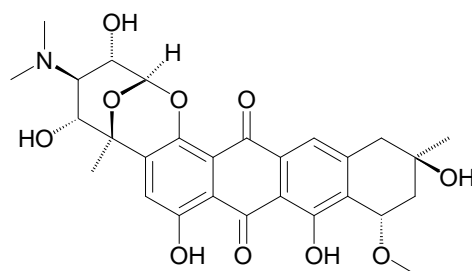
Menogaril
R= 0.536Deoxydoxorubicin
R= 0.427MX2 HCl (I)
R= 0.494Methyl mitomycin C
R= 0.426

Appendix 19. COMPARE analysis for compound 8p.



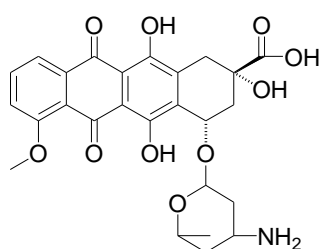
MX2 HCl

R= 0.471



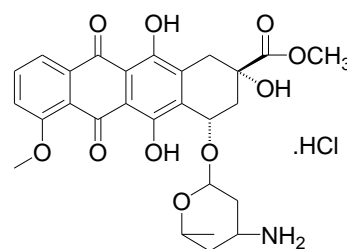
Menogaril

R= 0.404



Deoxydoxorubicin

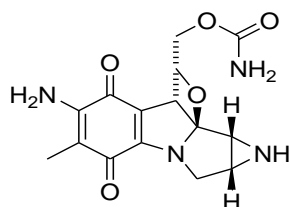
R= 0.394



Daunomycin

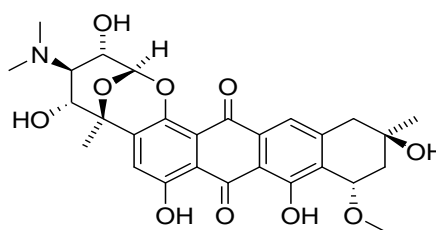
R= 0.342

Appendix 20. COMPARE analysis for compound 9p.



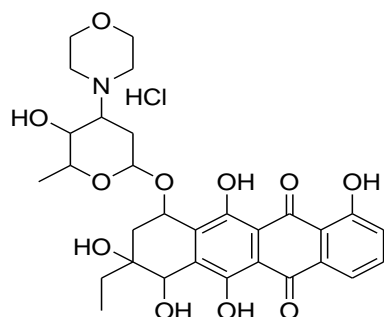
Mitomycin C

R= 0.414



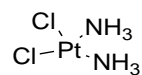
Menogaril

R= 0.363



MX2 HCl (I)

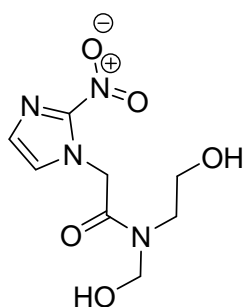
R= 0.332



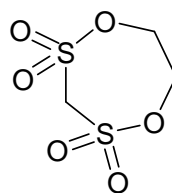
Cisplatin

R= 0.305

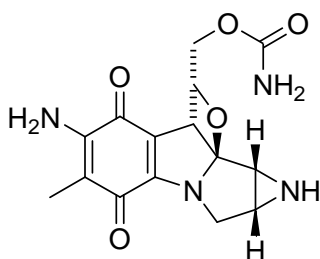
Appendix 21. COMPARE analysis for compound 11p.



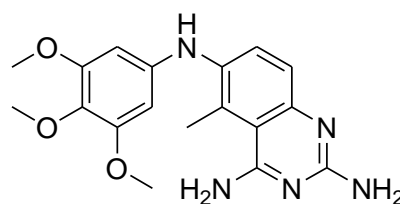
SR2555 (nitroimidazole)
R= 0.449



Cyclodisone
R= 0.461

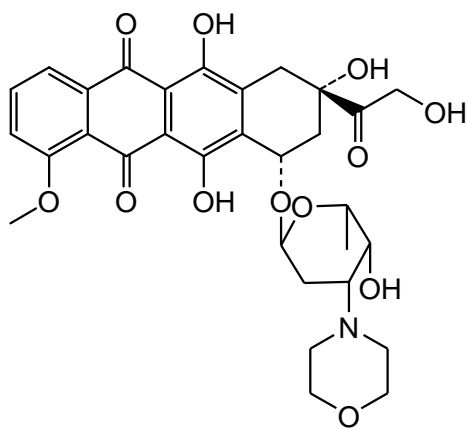


Mitomycin C
R= 0.270

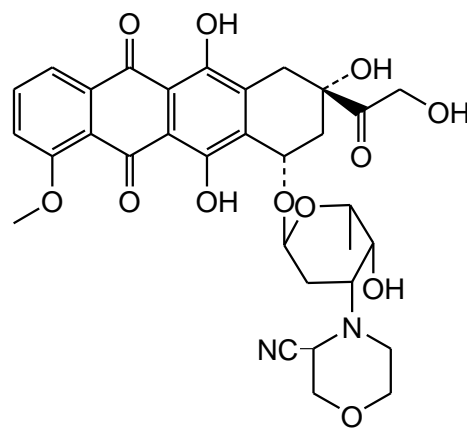


Trimetrexate
R= 0.300

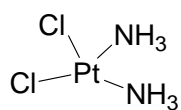
Appendix 22. COMPARE analysis for compound 12p.



Morpholino-ADR
R = 0.291

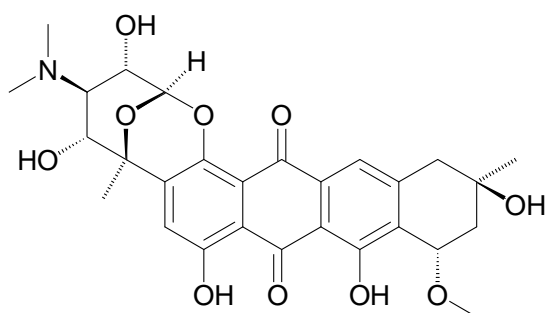


Cyanomorpholino-ADR
R = 0.25



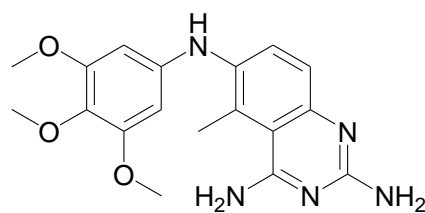
Cisplatin
R= 0.245

Appendix 23. COMPARE analysis for compound 3u.



Menogaril

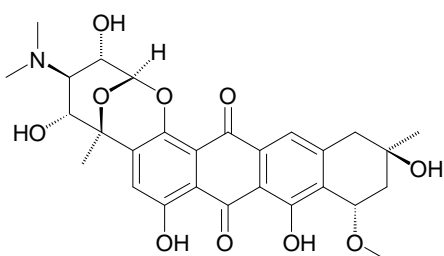
R= 0.345



Trimetrexate

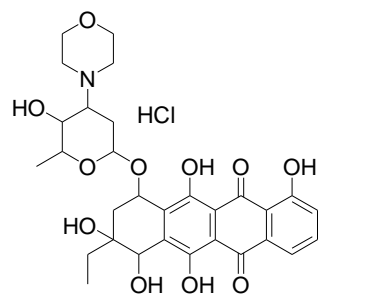
R= 0.462

Appendix 24. COMPARE analysis for compound 6u.



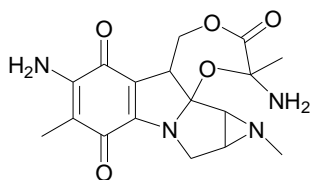
Menogaril

R= 0.365



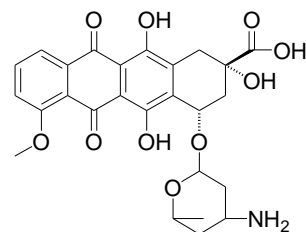
MX2 HCl

R= 0.364



Methyl mitomycin C

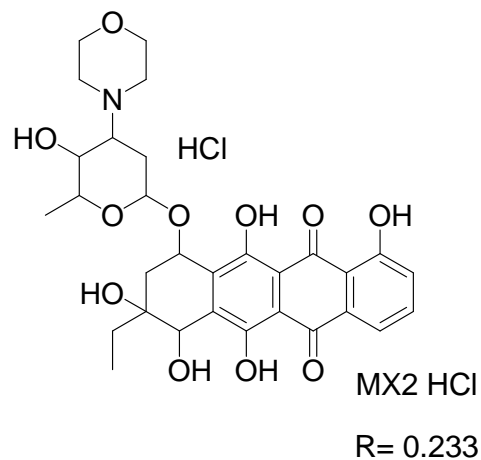
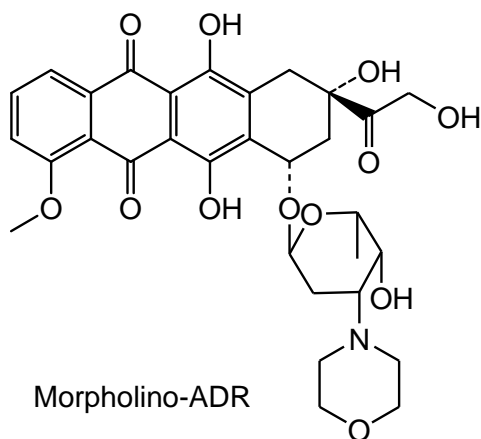
R= 0.336



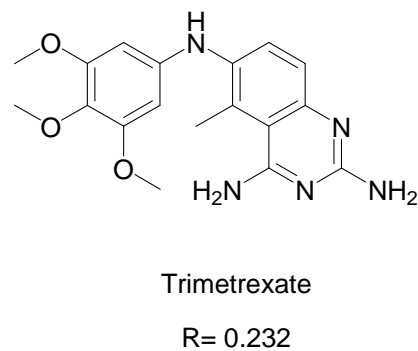
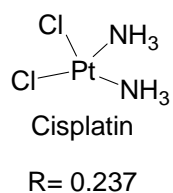
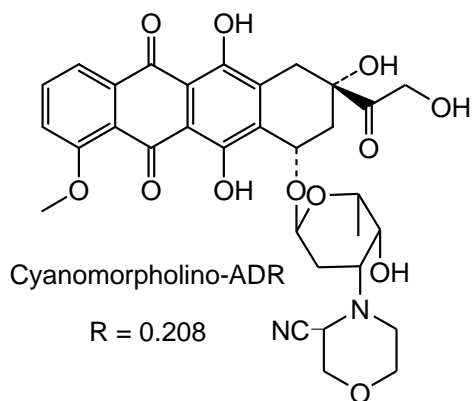
Deoxydoxorubicin

R= 0.316

Appendix 25. COMPARE analysis for compound 9u.



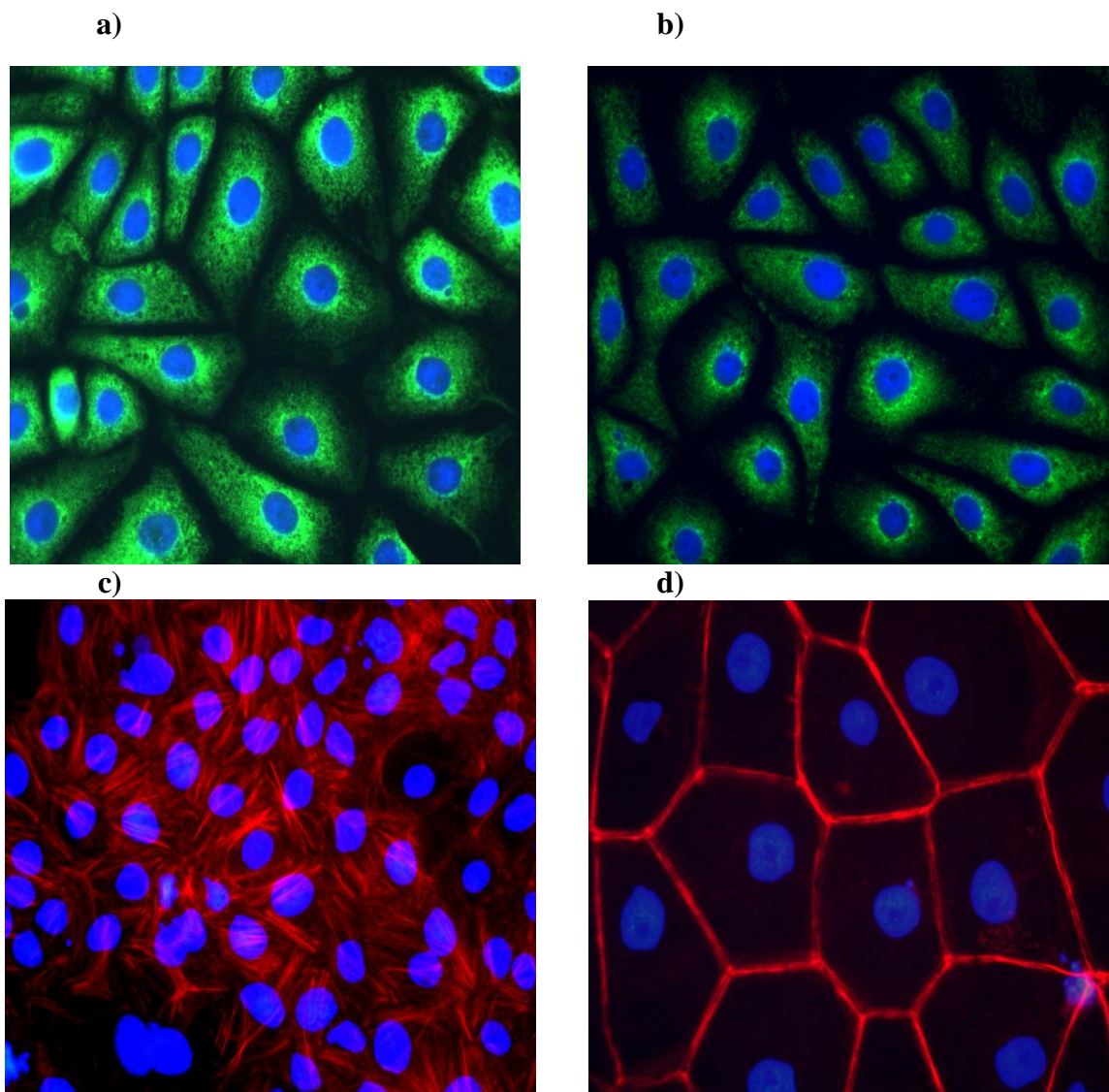
Appendix 26. COMPARE analysis for compound 15p.



Appendix 27. Name and description of the *S. cerevisiae* mutants identified by the chemogenomic assay.

Mutant Name (Systematic name)	Description
YPL188W (POS5)	Mitochondrial NADH kinase, phosphorylates NADH; also phosphorylates NAD(+) with lower specificity; required for the response to OS.
YDR032C (PST2)	Protein with similarity to members of a family of flavodoxin-like proteins; induced by OS in a Yap1p dependent manner; the authentic, non-tagged protein is detected in highly purified mitochondria in high-throughput studies.
YHL028W (WSC4)	ER membrane protein involved in the translocation of soluble secretory proteins and insertion of membrane proteins into the ER membrane; may also have a role in the stress response but has only partial functional overlap with WSC1-3.
YLL060C (GTT2)	Glutathione S-transferase capable of homodimerization; functional overlap with Gtt2p, Grx1p, and Grx2p.
YGL158W (RCK1)	Protein kinase involved in the response to OS; identified as suppressor of <i>S. pombe</i> cell cycle checkpoint mutations.
YOL049W (GSH2)	Glutathione synthetase, catalyzes the ATP-dependent synthesis of glutathione (GSH) from gamma-glutamylcysteine and glycine; induced by OS and heat shock.
YLL009C (COX17)	Copper metallochaperone that transfers copper to Sco1p and Cox11p for eventual delivery to cytochrome c oxidase; contains twin cysteine-x9-cysteine motifs
YDL190C (UFD2)	Ubiquitin chain assembly factor (E4) that cooperates with a ubiquitin-activating enzyme (E1), a ubiquitin-conjugating enzyme (E2), and a ubiquitin protein ligase (E3) to conjugate ubiquitin to substrates; also functions as an E3.
YJR104C (SOD1)	Cytosolic copper-zinc superoxide dismutase; some mutations are analogous to those that cause ALS (amyotrophic lateral sclerosis) in humans.
YHR008C (SOD2)	Mitochondrial superoxide dismutase, protects cells against oxygen toxicity.

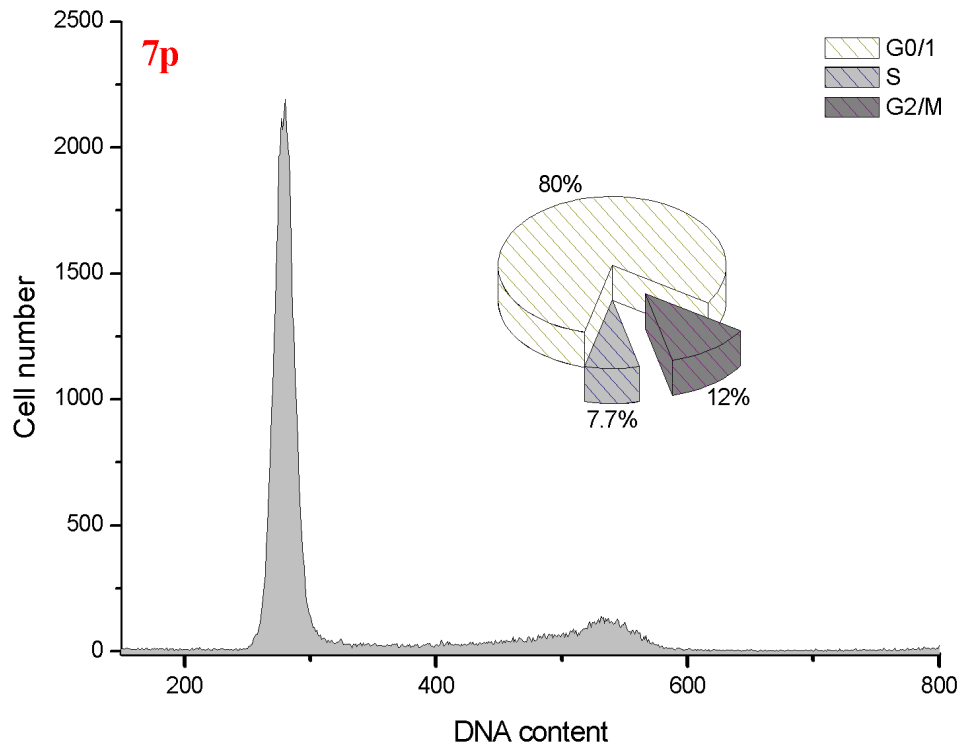
Appendix 28. Immunofluorescence investigations of the ER (panel a and b) and the actin cytoskeleton (panel c and d) of PtK2 cells.



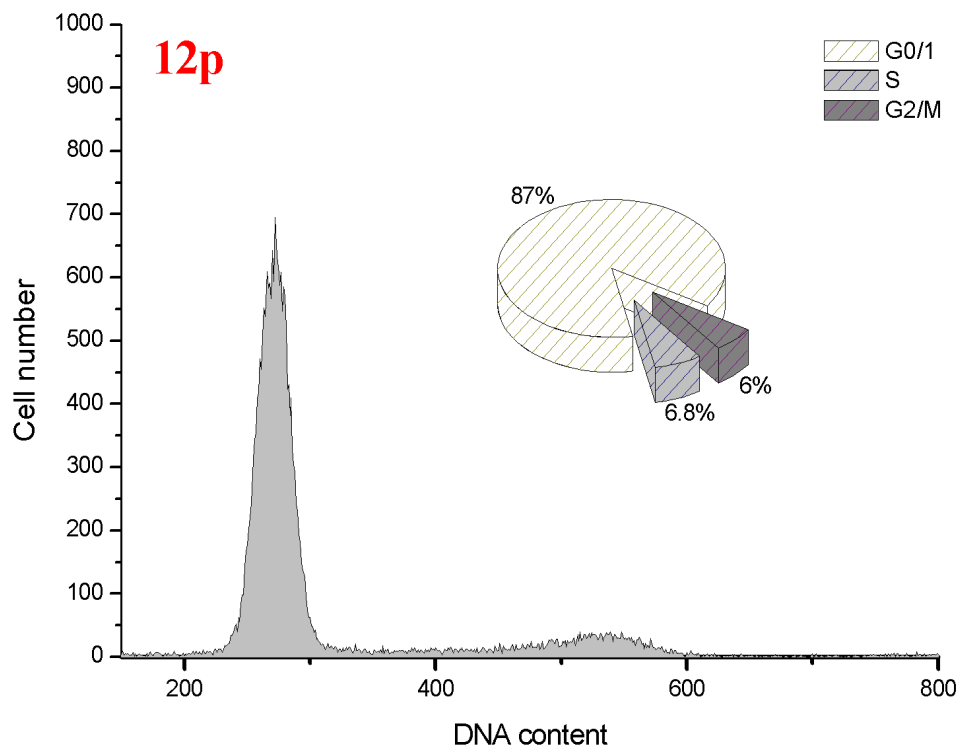
PtK2 cells were incubated with **17p** in comparison with control cells. Treated cells show that the ER is affected in general (panel b) and Actin stress fibers are barely detectable (panel d). Adhesion seems to be reduced and cells become rounded and detached from each other.

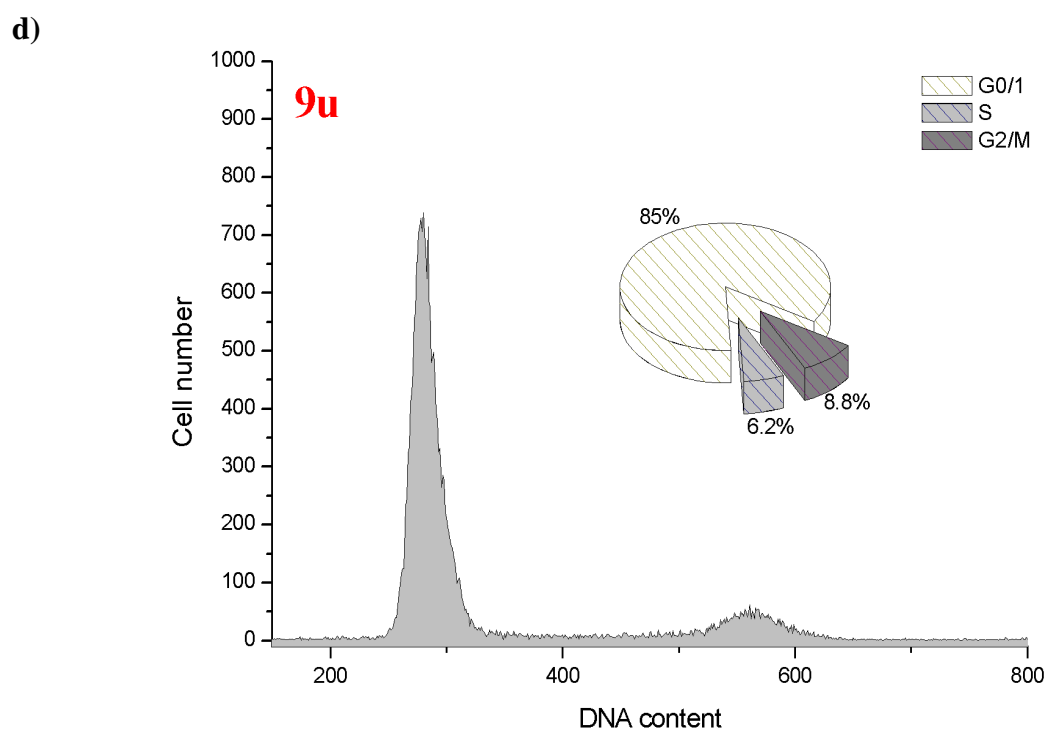
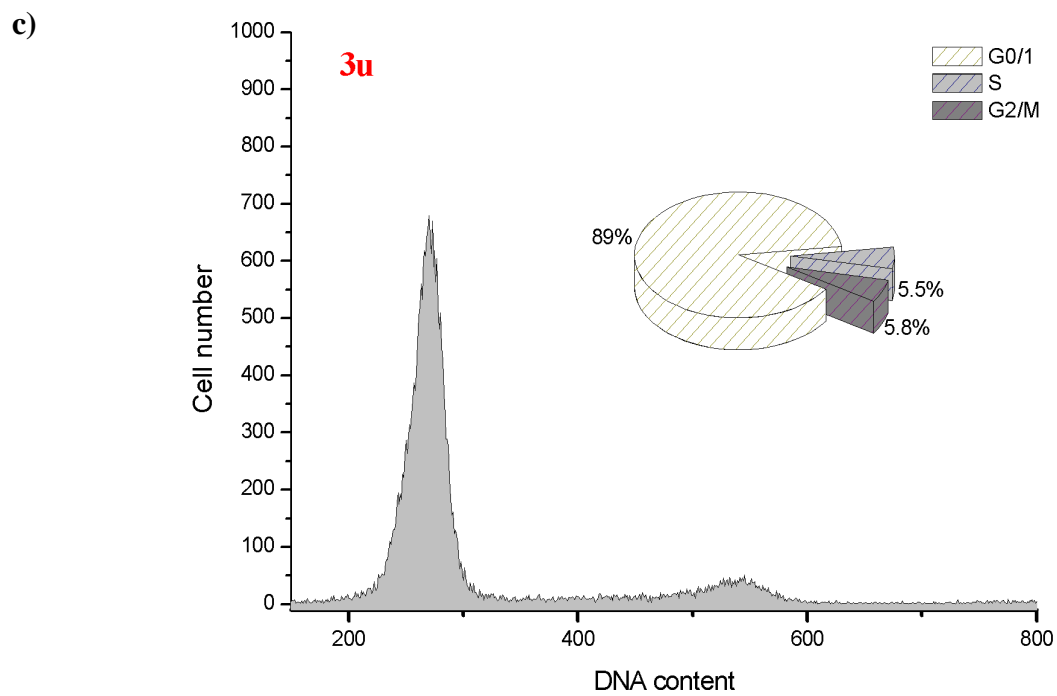
Appendix 29. Cell cycle analysis of MCF-7 breast cancer cells.

a)



b)





MCF-7 cells were treated with **7p** (panel a), **12p** (panel b), **3u** (panel c), and **9u** (panel d) at their respective IC_{50} s for 24 h. The diagrams show the distribution of the cells according to their DNA content. The inserts give the percentages of cells in different cell cycle phases.

Quantitative structure-activity relationship studies (QSAR)

QSAR studies were performed in order to quantitatively correlate the chemical structure of the synthesized compounds to its biological activity (or chemical reactivity). The IC_{50} (μM) values were converted into activities ($\log 1/C$, where C is the IC_{50} in molar concentration) and used as dependent variables for the QSAR models. All the QSAR models were developed by multi-regression analyses (MRA) using the C-QSAR program.¹ The details about this program can be found in earlier publications.^{2,3} Compounds were deemed to be an outlier on the basis of their deviation between the observed and predicted activities obtained from the individual QSAR model ($obsd - pred > 2s$, where s is the standard deviation).⁴ QSARs were validated using statistical diagnostics and internal validation. In statistical diagnostics, QSARs were filtered through a number of specific conditions such as (i) $n/p \geq 4$ (ii) $r^2 > 0.6$ (iii) $q^2 > 0.5$ (iv) $F > F_{(iii)}$ at 95% level (vi) high Q value, and (vii) low s value.^{5,6} The internal validation was carried out using cross-validation and Y-randomization tests.^{7,8} The poor values of r^2 and q^2 in Y-randomization tests (average of the five runs for QSARs; r^2/q^2 : 0.406/-1.021, 0.422/-0.479, 0.259/-0.915, 0.738/0.401, and 0.188/-3.448) ensure the robustness of the QSAR models and also the lack of over fitting. Due to the small data sets, the external validation test was not performed.

References

1. C-QSAR Program, BioByte Corp., 201W. 4th st., Suit 204, Claremont, USA. **2003**, CA 91711, www.biobyte.com.
2. Hansch, C.; Hoekman, D.; Leo, A.; Weininger, D.; Selassie, C.D. Chem-Bioinformatics: Comparative QSAR at the interface between chemistry and biology. *Chem. Rev.* **2002**, 102, 783–812.
3. Verma, R. P.; Hansch, C. Development of QSAR models using C-QSAR program: a regression program that has dual databases of over 21,000 QSAR models. *Nat. Protoc.* **2007**.
4. Selassie, C. D.; Kapur, S.; Verma, R. P.; Rosario, M. Cellular apoptosis and cytotoxicity of phenolic compounds: a quantitative structure-activity relationship study. *J. Med. Chem.* **2005**, 48, 7234–7242.

5. Bennett, C. A.; Franklin, N. L. Statistical Analysis in Chemistry and the Chemical Industry. *John Wiley & Sons: New York*. **1967**; 708–709; 5th printing.
6. Hansch, C.; Verma, R. P. 20-(S)-Camptothecin analogues as DNA Topoisomerase I inhibitors: A QSAR study. *Chem. Med. Chem.* **2007**, 2, 1807-1813.
7. Tropsha, A.; Gramatica, P.; Gombar, V. K. The importance of being earnest: Validation is the absolute essential for successful application and interpretation of QSPR models. *QSAR Comb. Sci.* **2003**, 22, 69–77.
8. Wold, S.; Eriksson, L. Statistical validation of QSAR results. Validation tools. In: van de Waterbeemd H., editor. *Chemometrics Methods in Molecular Design (Methods and Principles in Medicinal Chemistry, Vol 2)*. Weinheim, Germany: VCH, **1995**; 309–318.

Appendix 30. Terms and abbreviations used as in the development of QSAR models

Abbreviations	Details
QSAR	Quantitative structure activity relationship
Activity	$\log 1/C$, where C is the IC_{50} in molar concentration
MRA	Multi-regression analyses
n	Number of data points
r^2	Square of the correlation coefficient
q^2	Cross-validated r^2
s	Standard deviation
Q	Quality factor
F	Fischer ratio
P_{ow}	Experimental partition coefficient of the compound in octanol-water system
$\log P_{ow}$	Measure of hydrophobicity
HBA	Number of hydrogen bond acceptors
NOR	Number of rings
RC	Number of redox centres

Appendix 19. QSAR models for the multifunctional redox compounds on the viability and proliferation of human cancer cell lines and primary human endothelium cell lines.

QSAR Nr.	Cell lines	QSAR Models [C = IC ₅₀ (mol/L)]	Statistics						Outliers (Cpd.Nr.)
			n	r ²	q ²	s	Q	F	
1	MCF-7	$\log 1/C = -0.27(\pm 0.15)\log Pow + 0.12(\pm 0.07)HBA + 4.84(\pm 0.81)$	11	0.808	0.715	0.159	5.654	16.834	2p
2	A-498	$\log 1/C = -0.09(\pm 0.07)HBA + 6.04(\pm 0.64)$	6	0.783	0.603	0.066	13.409	14.433	9p and 11p
3	A-431	$\log 1/C = -0.12(\pm 0.07)NOR + 5.70(\pm 0.22)$	6	0.855	0.727	0.063	14.682	23.586	2p, 4p and 10p
4	HUVEC	$\log 1/C = -0.33(\pm 0.22)\log Pow + 0.37(\pm 0.22)RC + 4.74(\pm 1.25)$	9	0.913	0.798	0.182	5.247	31.483	2p, 7p and 12p
5	HF	$\log 1/C = 1.68(\pm 0.69)HBA - 0.09(\pm 0.04)HBA2 - 2.45(\pm 3.03)$ Optimum HBA = 9.16(8.73-9.68)	8	0.887	0.738	0.147	6.408	19.624	1p, 3p and 5p

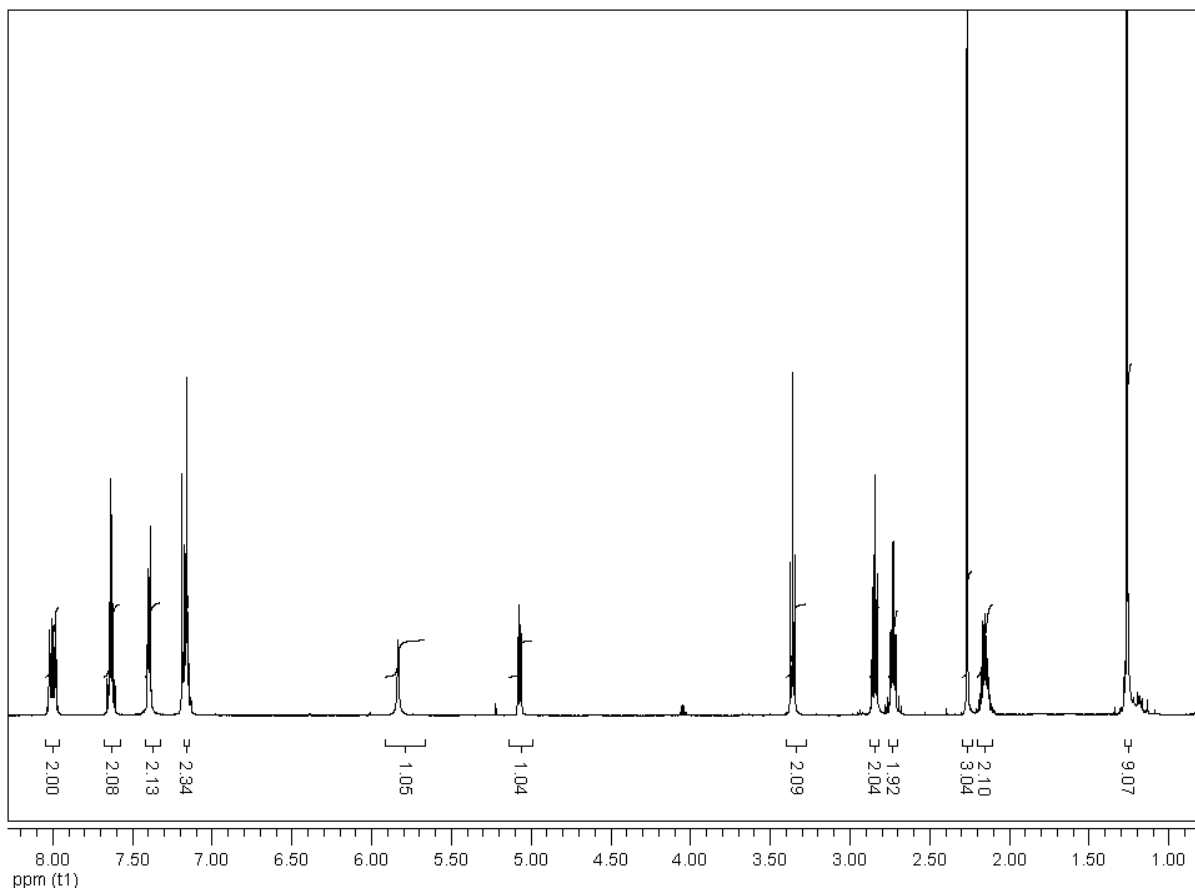
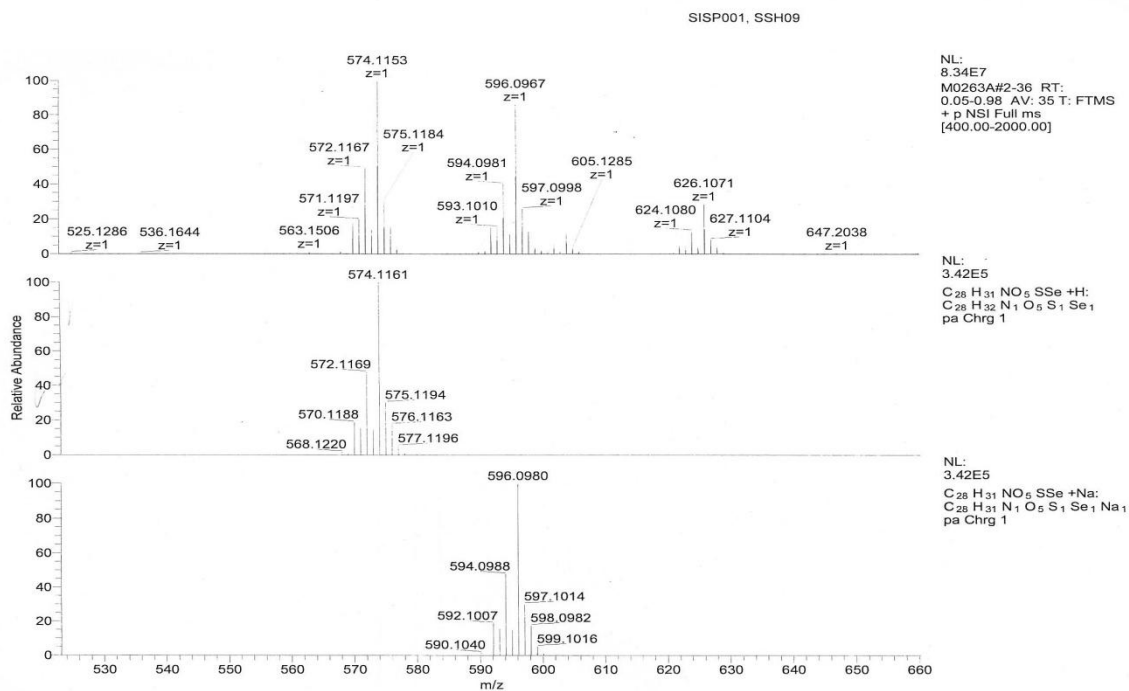
Appendix 20. Biological, Physicochemical, and structural parameters used to derive QSARs 1-5.

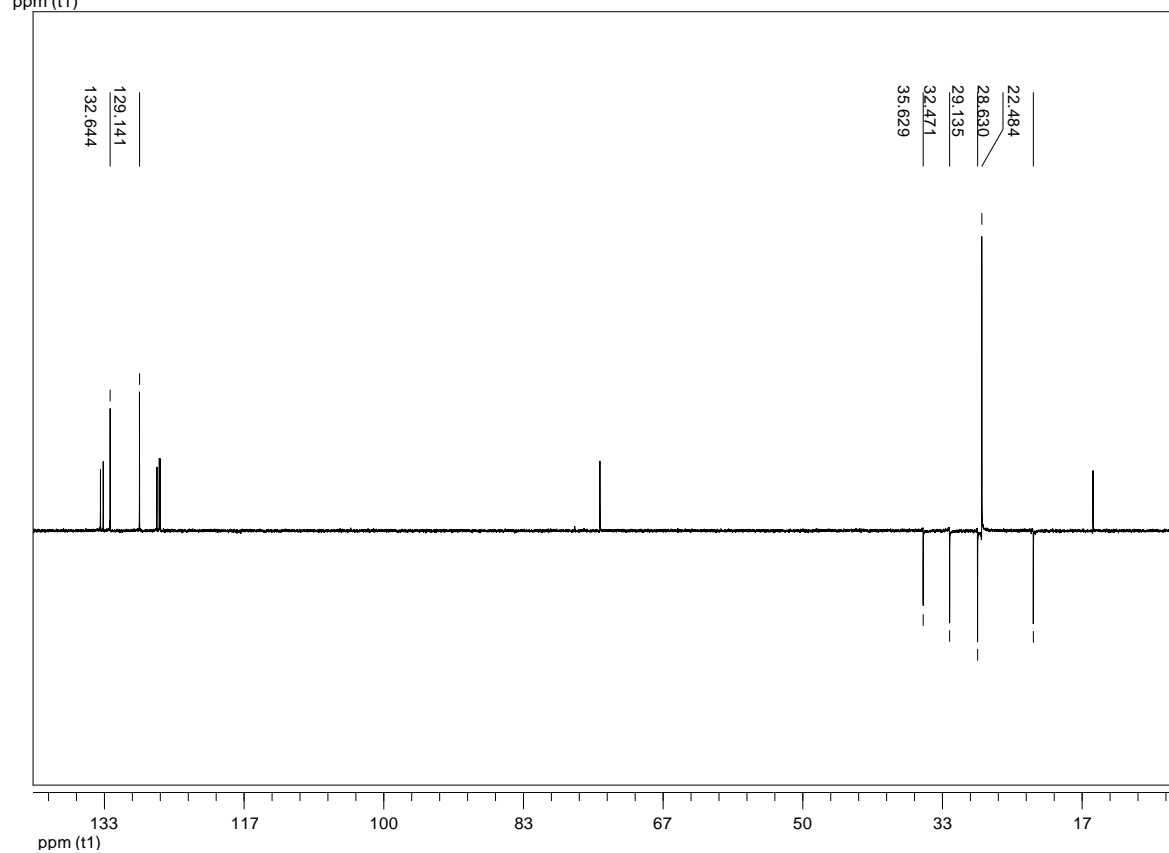
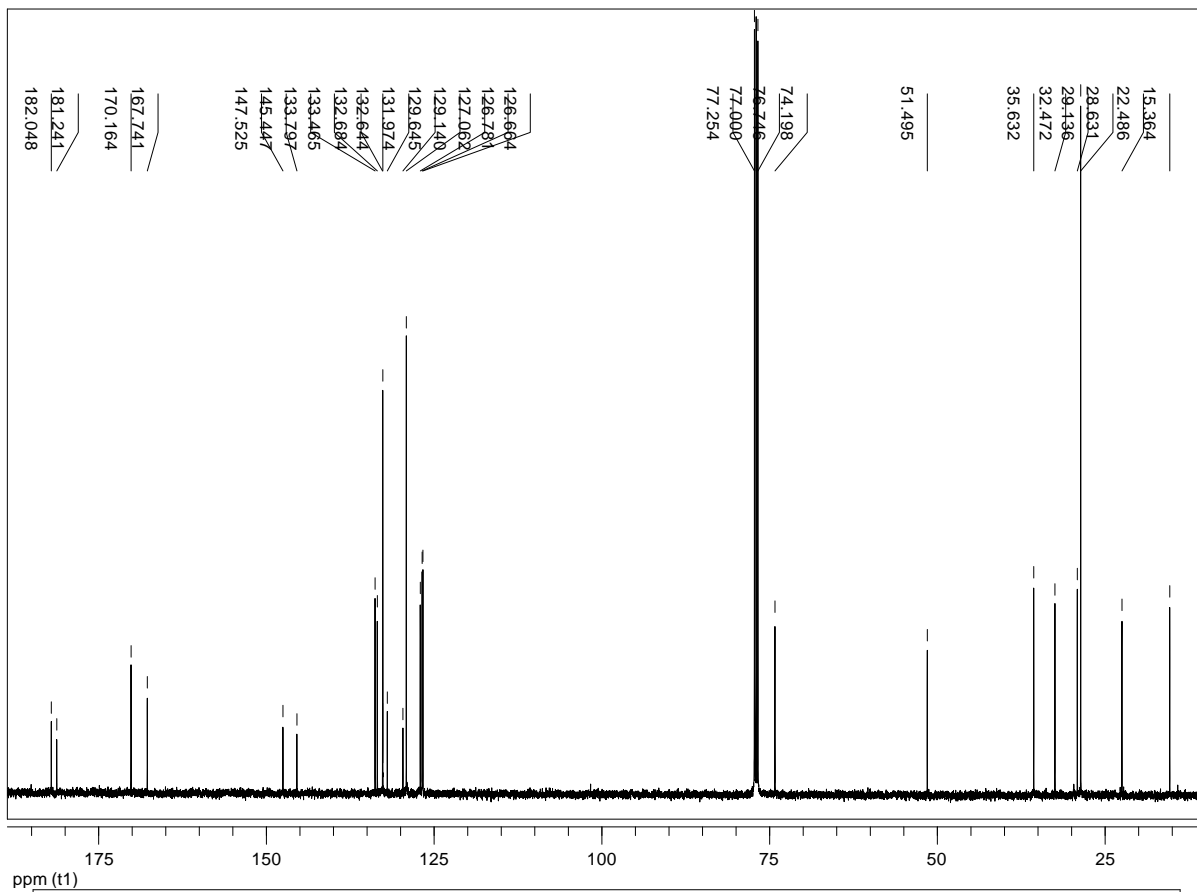
Cpd. Nr.	log 1/C (QSAR 1)		log 1/C (QSAR 2)		log 1/C (QSAR 3)		log 1/C (QSAR 4)		log 1/C (QSAR 5)		log P _{ow}	HBA	NOR	RC
	Obsd.	Pred.												
	1p	4.34	4.33	NA	5.48	NA	5.35	4.64	4.39	4.72a				
2p	4.60a	5.03	NA	5.48	4.90a	5.35	4.22a	5.23	4.33	4.32	1.94	6	3	3
3p	4.85	4.86	NA	5.29	NA	5.23	4.49	4.74	4.15a	5.11	3.42	8	4	3
4p	5.34	5.27	5.34	5.29	5.81a	5.23	5.81	5.61	NA	5.11	1.92	8	4	4
5p	4.58	4.84	NA	5.29	NA	5.23	4.63	4.72	4.54a	5.11	3.50	8	4	3
6p	4.90	5.06	5.20	5.11	5.13	5.11	5.06	5.06	5.20	5.17	3.60	10	5	4
7p	5.29	5.03	5.07	5.11	5.46	5.47	5.29a	4.28	4.92	5.17	3.70	10	2	2
8p	5.36	5.38	5.14	5.20	5.54	5.47	5.54	5.58	5.23	5.23	1.99	9	2	4
9p	5.16	5.27	5.16a	4.92	5.26	5.35	4.32	4.28	4.43	4.50	3.70	12	3	2
10p	5.24	5.15	5.00	5.01	5.15a	5.35	4.29	4.28	5.07	4.92	3.70	11	3	2
11p	5.01	5.03	4.80a	5.11	5.31	5.35	4.91	5.03	5.31	5.17	3.70	10	3	4
12p	4.92	4.79	5.28	5.29	5.28	5.23	5.40a	4.65	5.10	5.11	3.70	8	4	3

^aNot included in the derivation of QSAR models; C = IC₅₀ [mol/l]

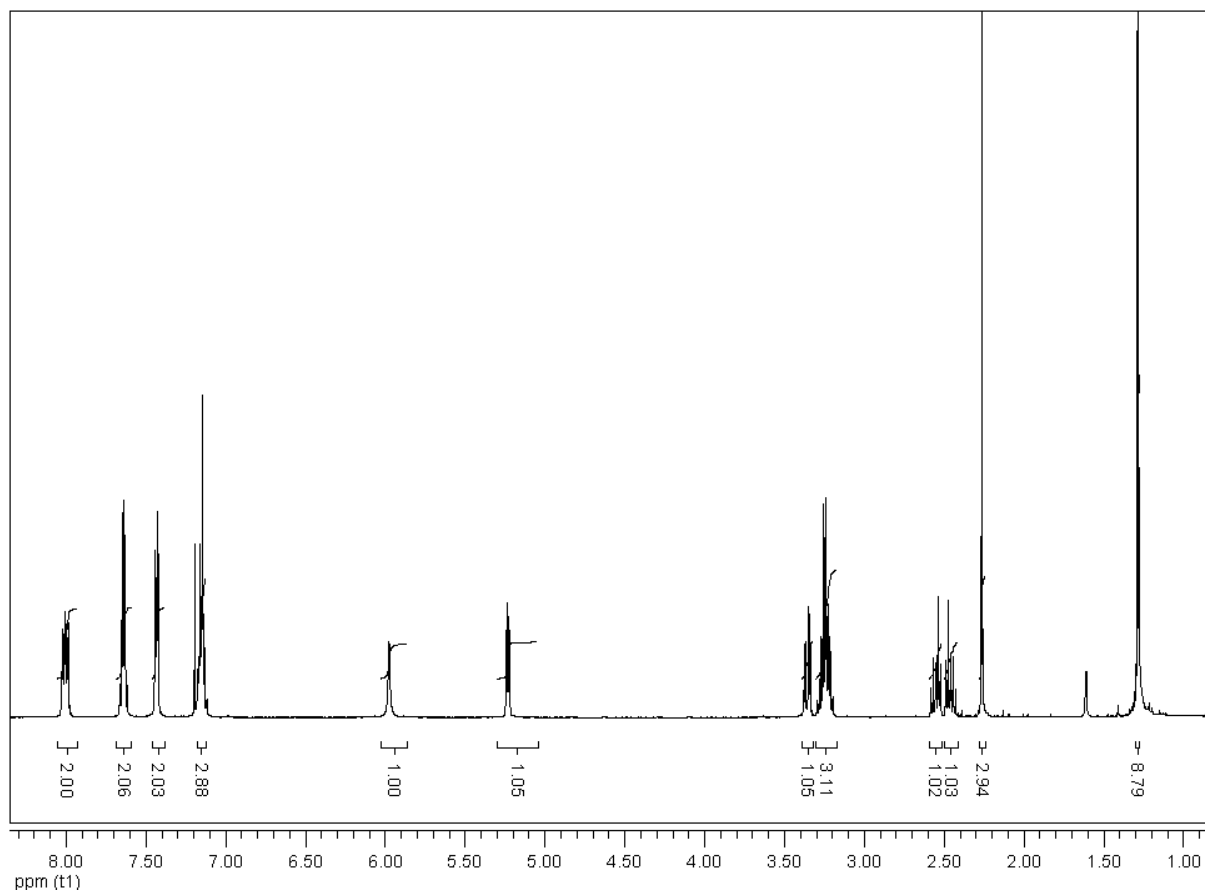
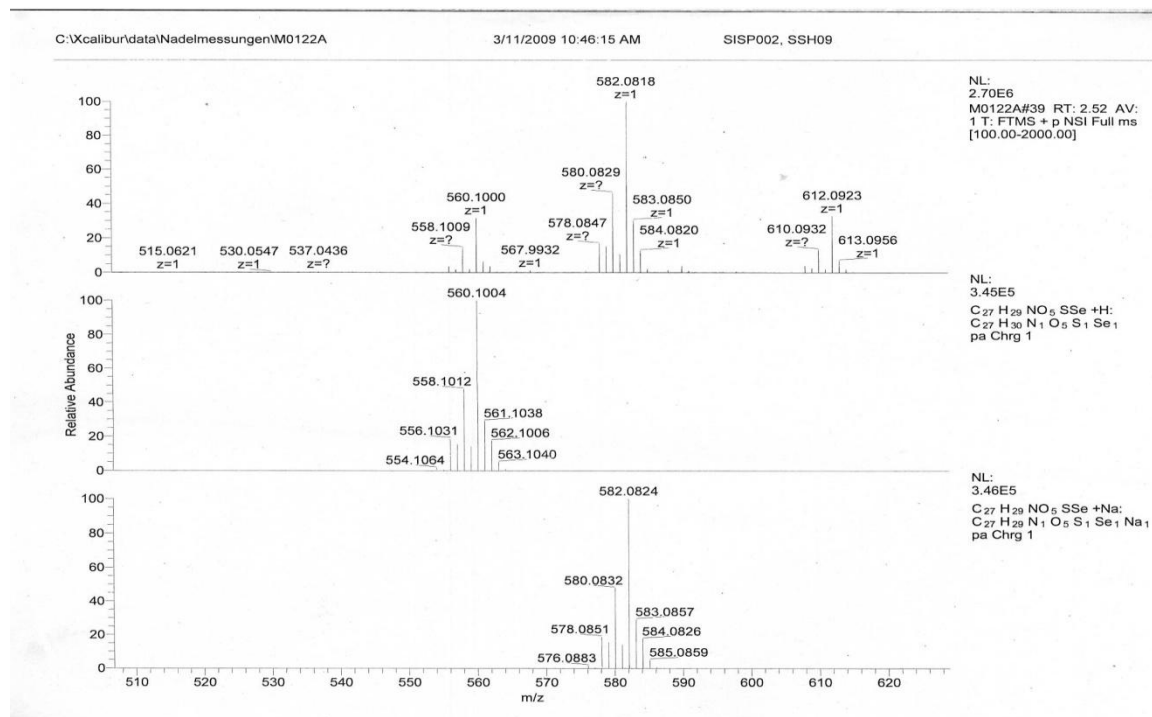
Appendix 21. High resolution mass, ^1H NMR, ^{13}C NMR and ^{13}C DEPT-135 spectra of novel compounds.

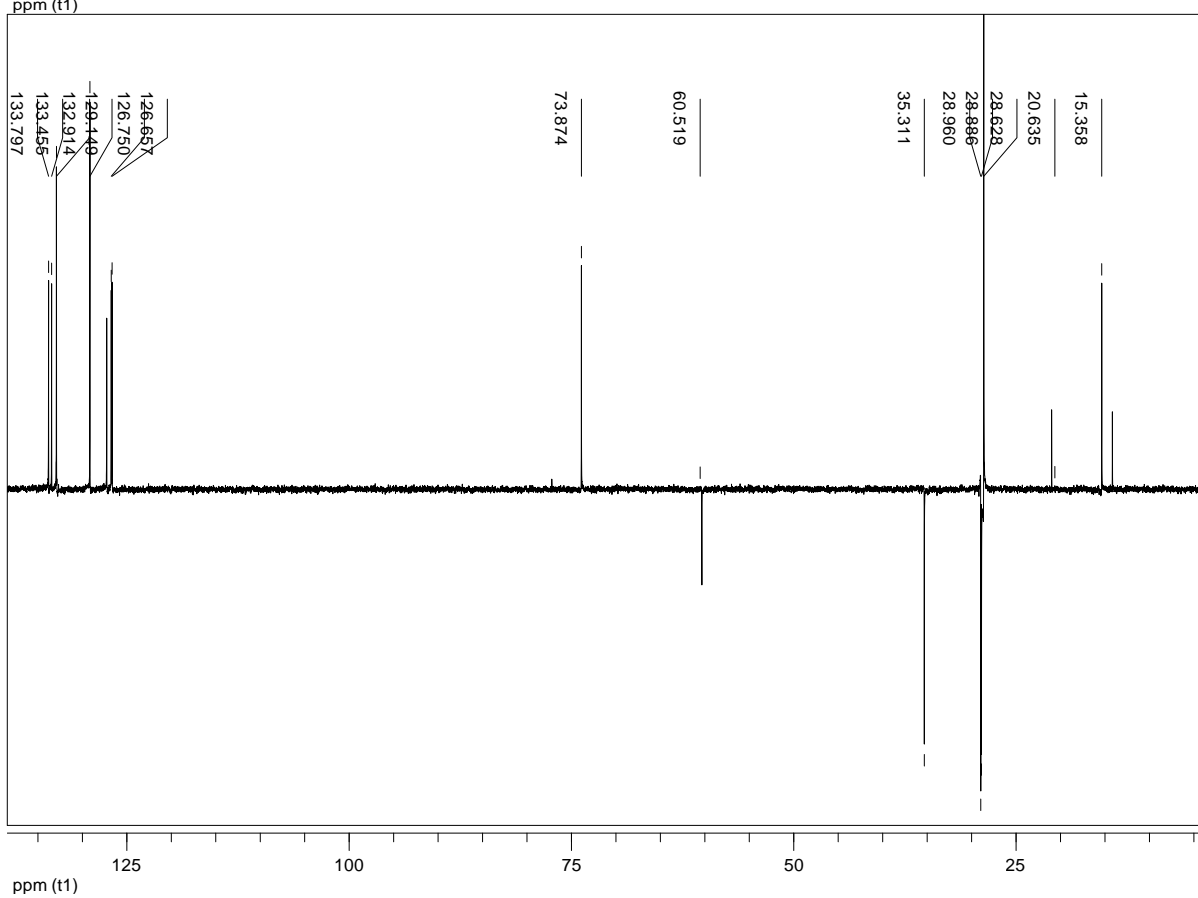
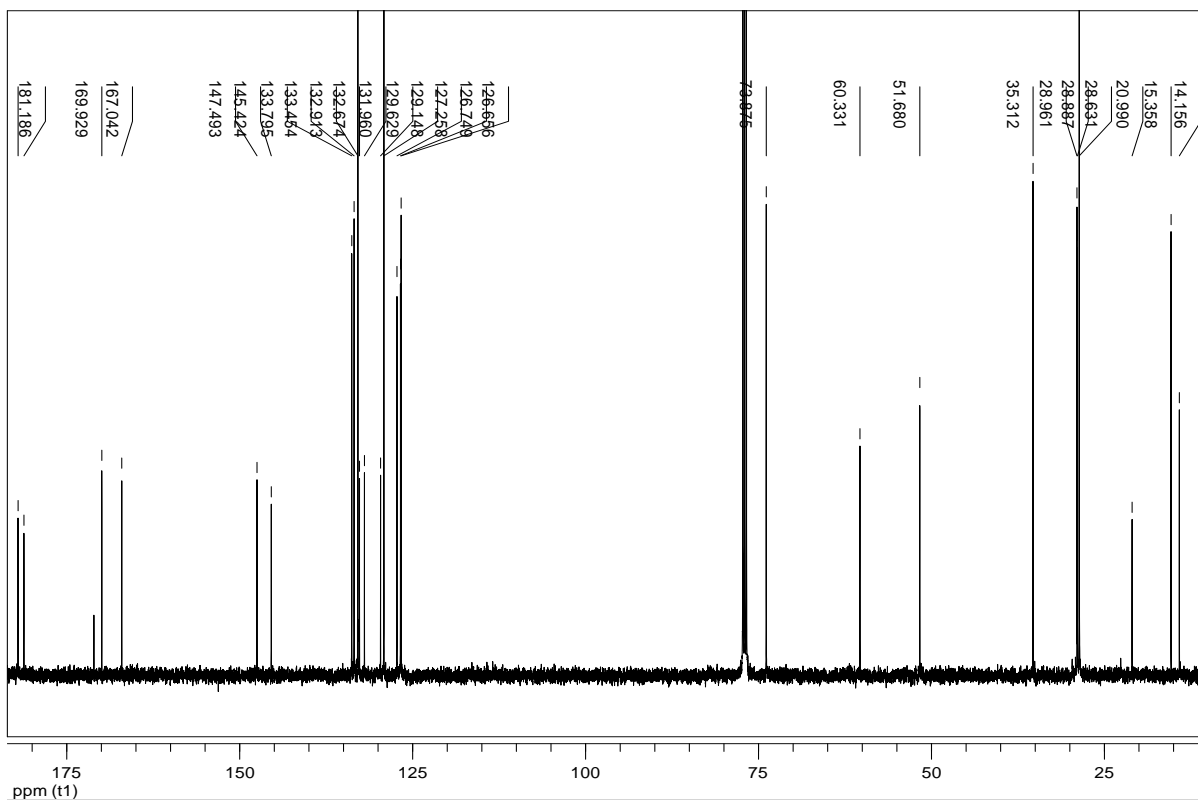
Compound 1p





Compound2p



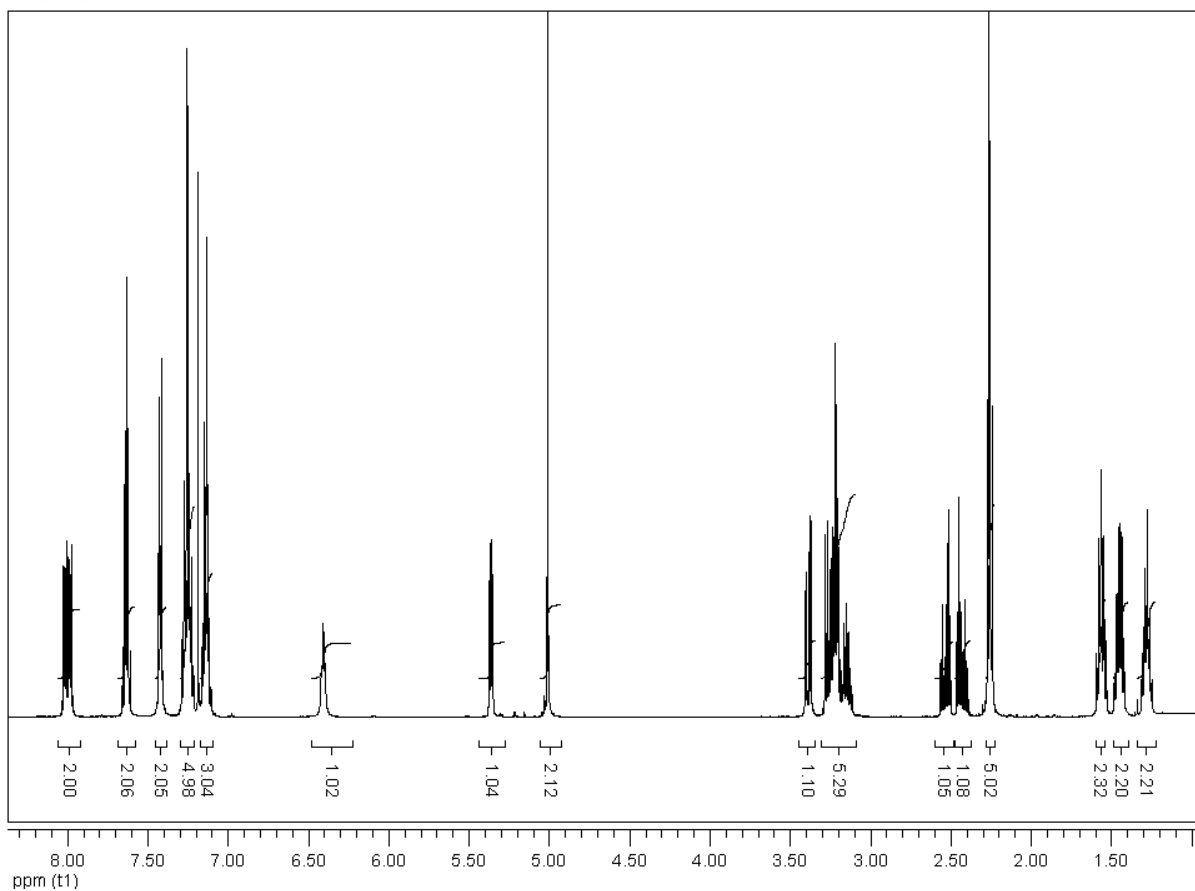
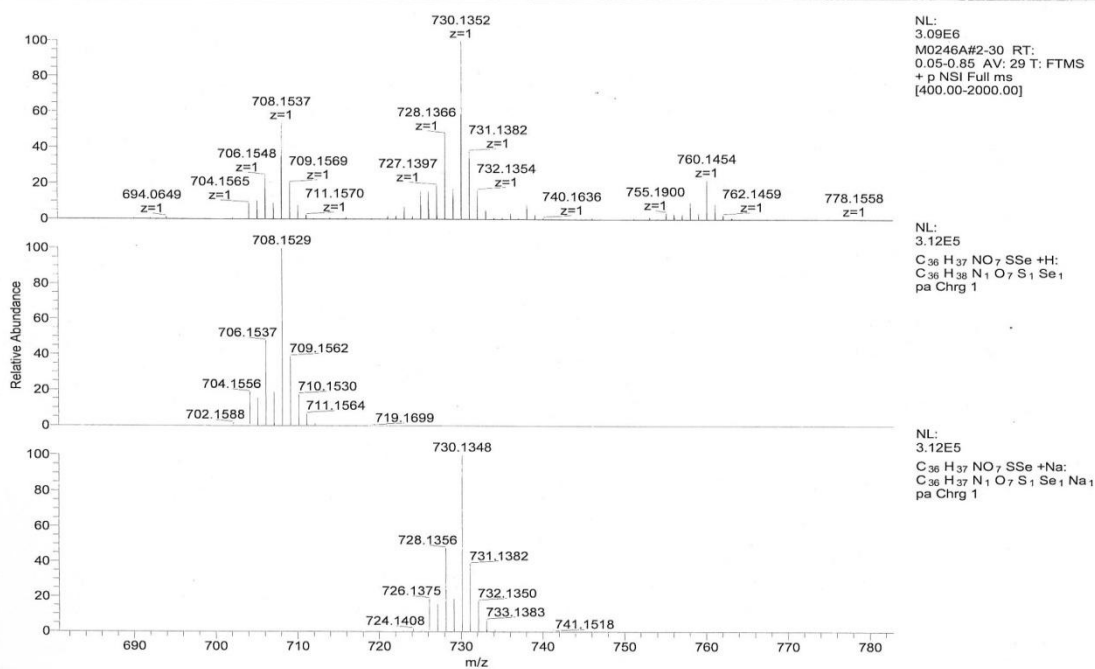


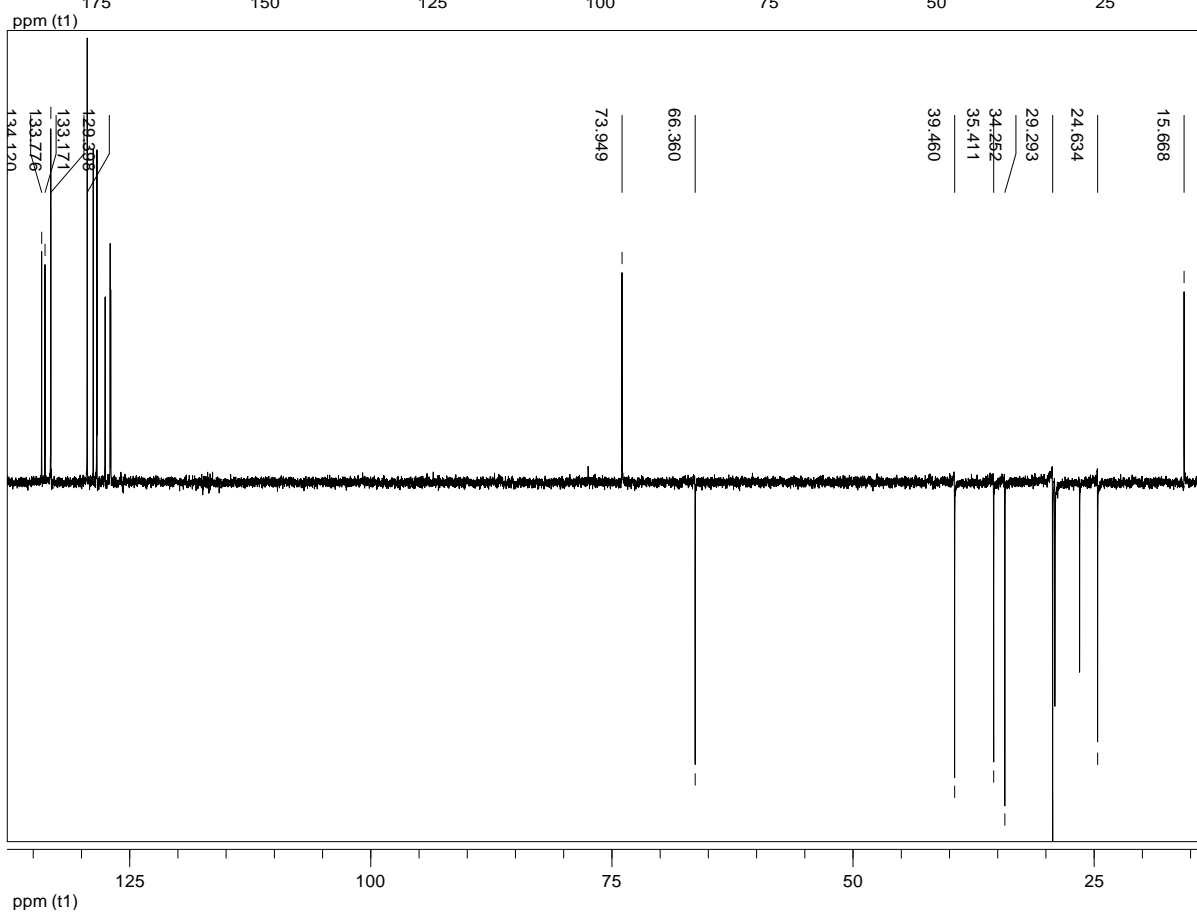
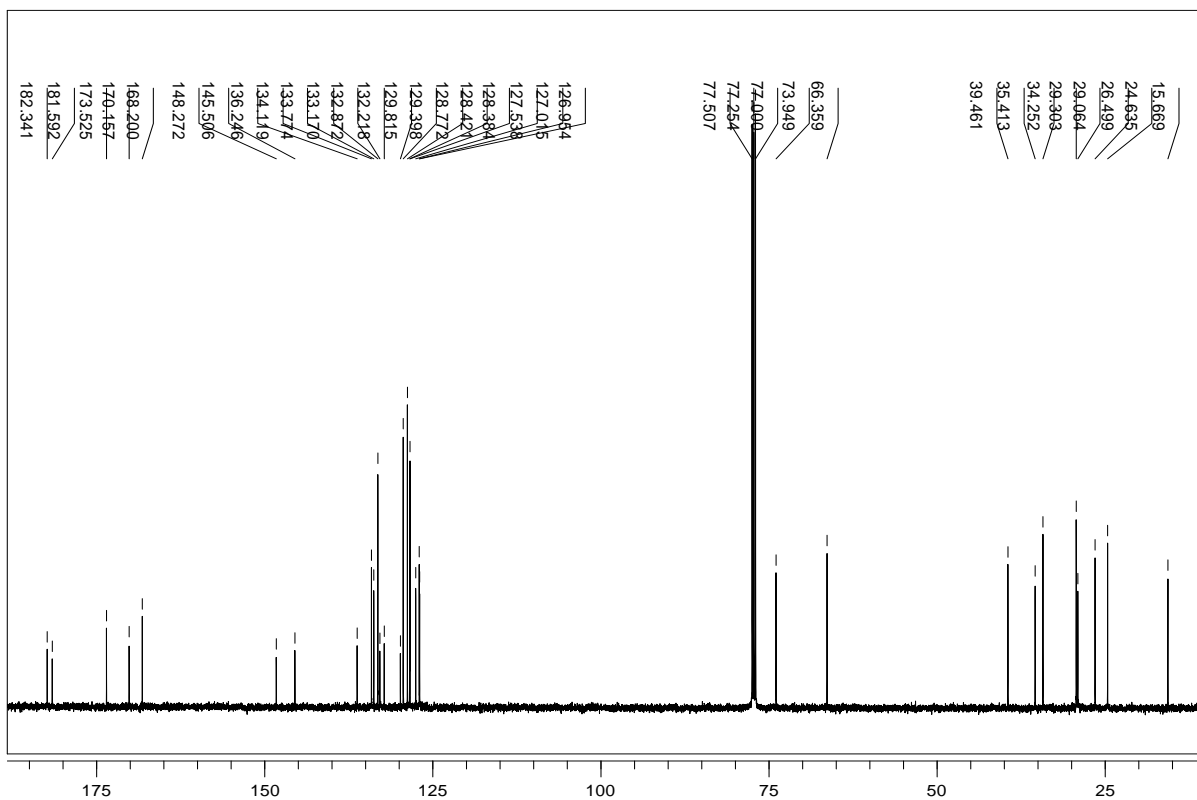
Compound 3p

C:\Xcalibur\data\Nadelmessungen\M0246A

8/25/2009 10:41:13 AM

SISP003, SSH09



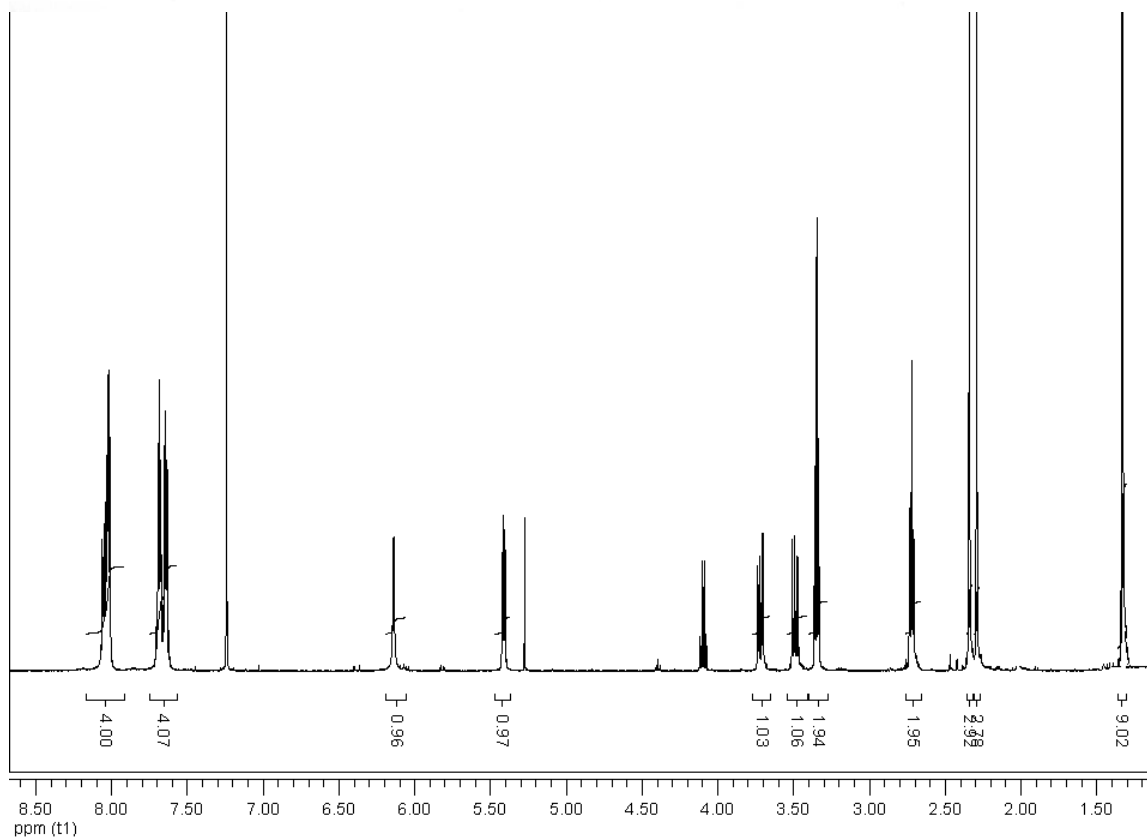
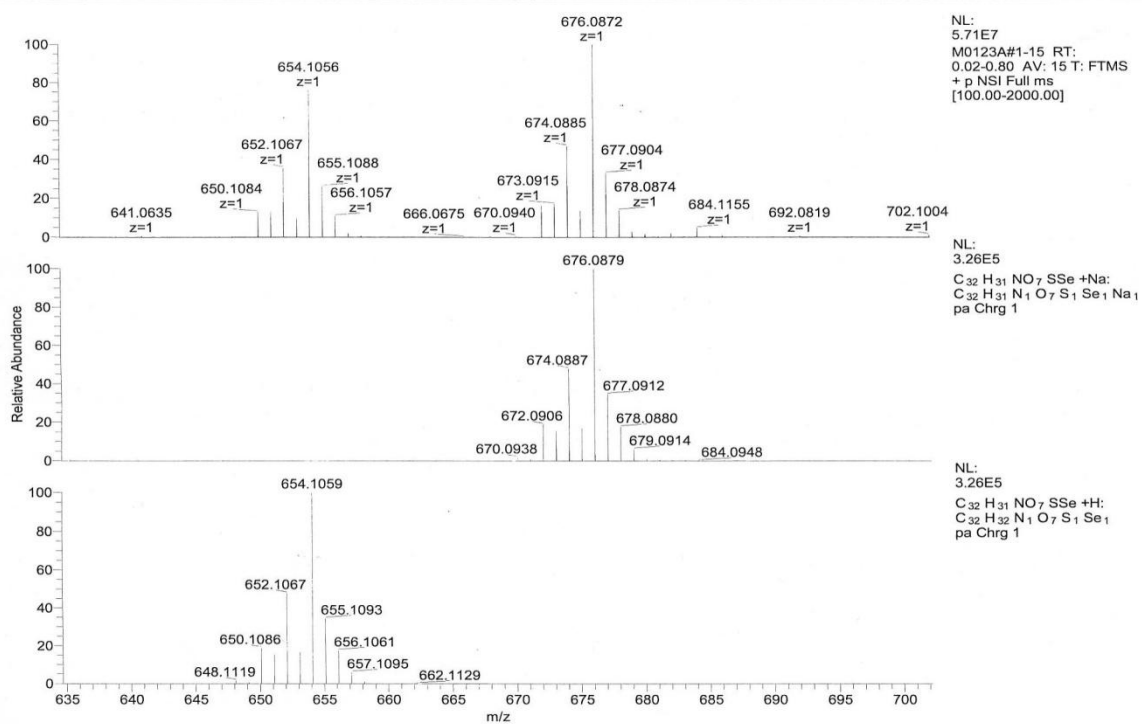


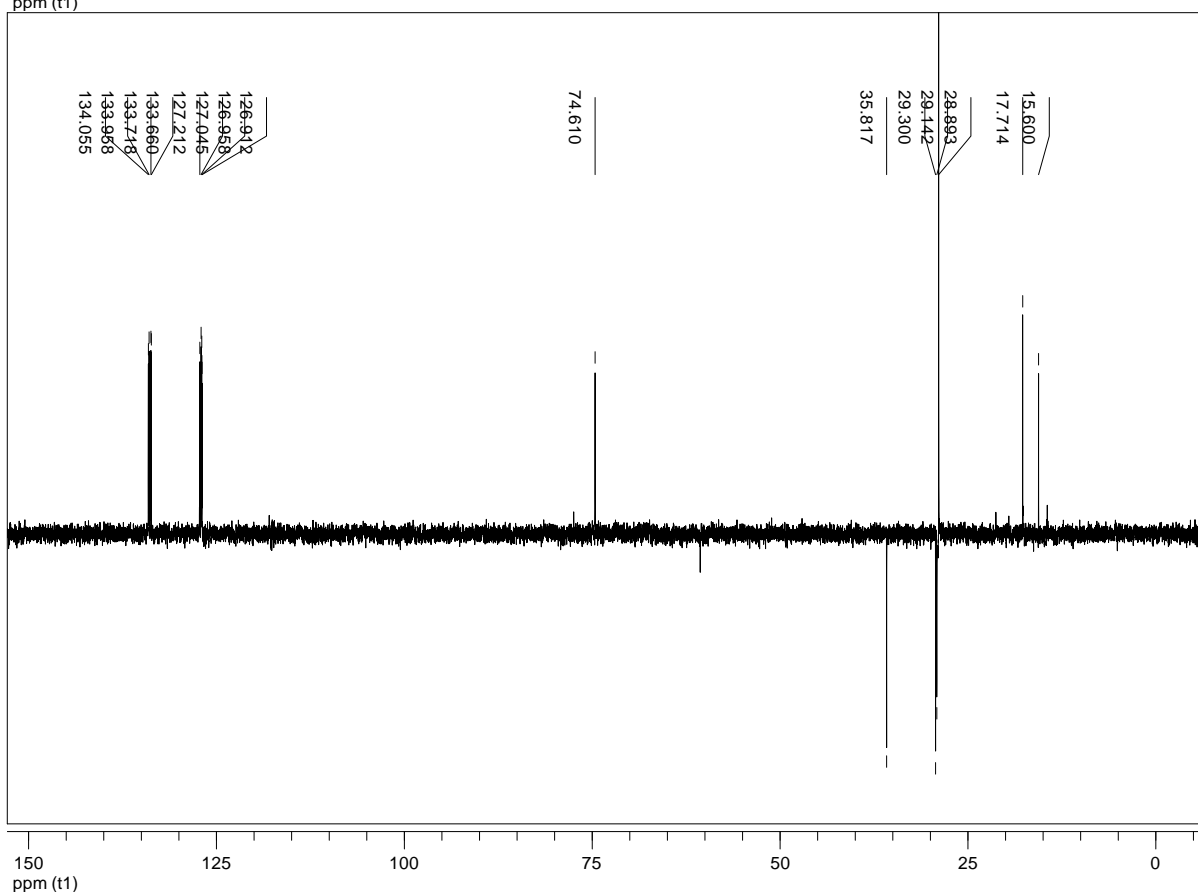
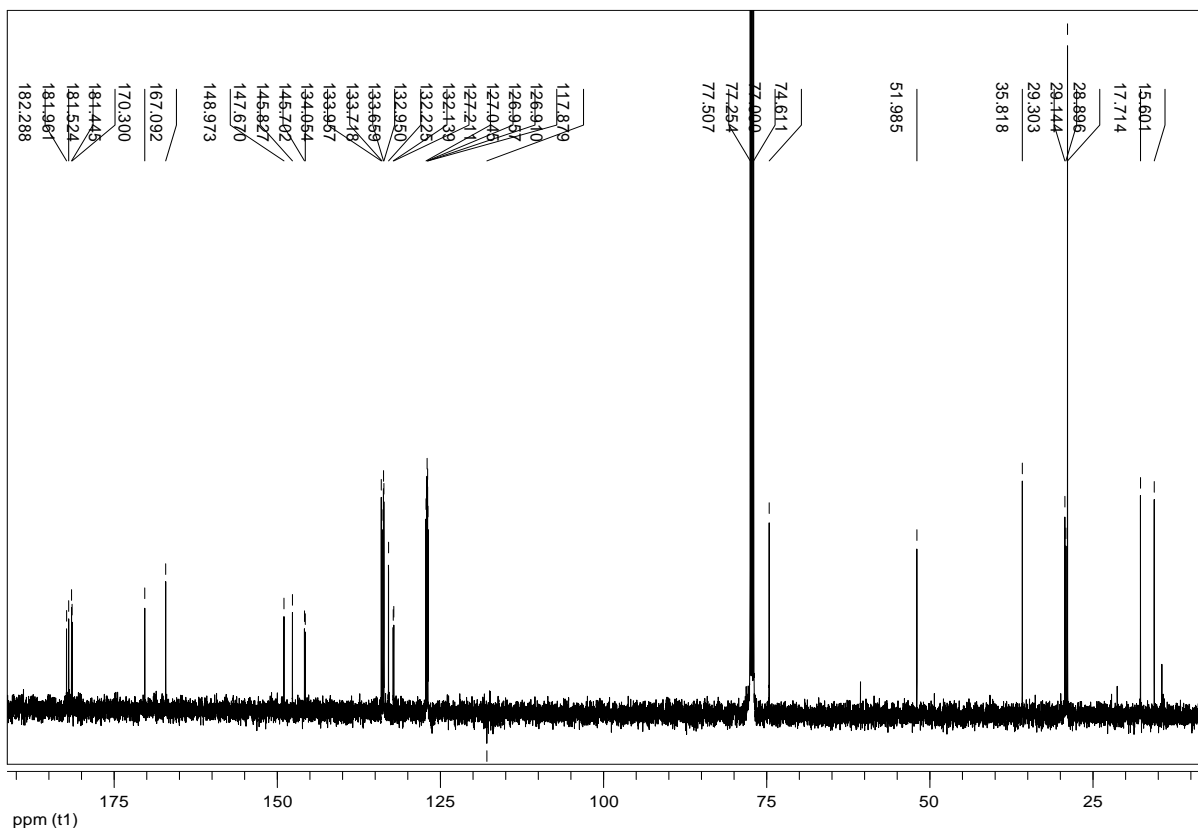
Compound 4p

C:\Xcalibur\data\Nadelmessungen\M0123A

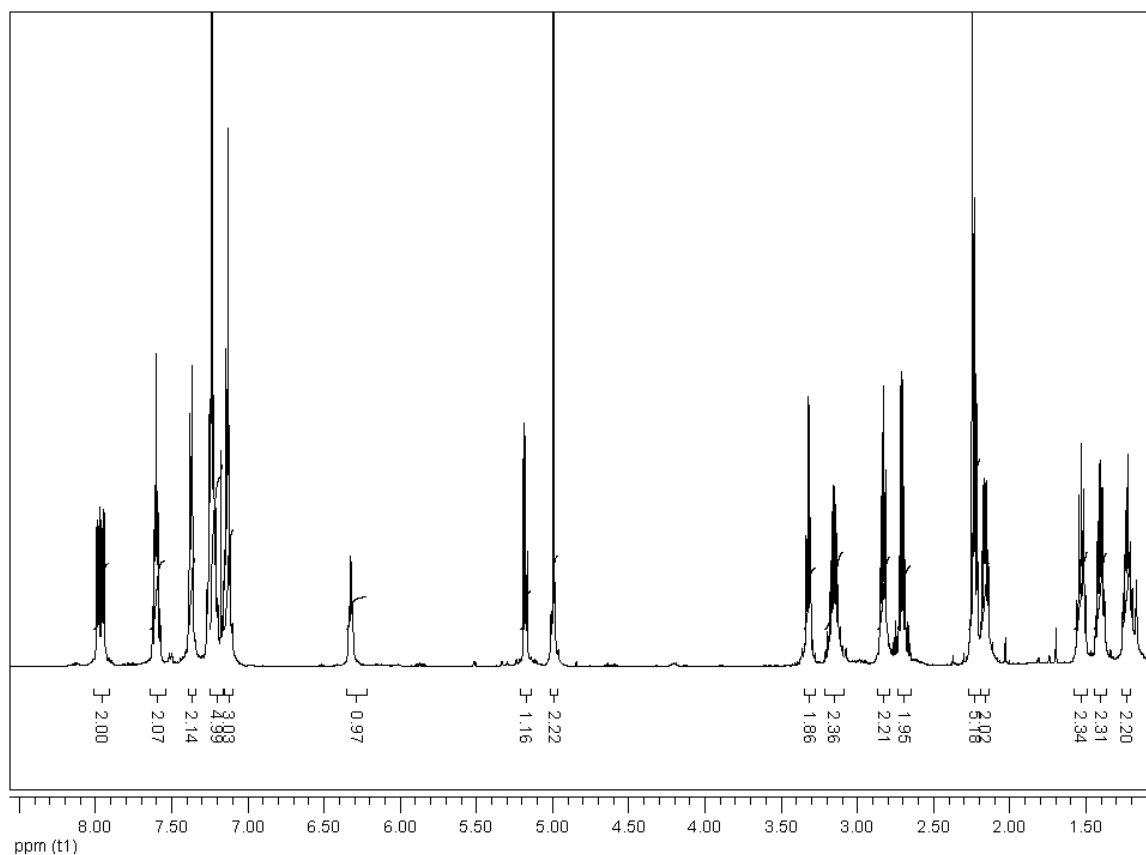
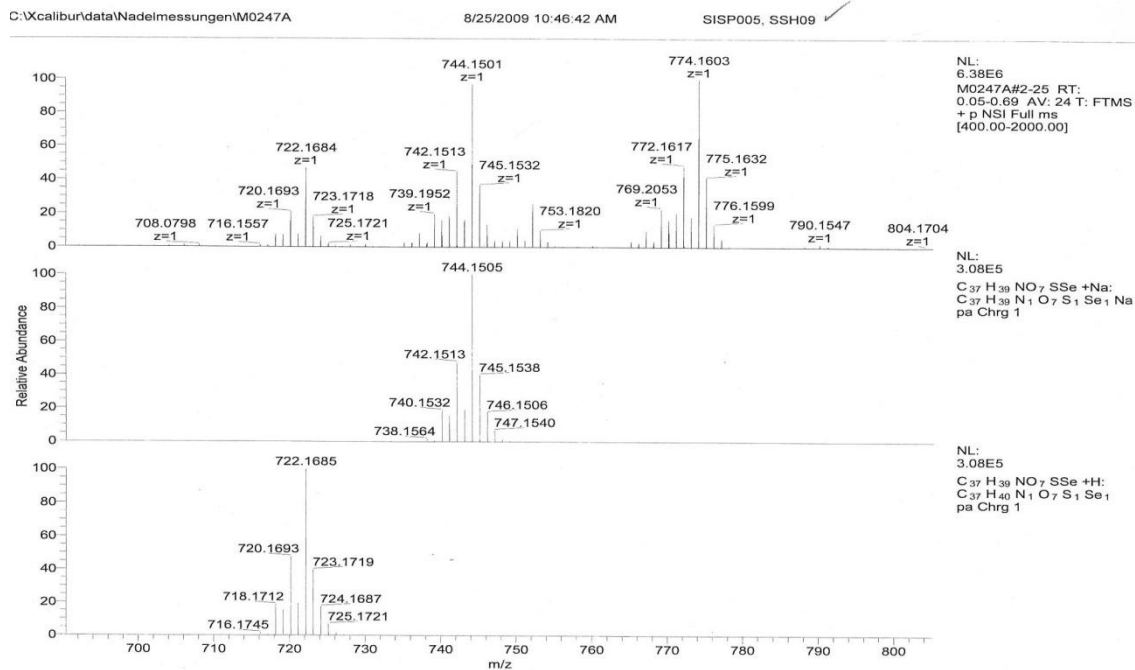
3/11/2009 11:08:52 AM

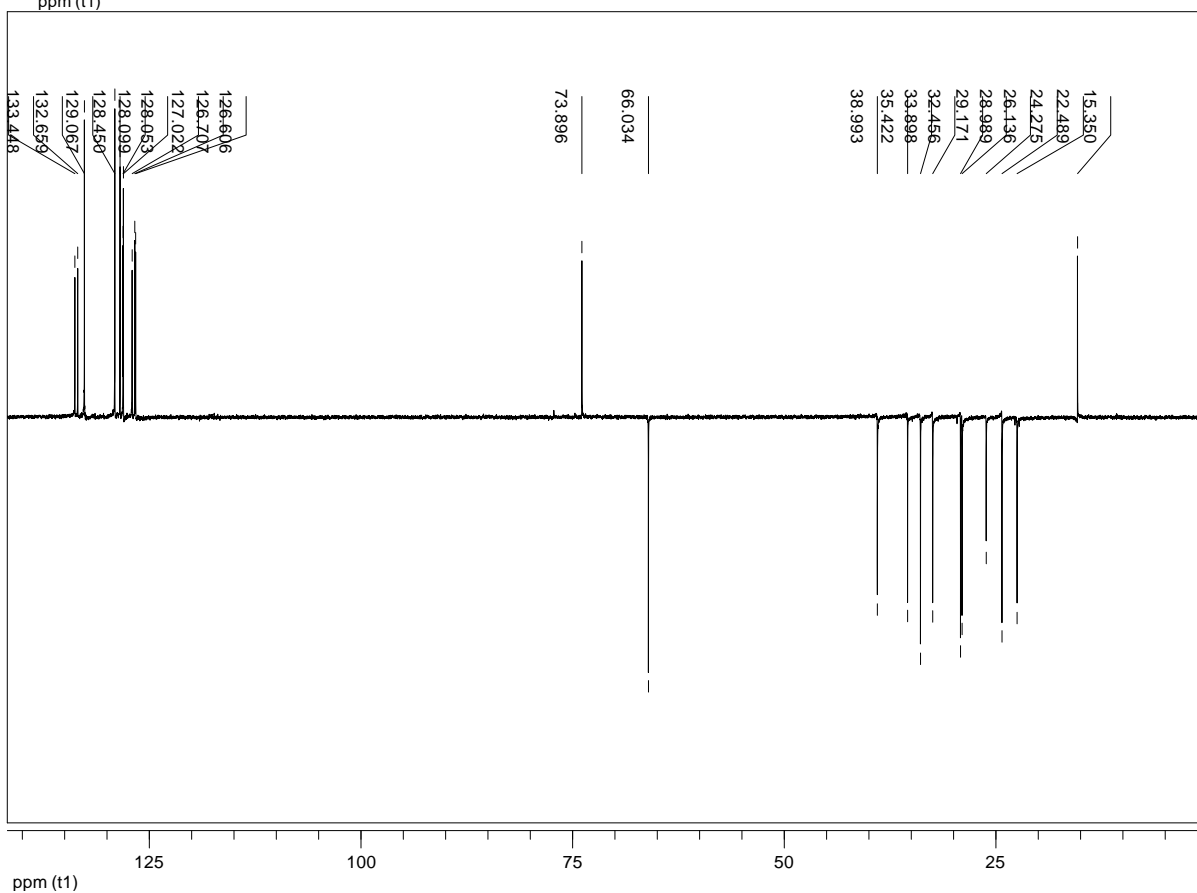
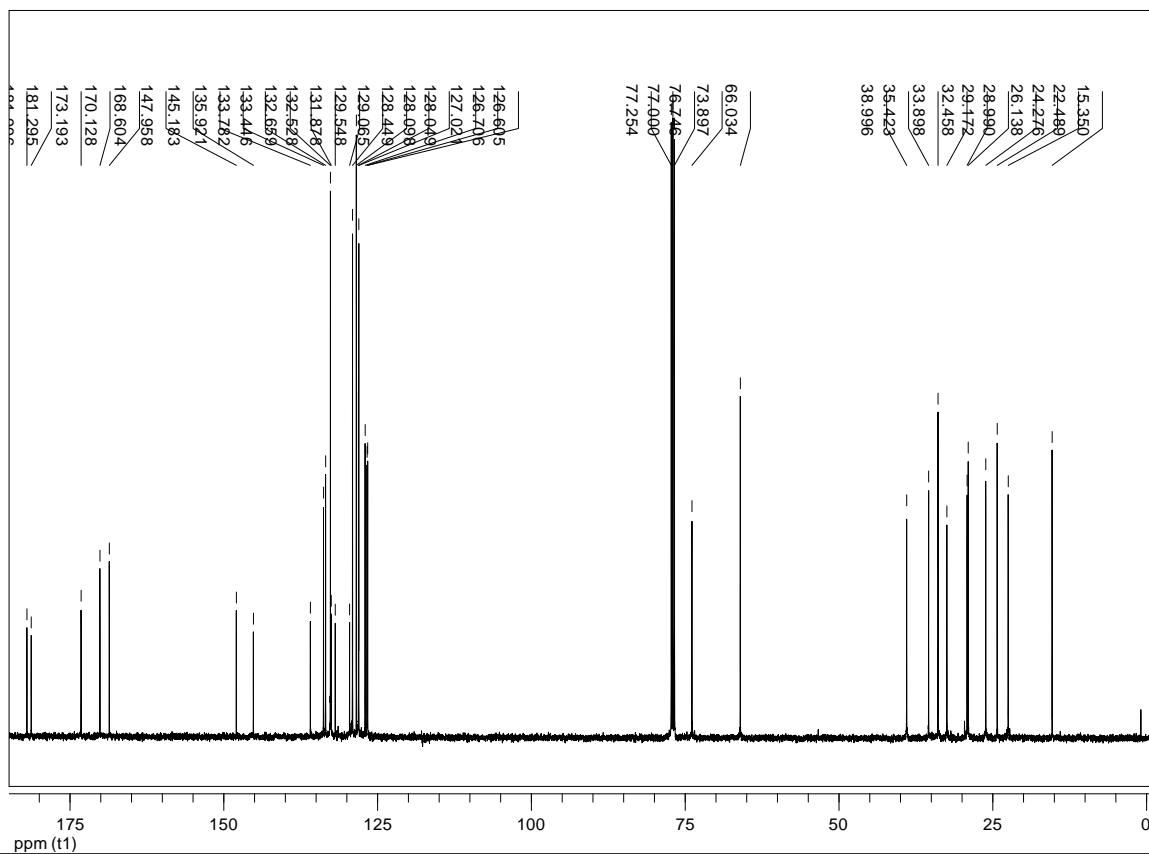
SISP004, SSH09



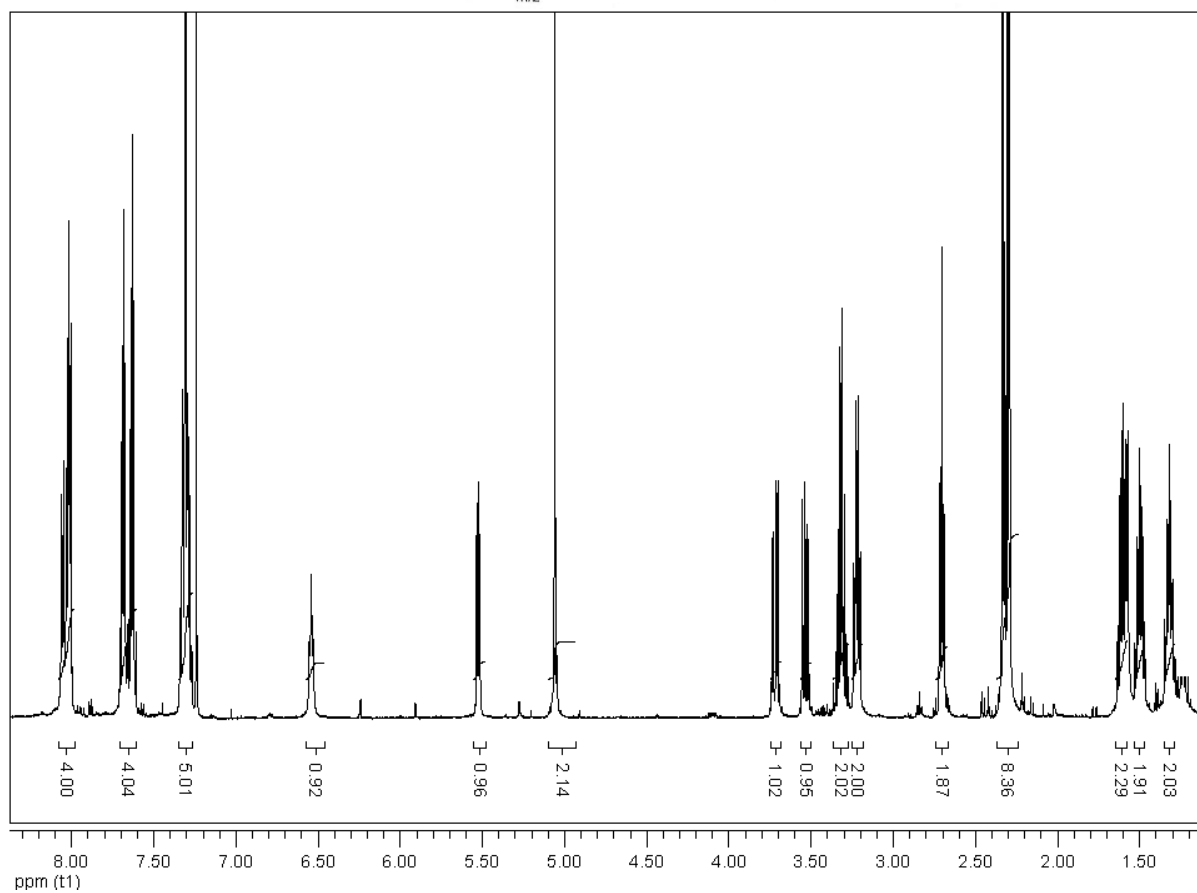
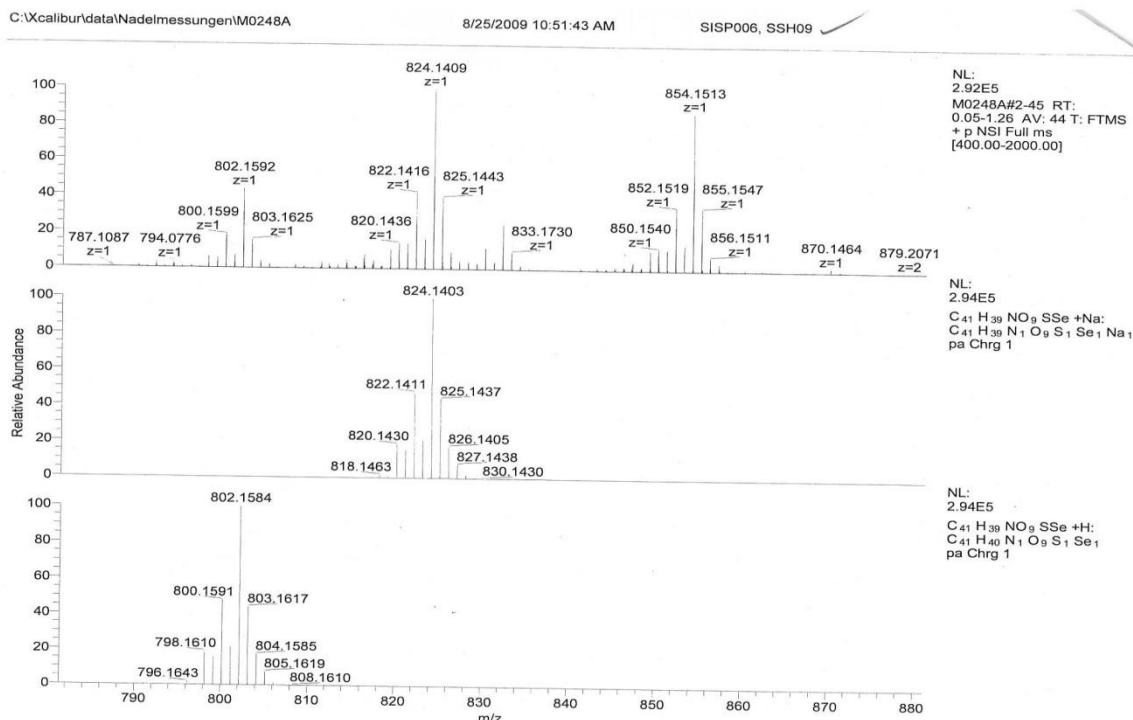


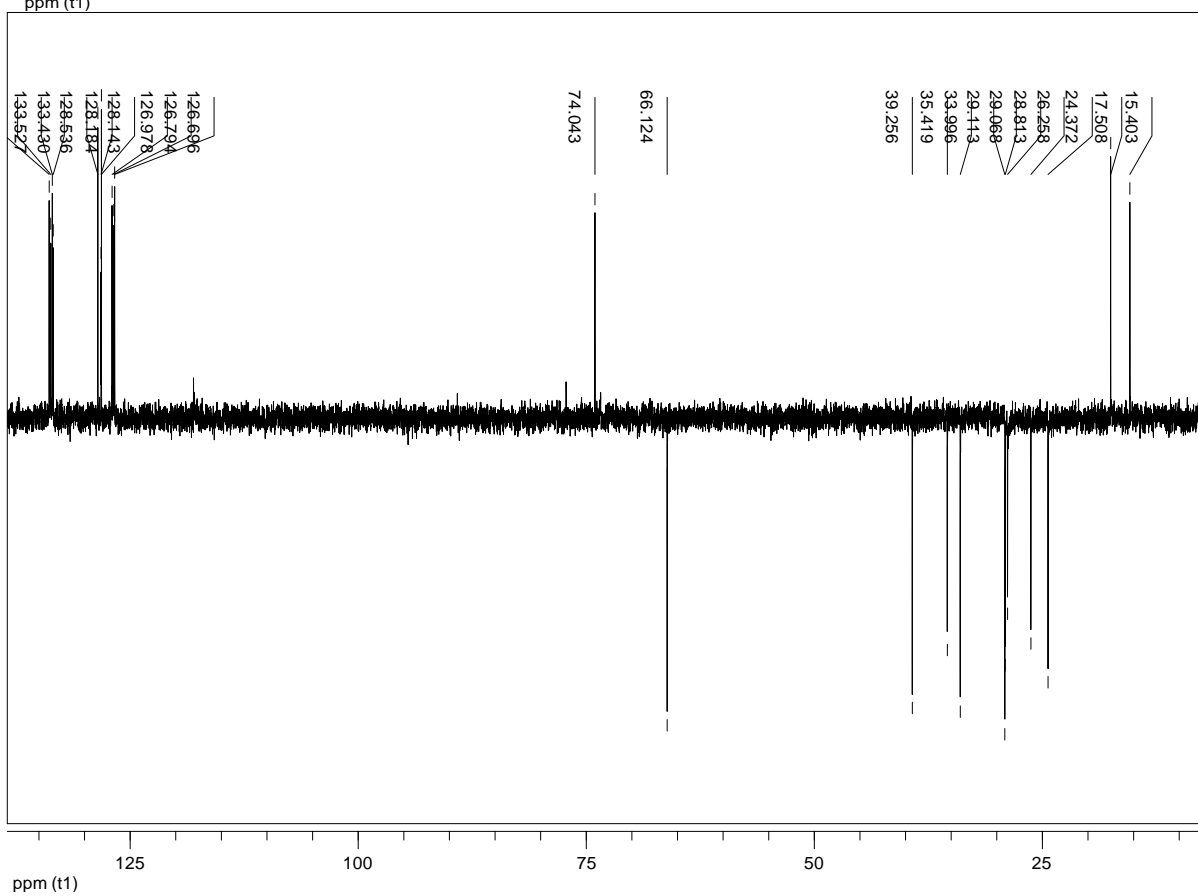
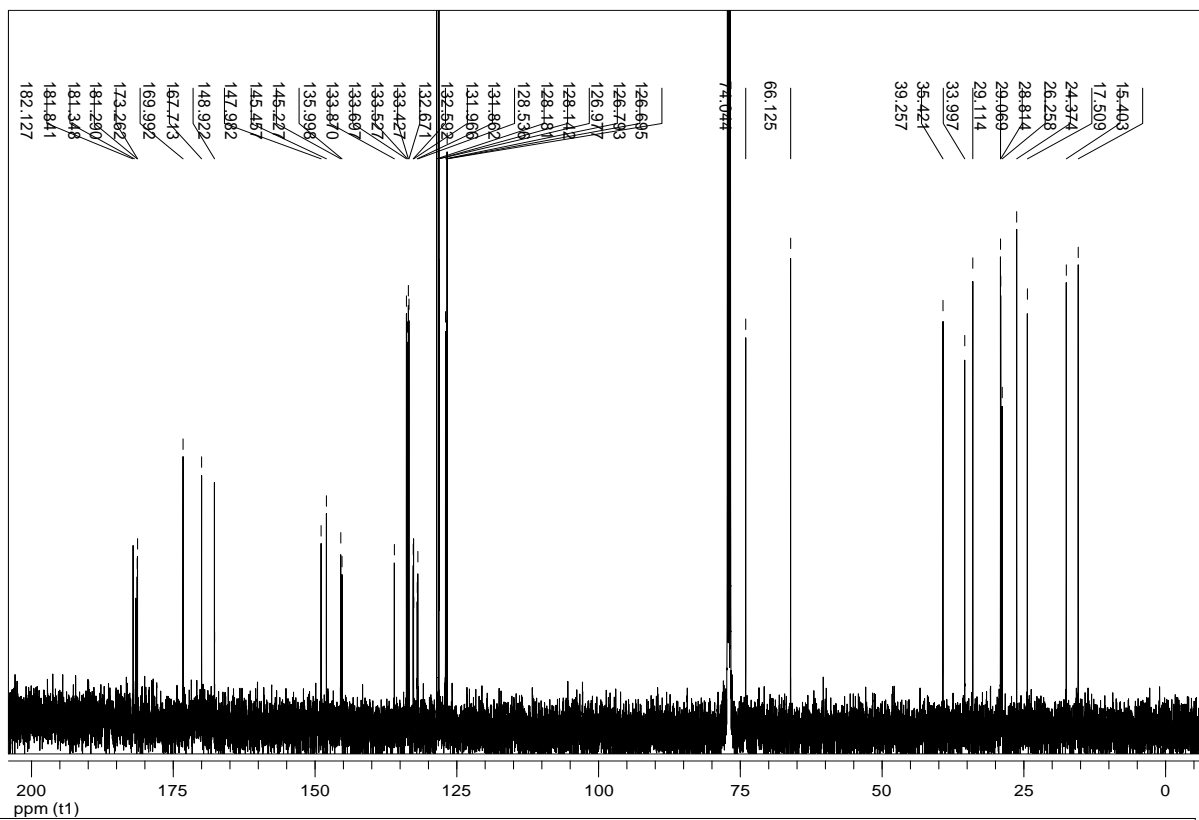
Compound 5p





Compound 6p



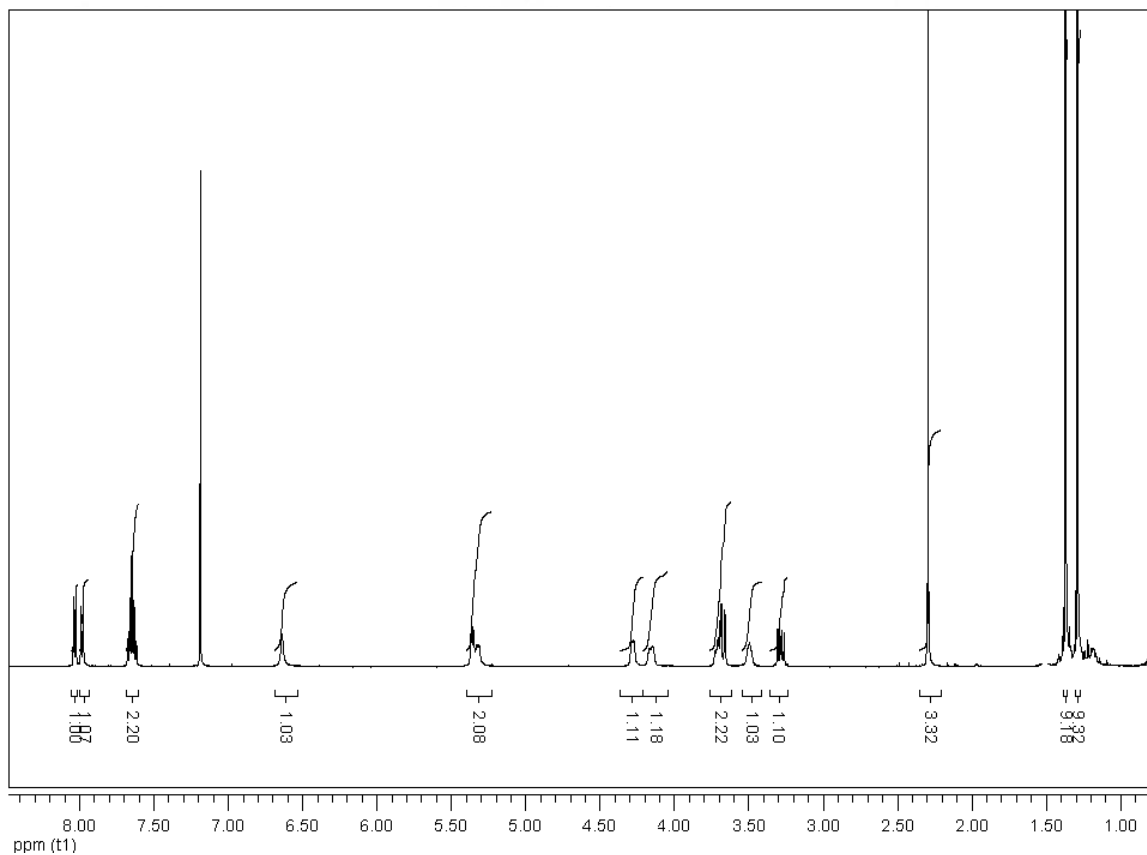
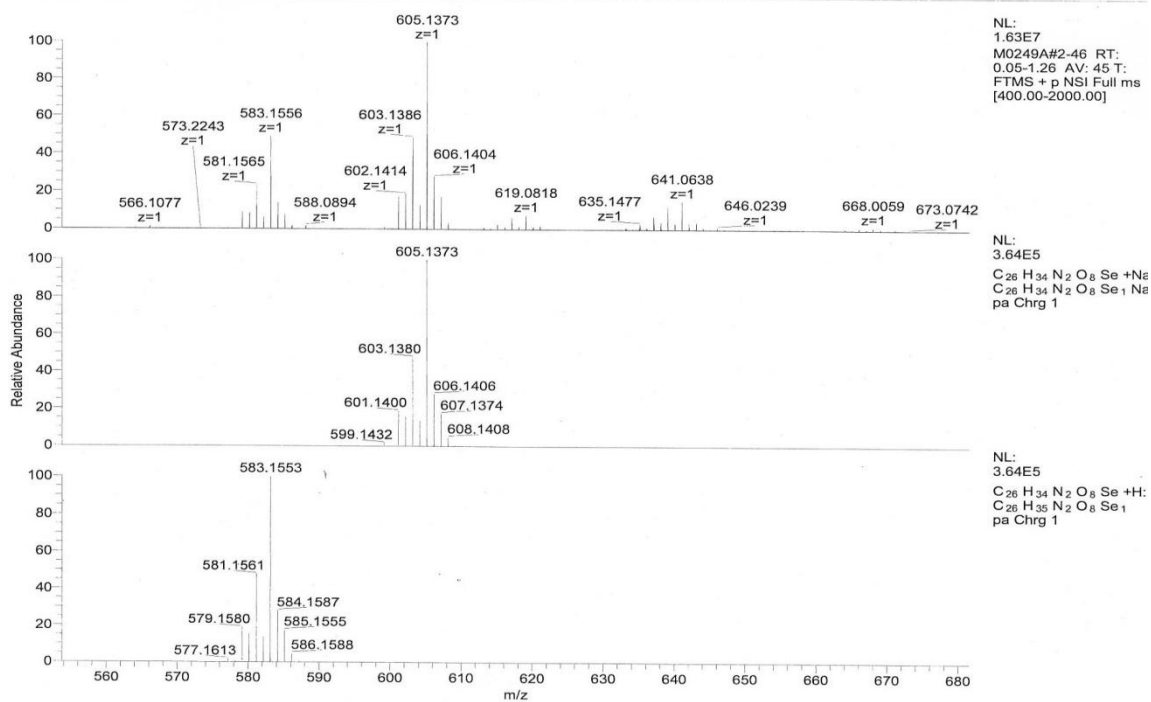


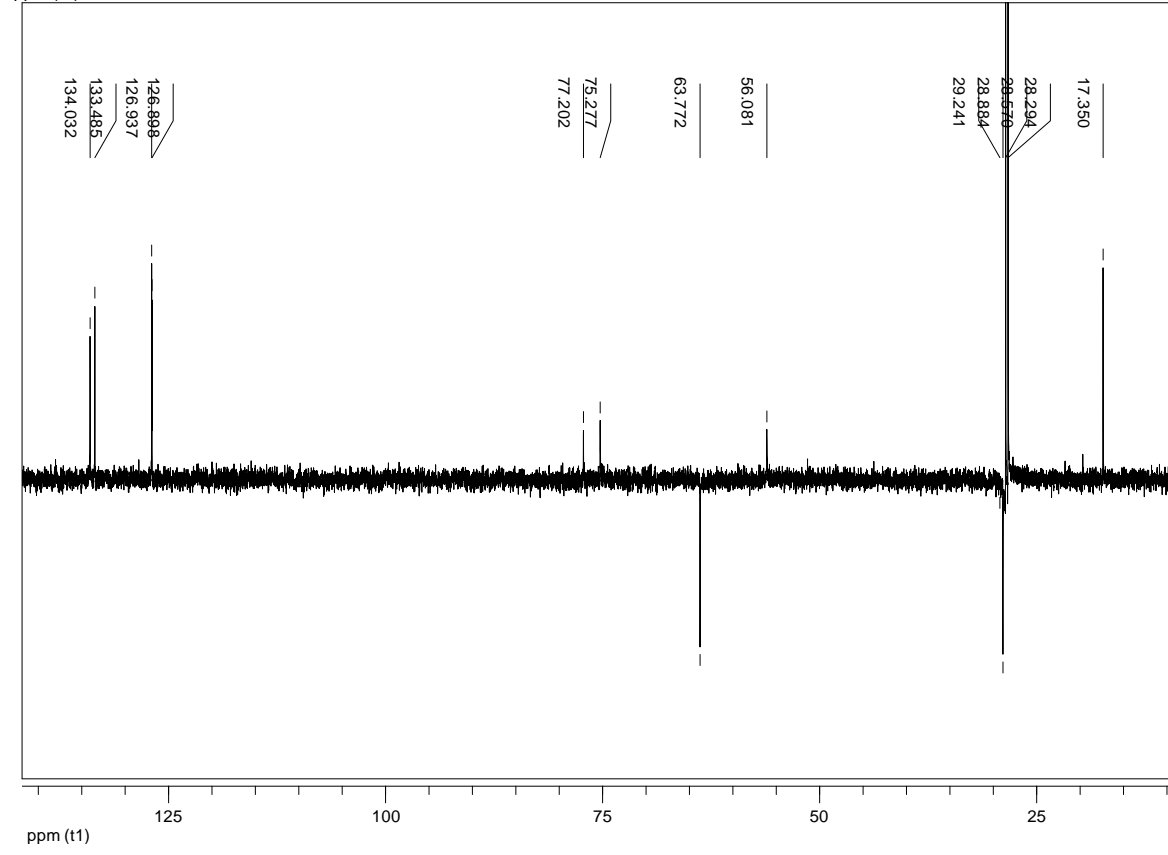
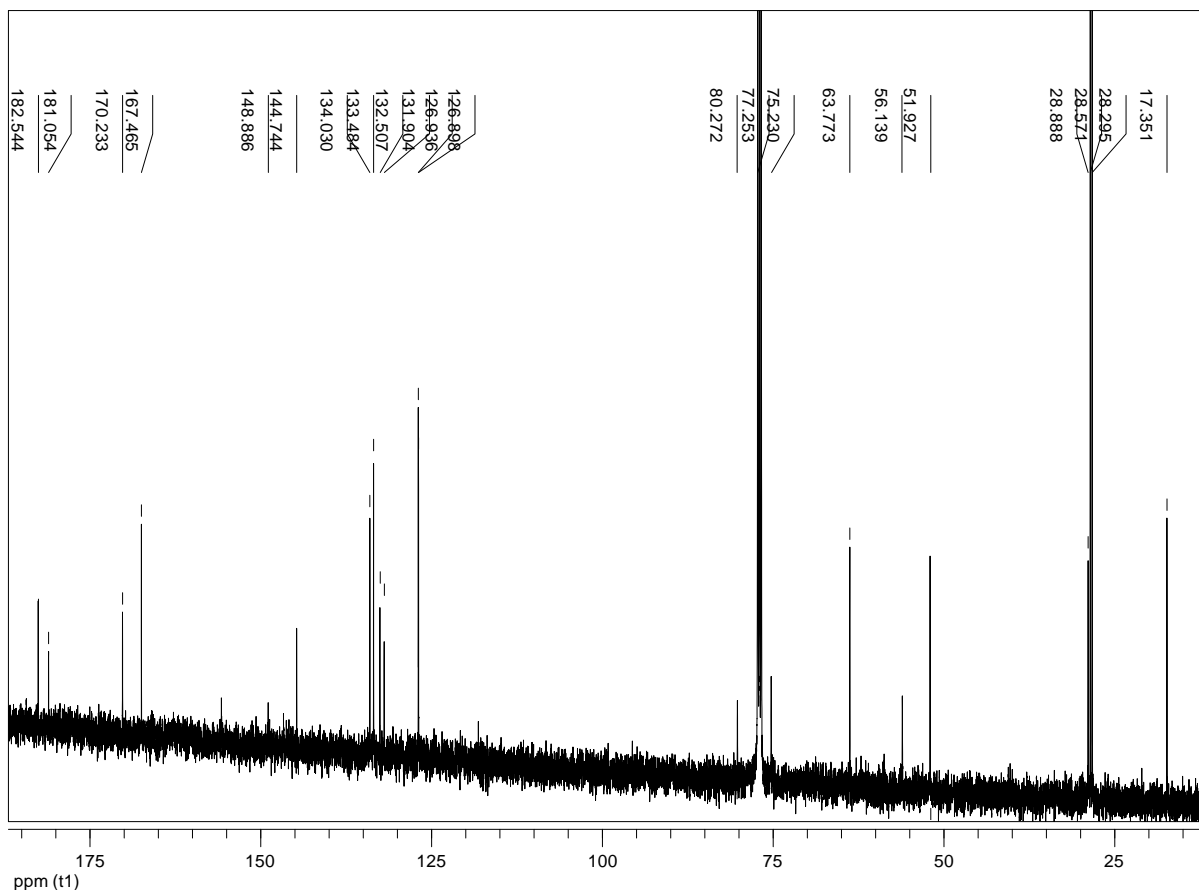
Compound 7p

C:\Xcalibur\data\Nadelmessungen\M0249A

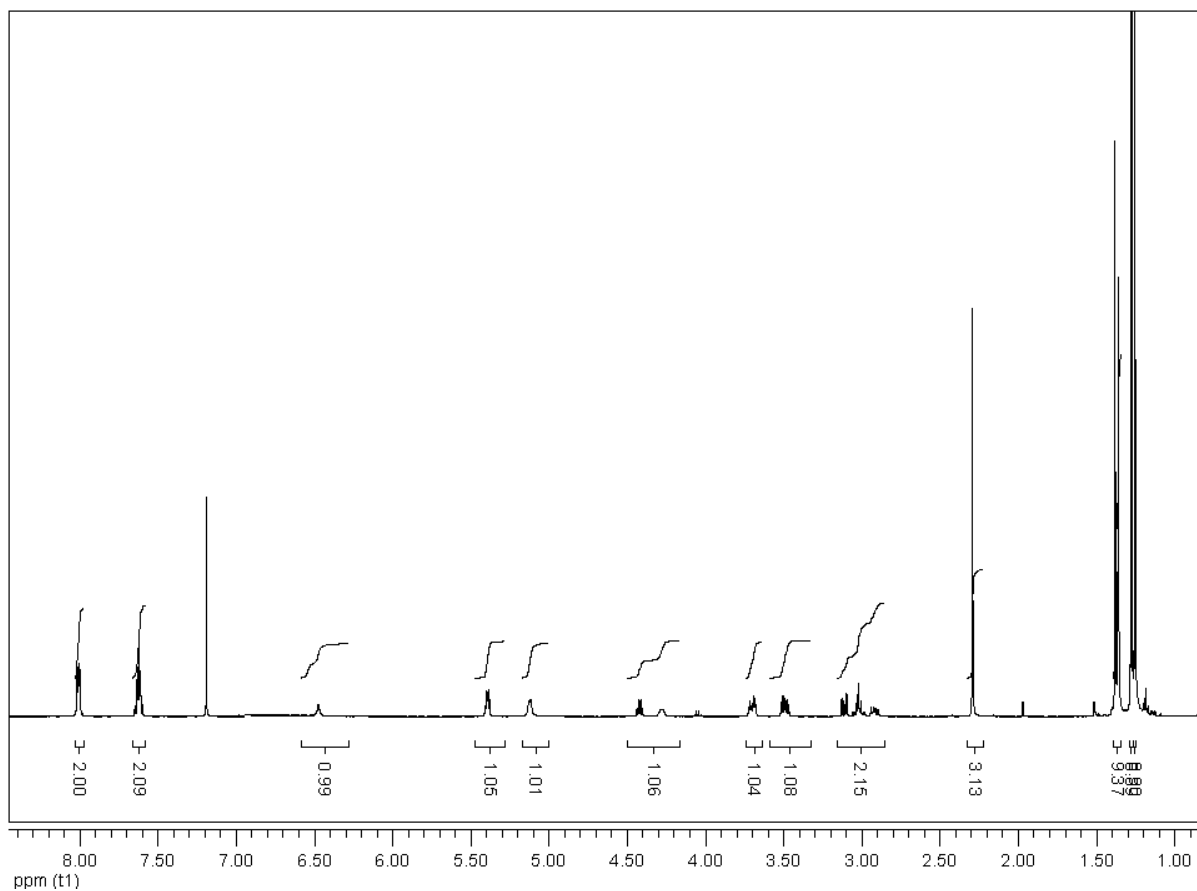
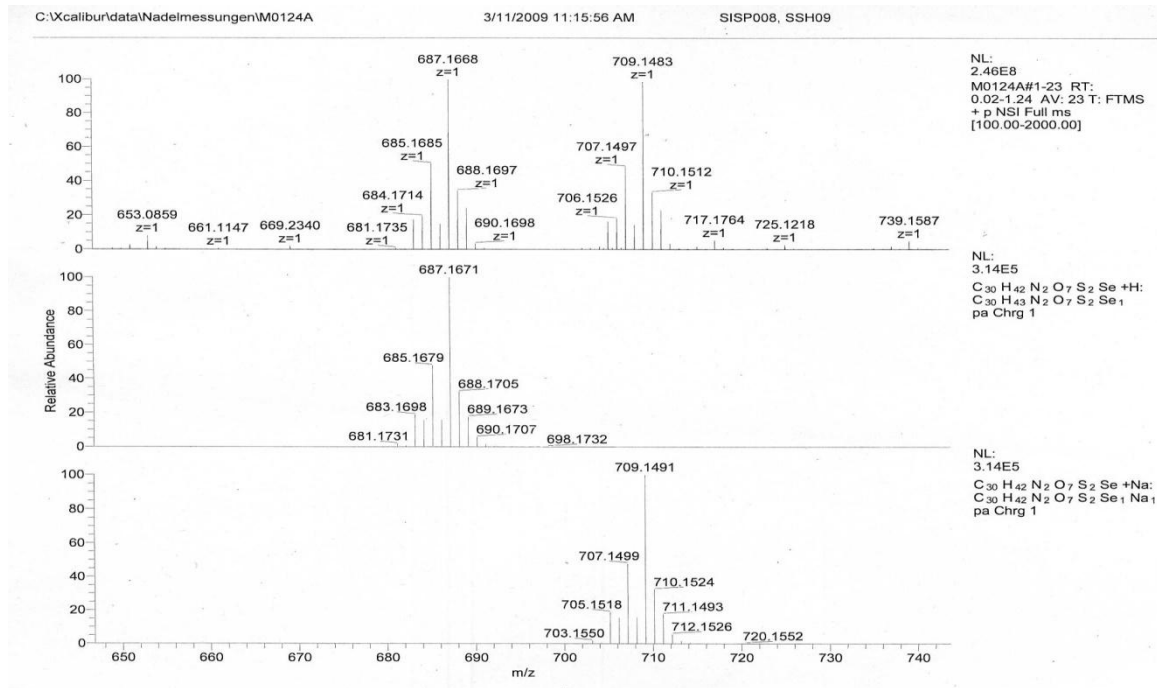
8/25/2009 11:01:24 AM

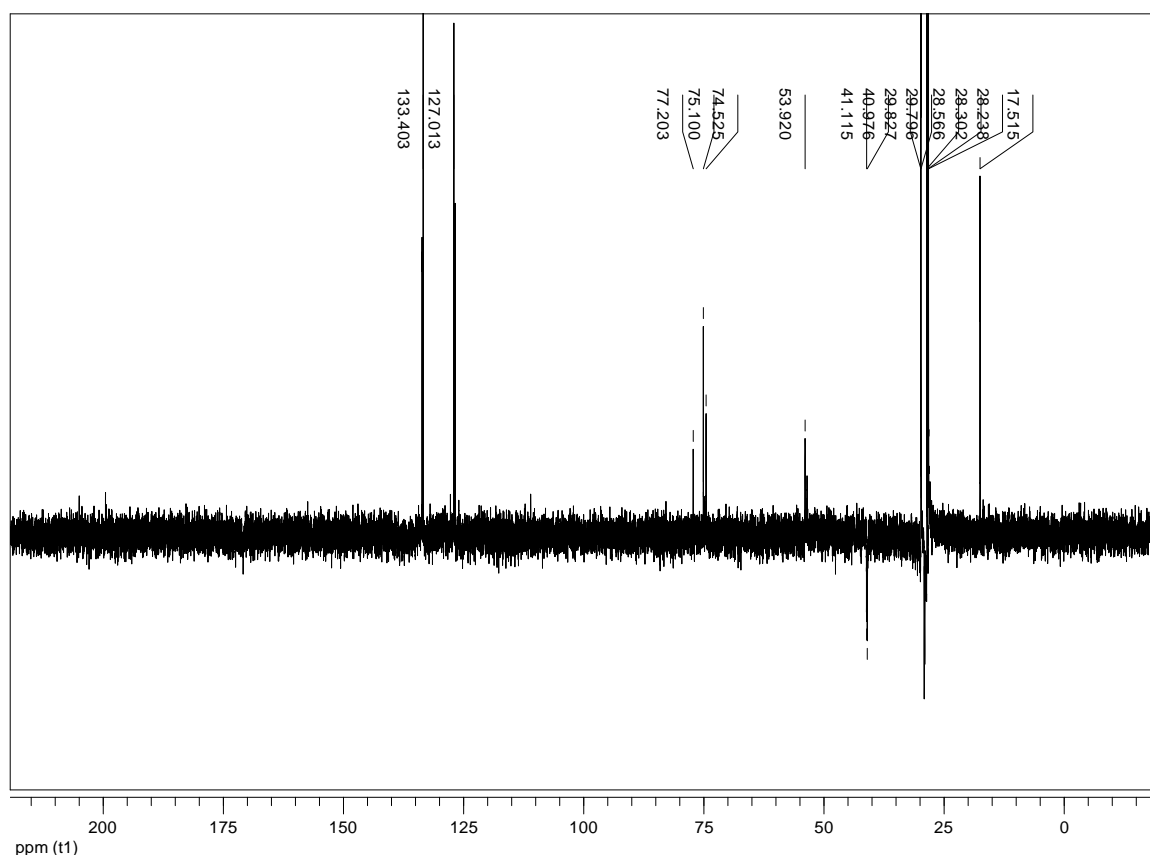
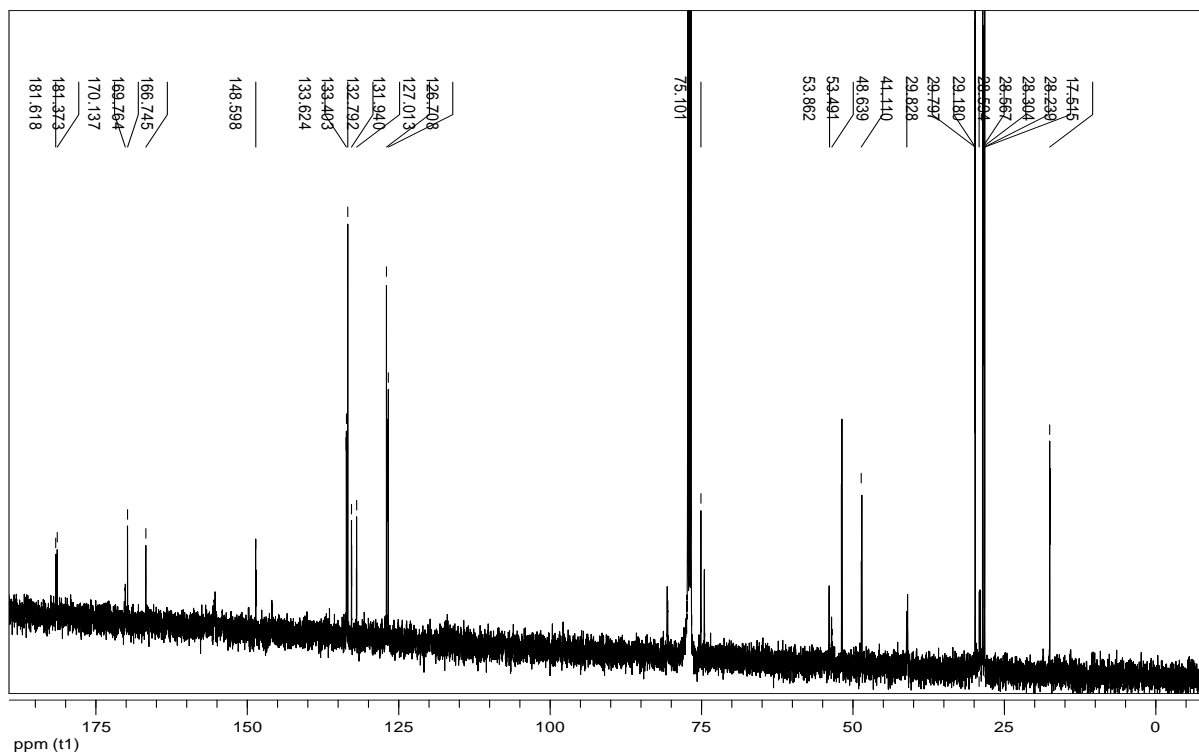
SISP007, SSH09 ✓



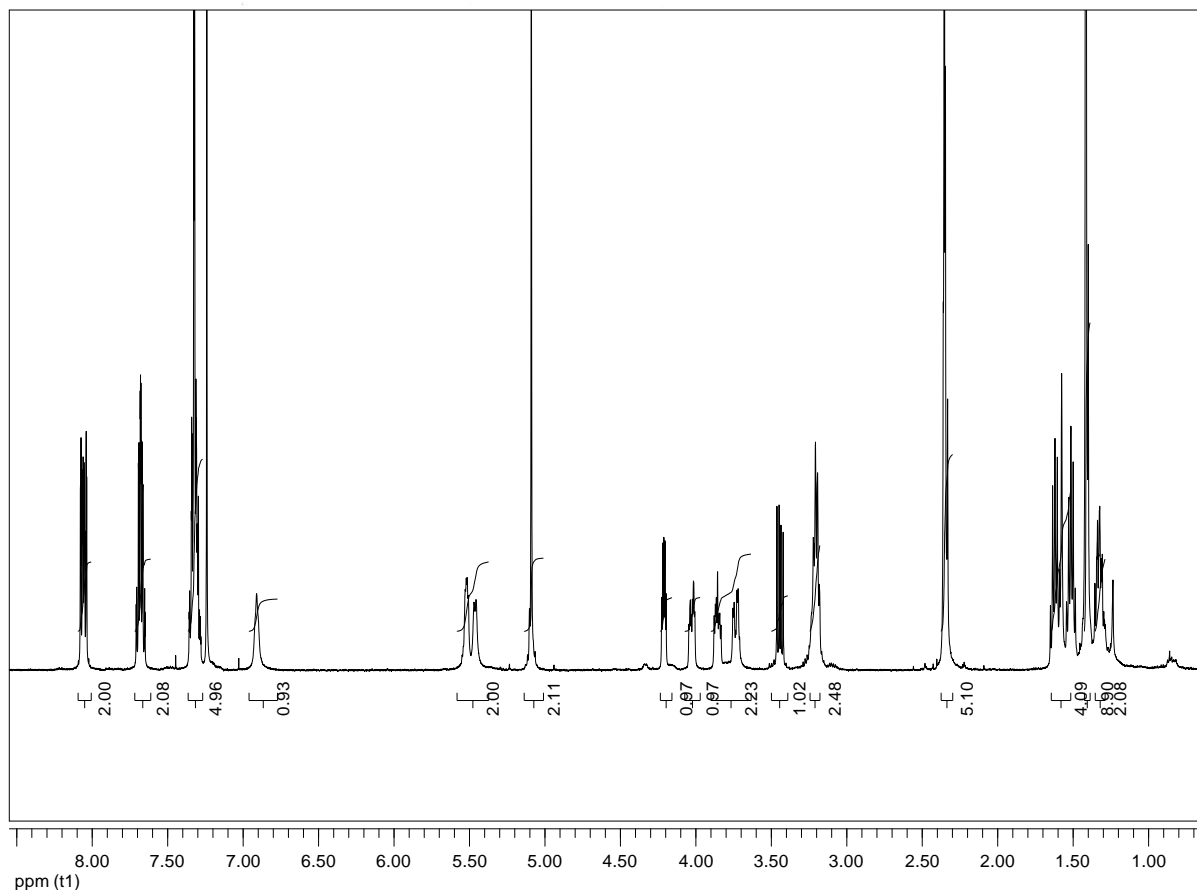
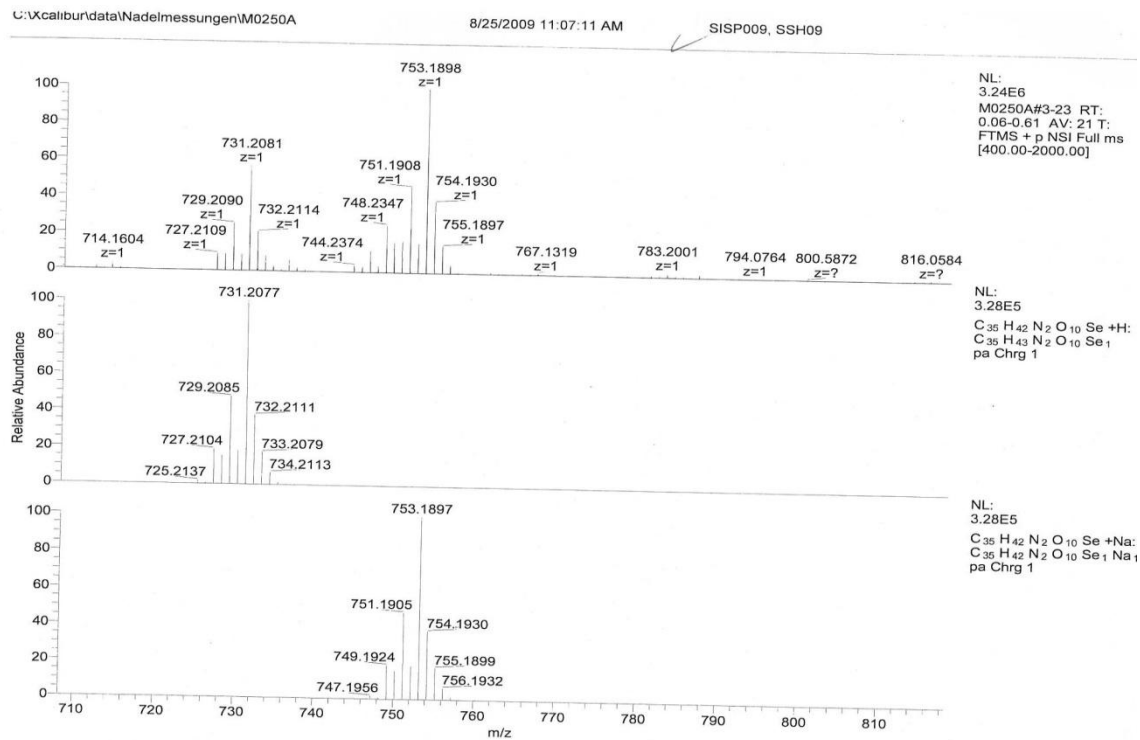


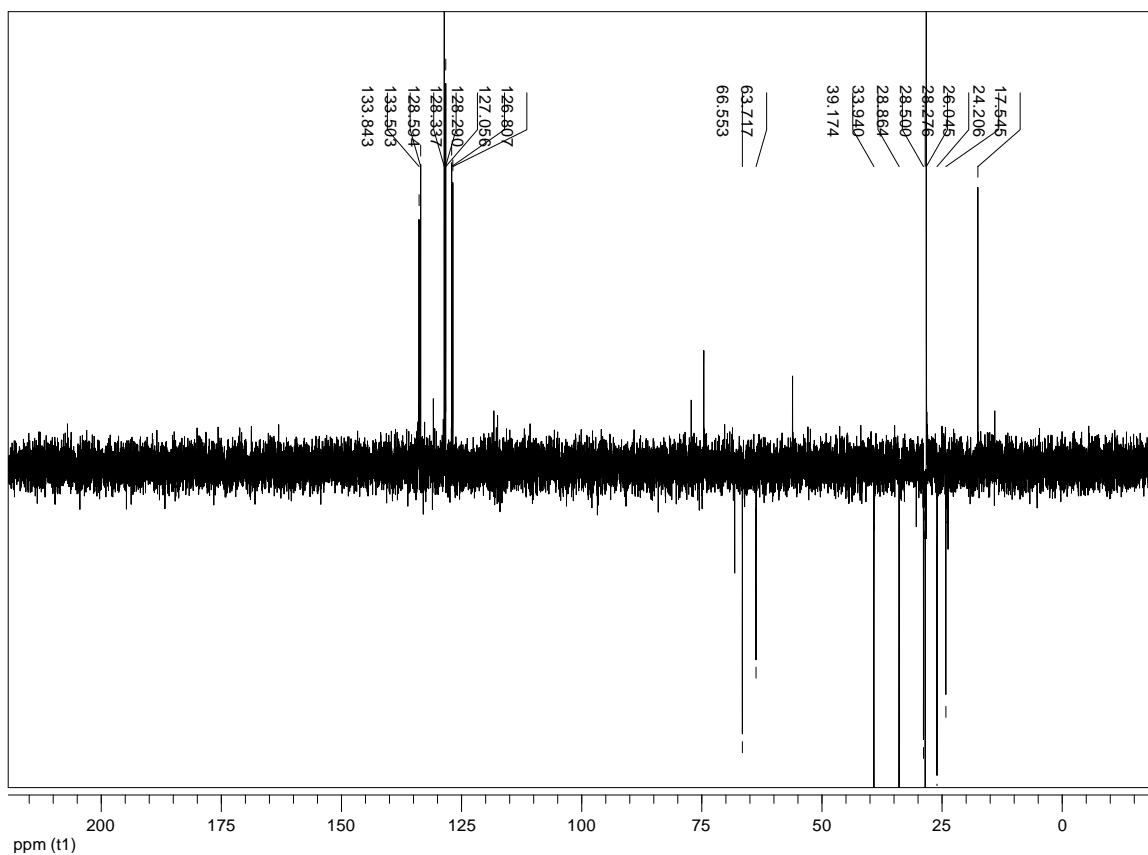
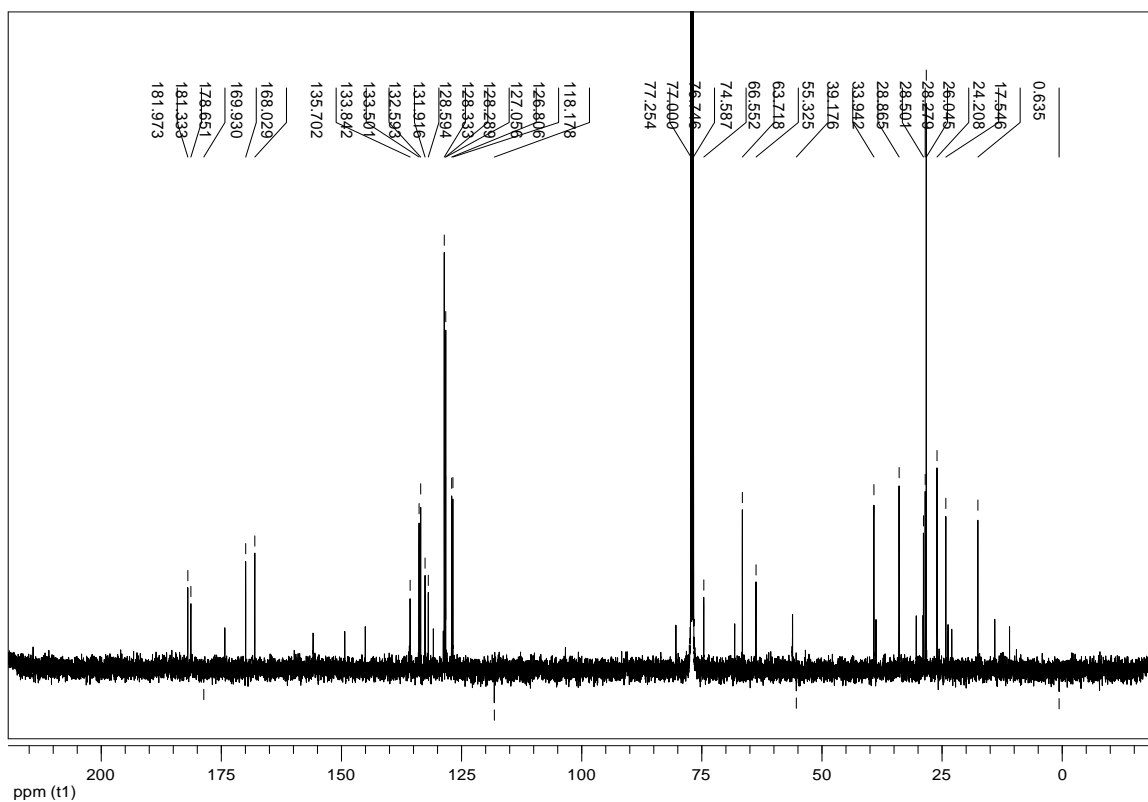
Compound 8p



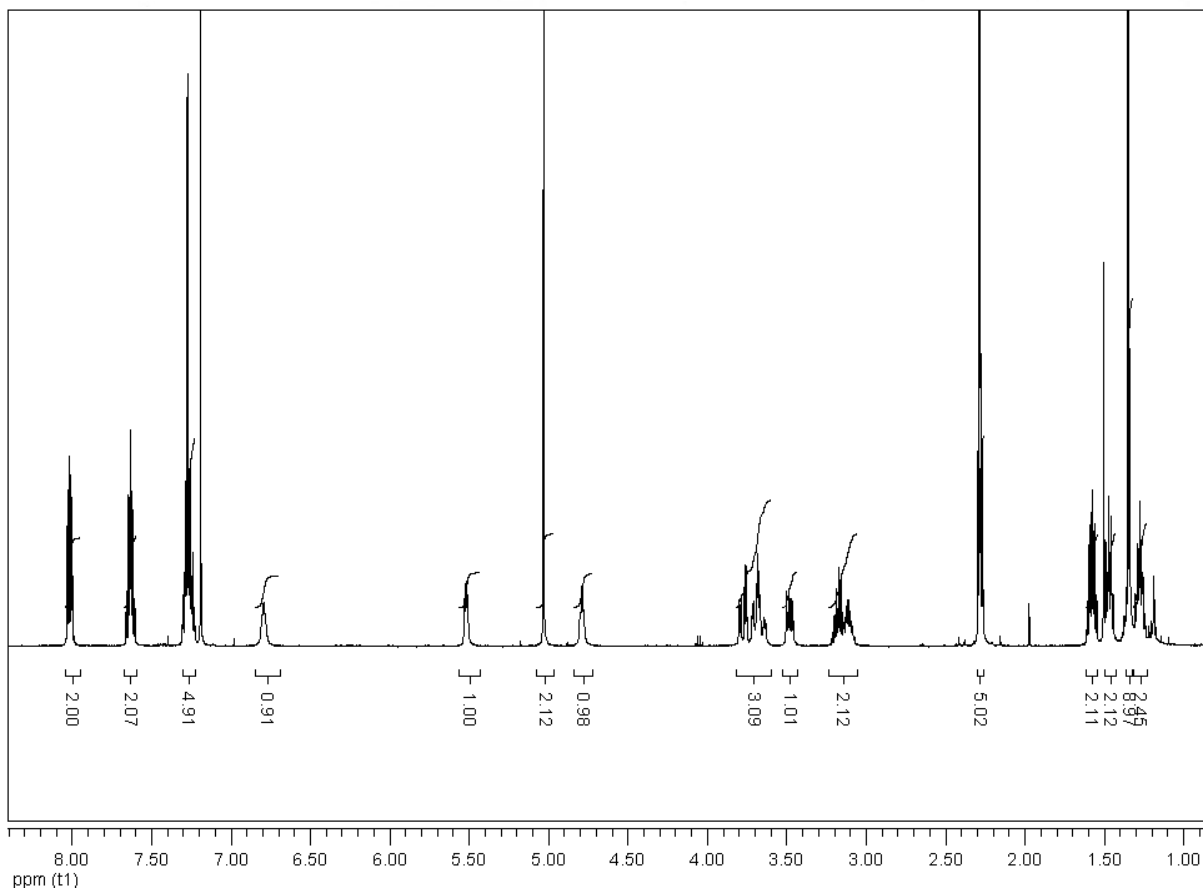
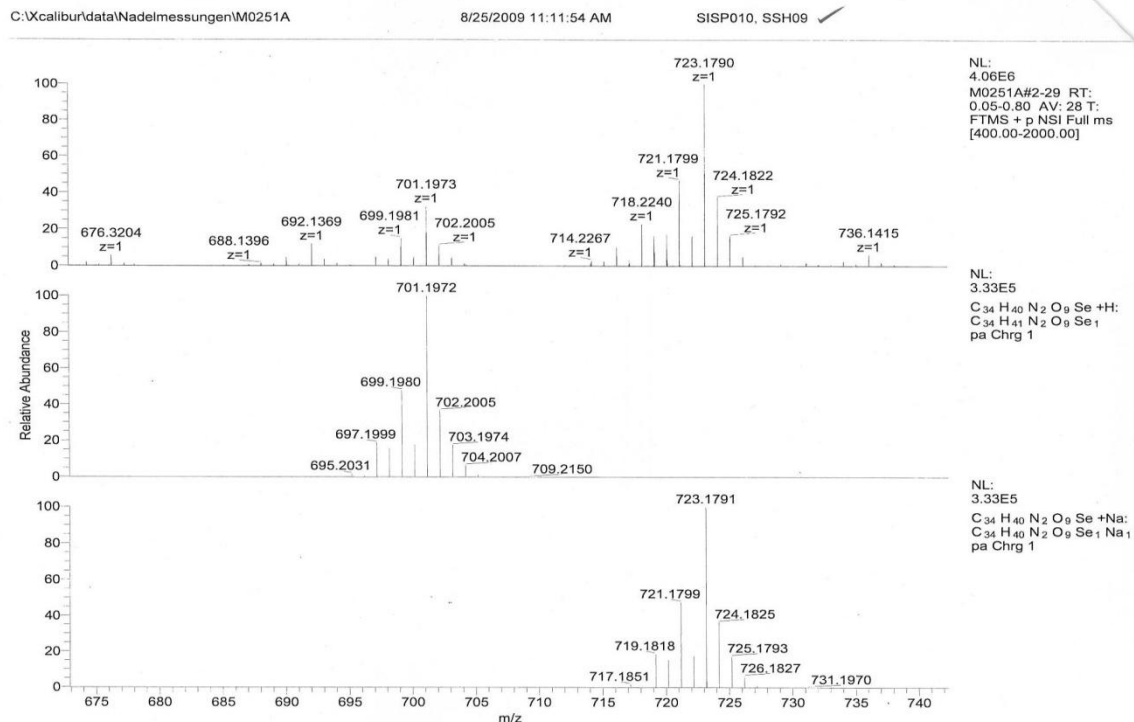


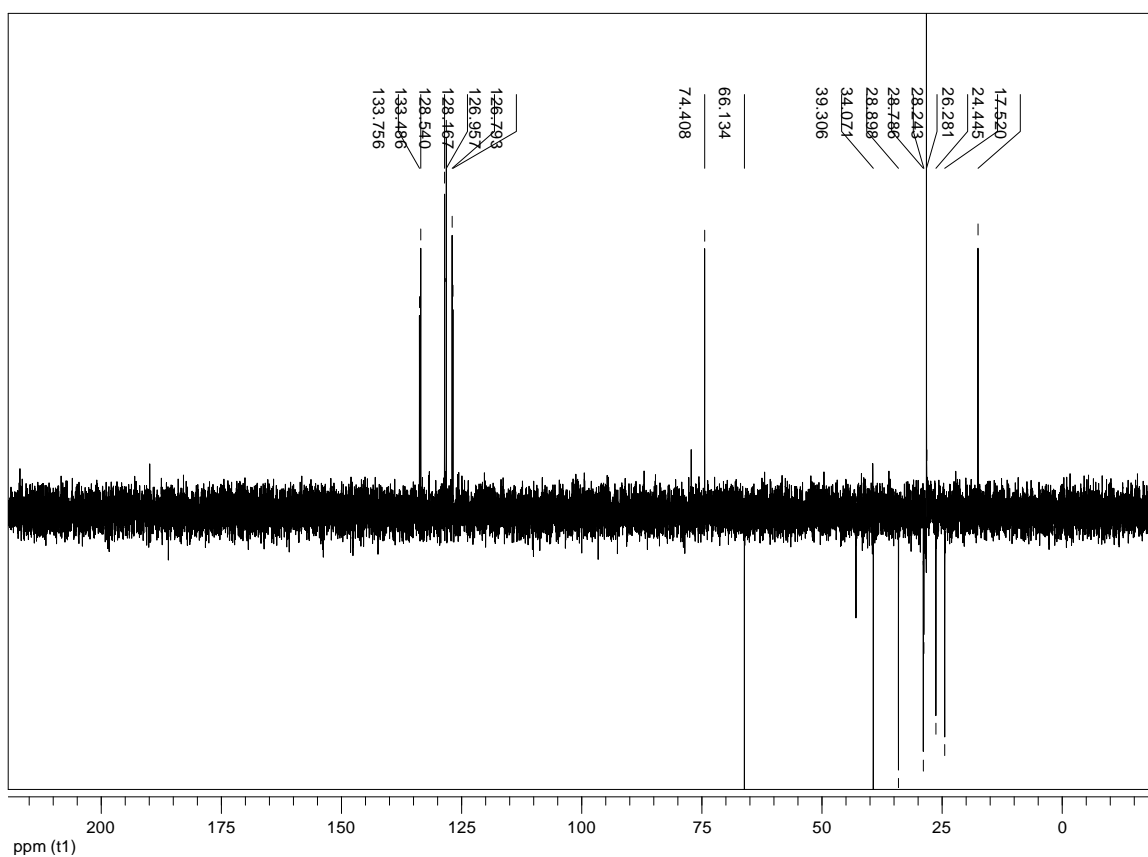
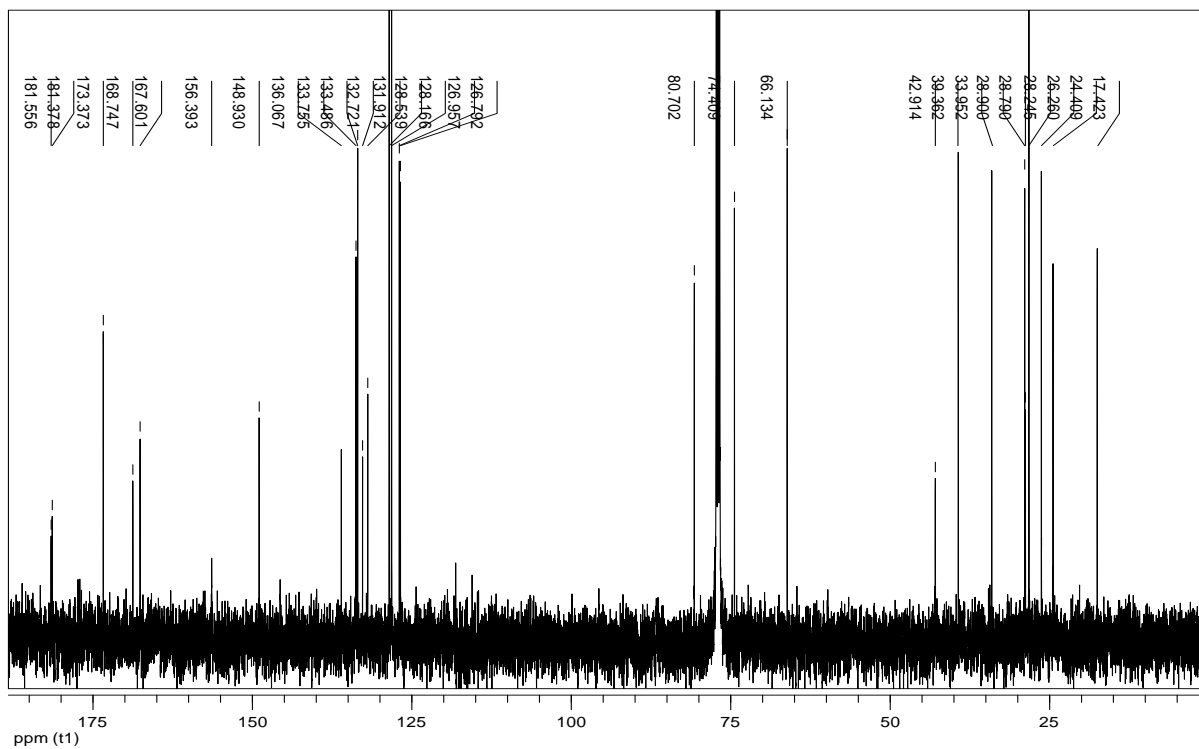
Compound 9p



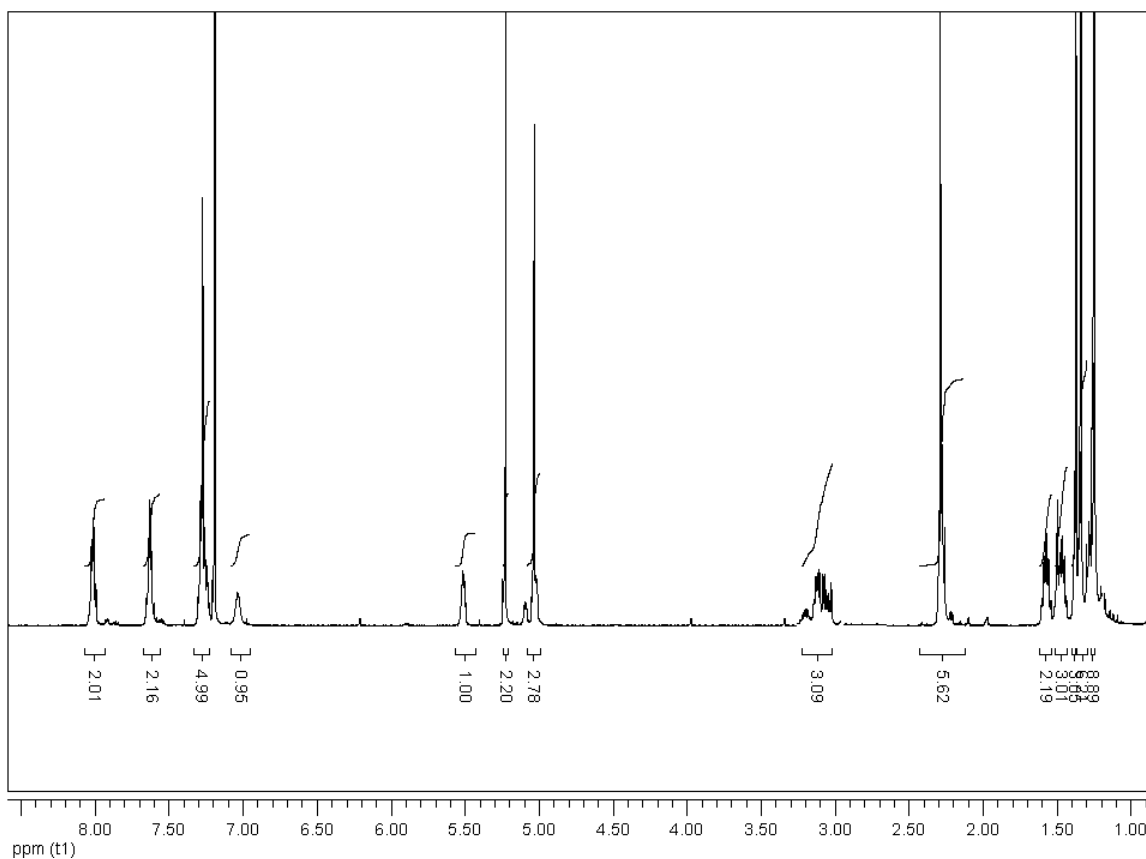
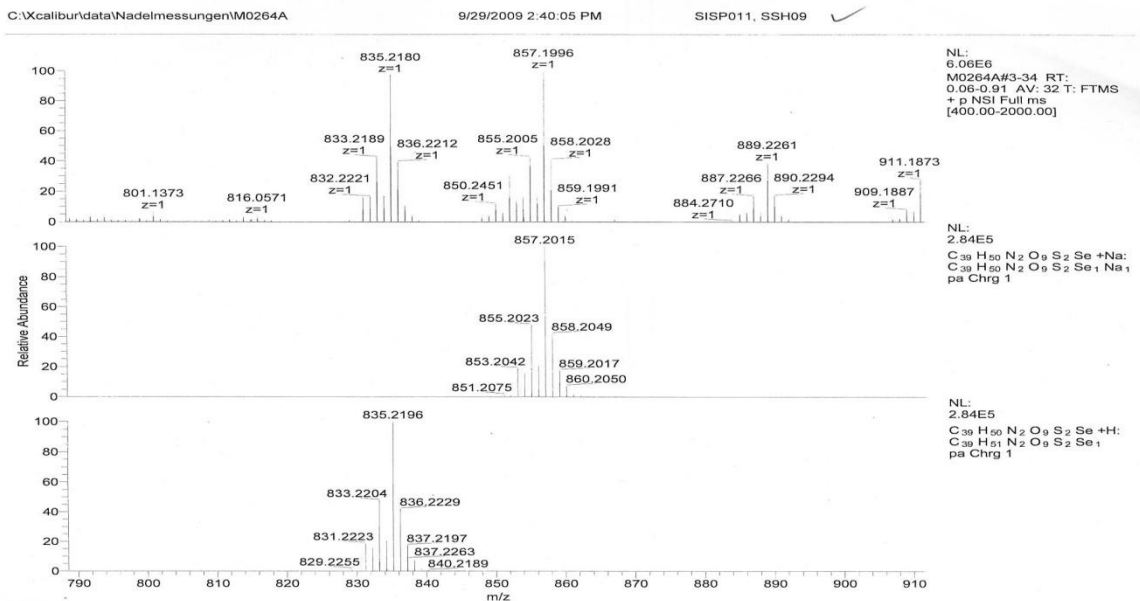


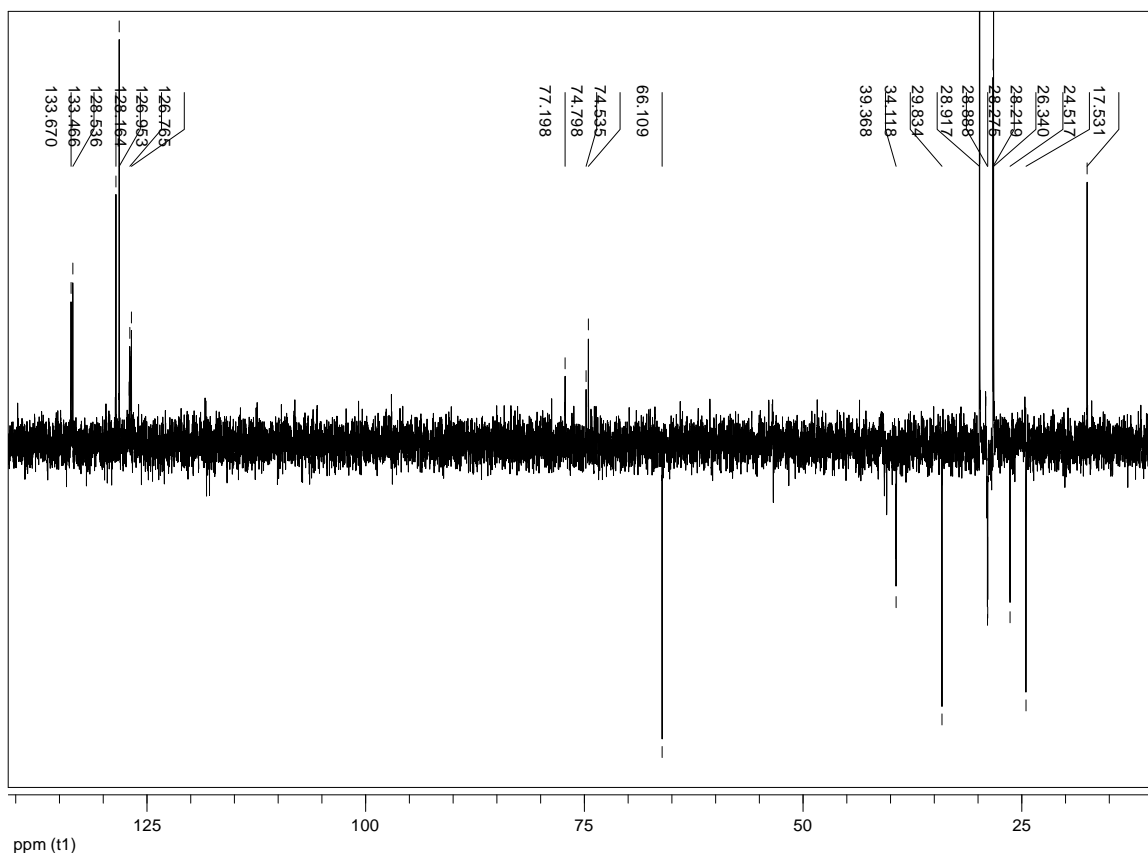
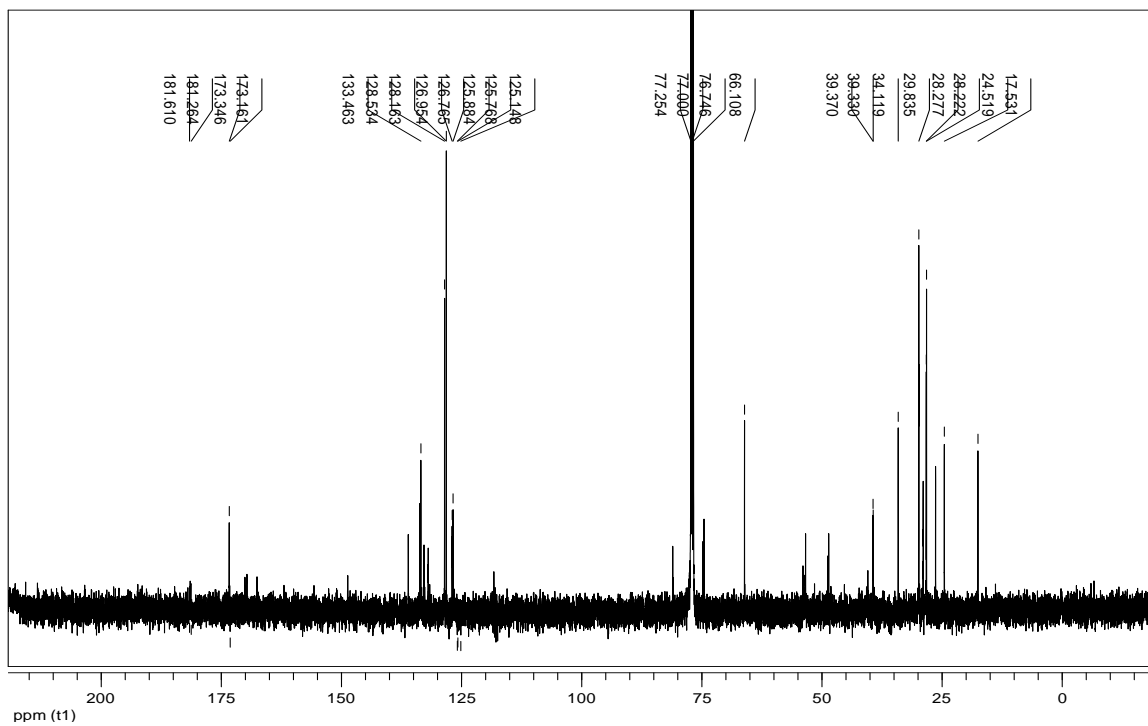
Compound 10p



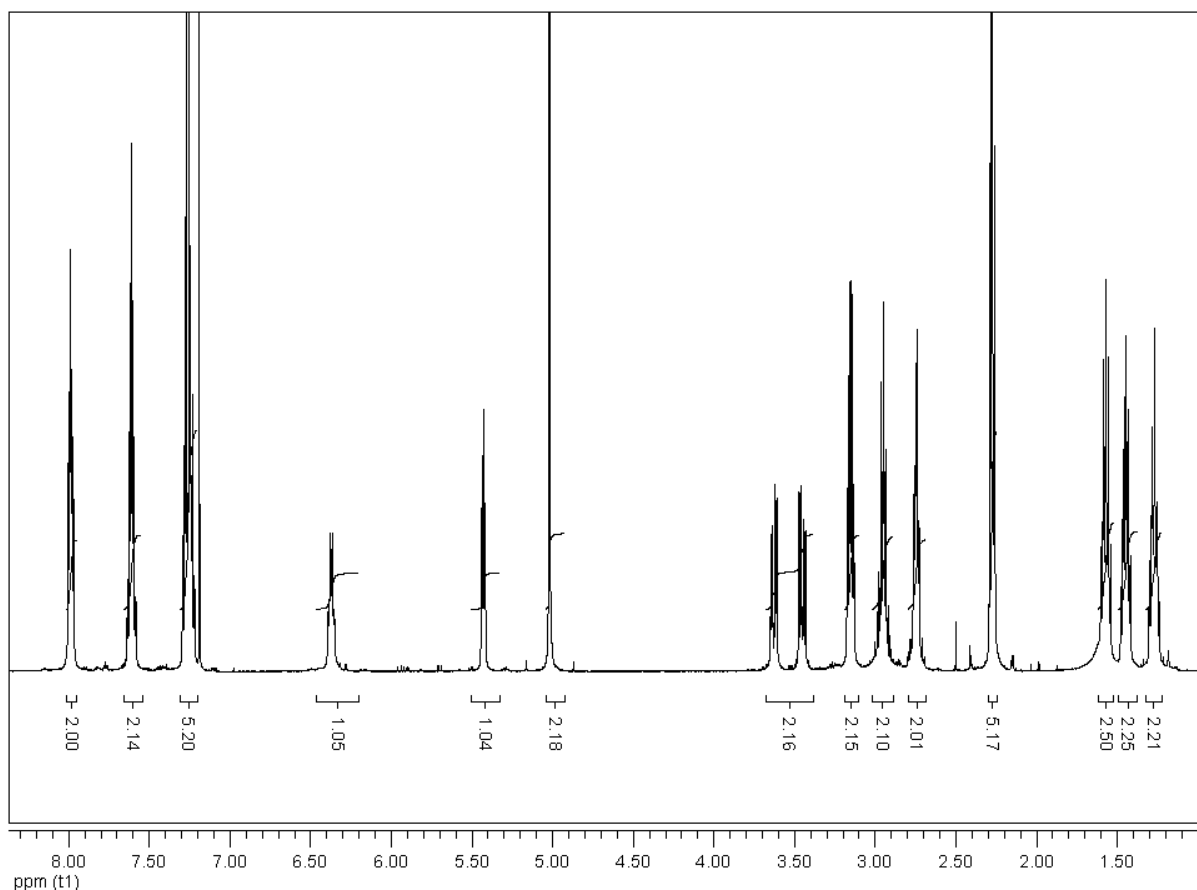
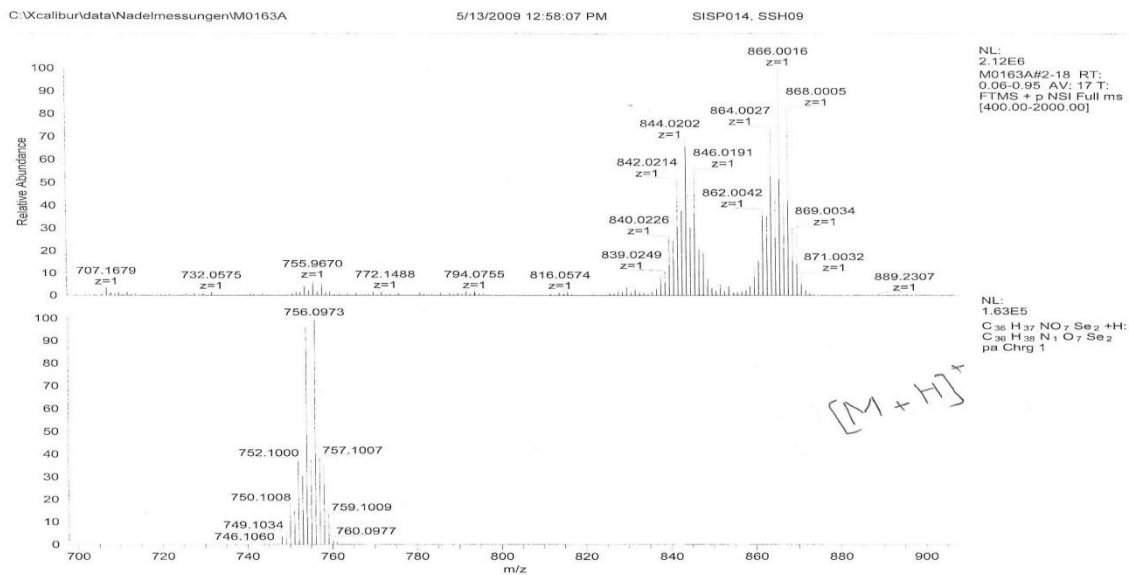


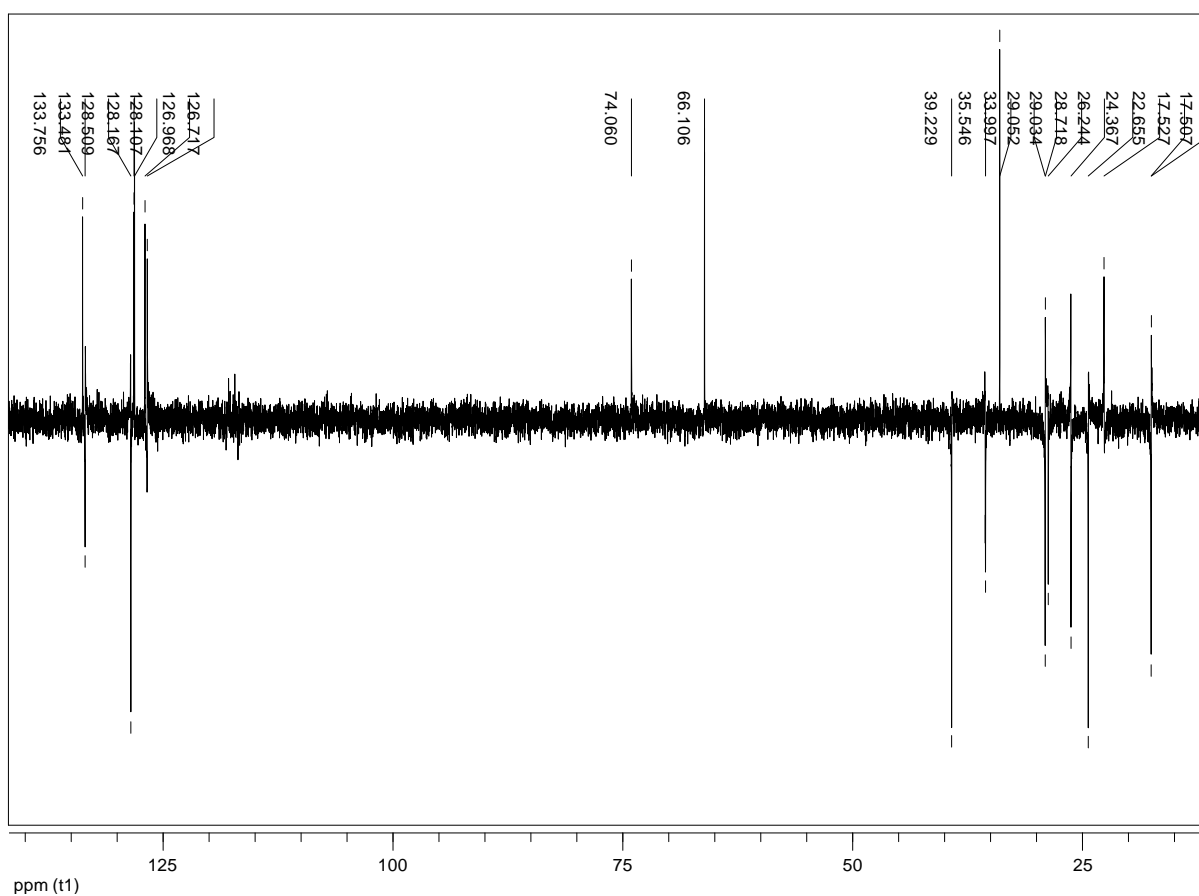
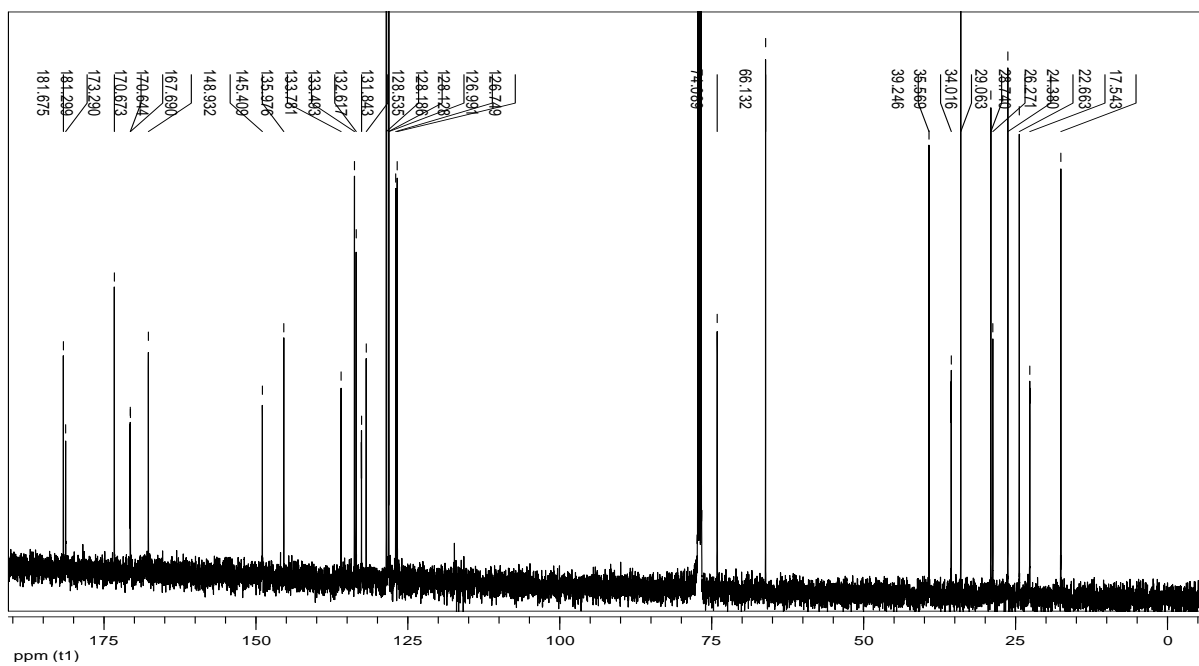
Compound 11p



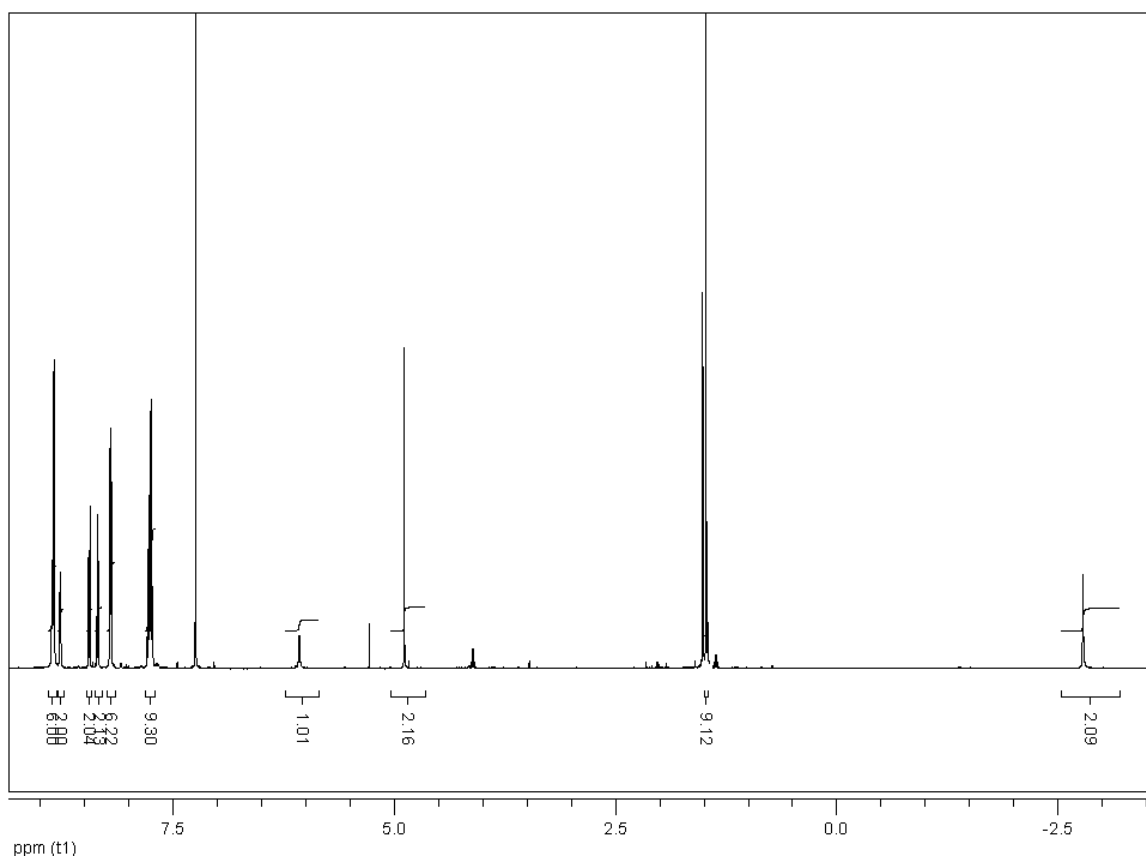
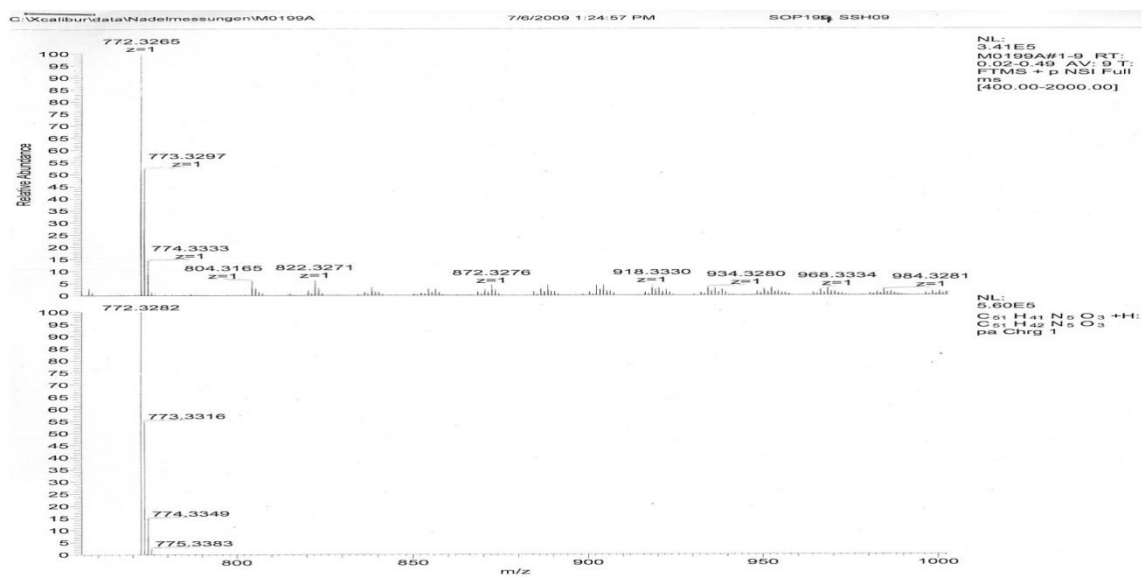


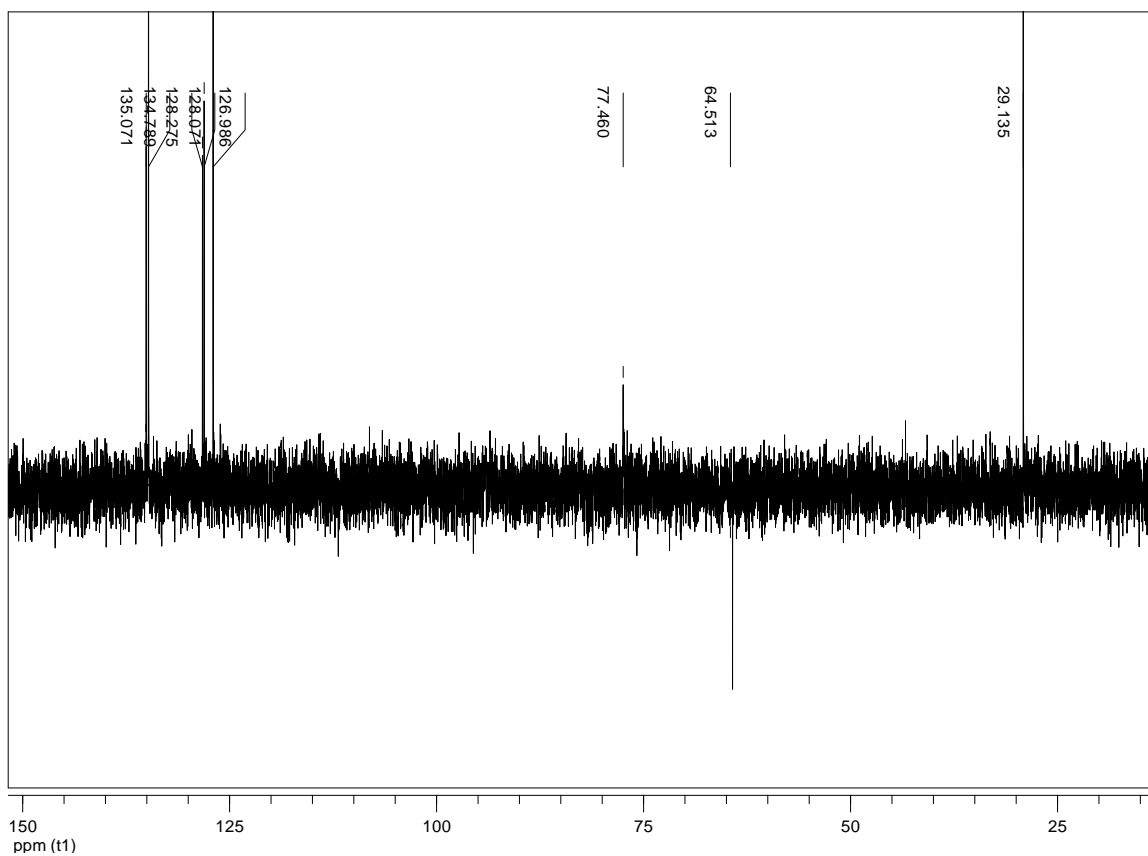
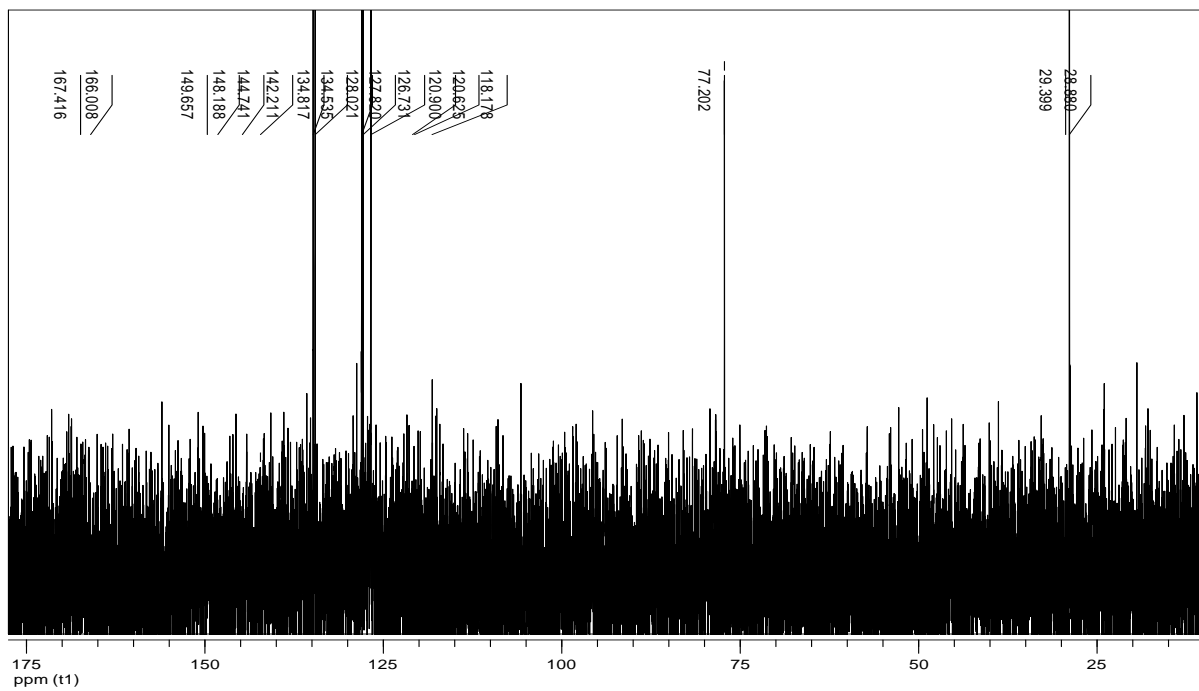
Compound 12p



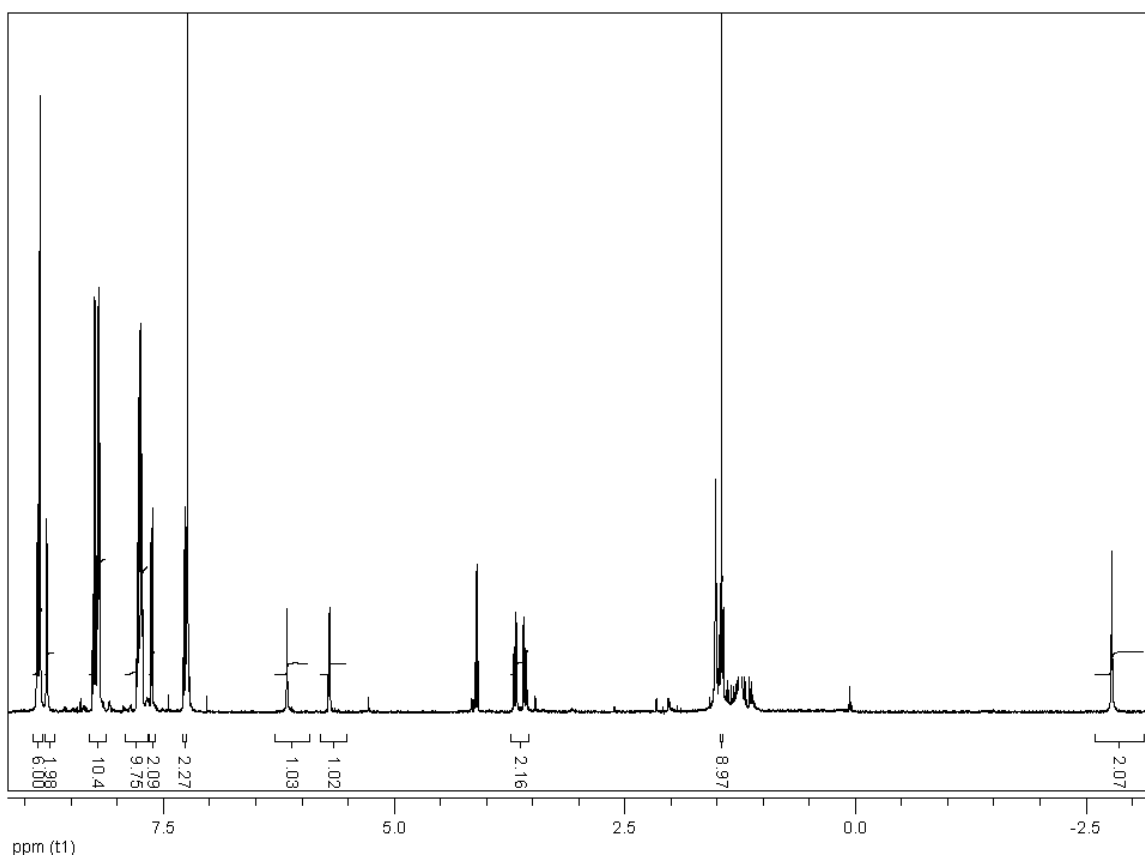
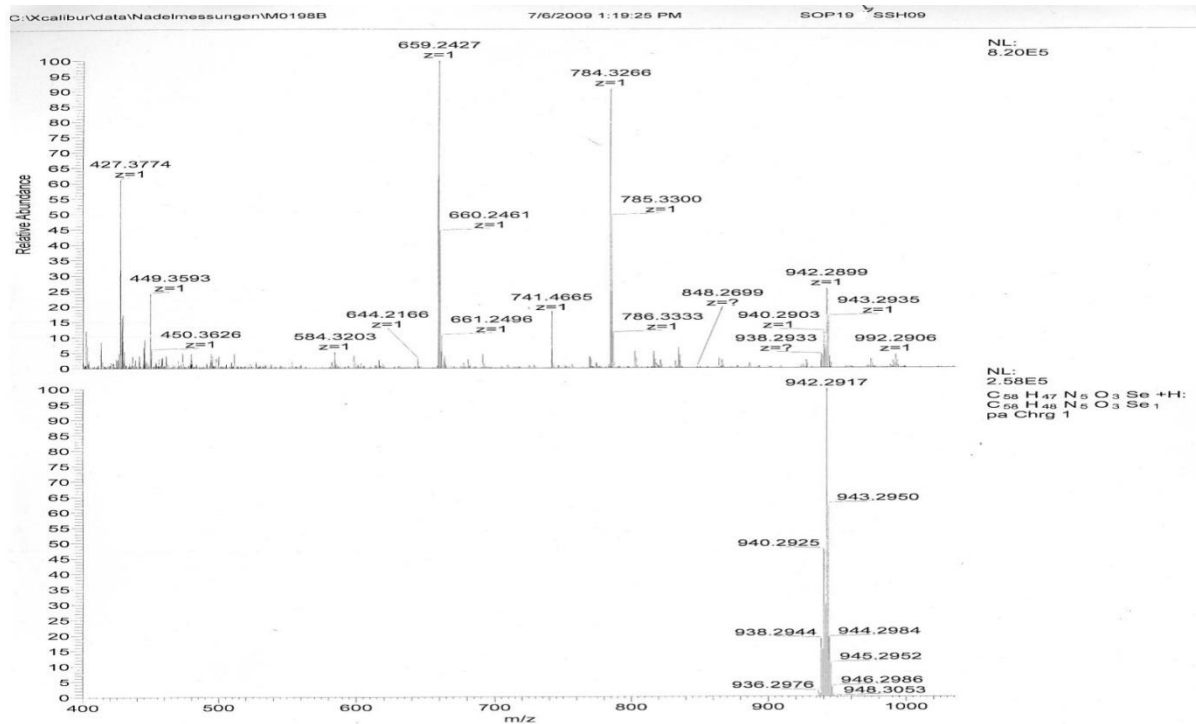


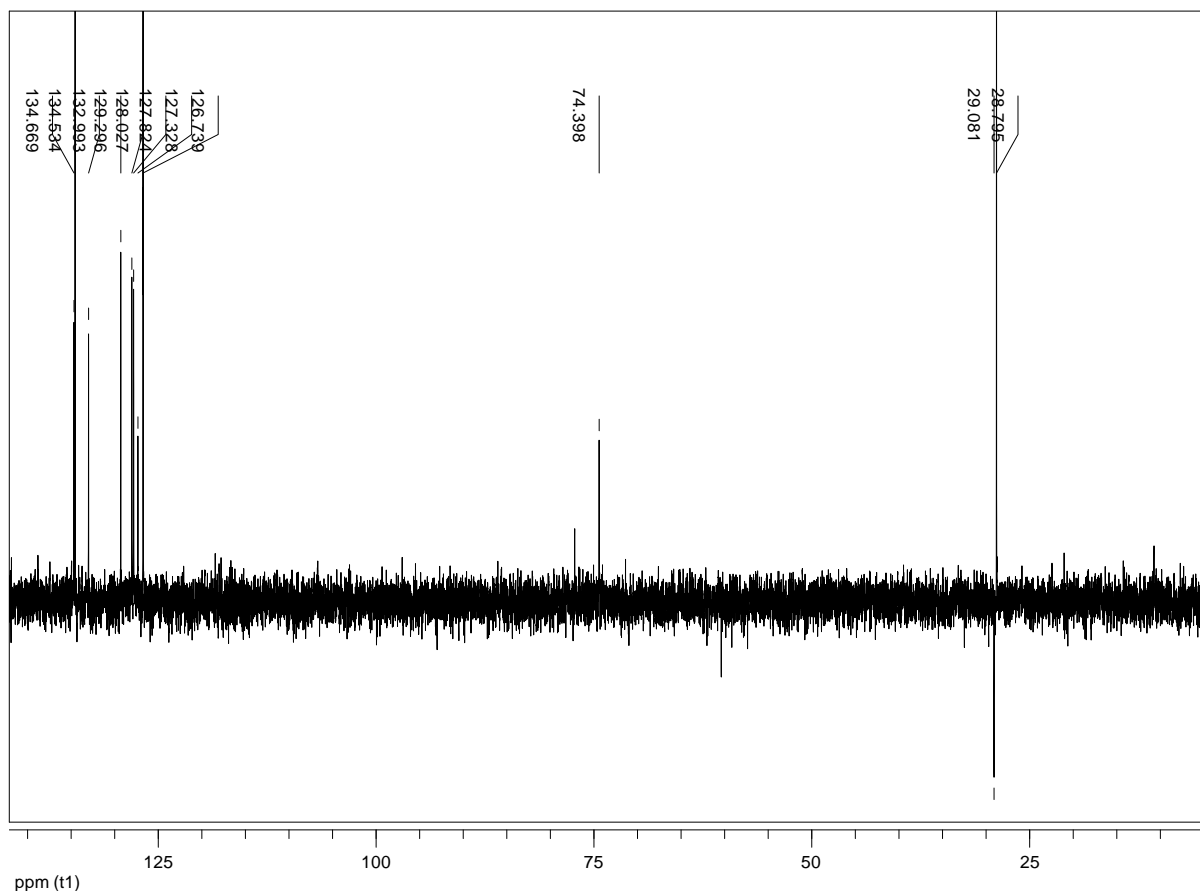
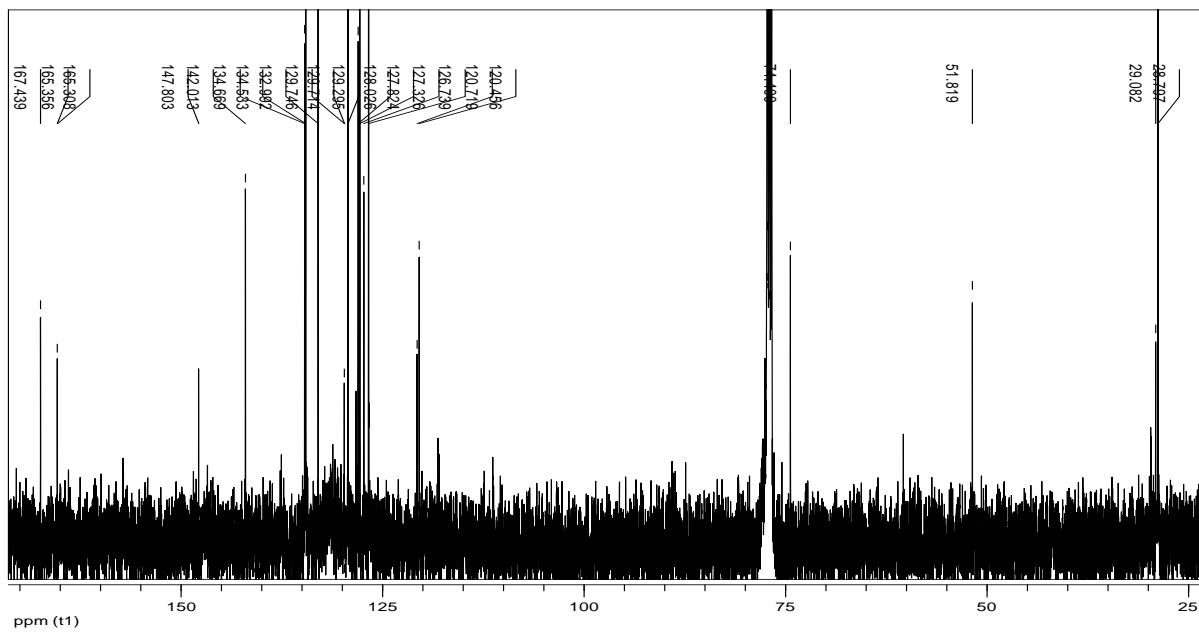
Compound 13p



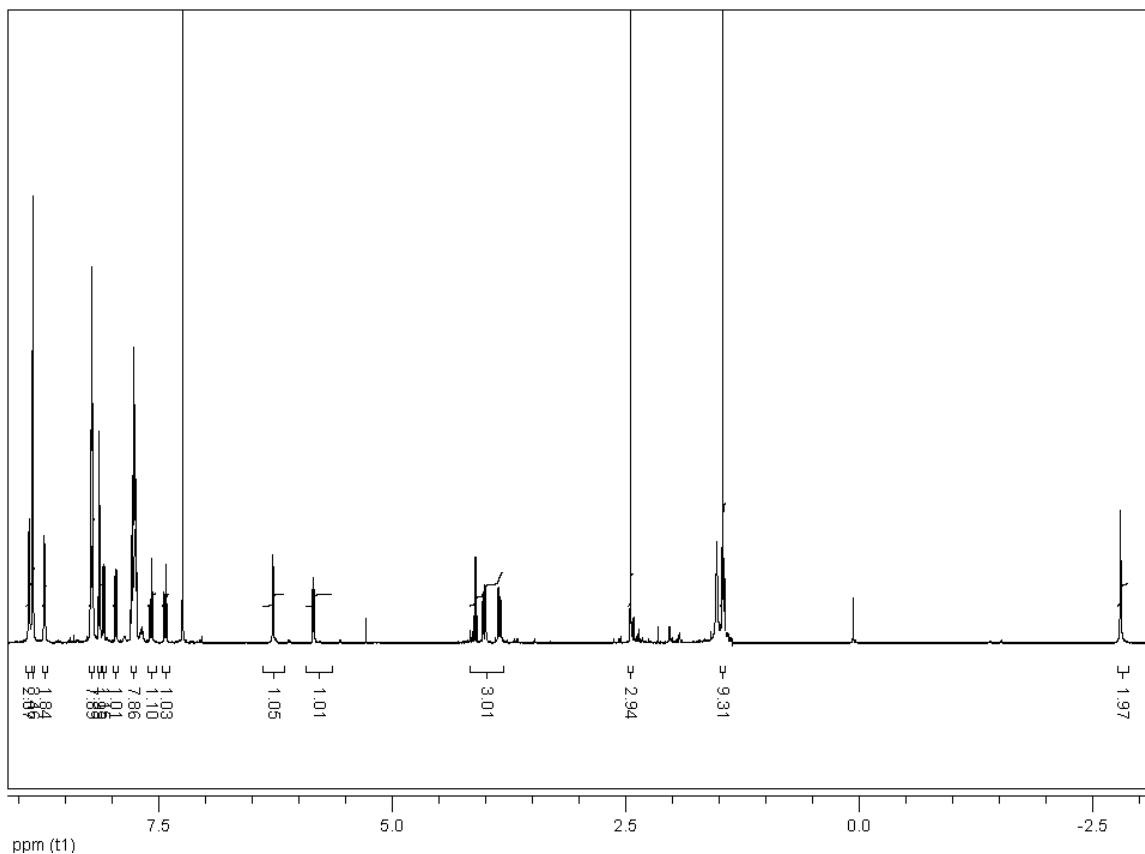
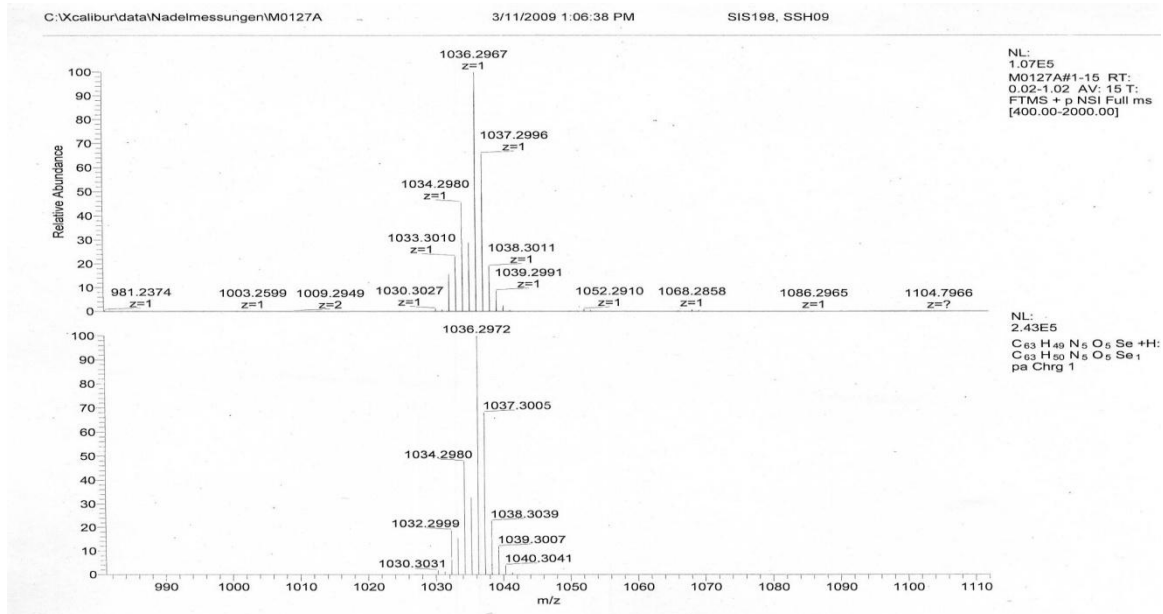


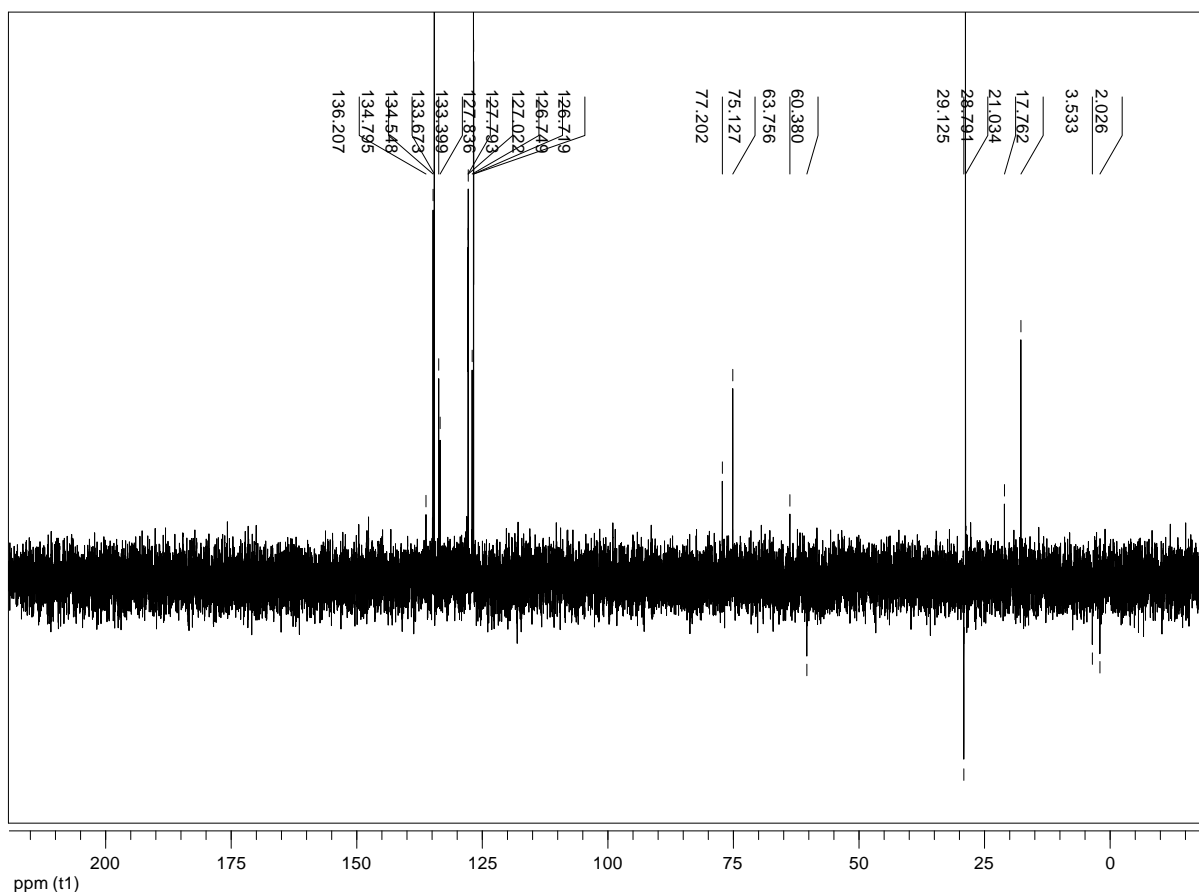
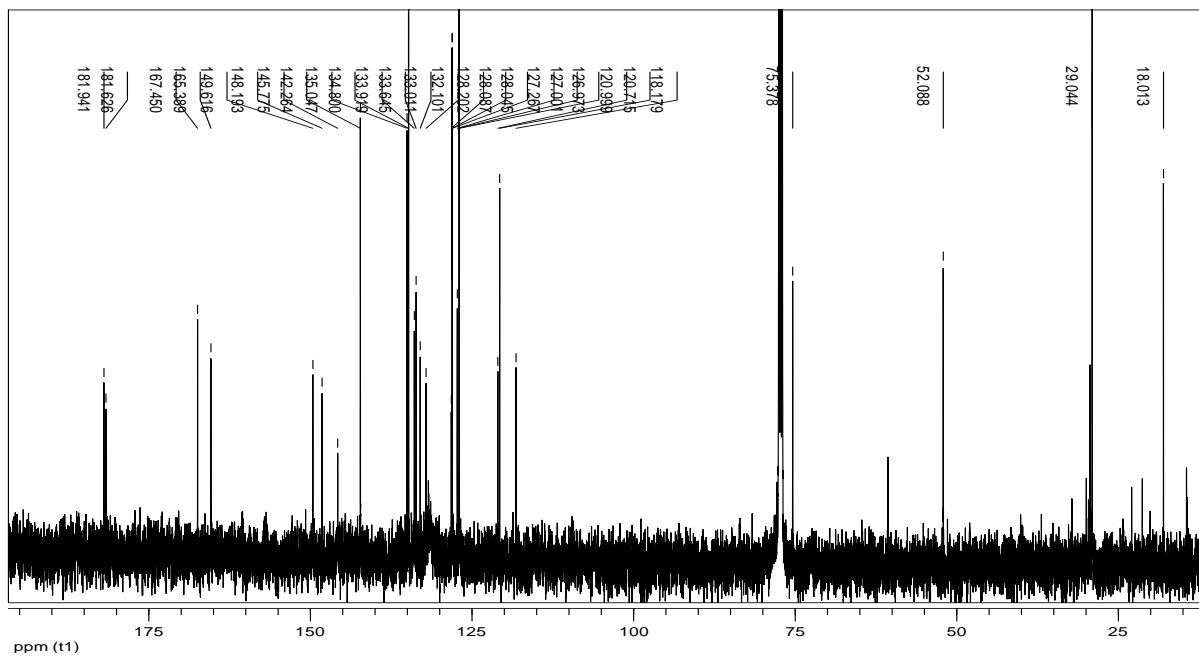
Compound 14p



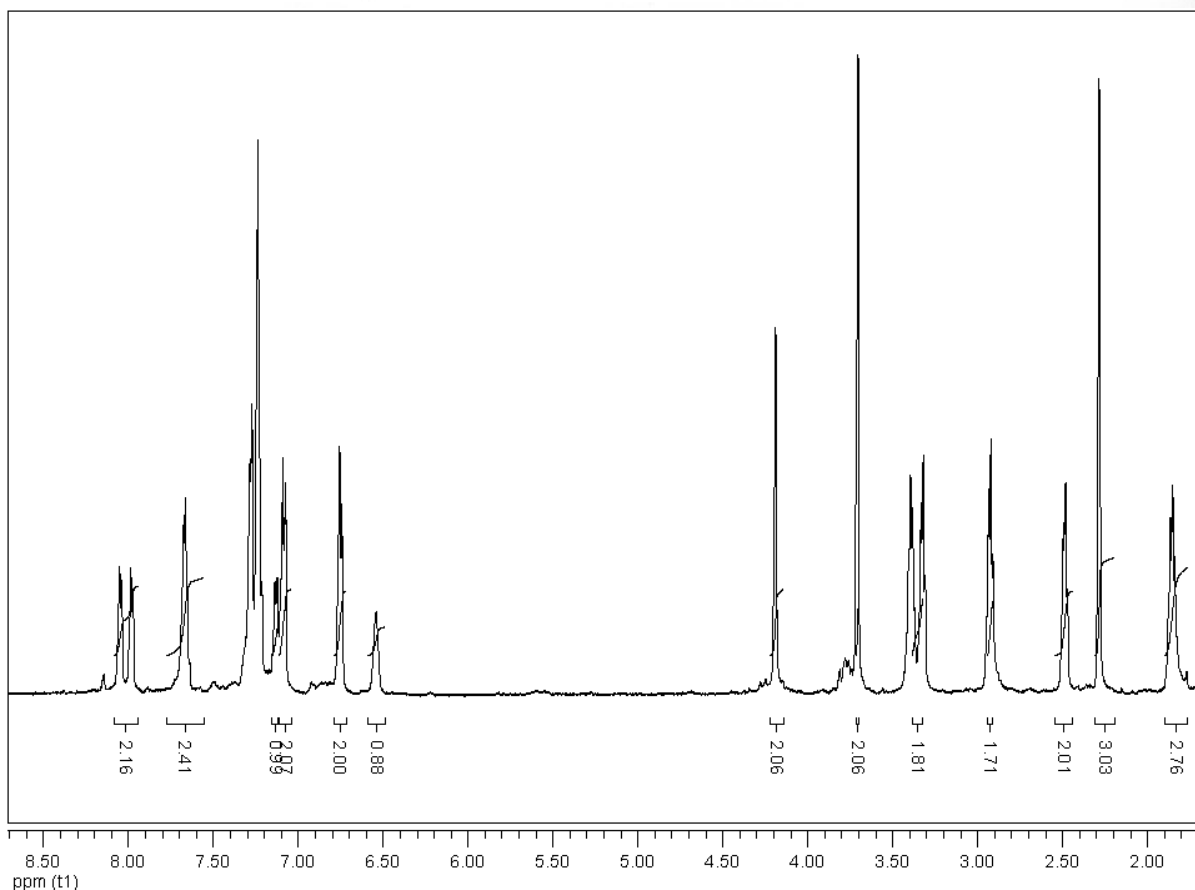
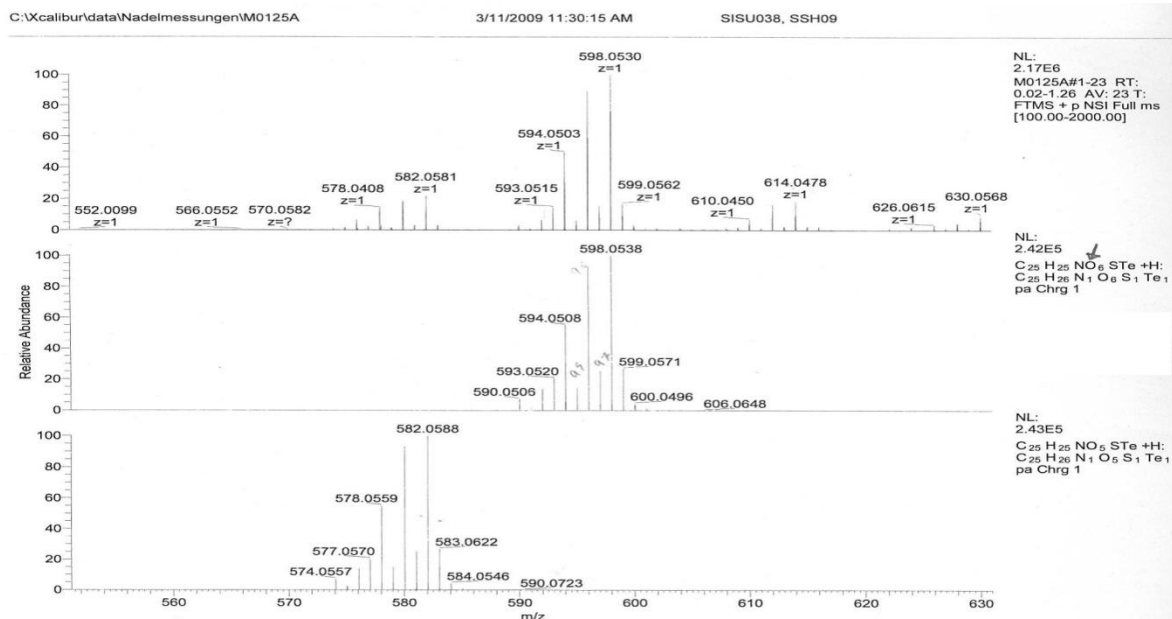


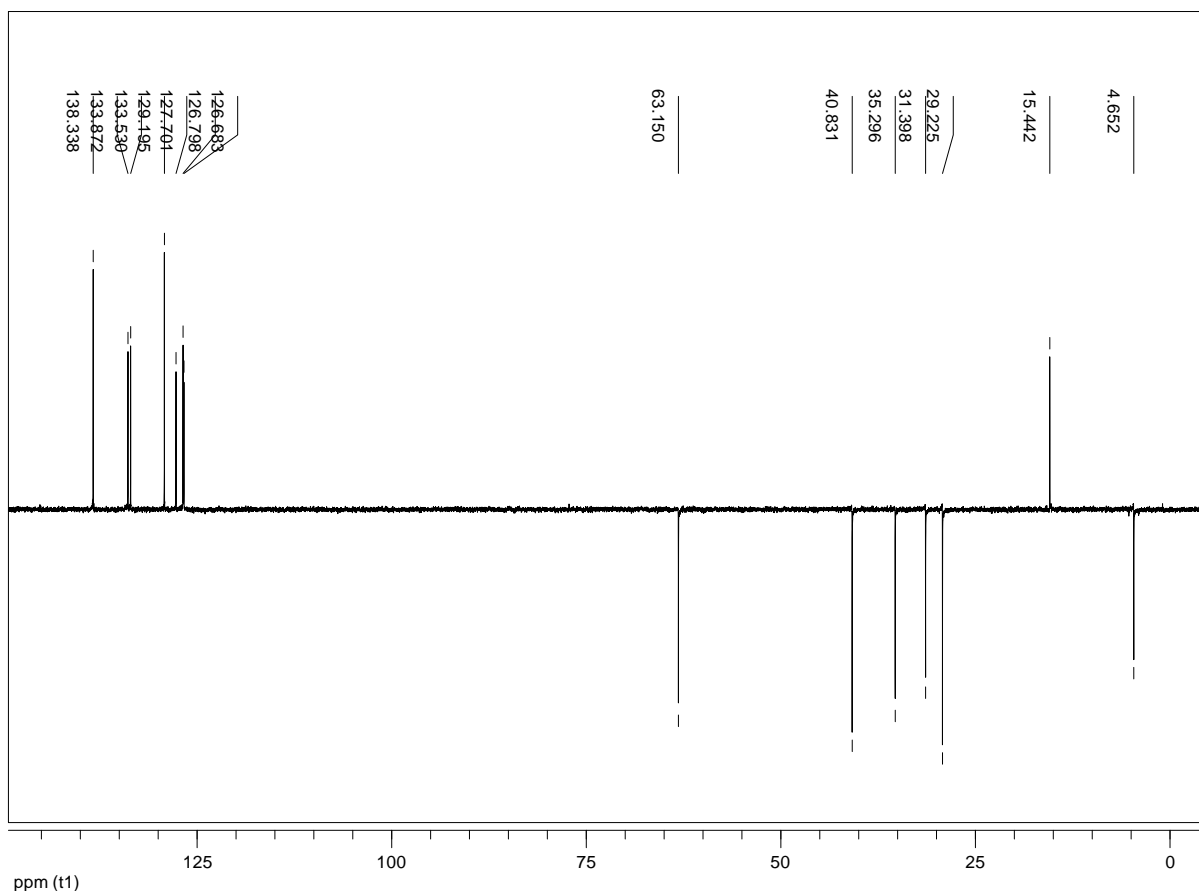
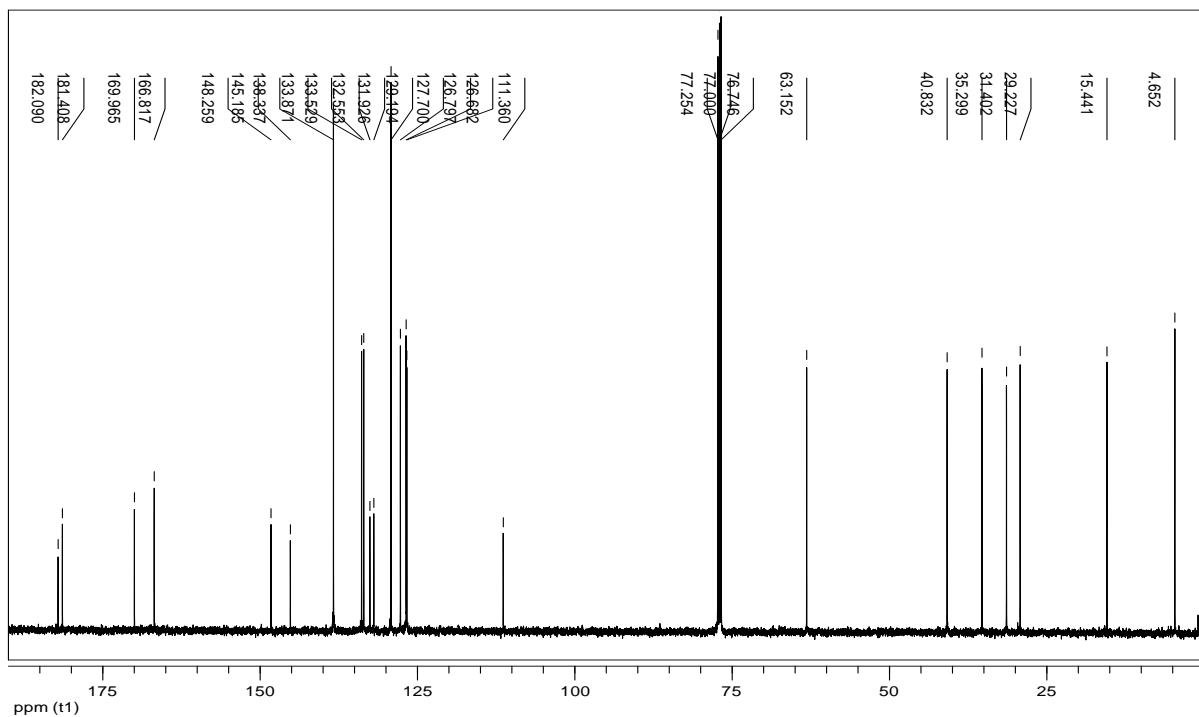
Compound 15p



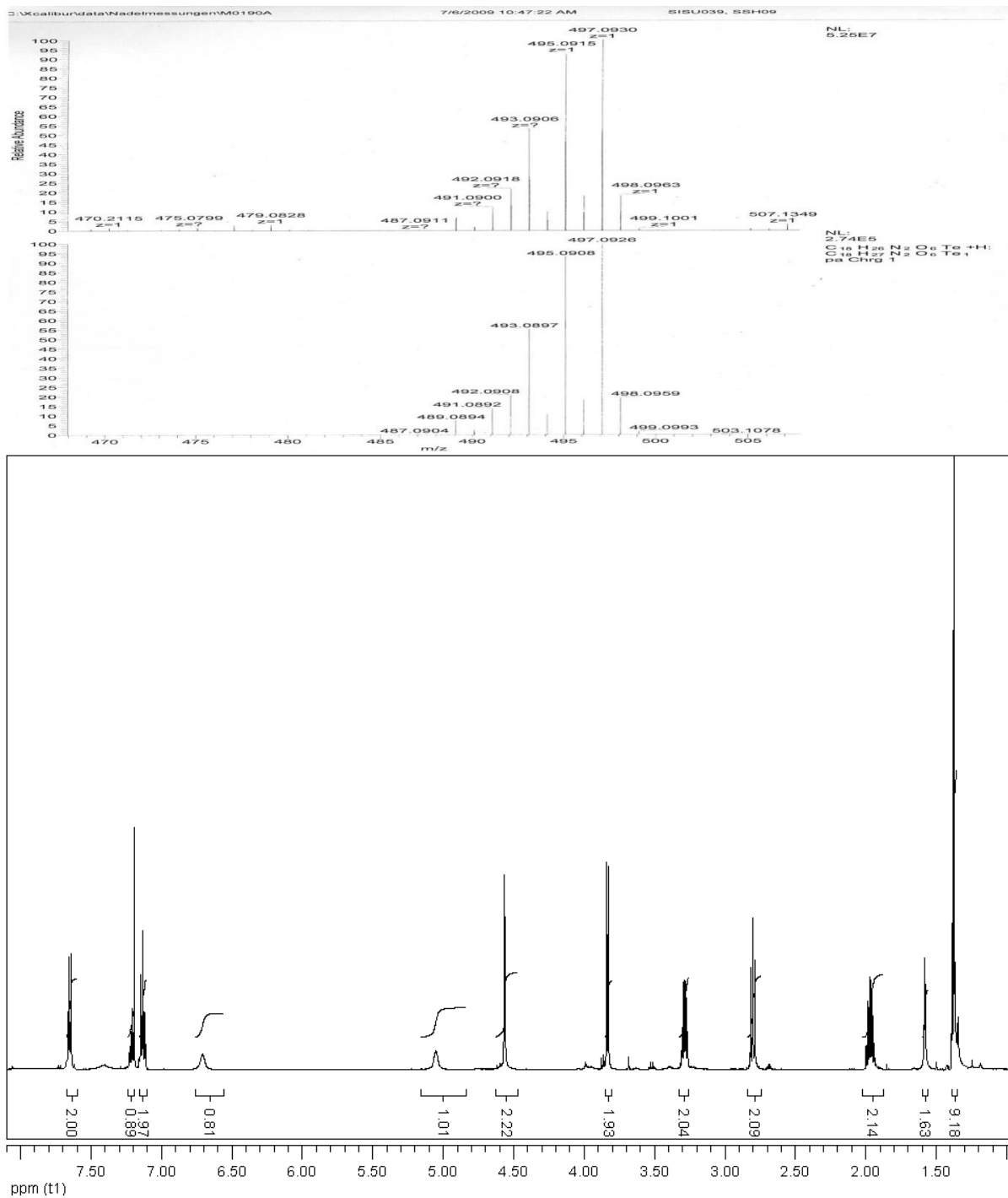


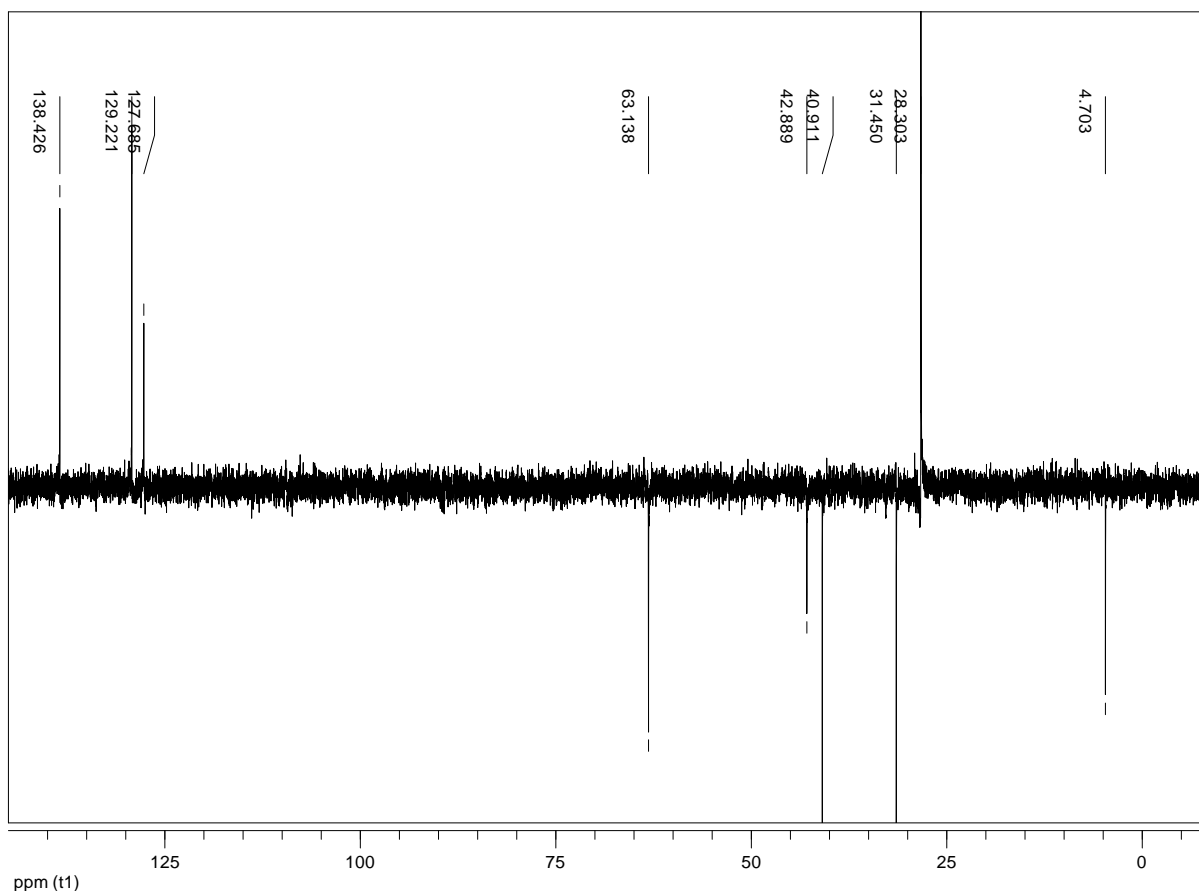
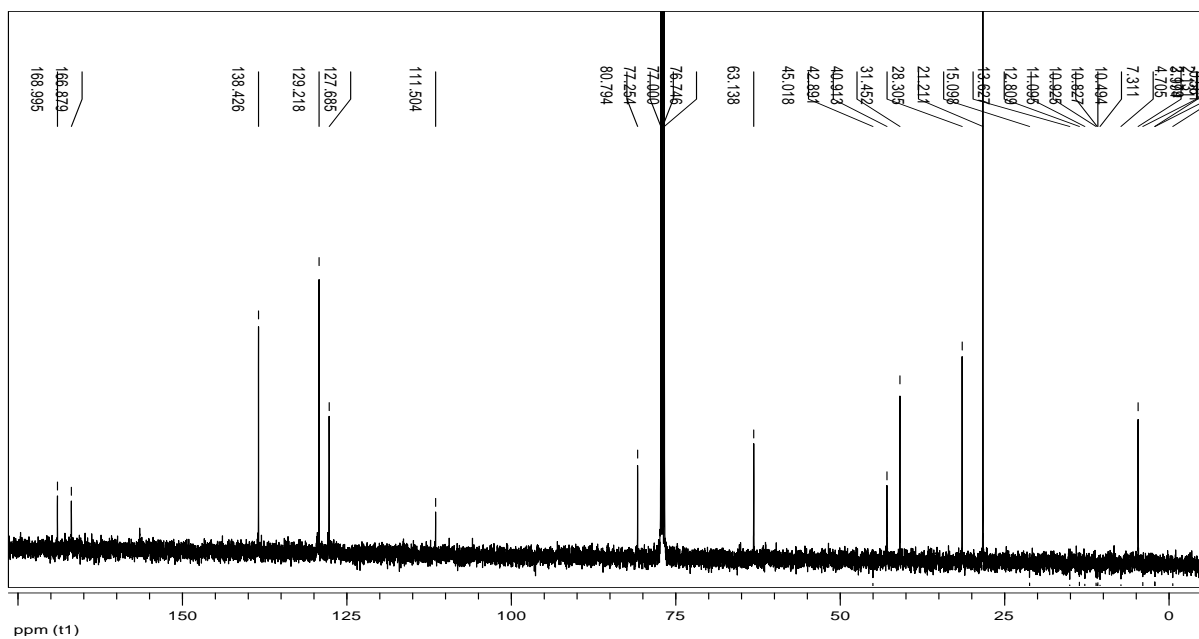
Compound16p



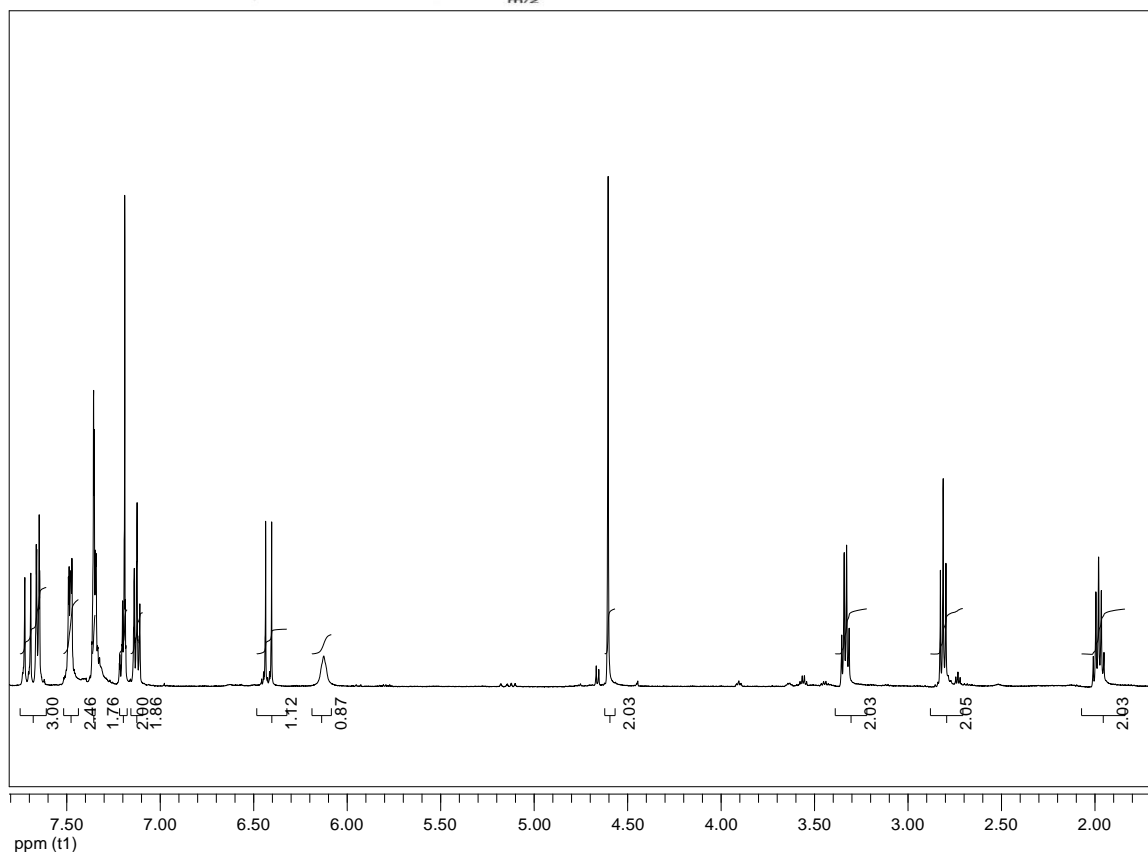
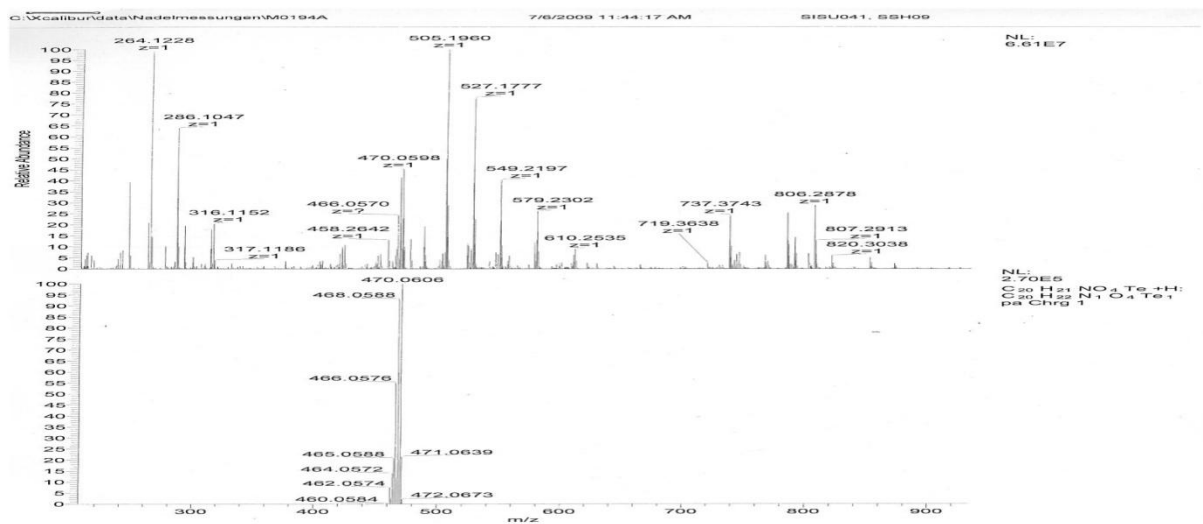


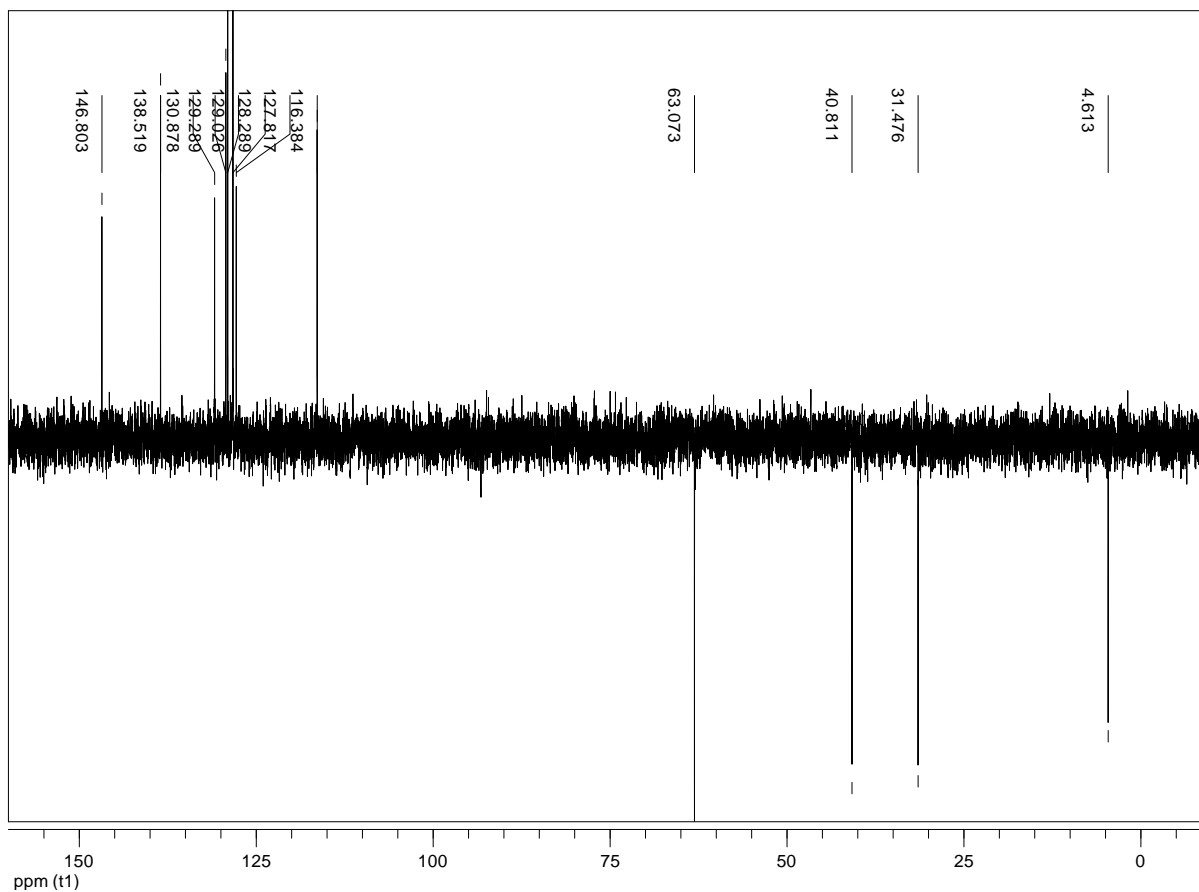
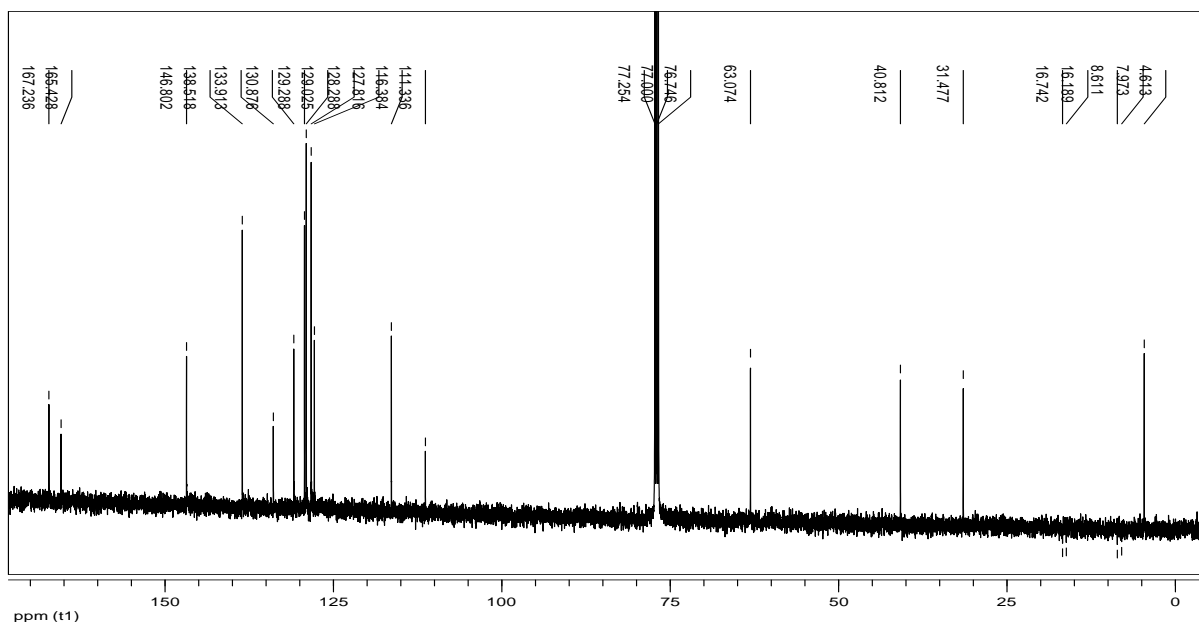
Compound17p



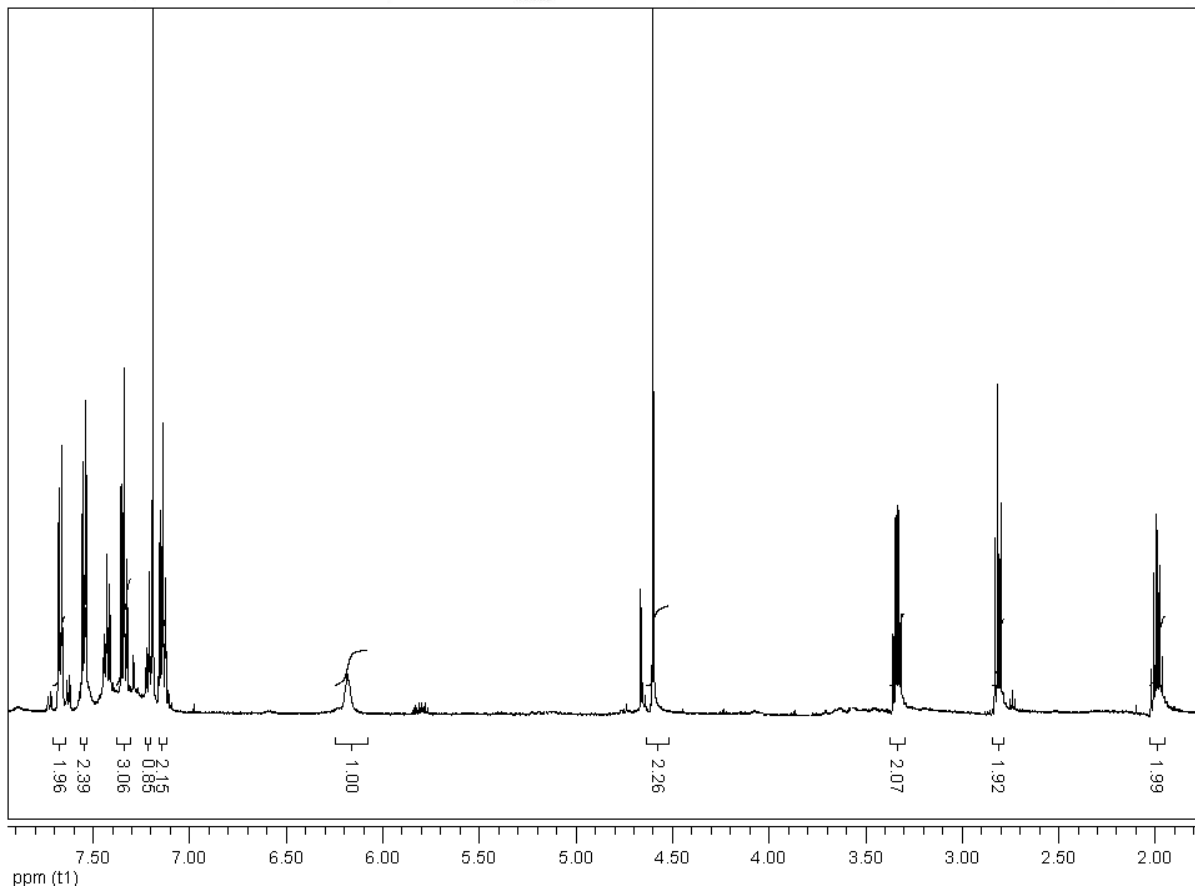
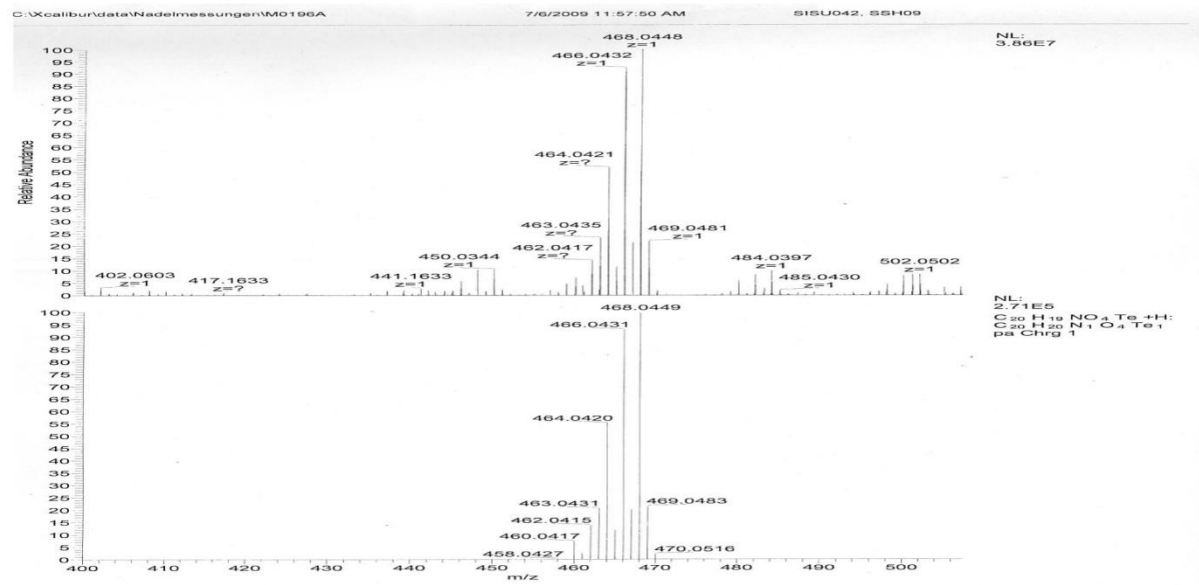


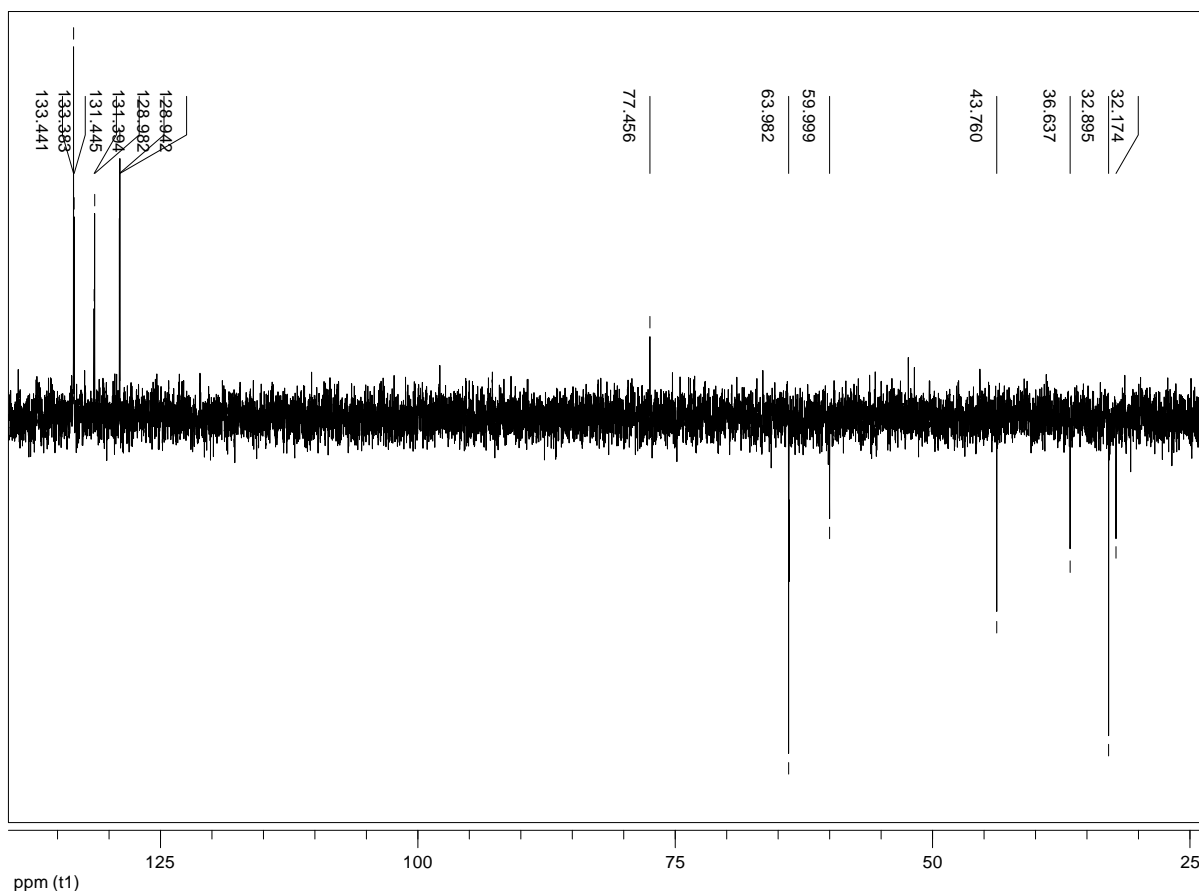
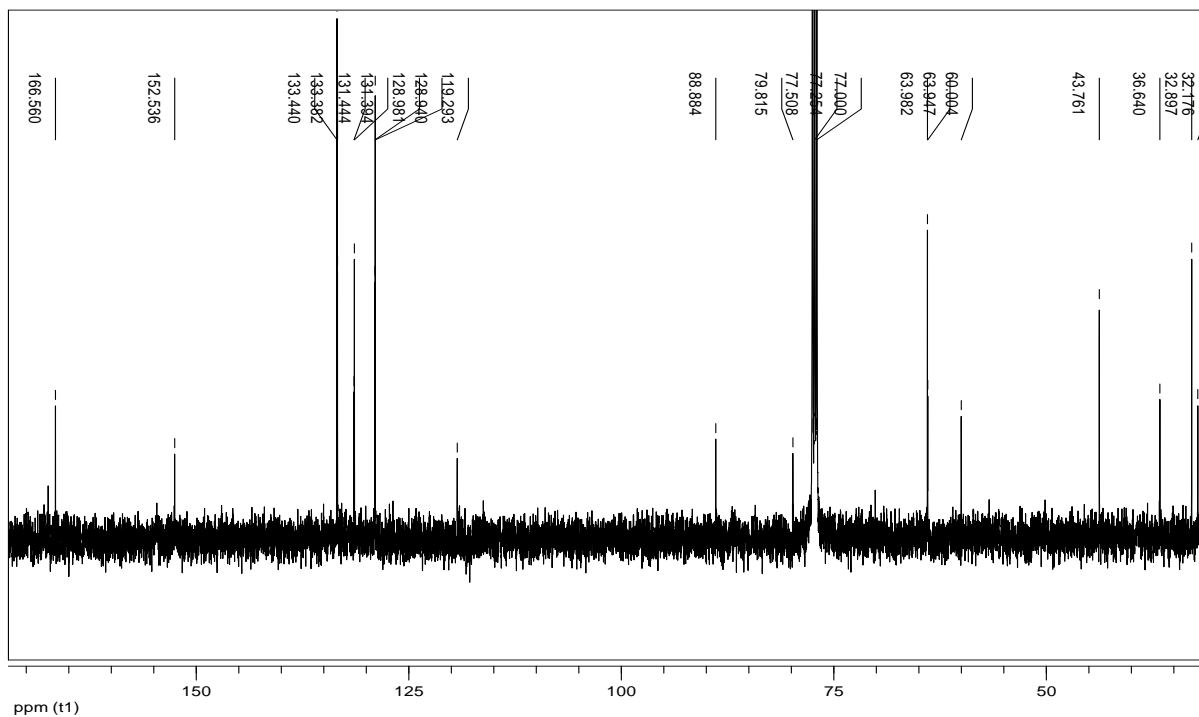
Compound18p



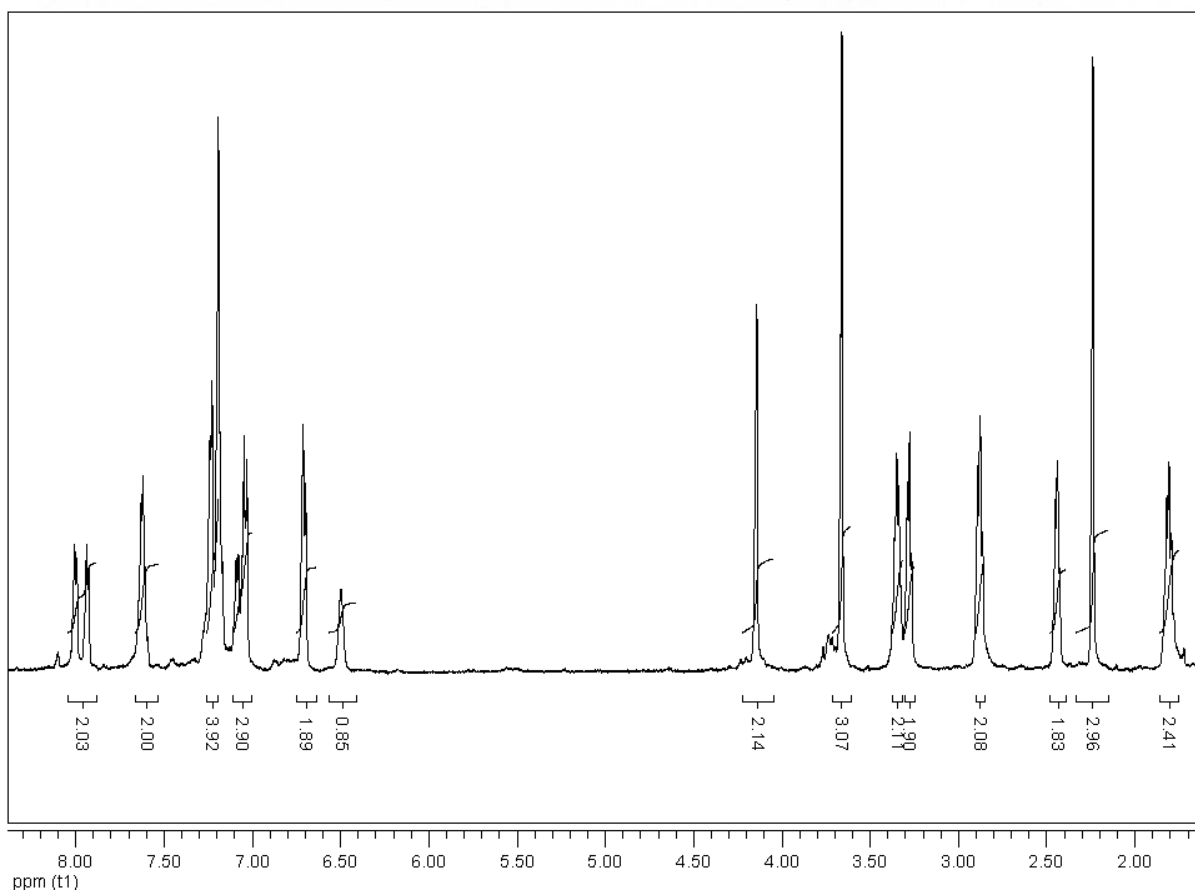
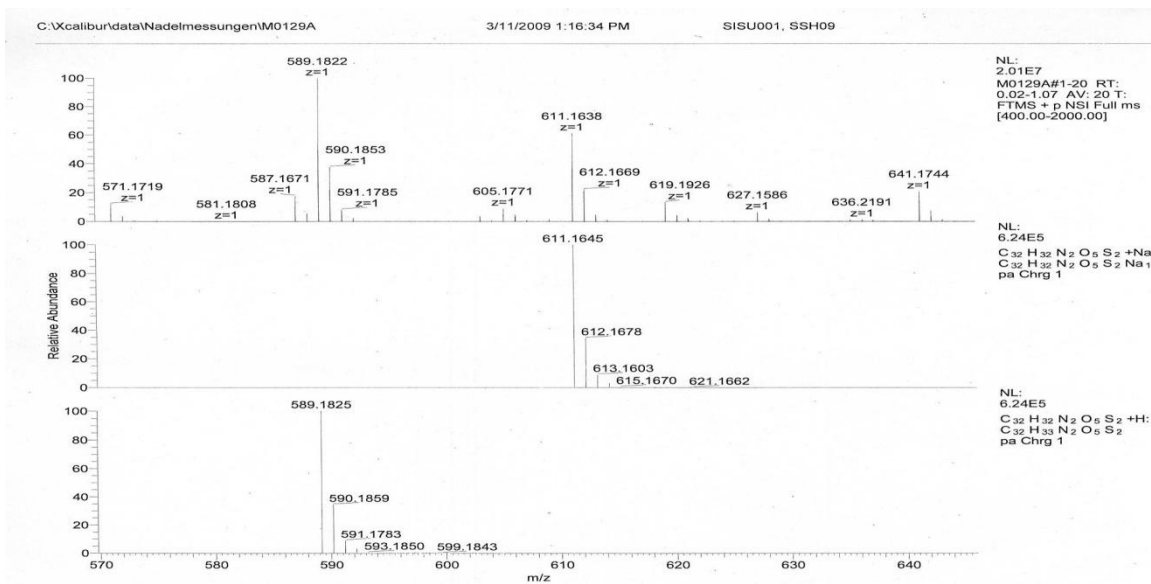


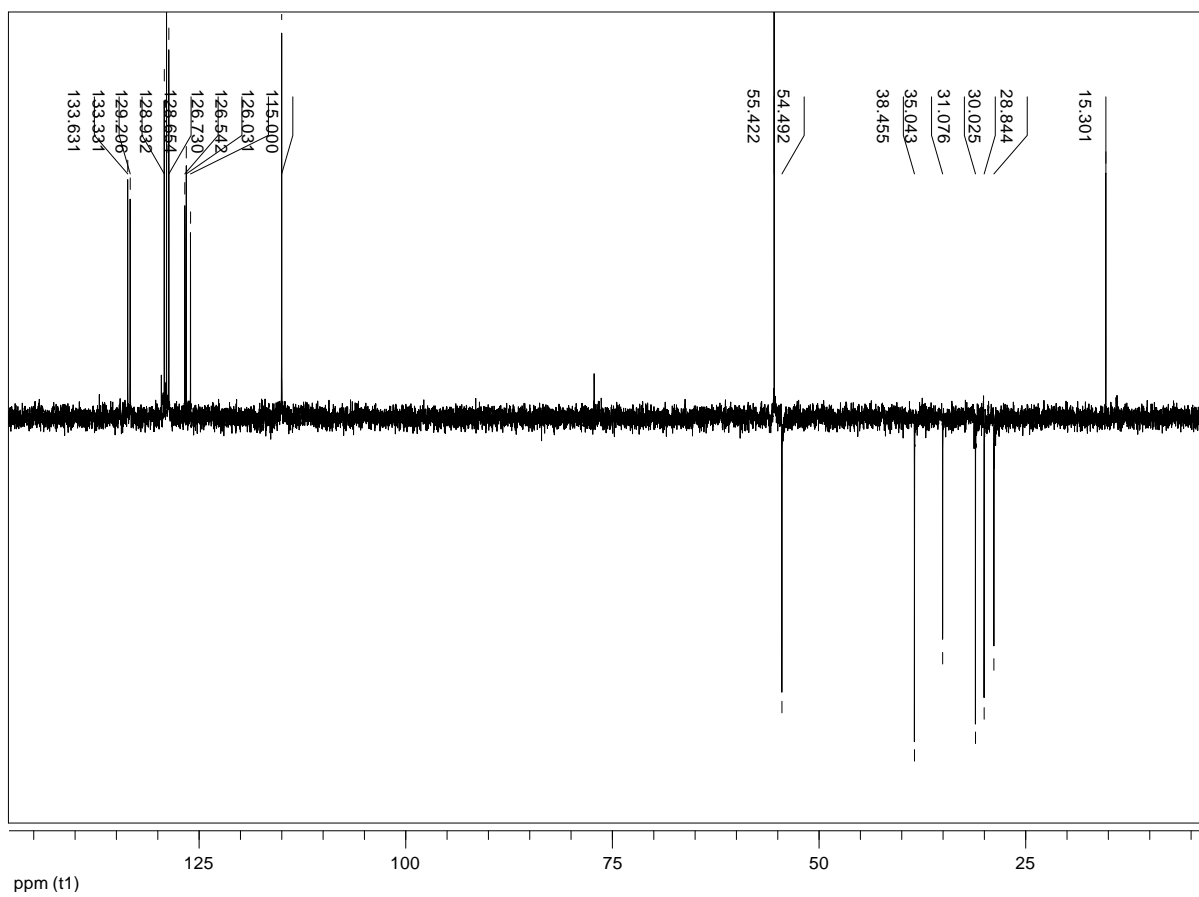
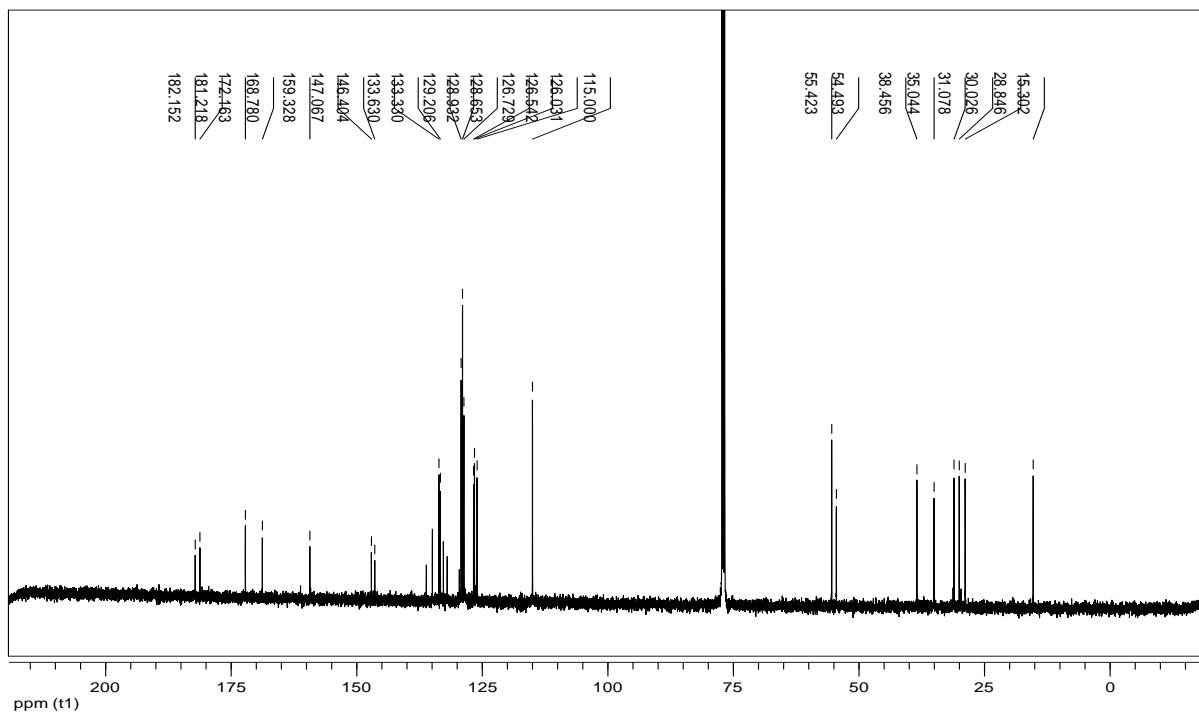
Compound 19p



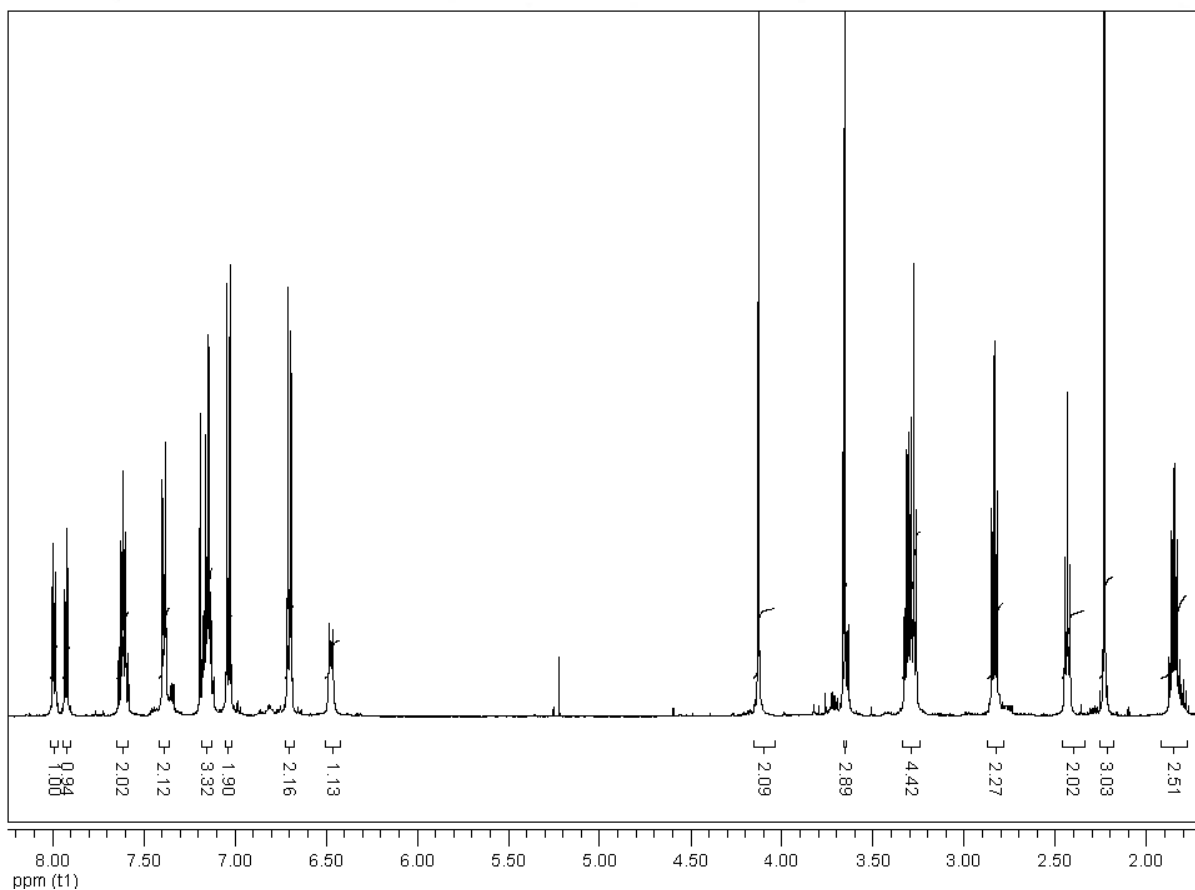
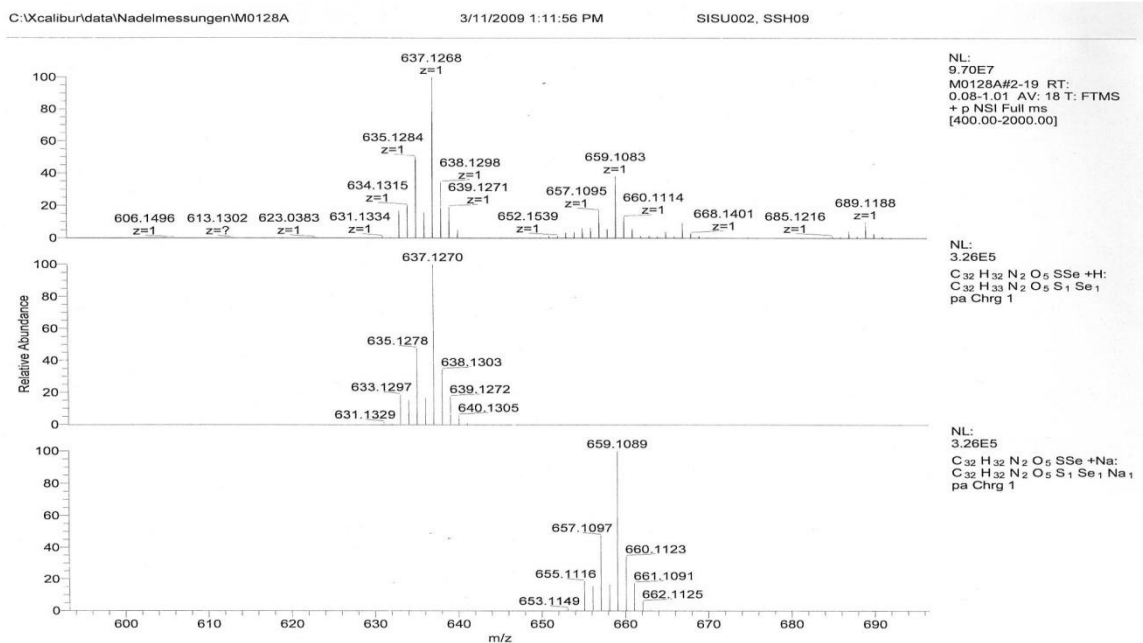


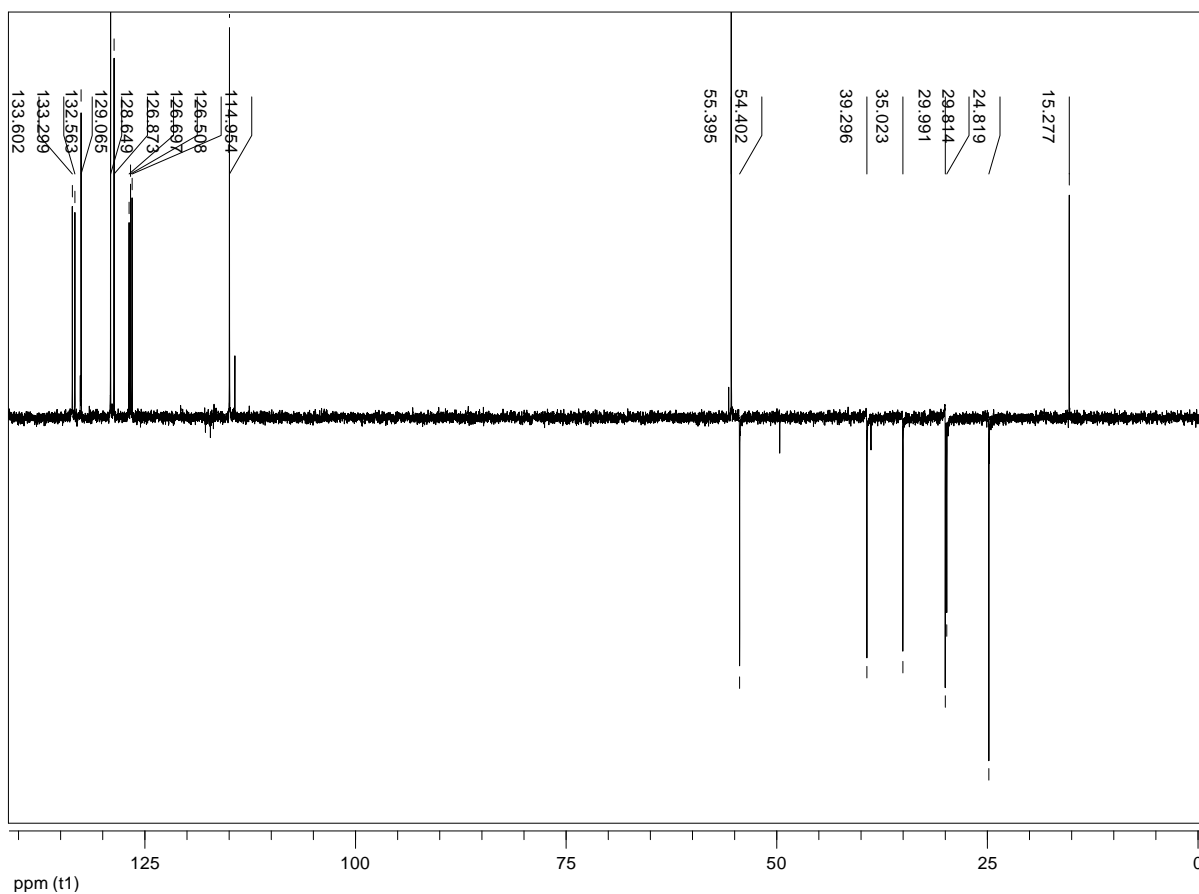
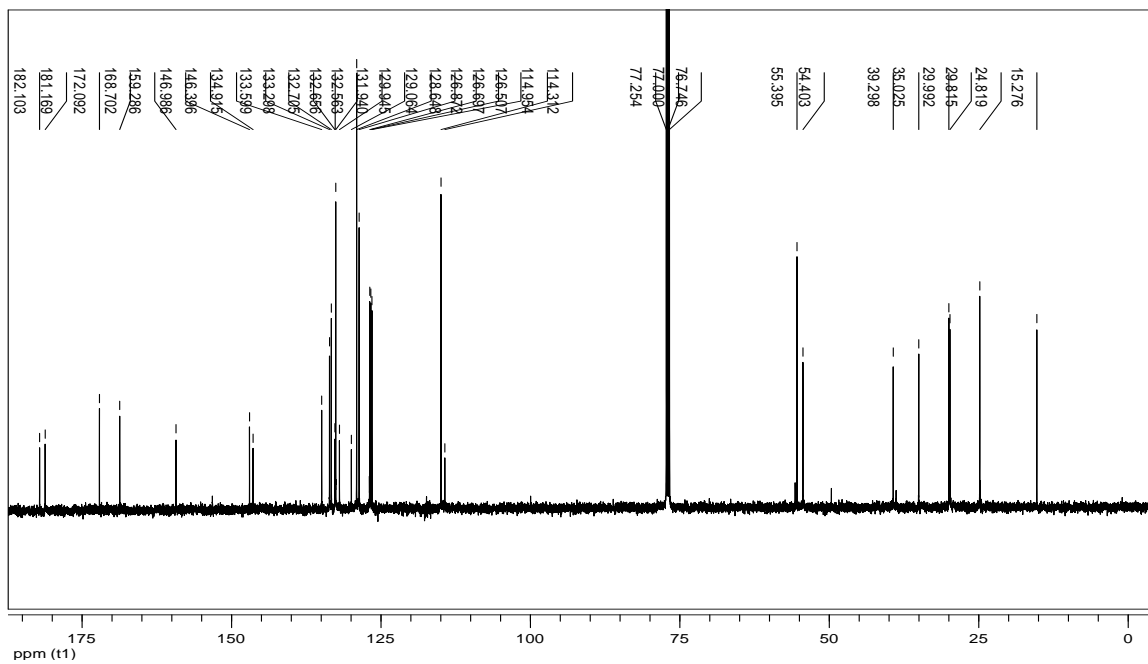
Compound 1u



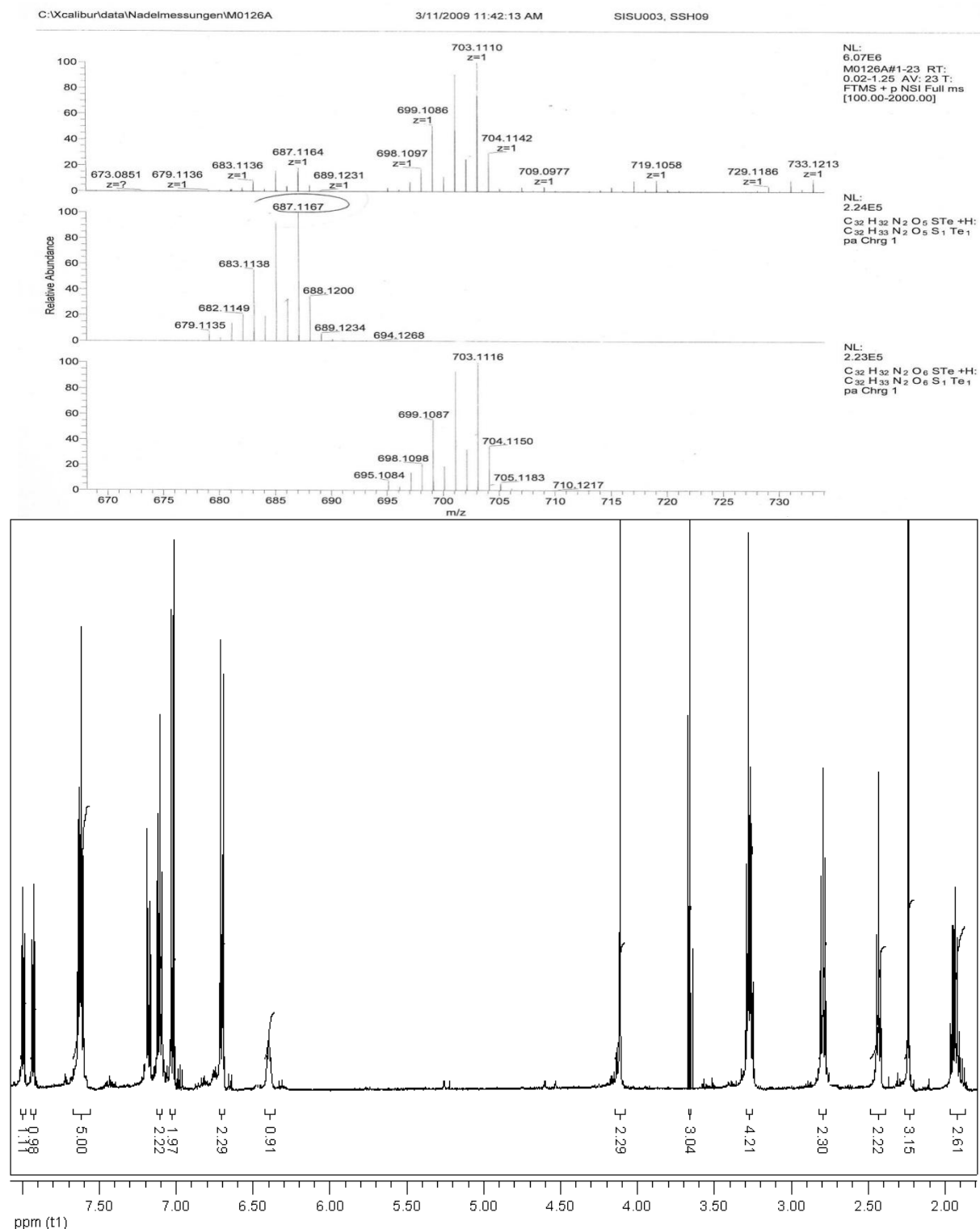


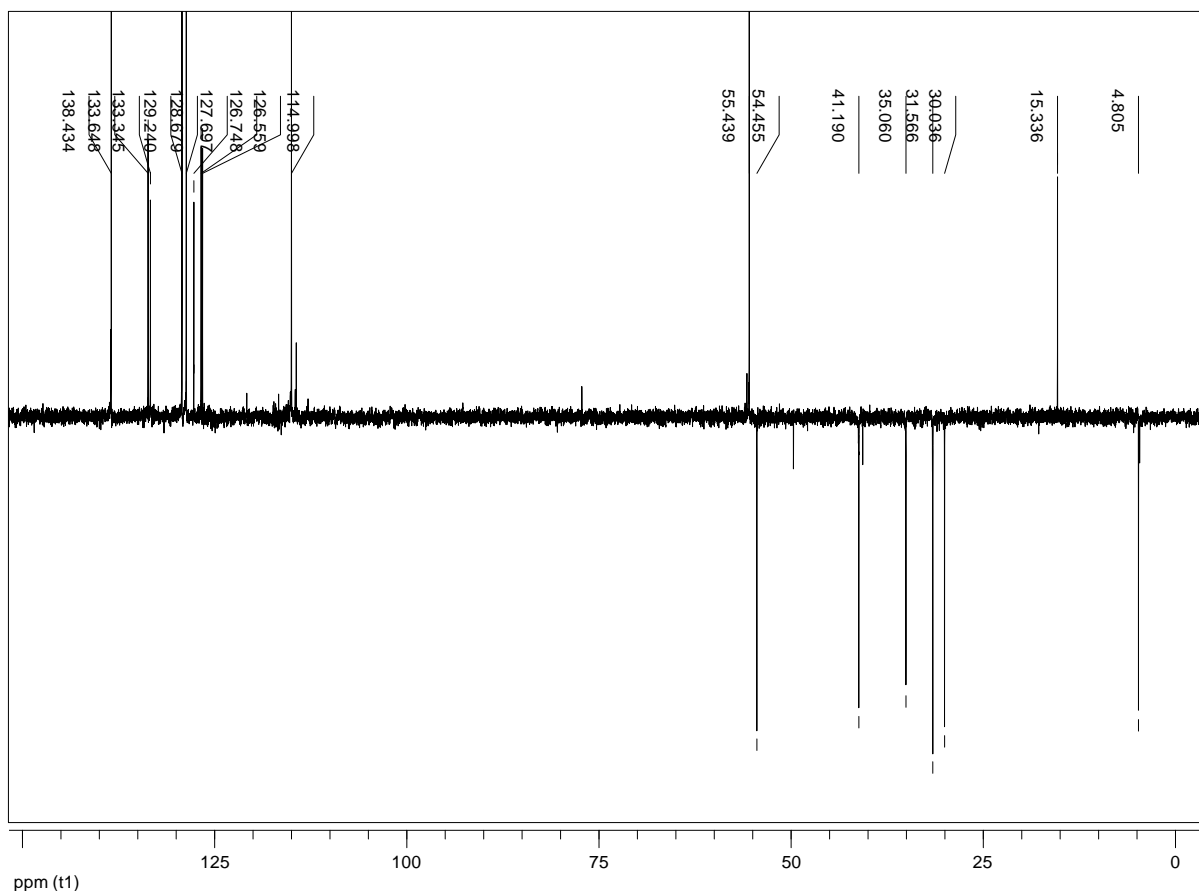
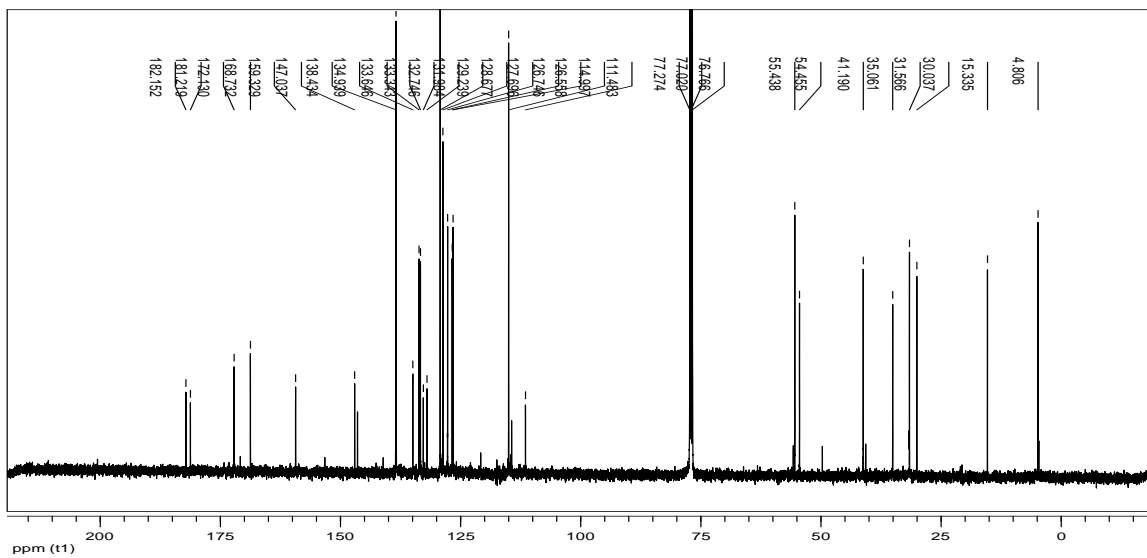
Compound 2u





Compound 3u



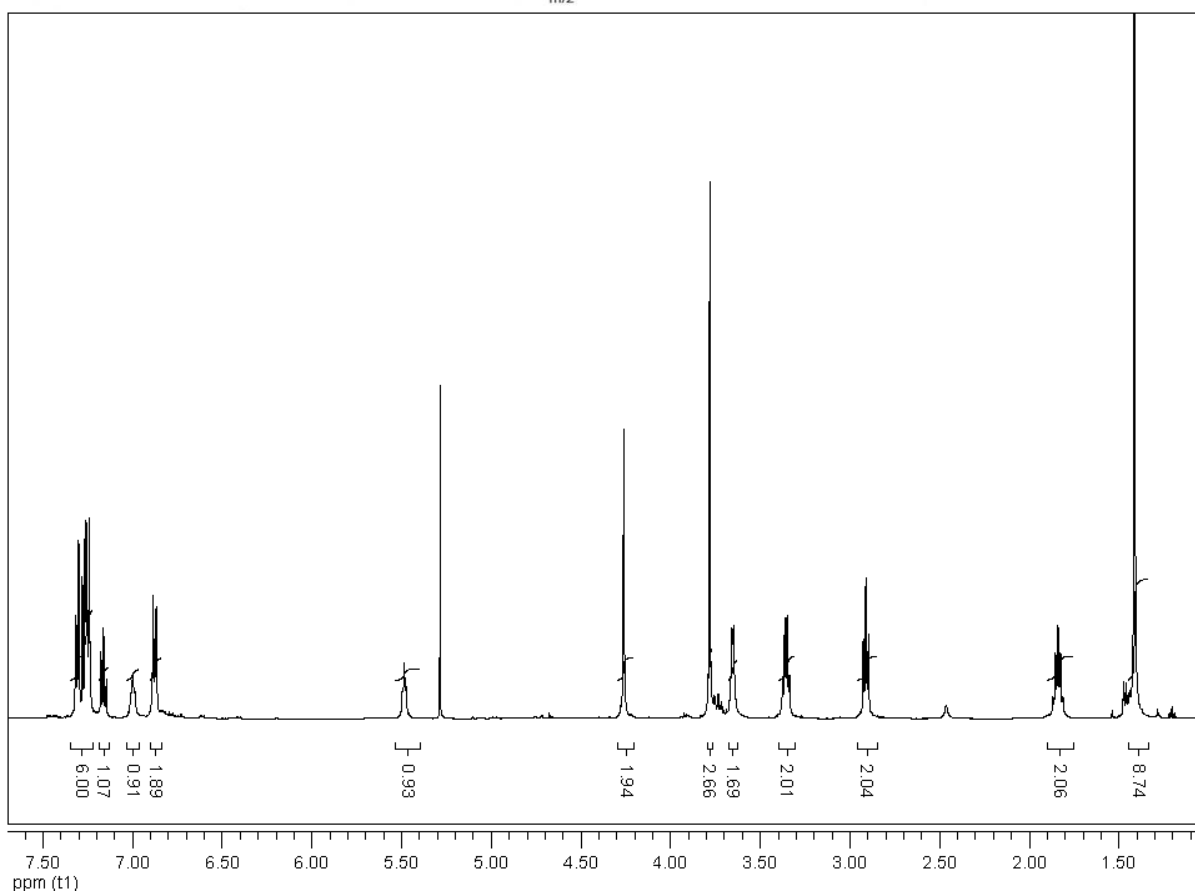
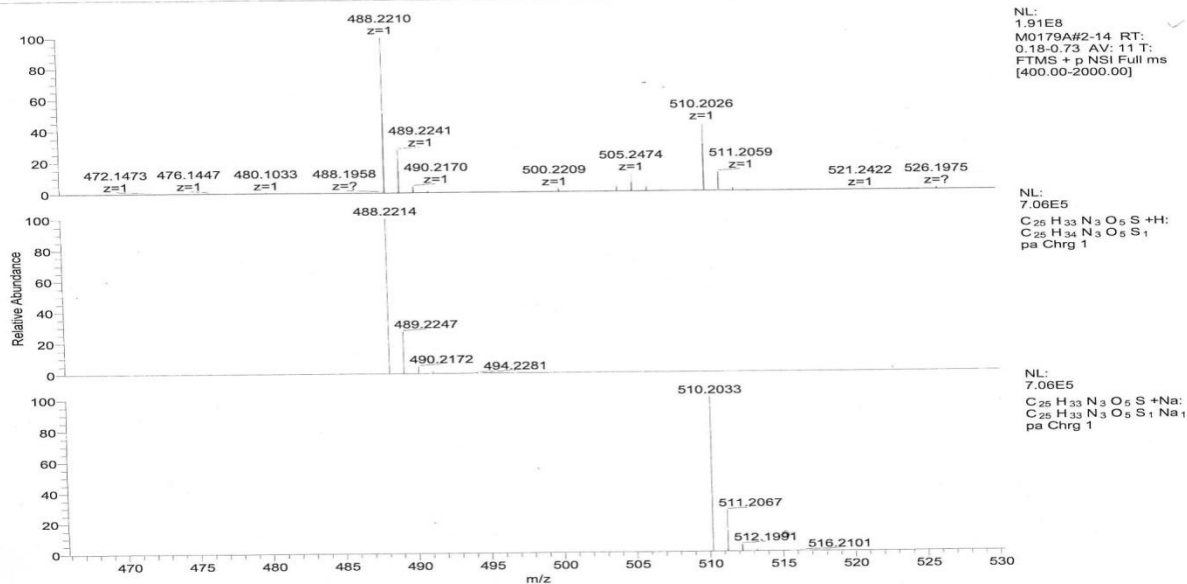


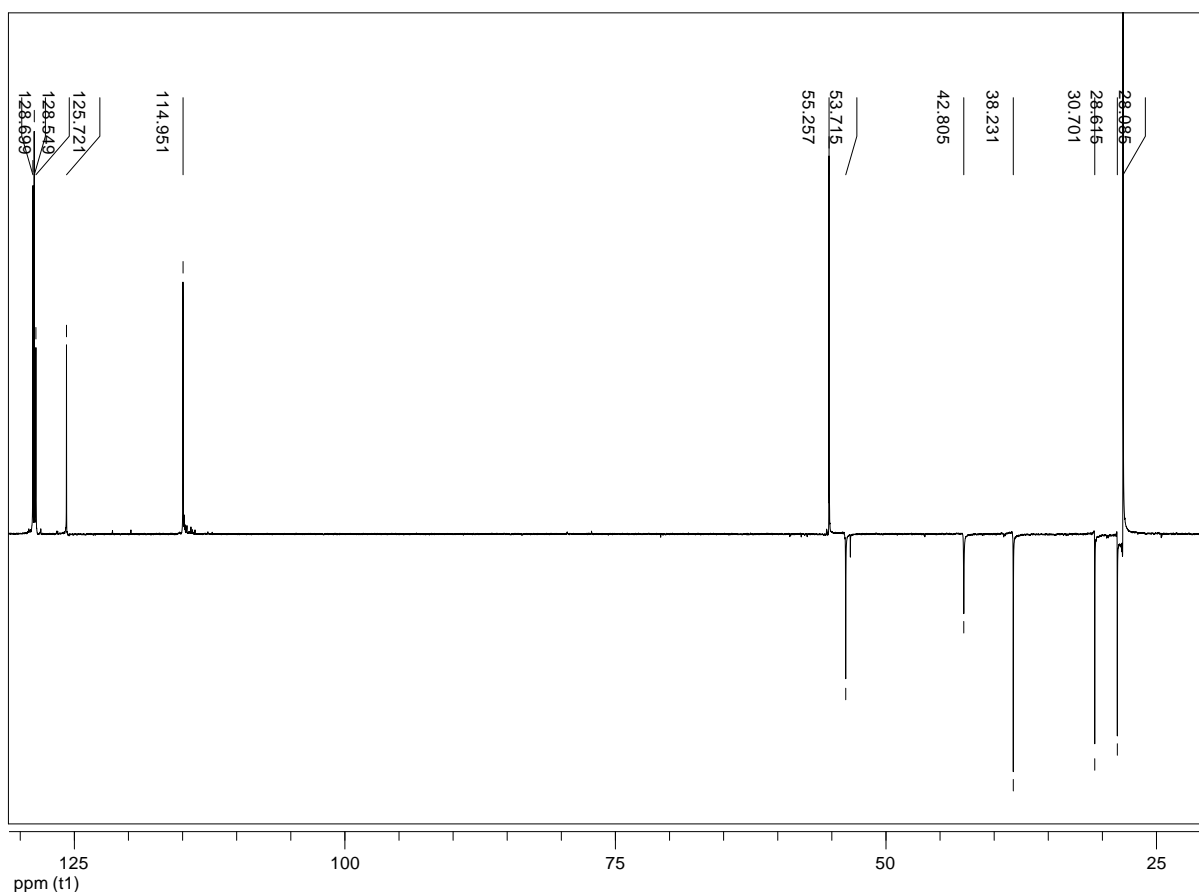
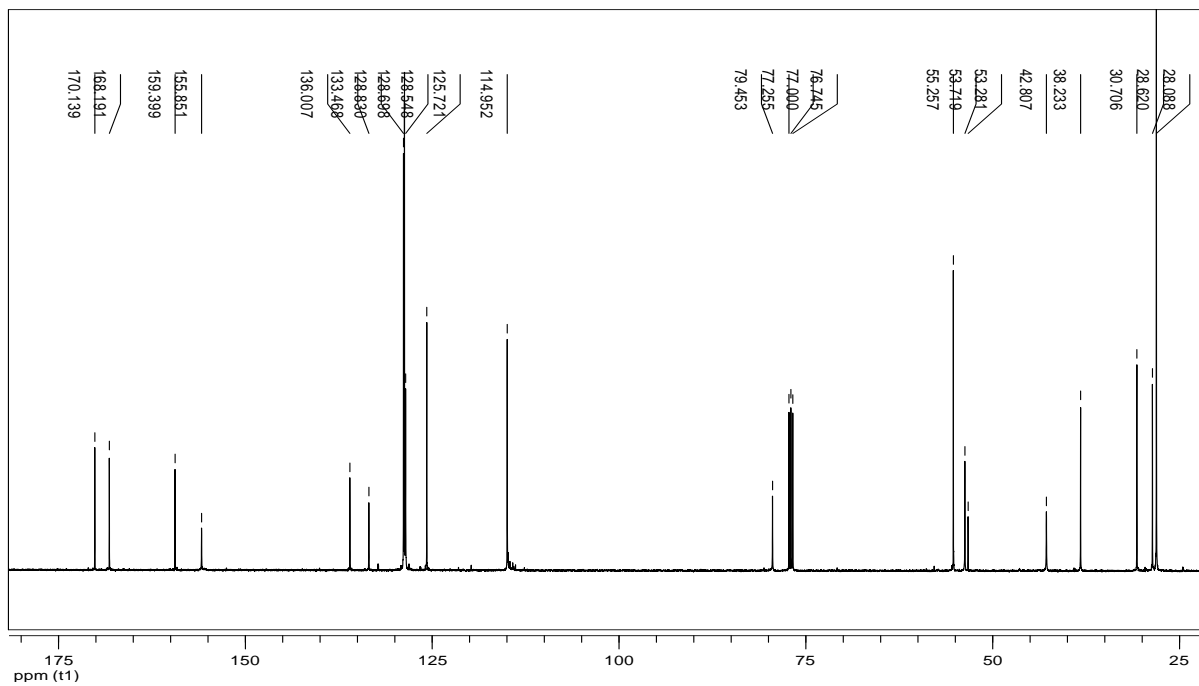
Compound4u

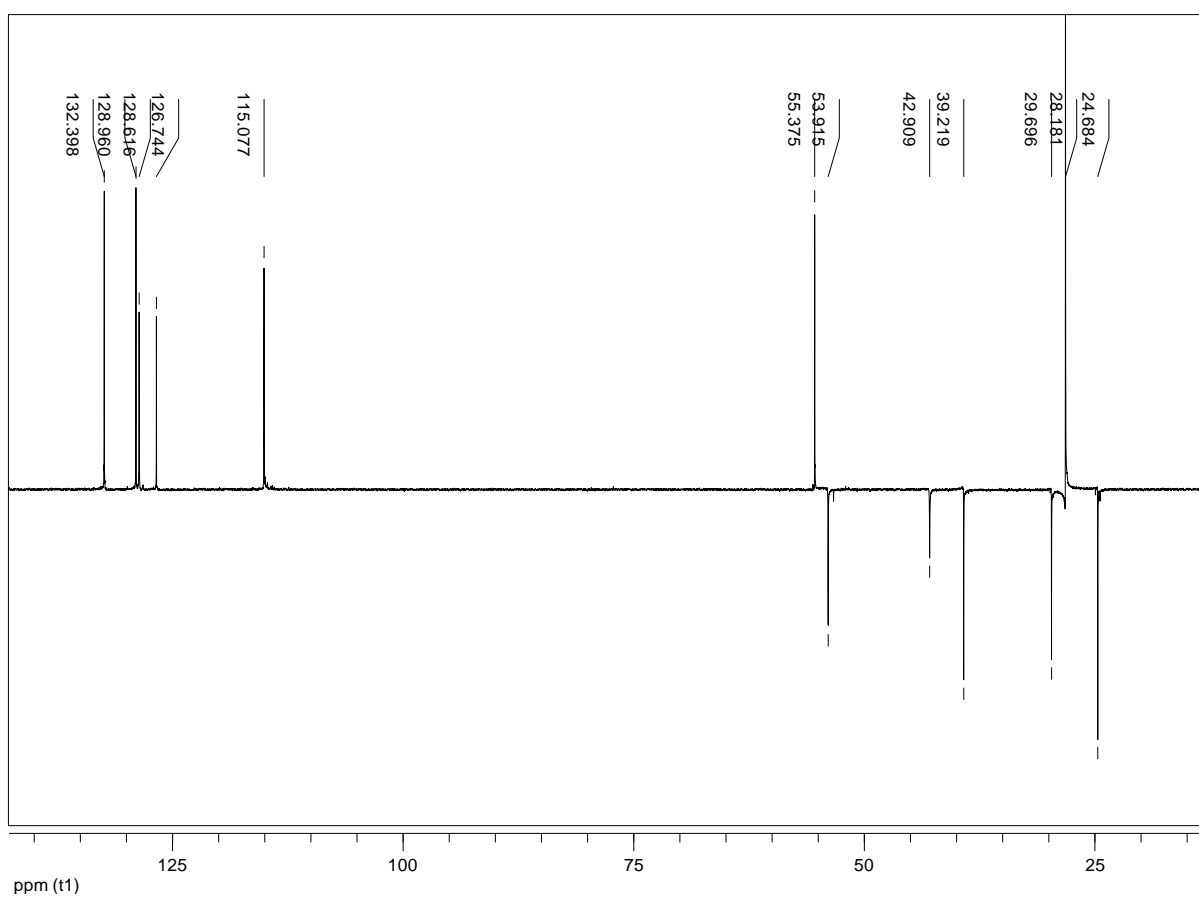
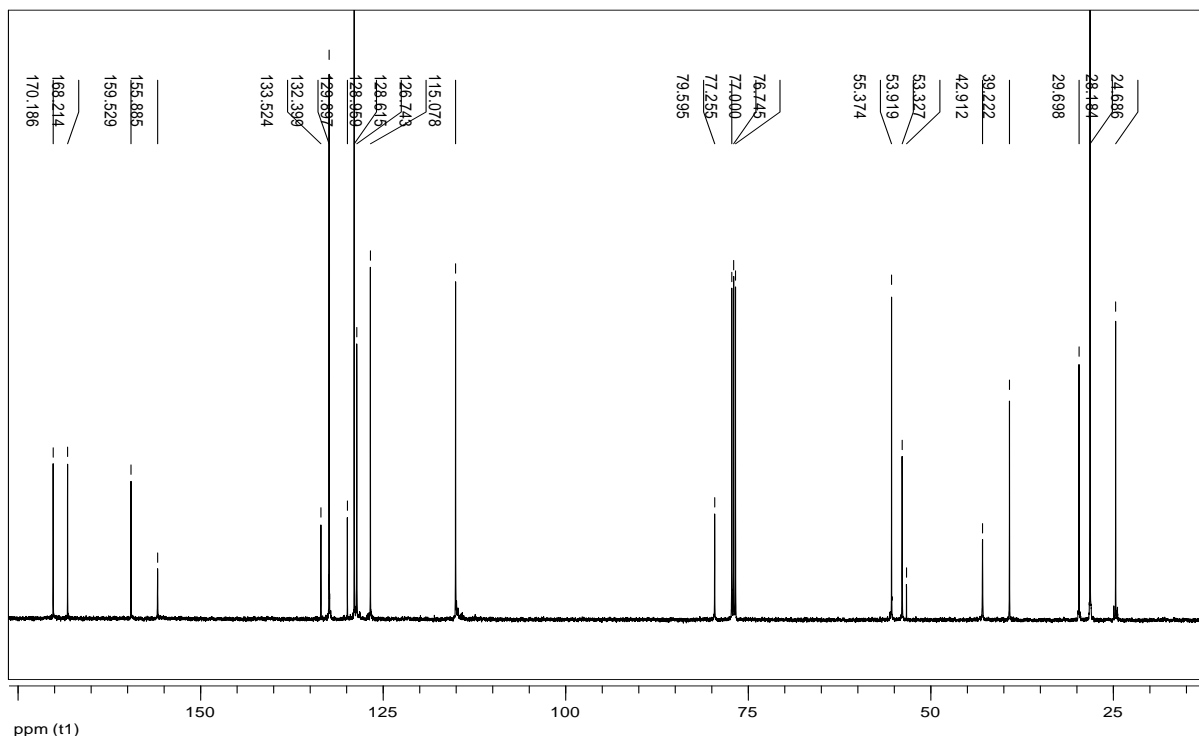
C:\xcalibur\data\Nadelmessungen\M0179A

6/11/2009 12:03:22 PM

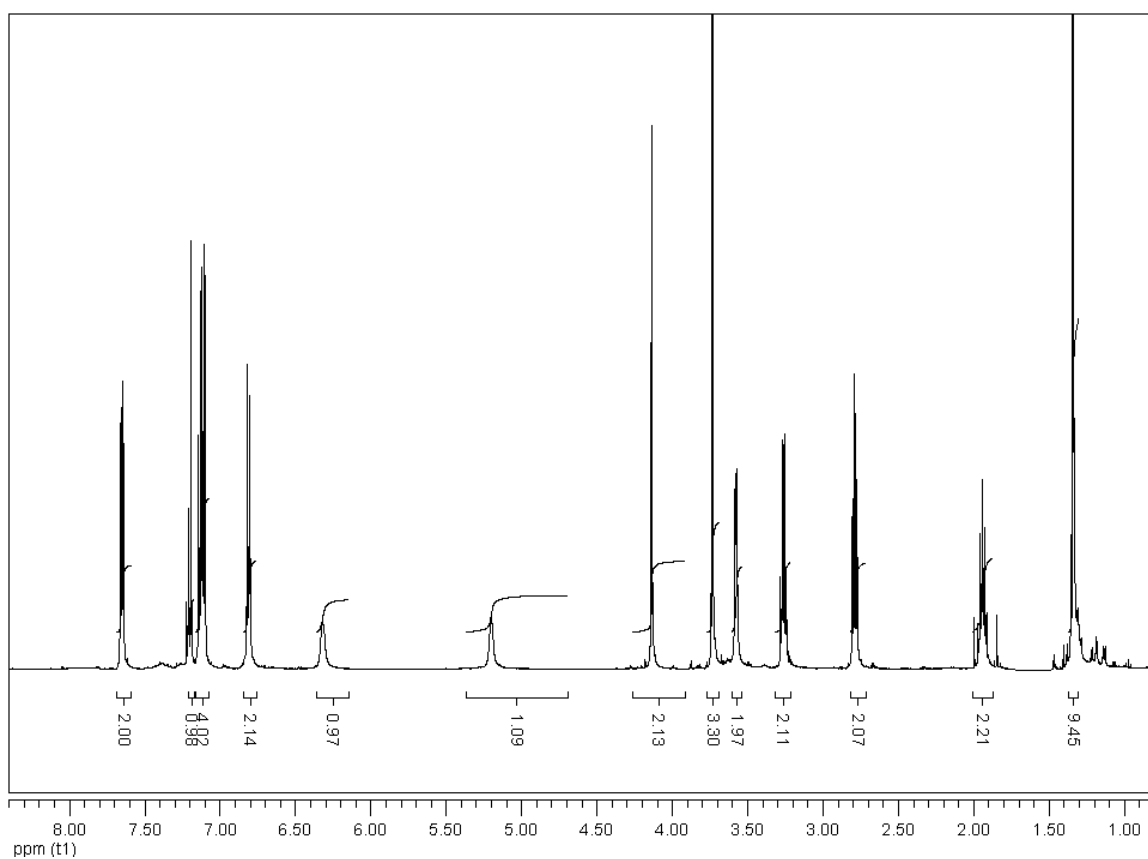
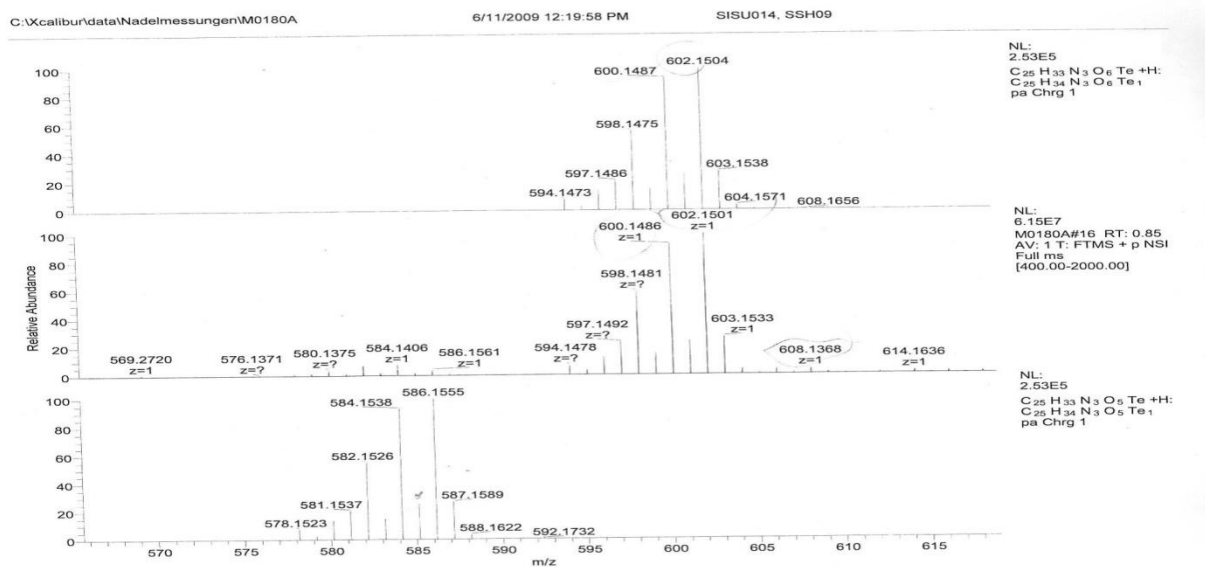
SISU012_SSH09

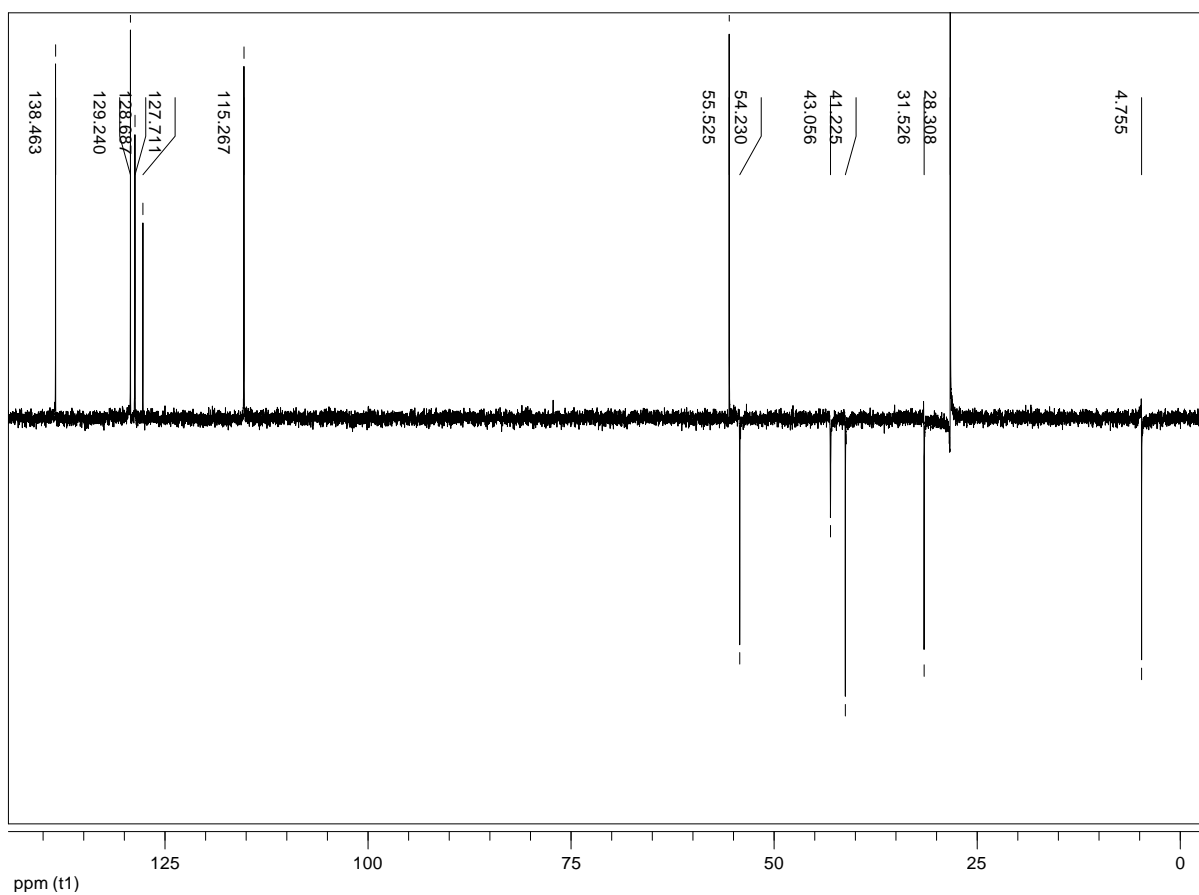
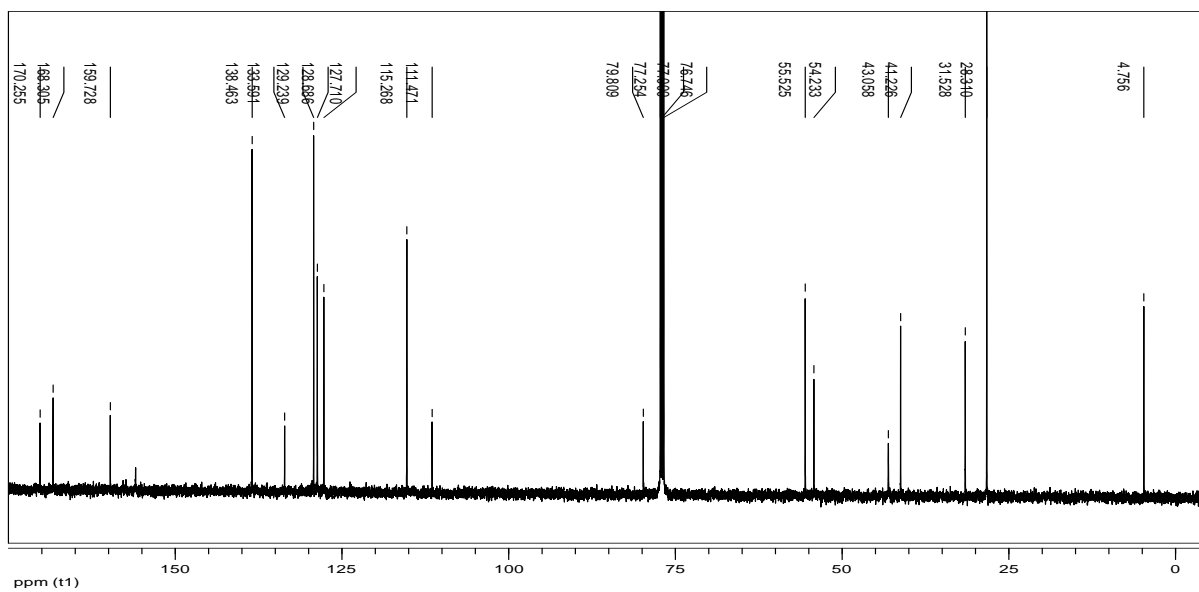




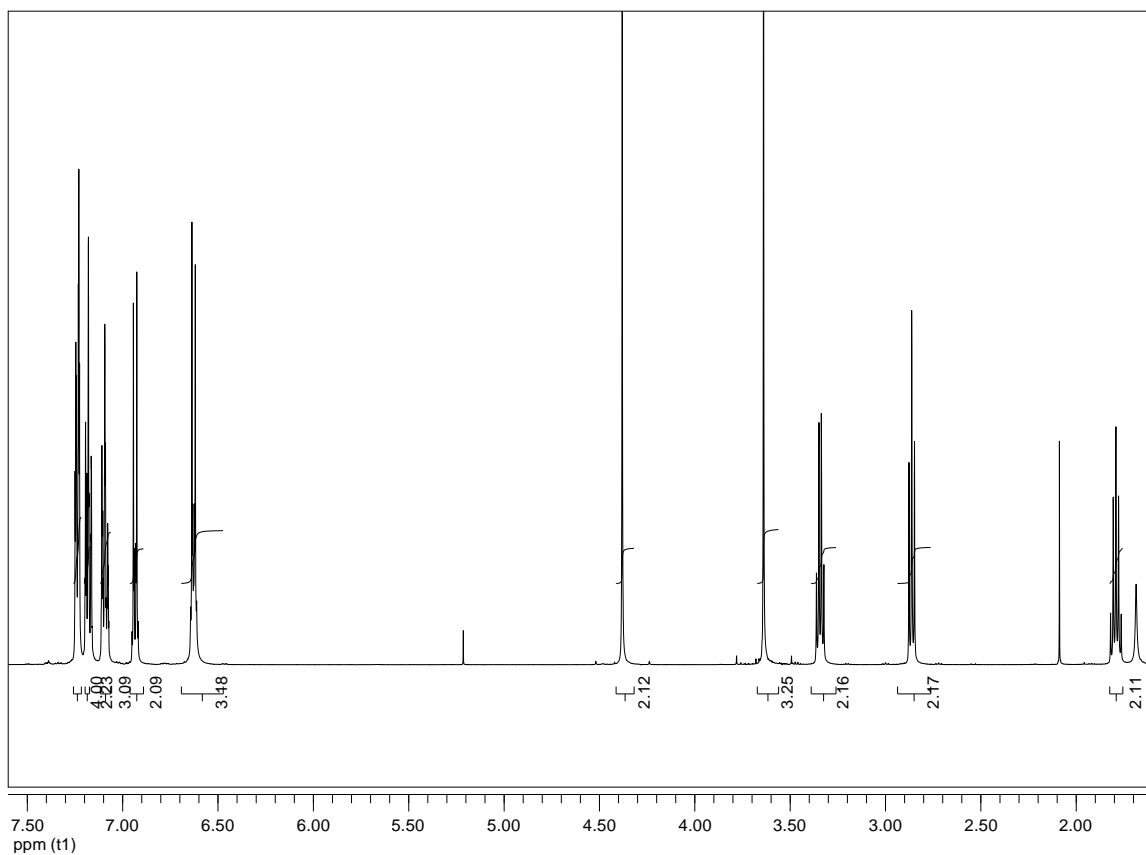
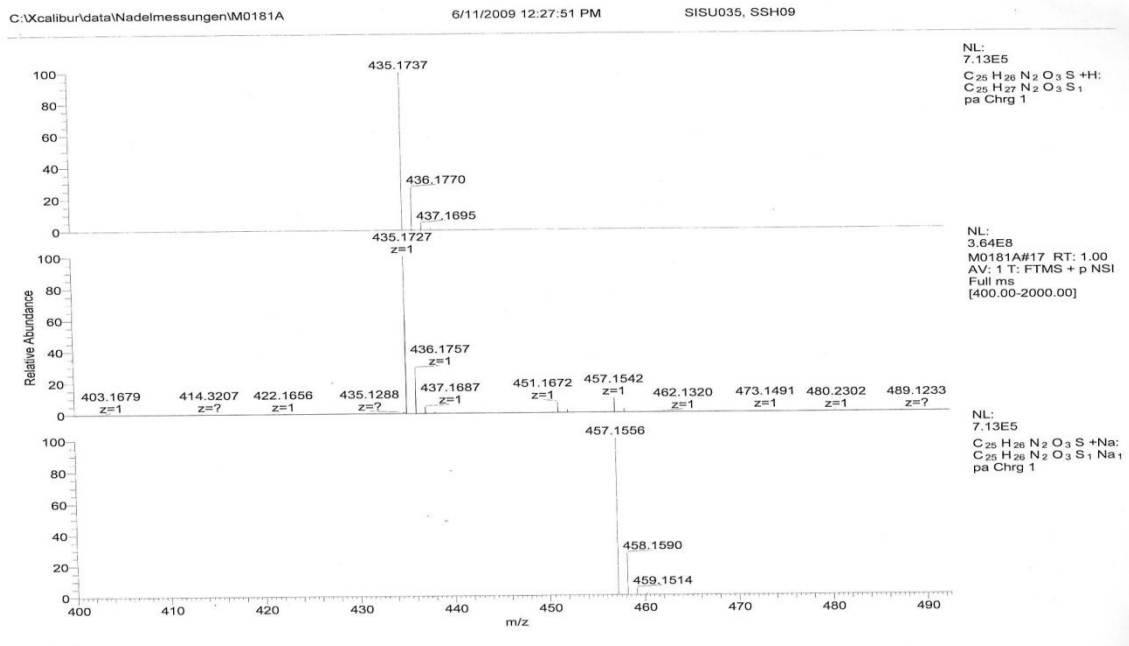


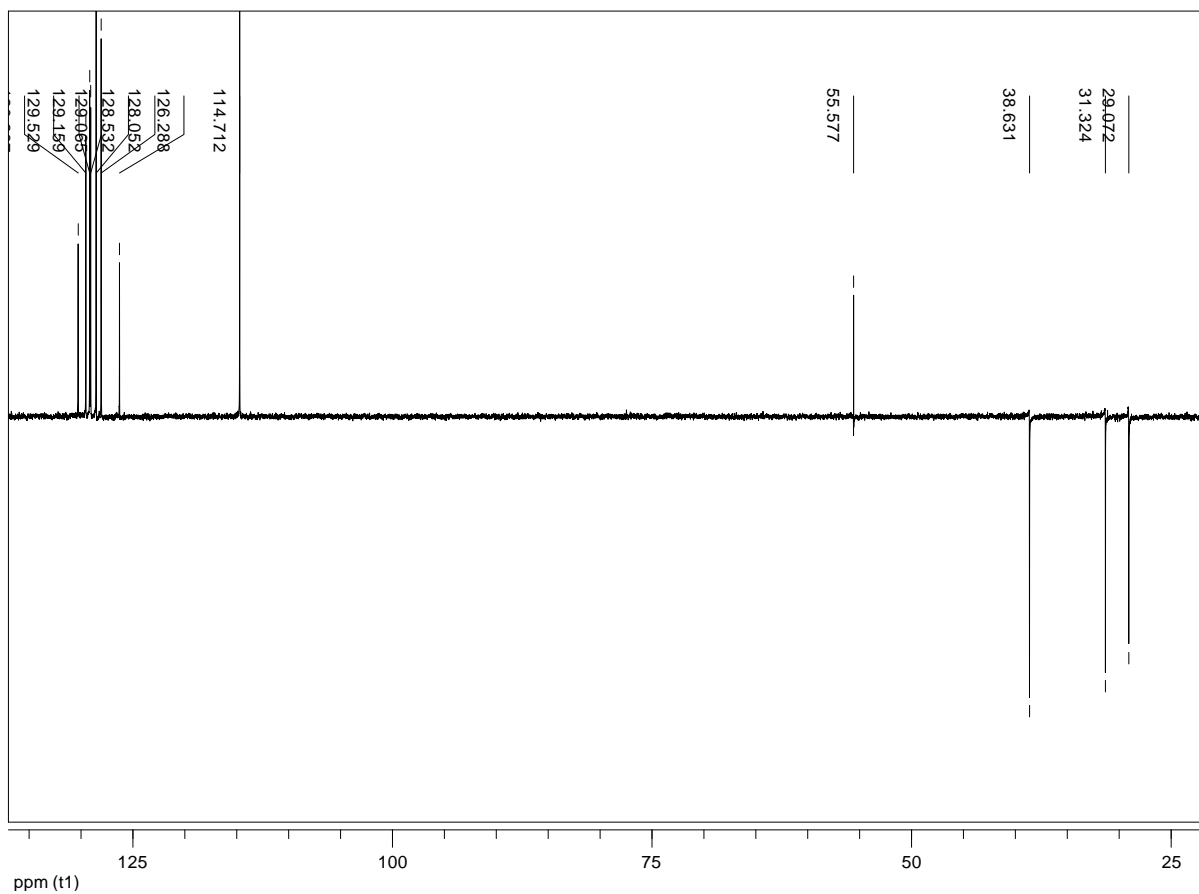
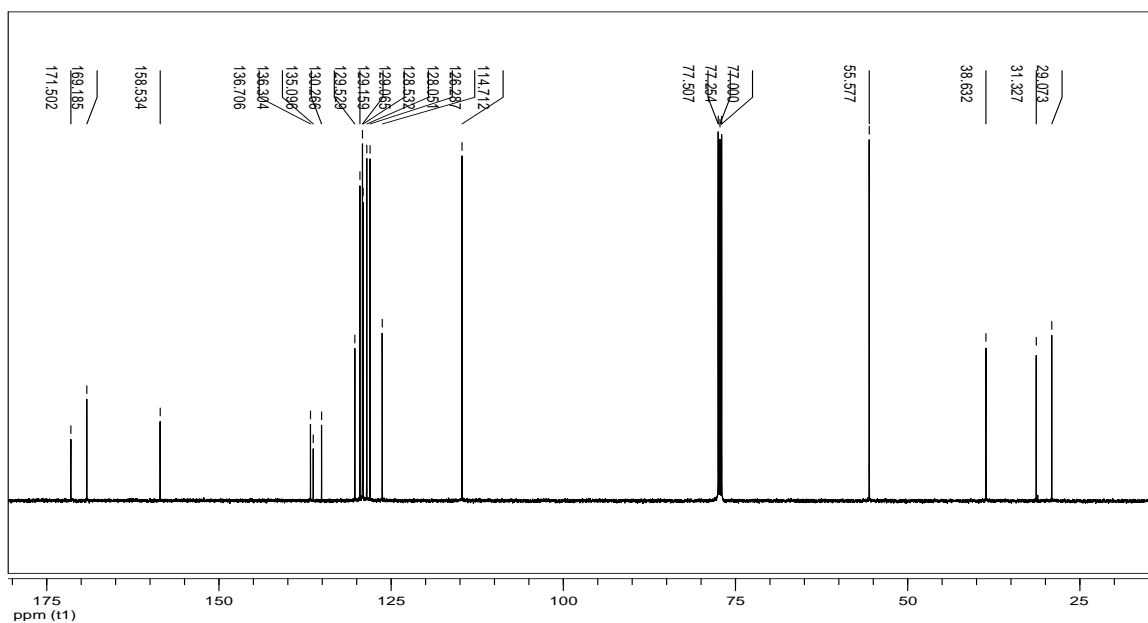
Compound 6u



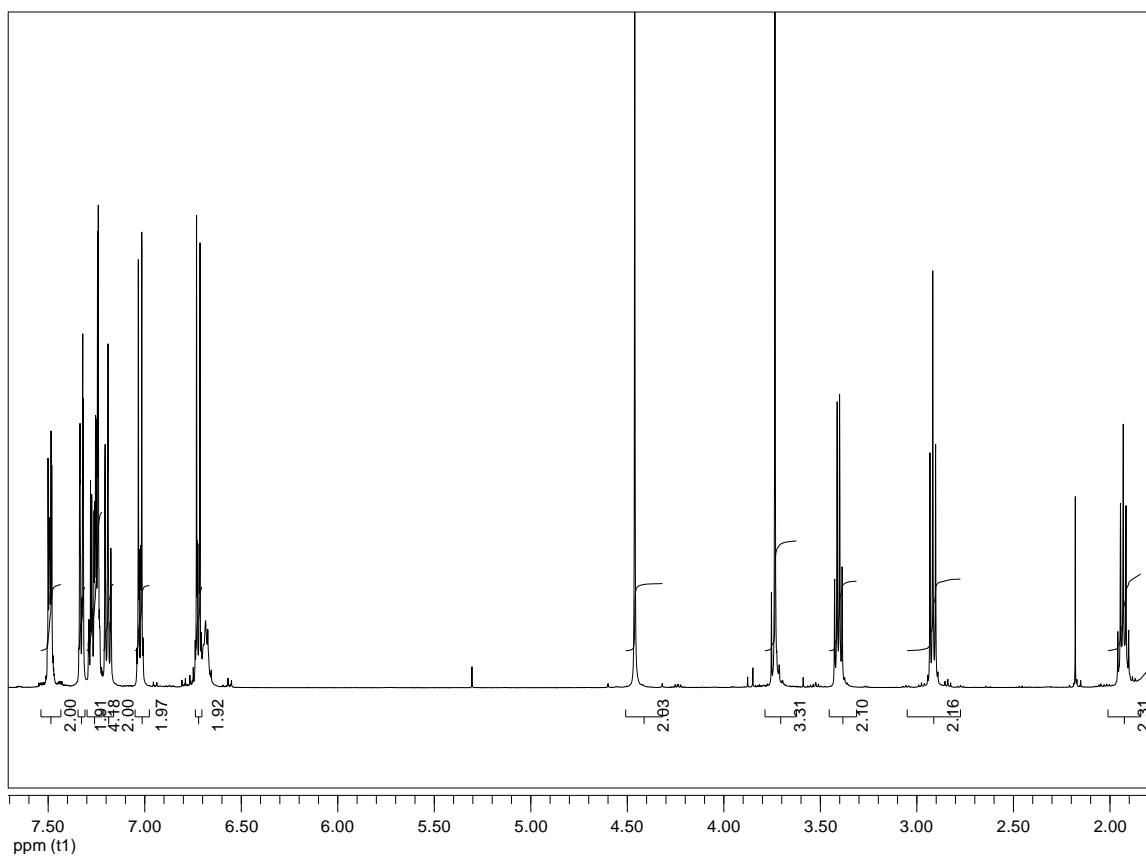
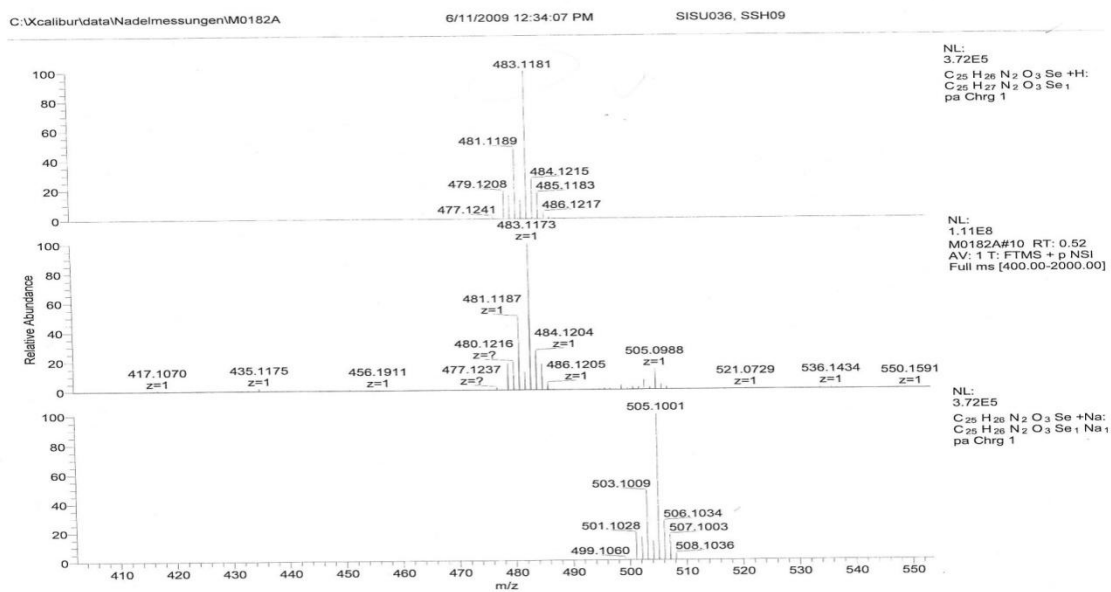


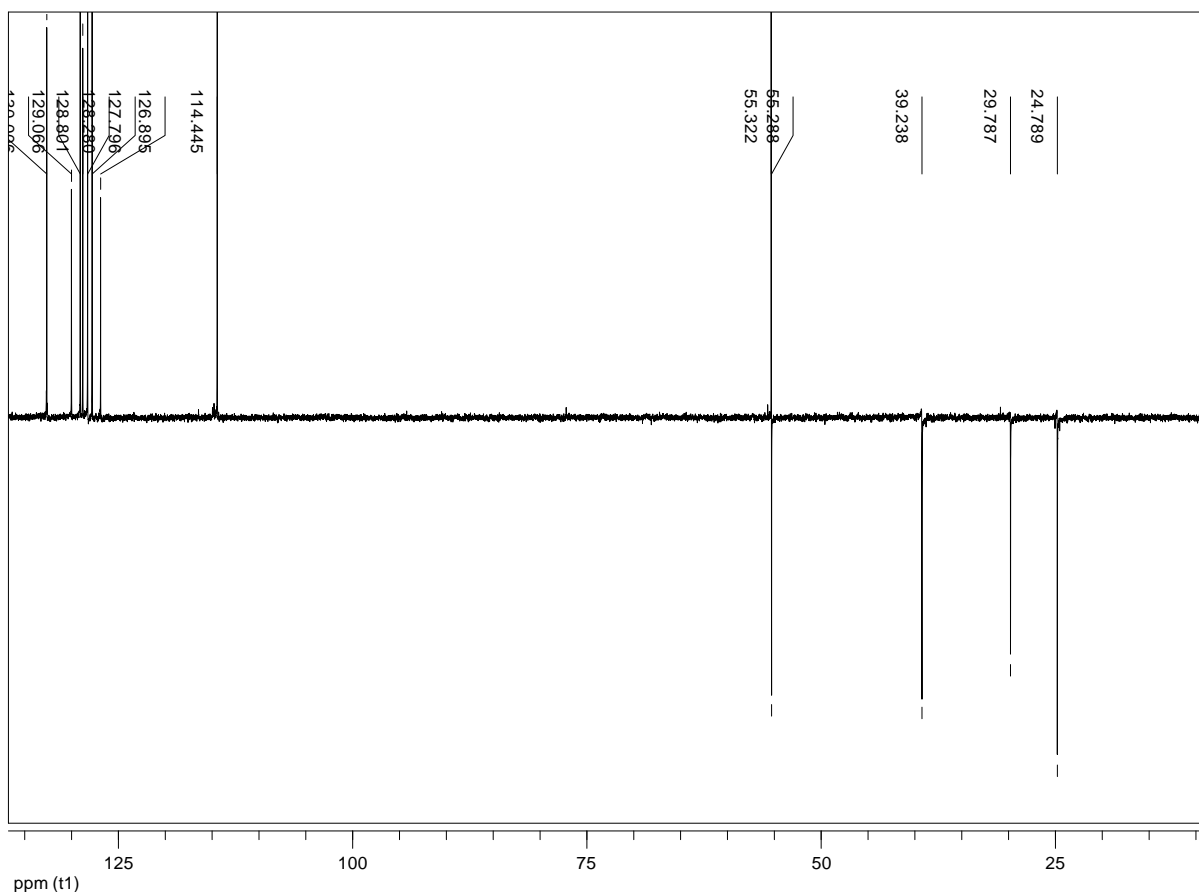
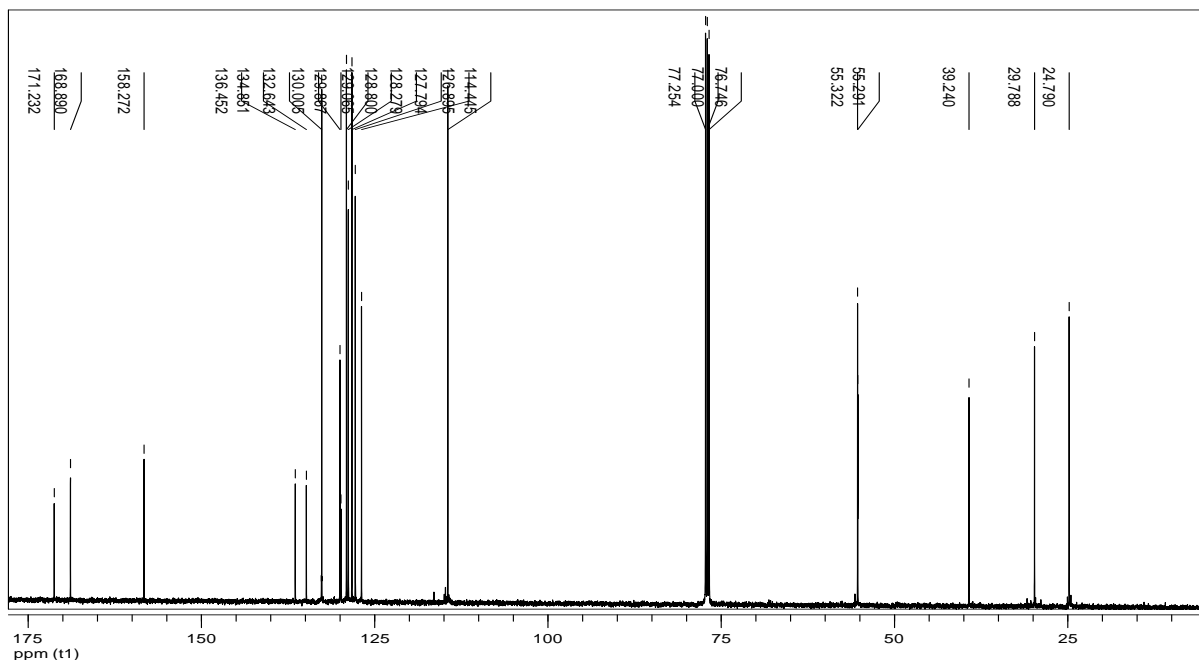
Compound7u



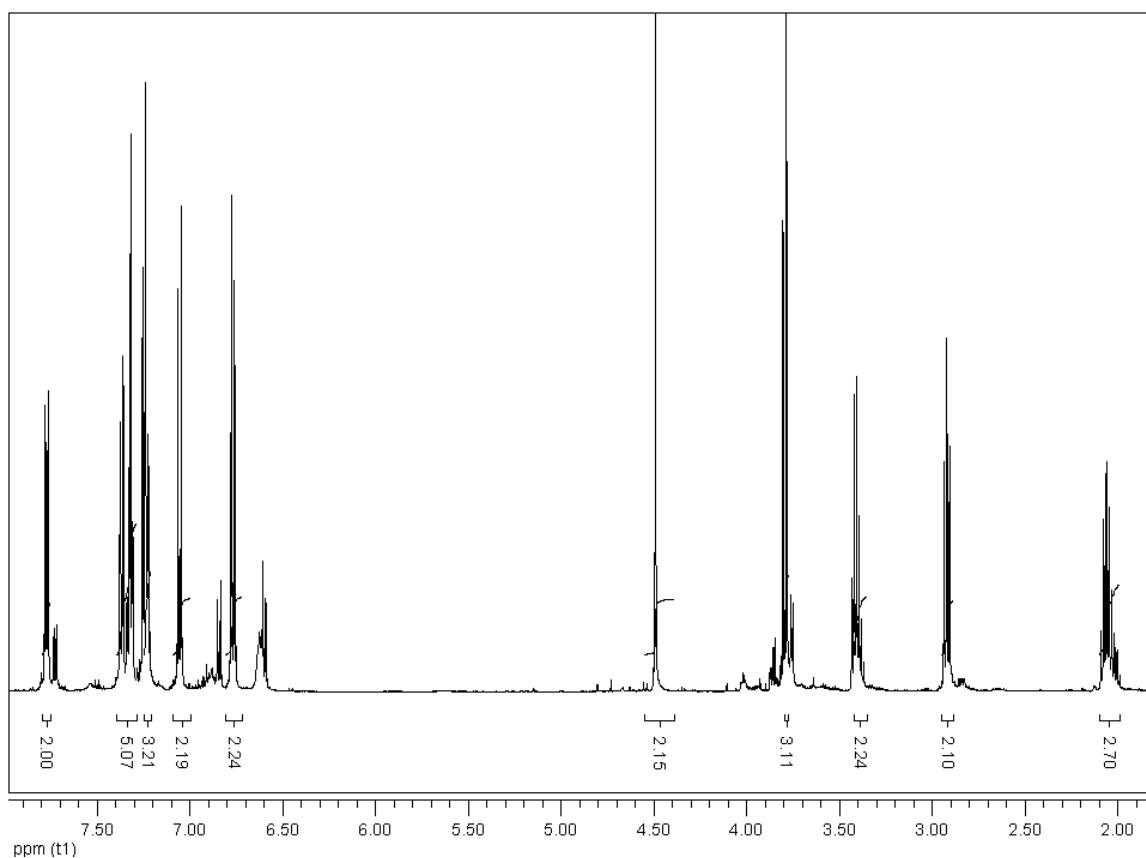
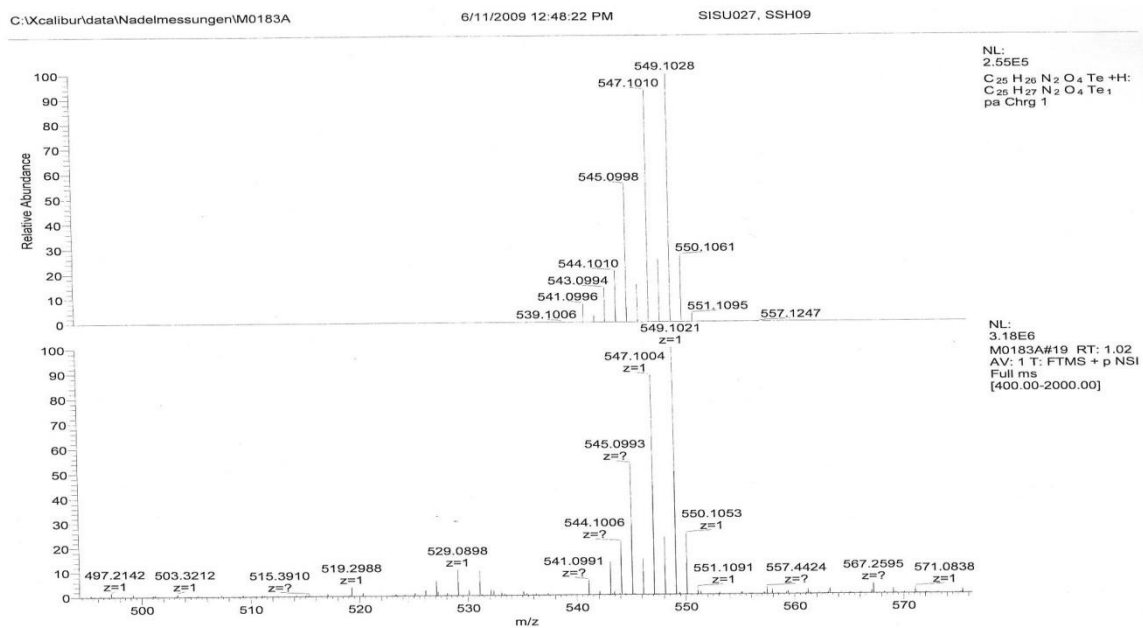


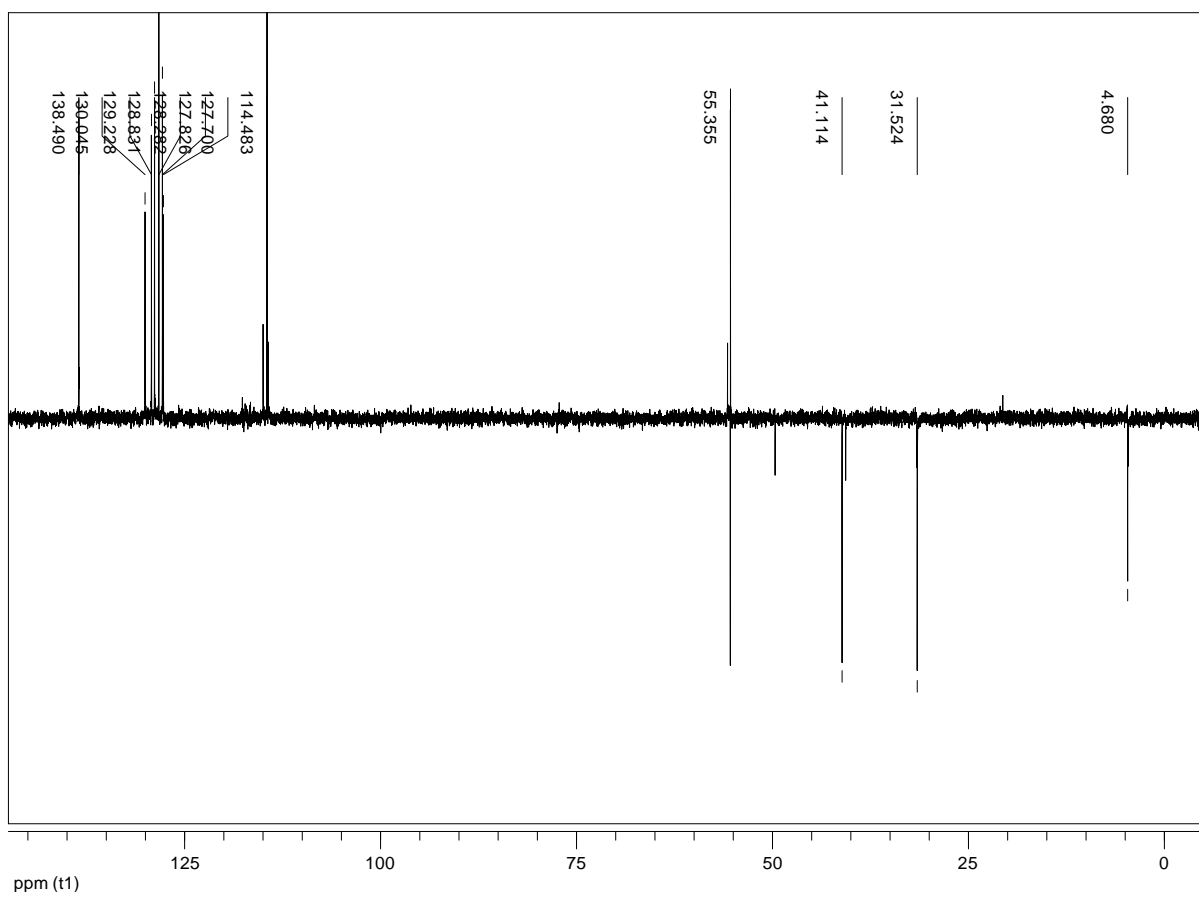
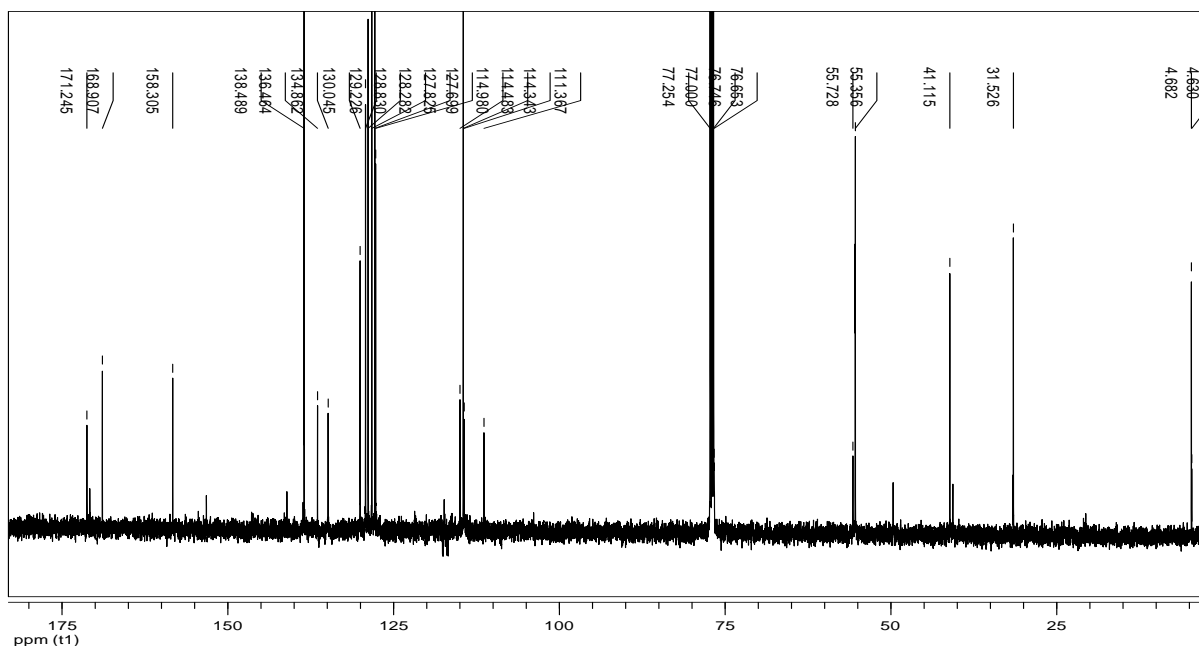
Compound 8u



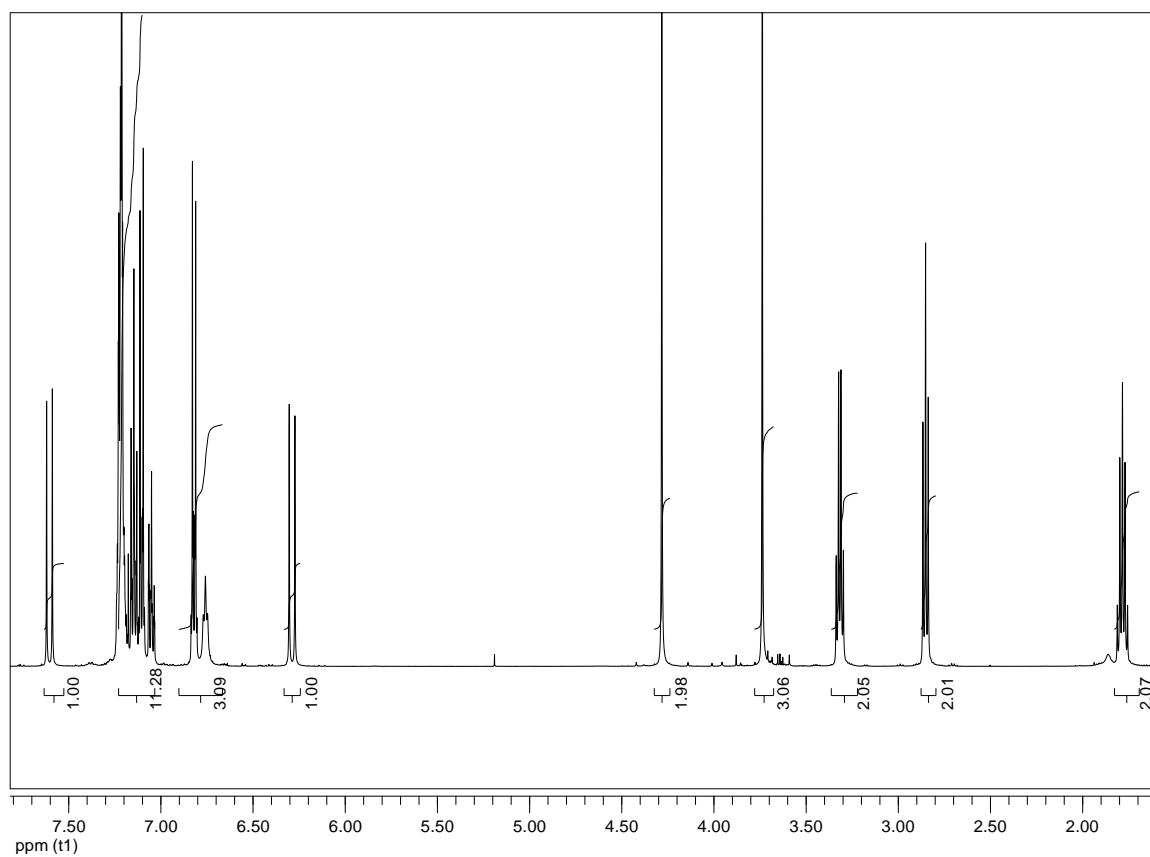
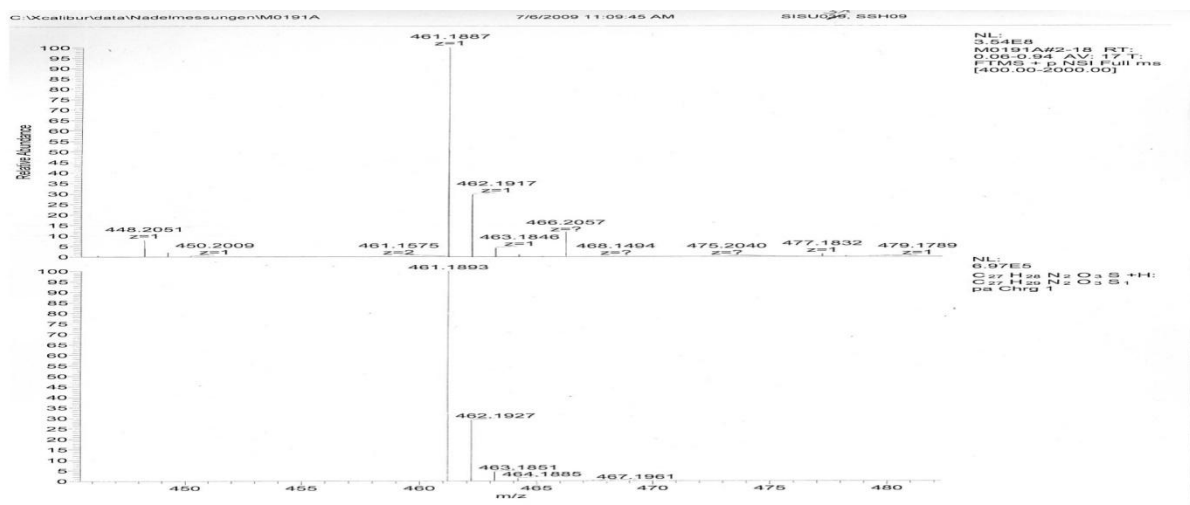


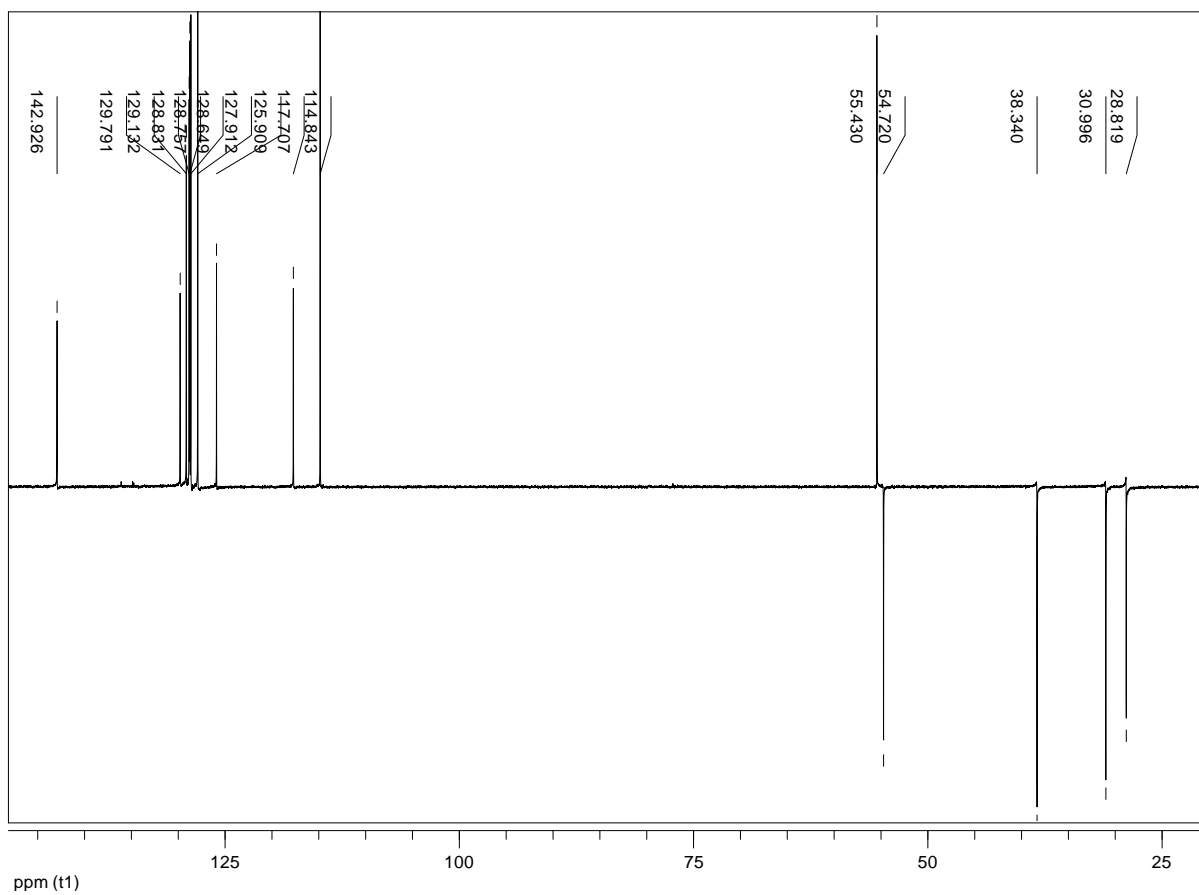
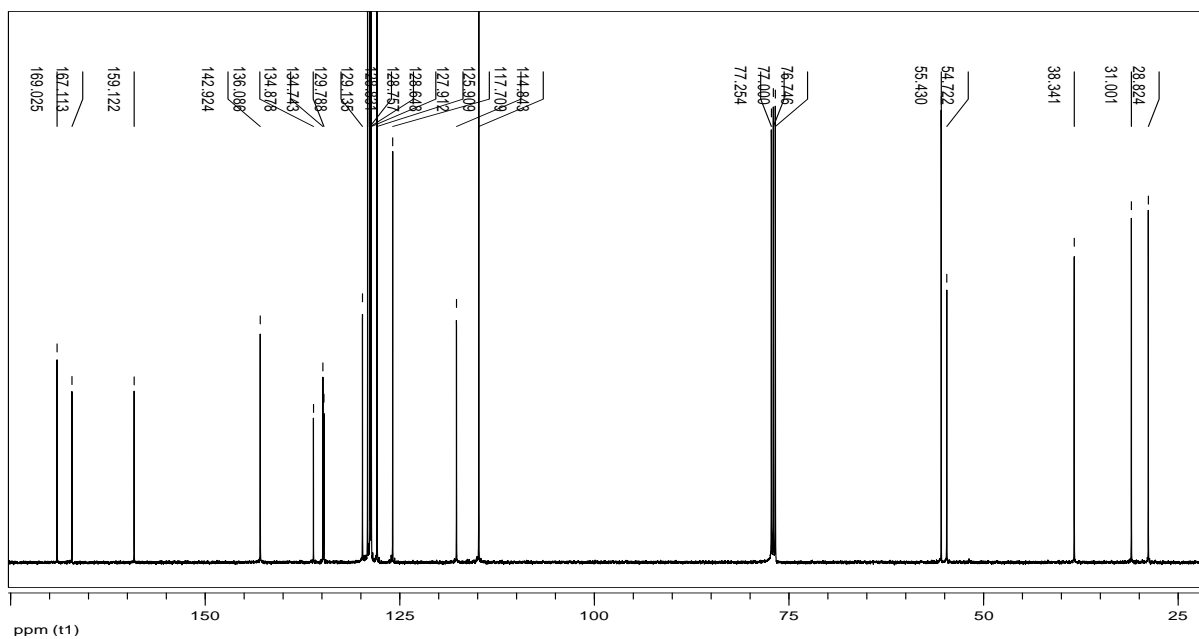
Compound 9u



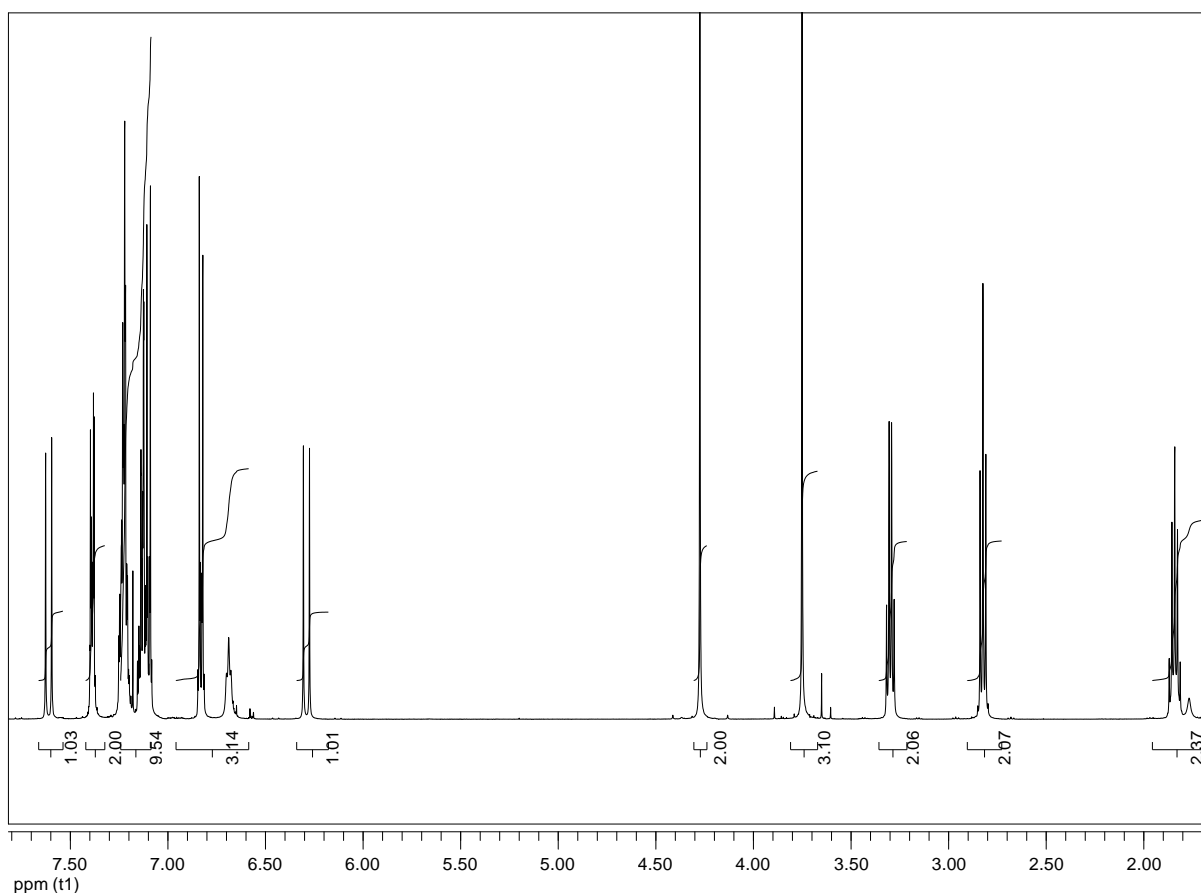
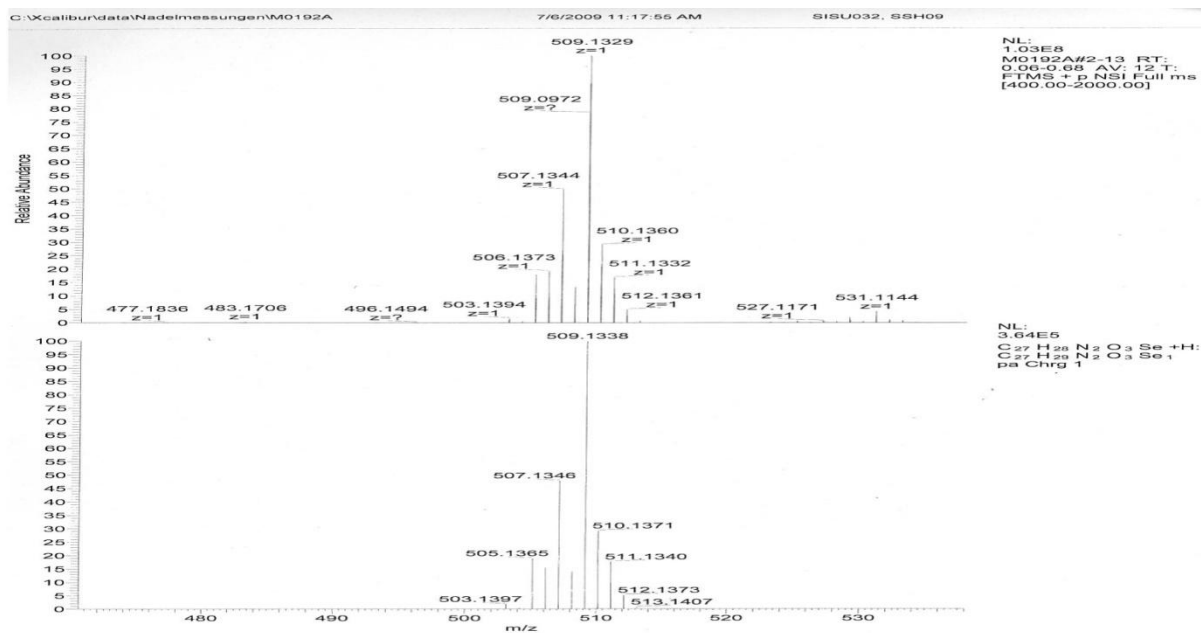


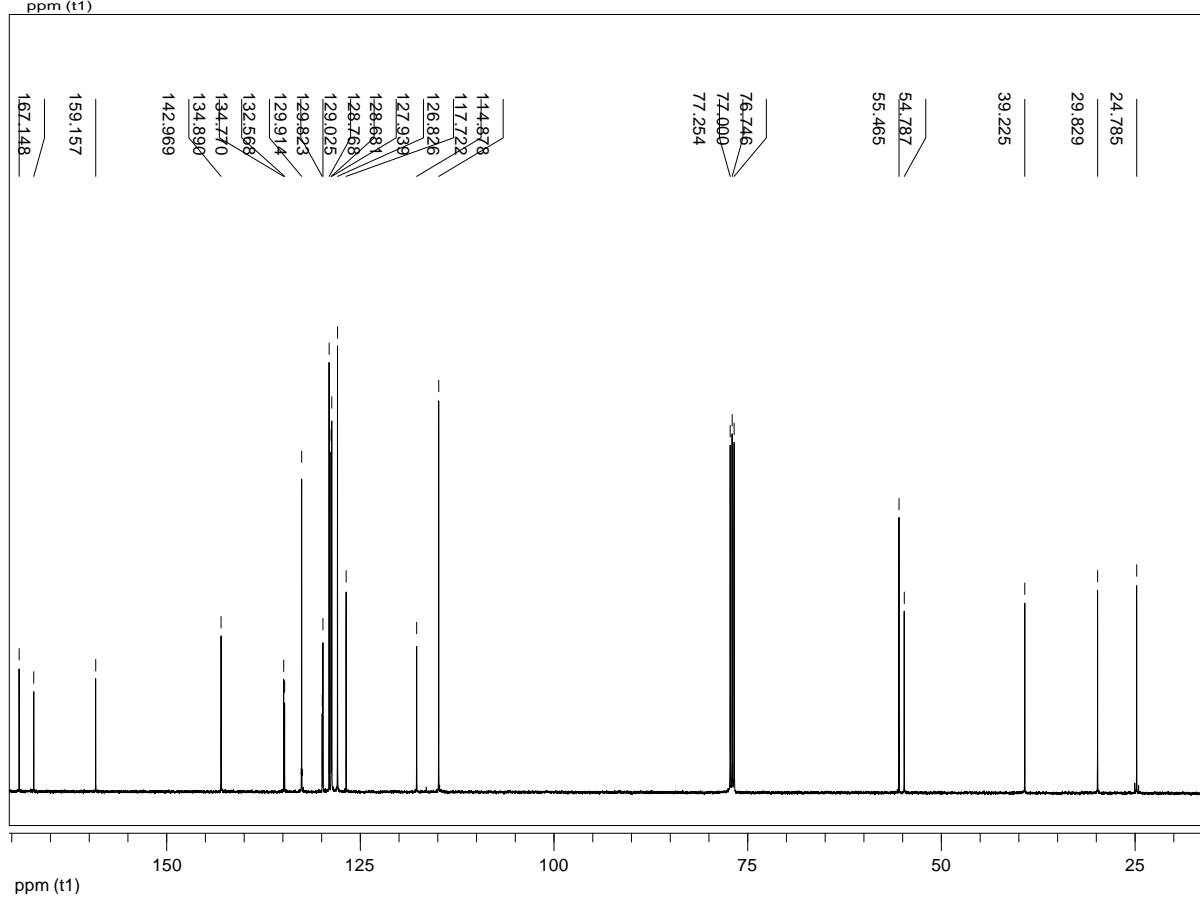
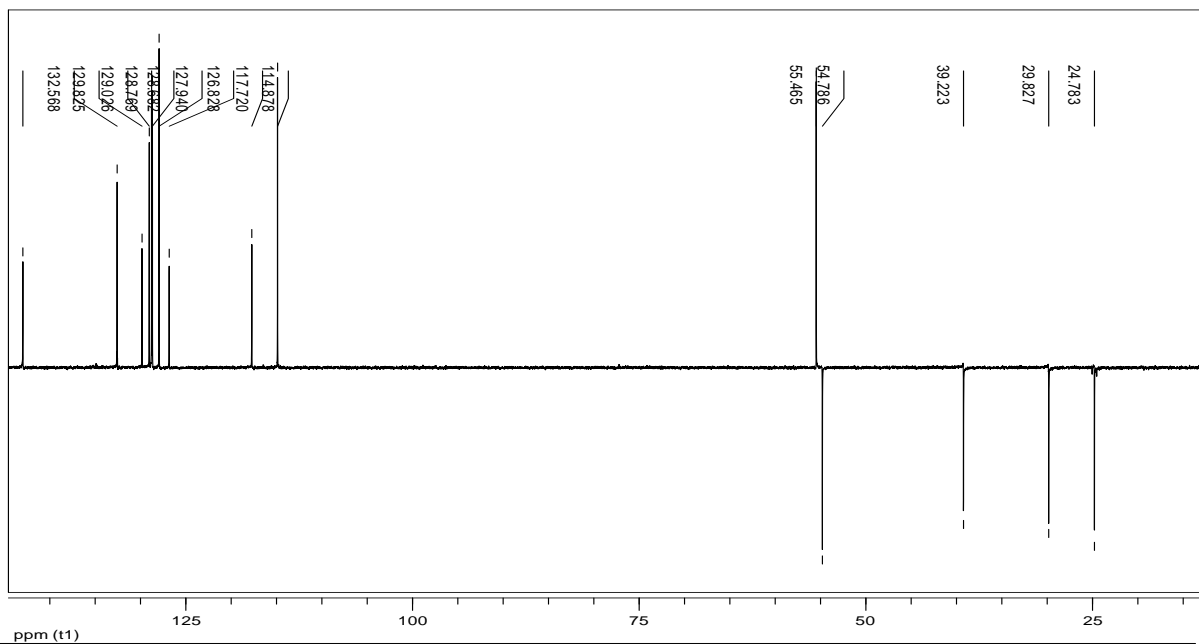
Compound 10u



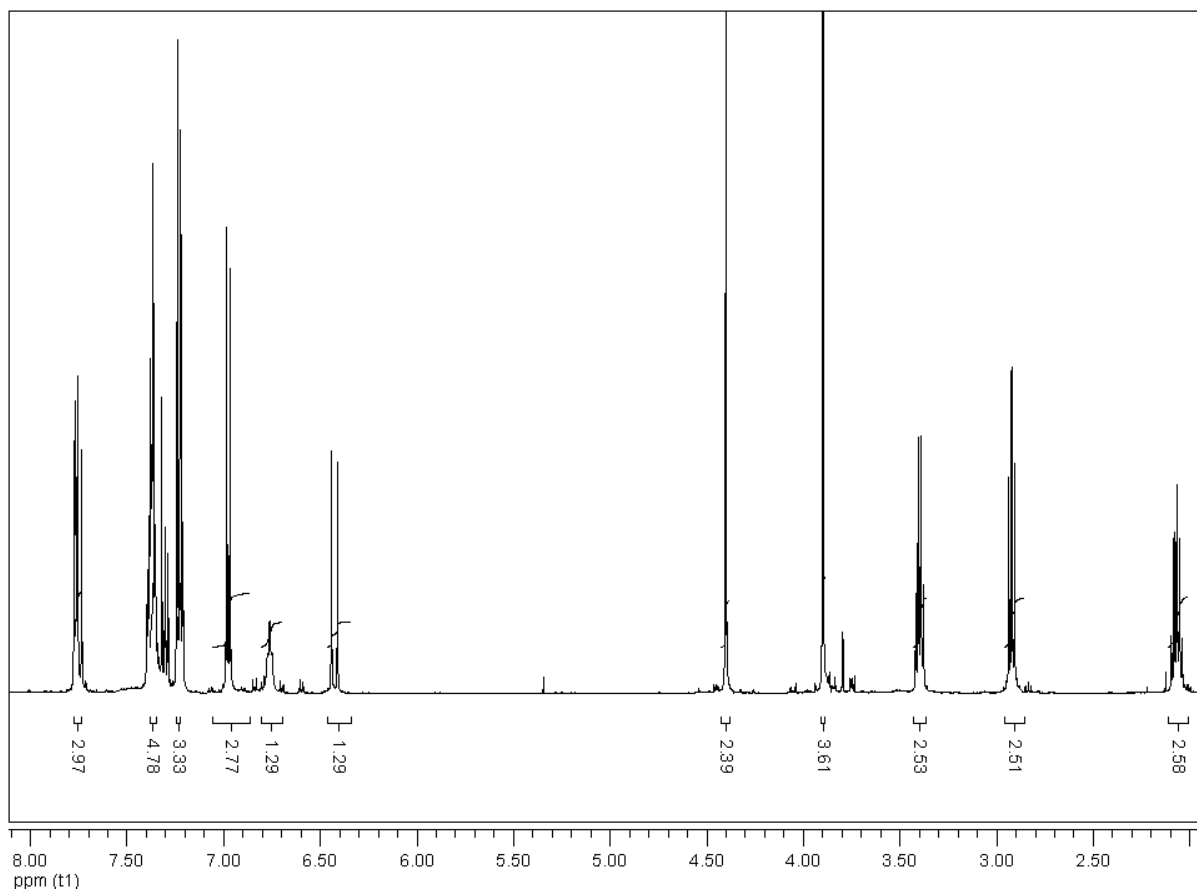
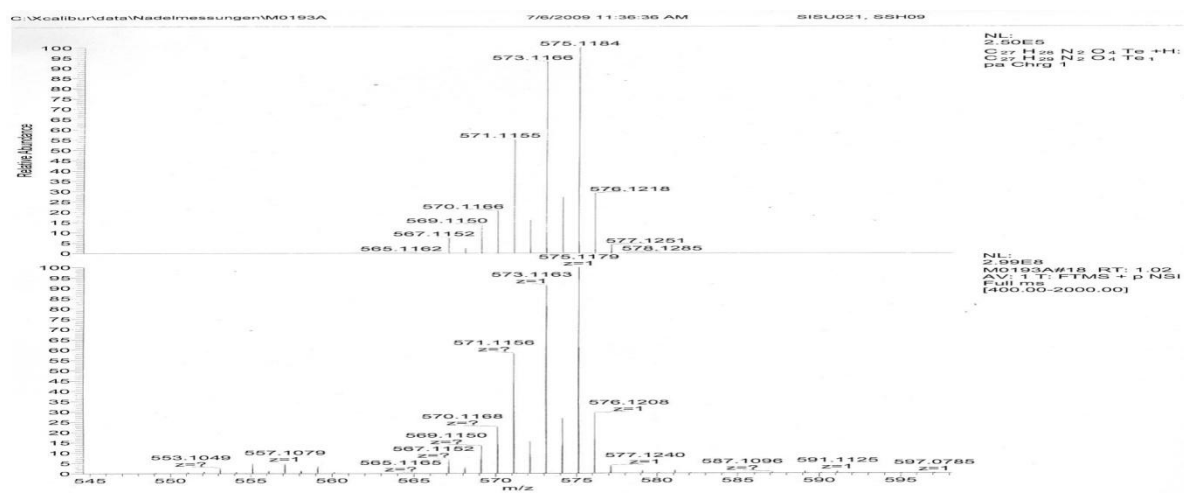


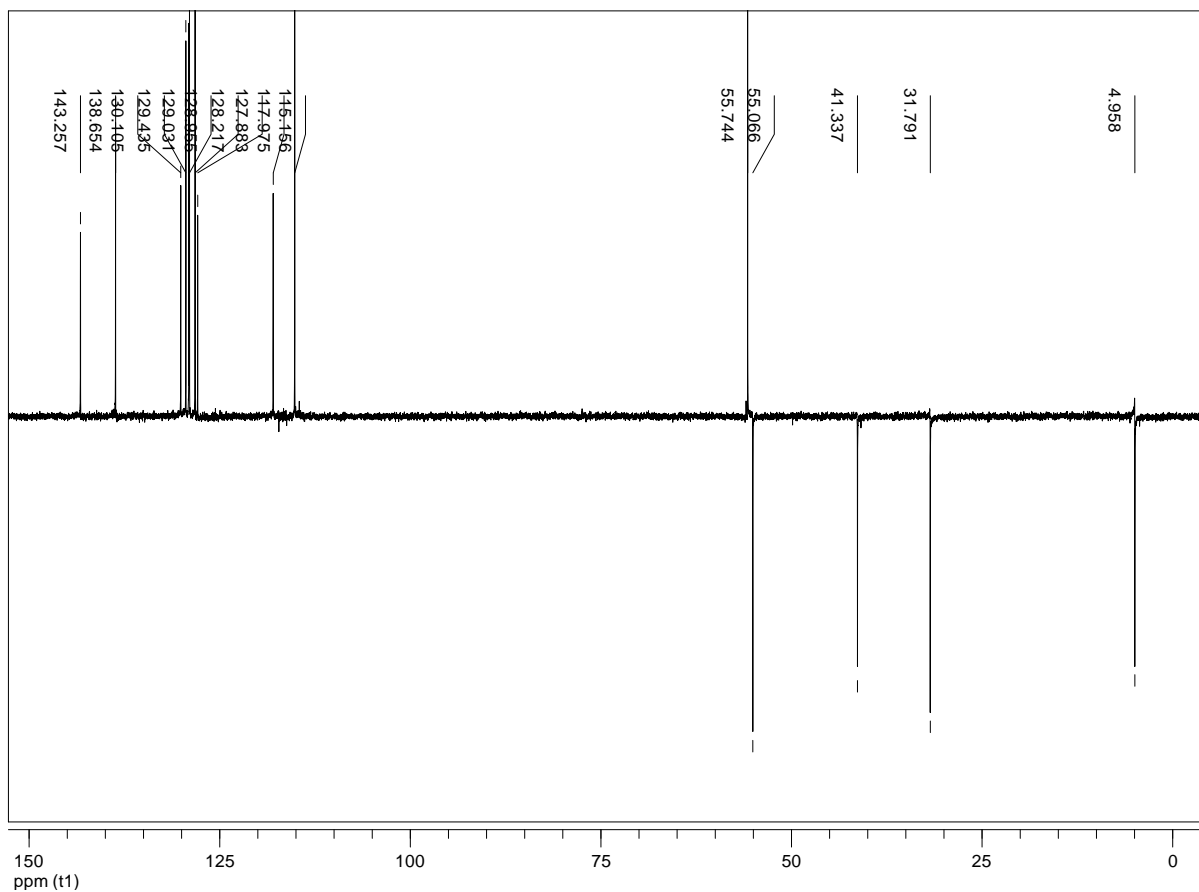
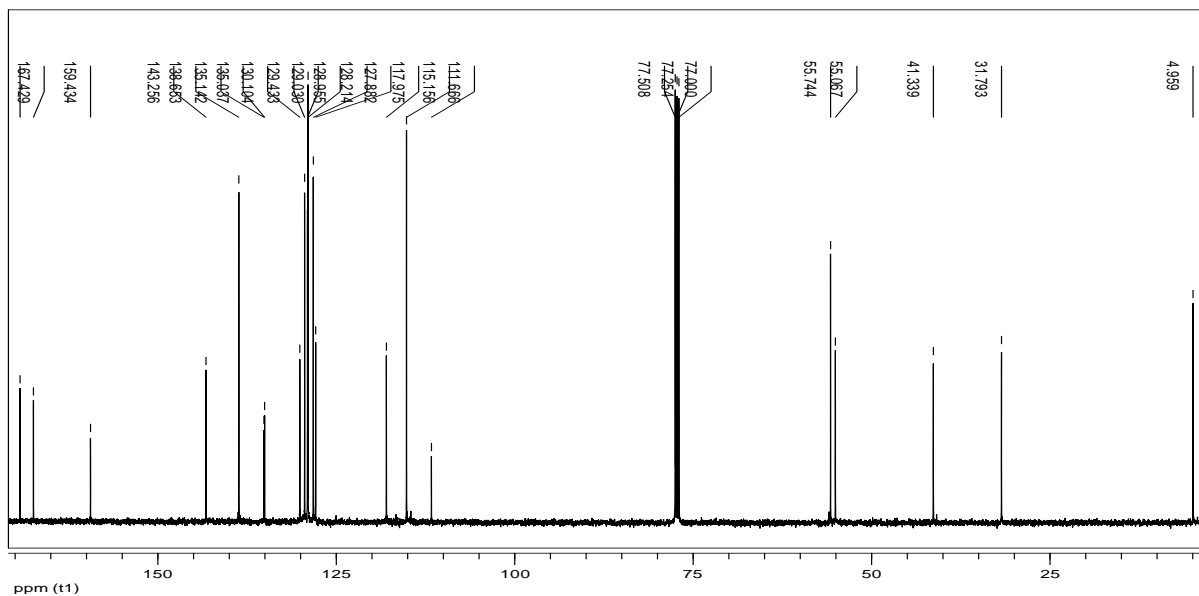
Compound 11u



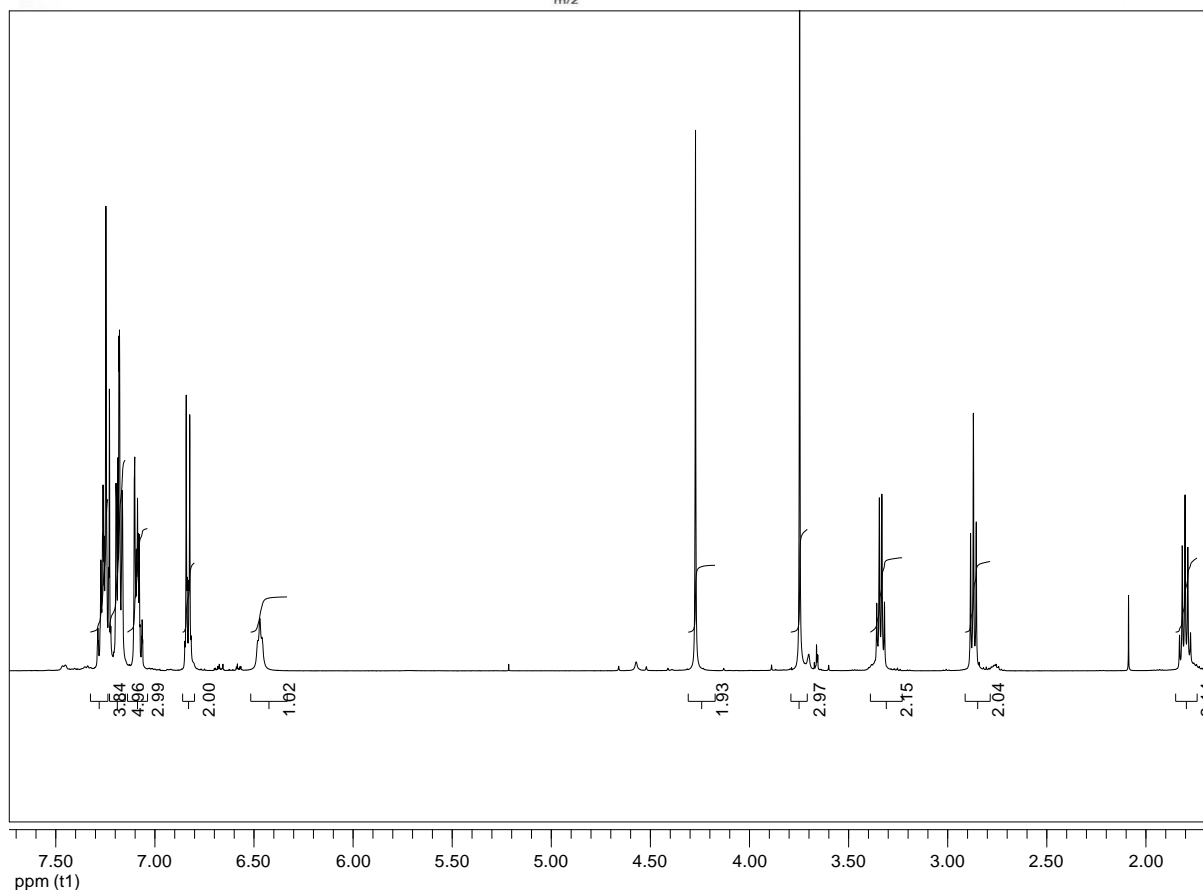
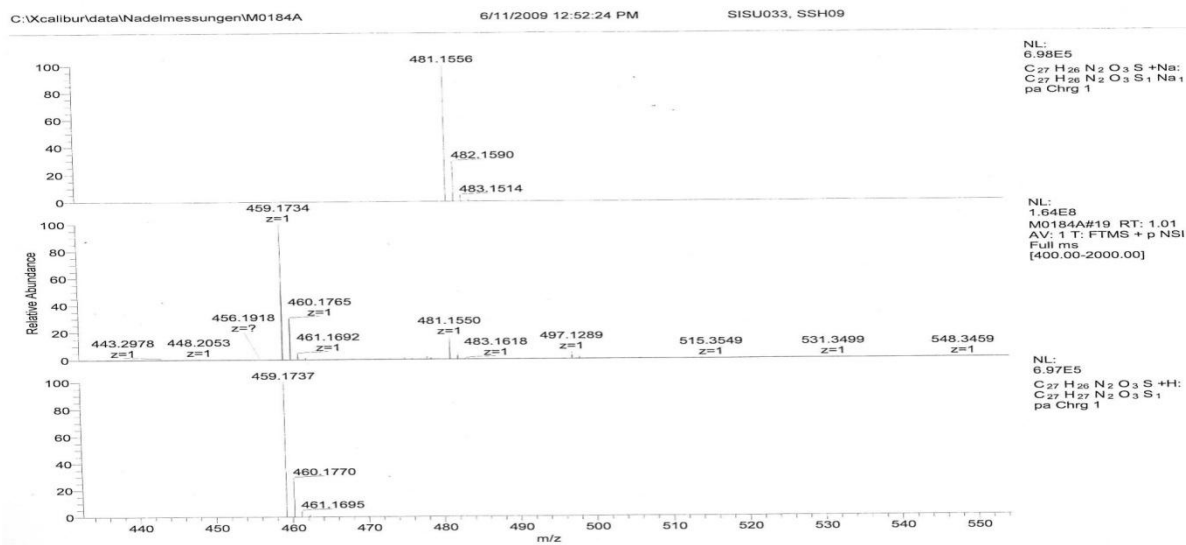


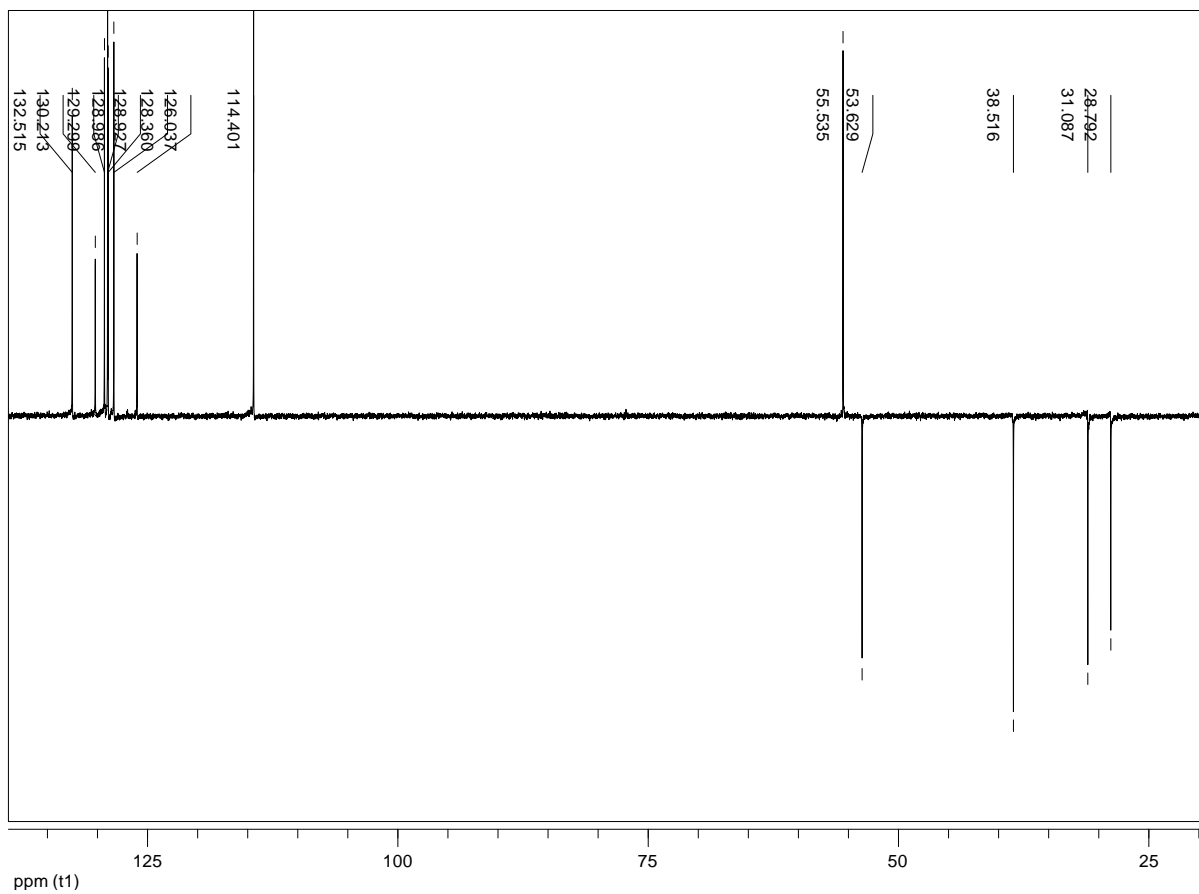
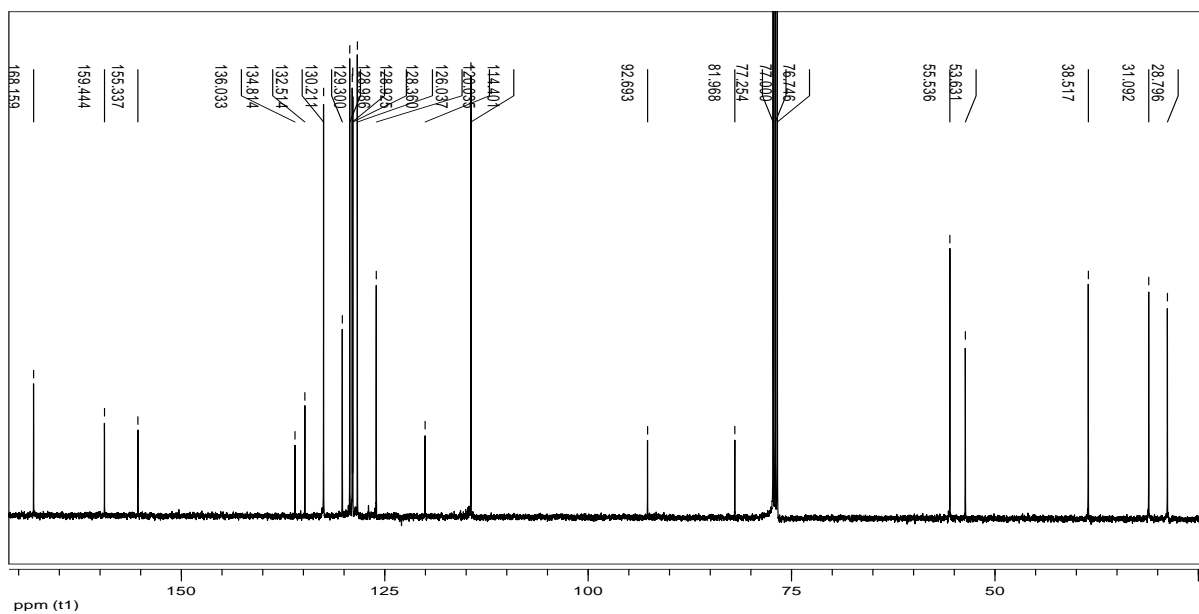
Compound 12u



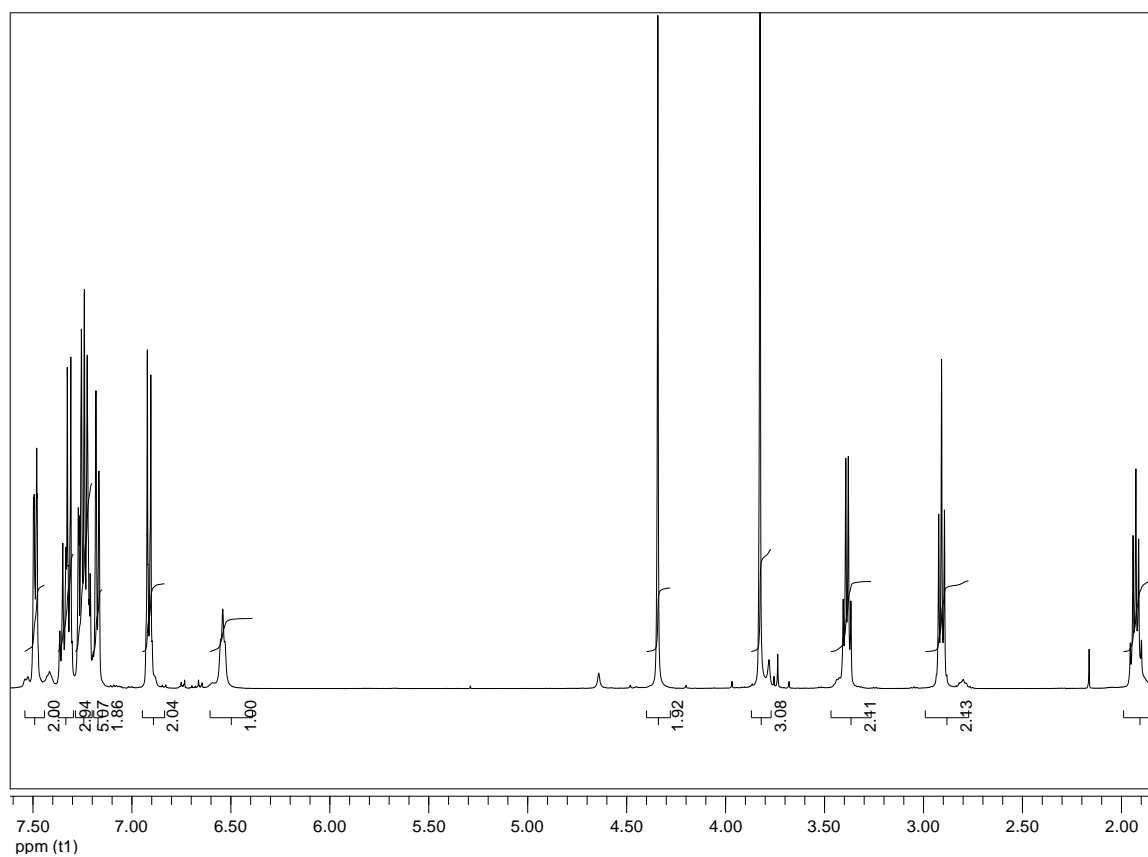
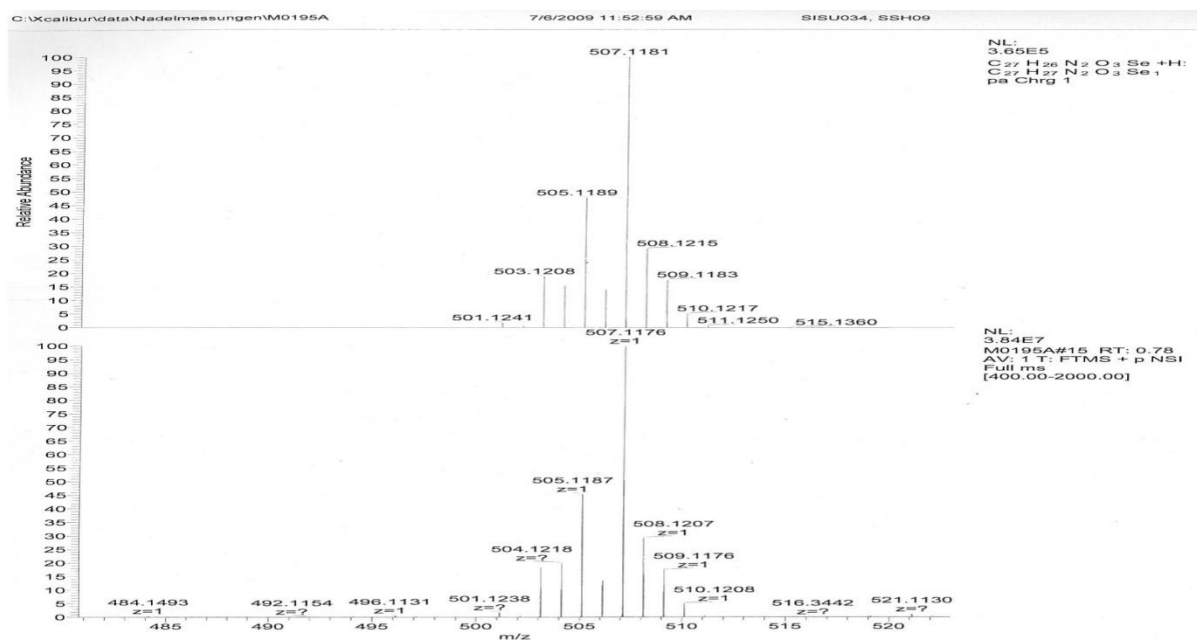


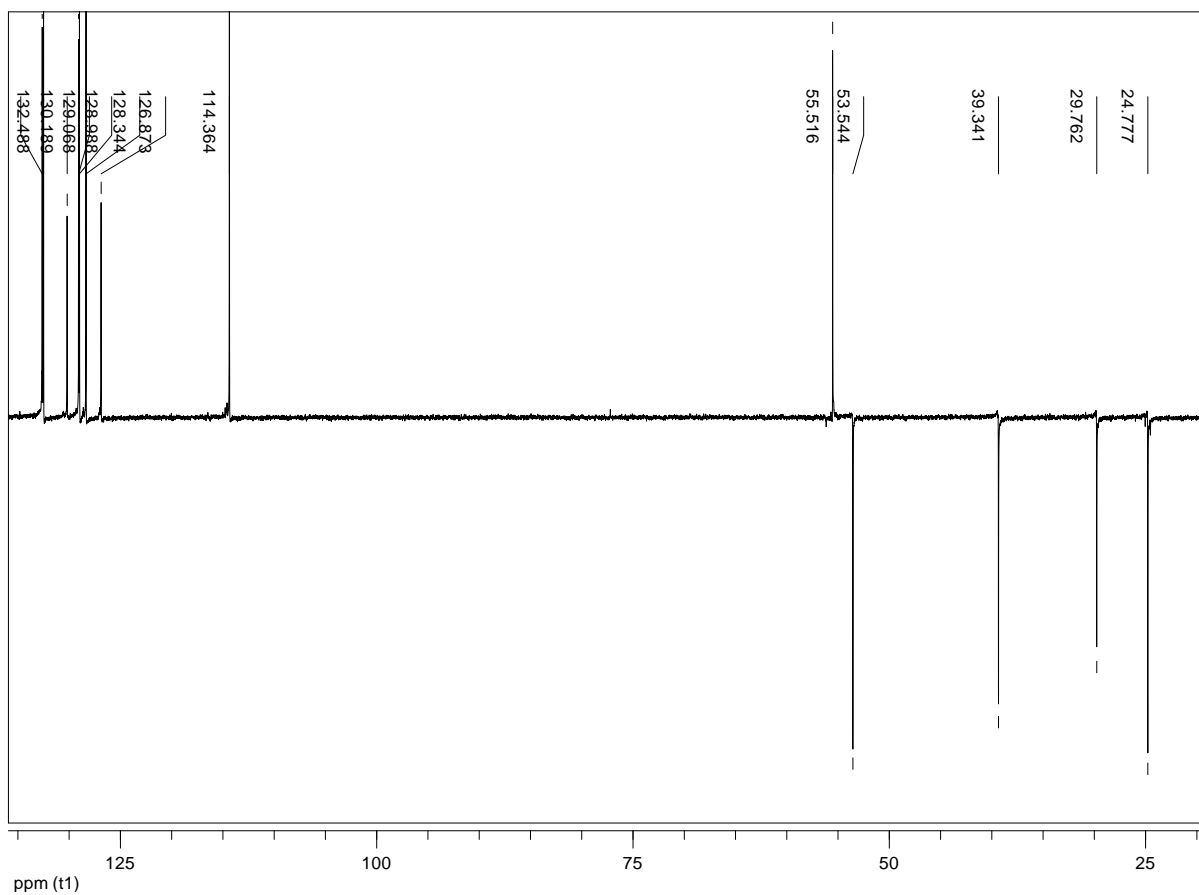
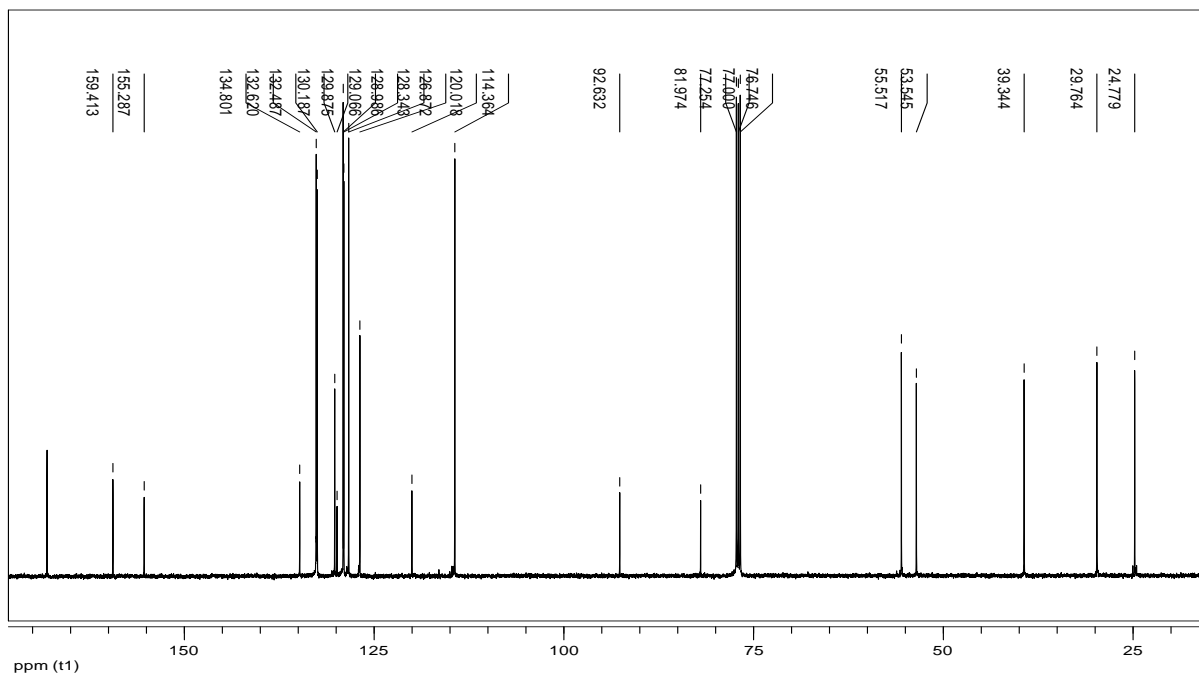
Compound 13u



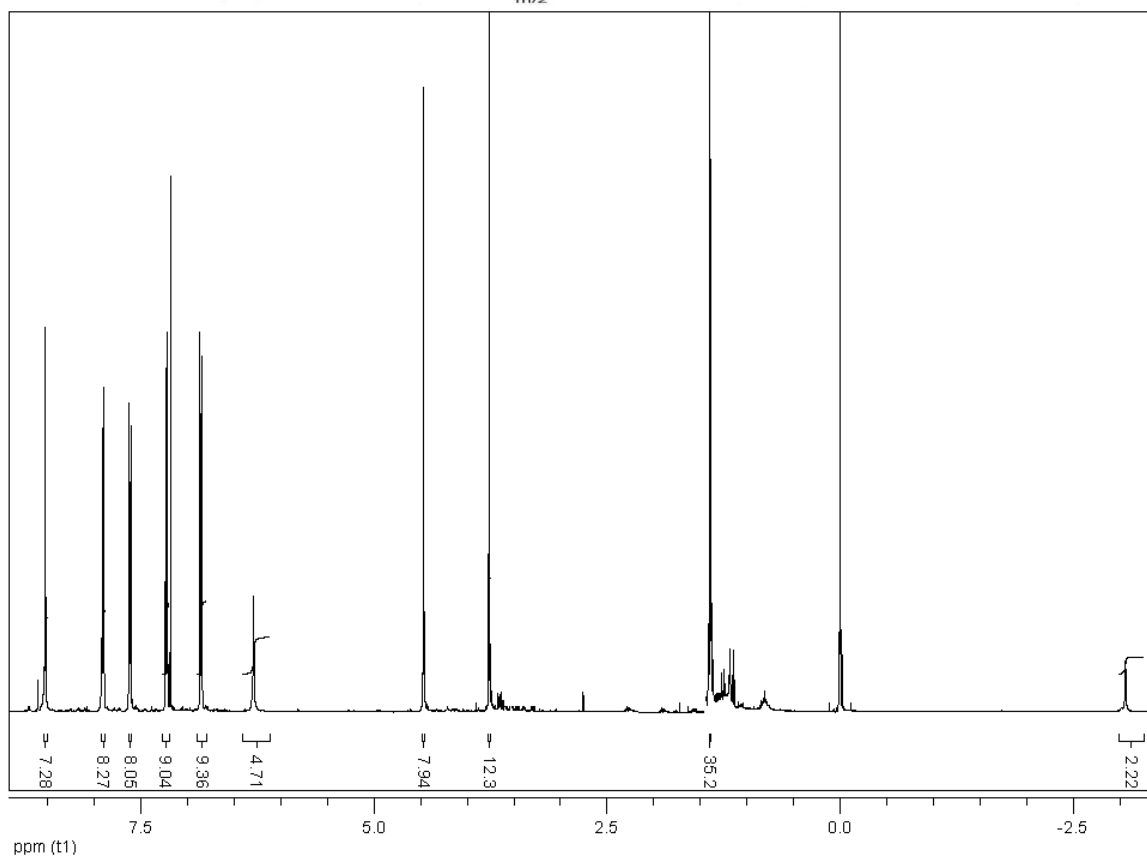
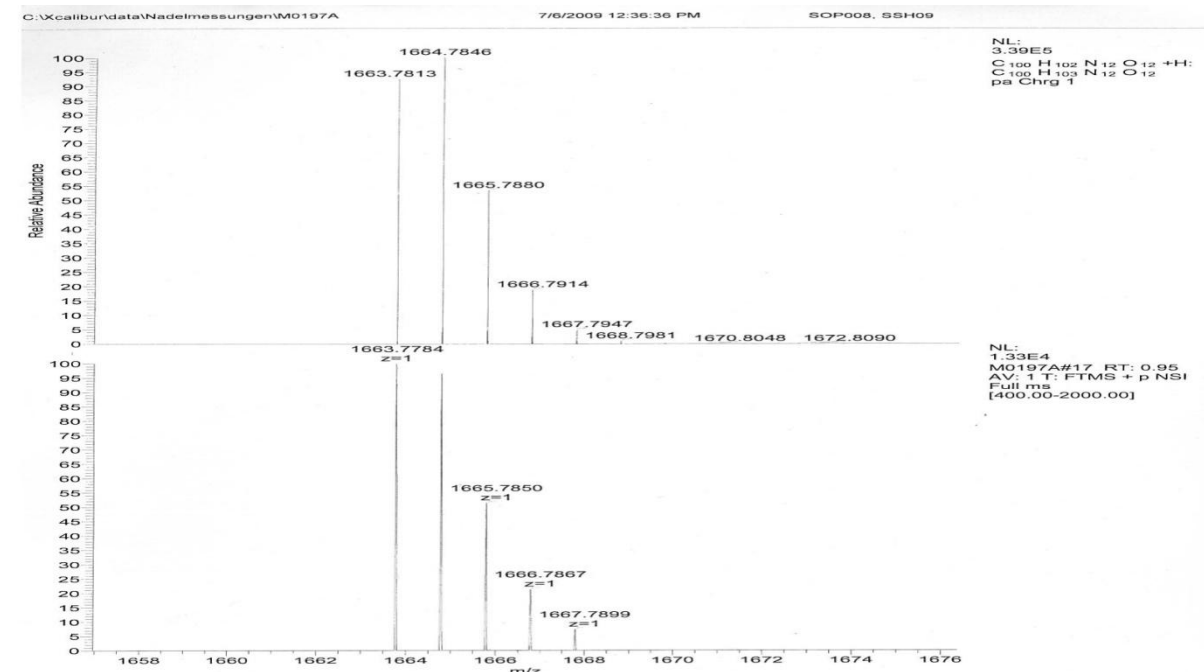


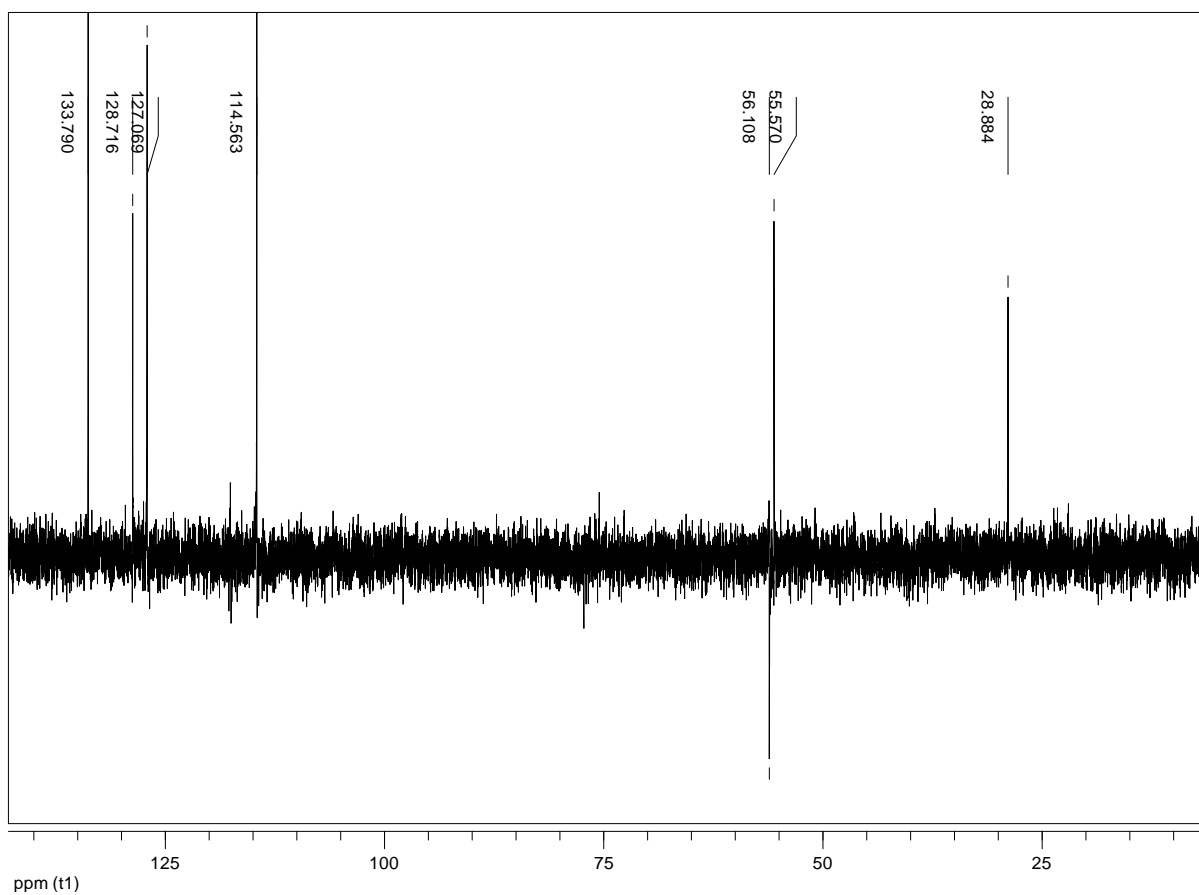
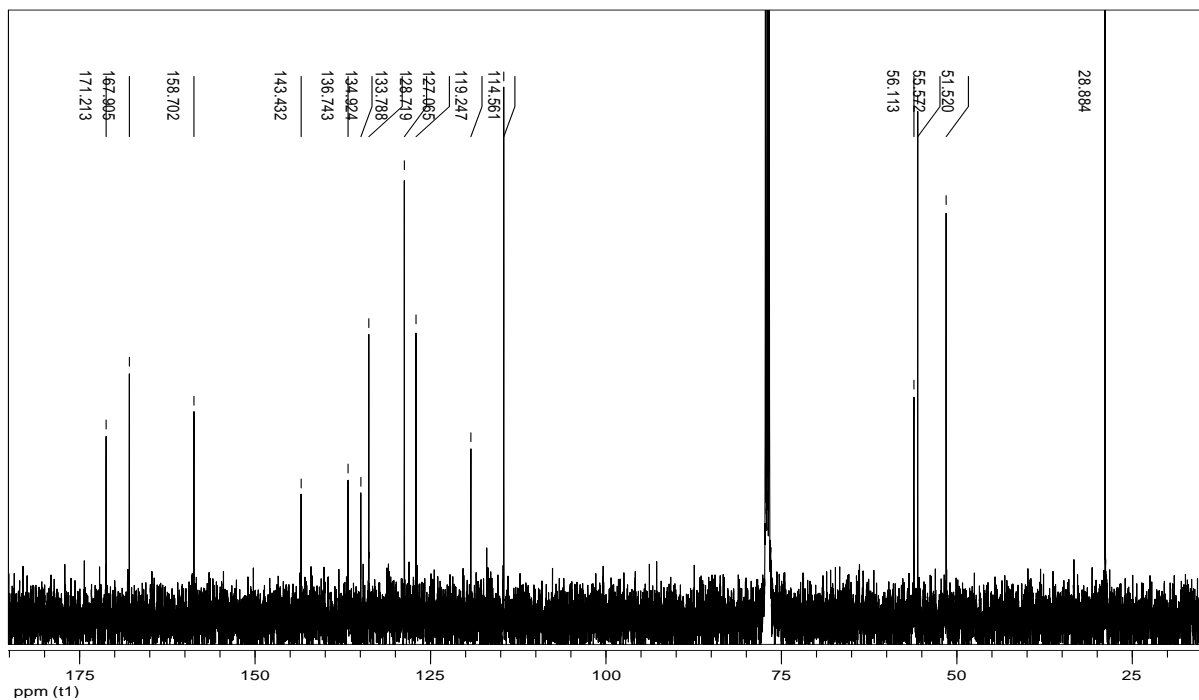
Compound 14u



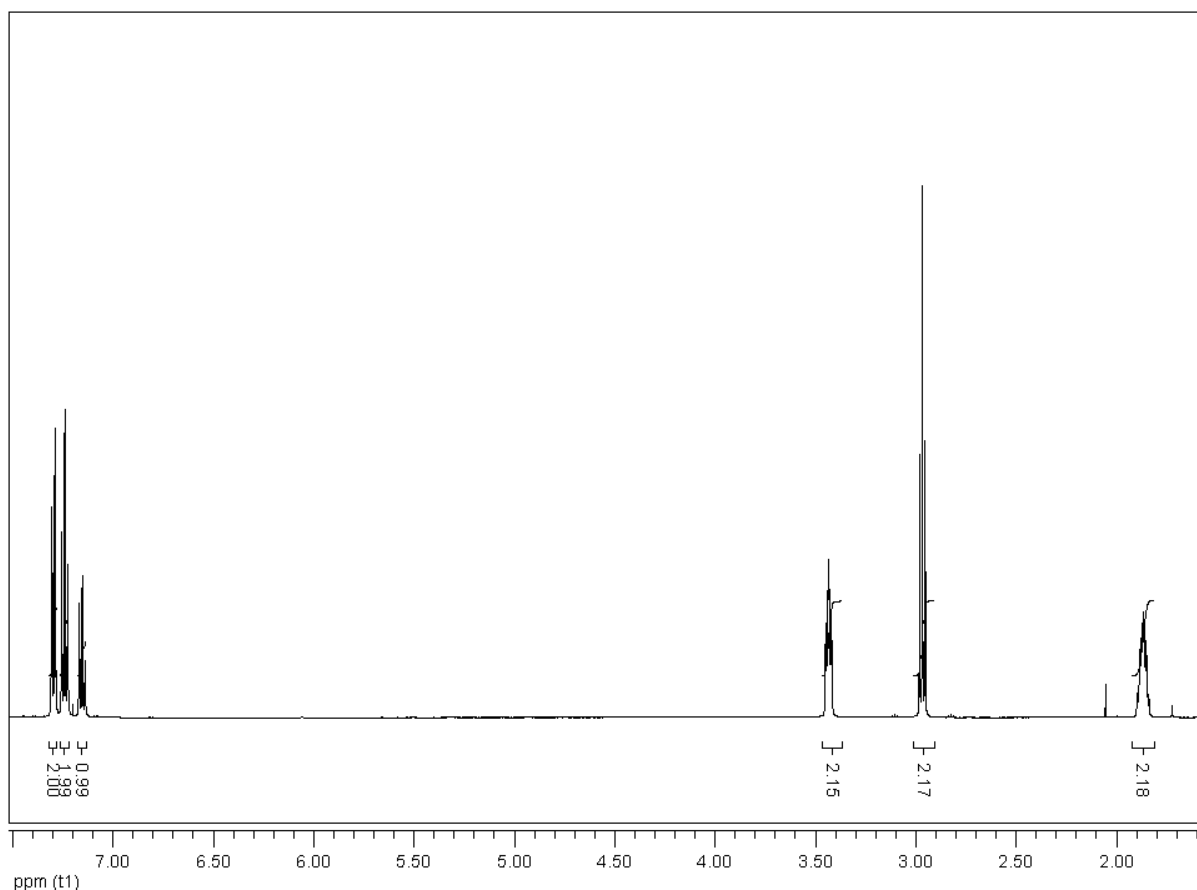
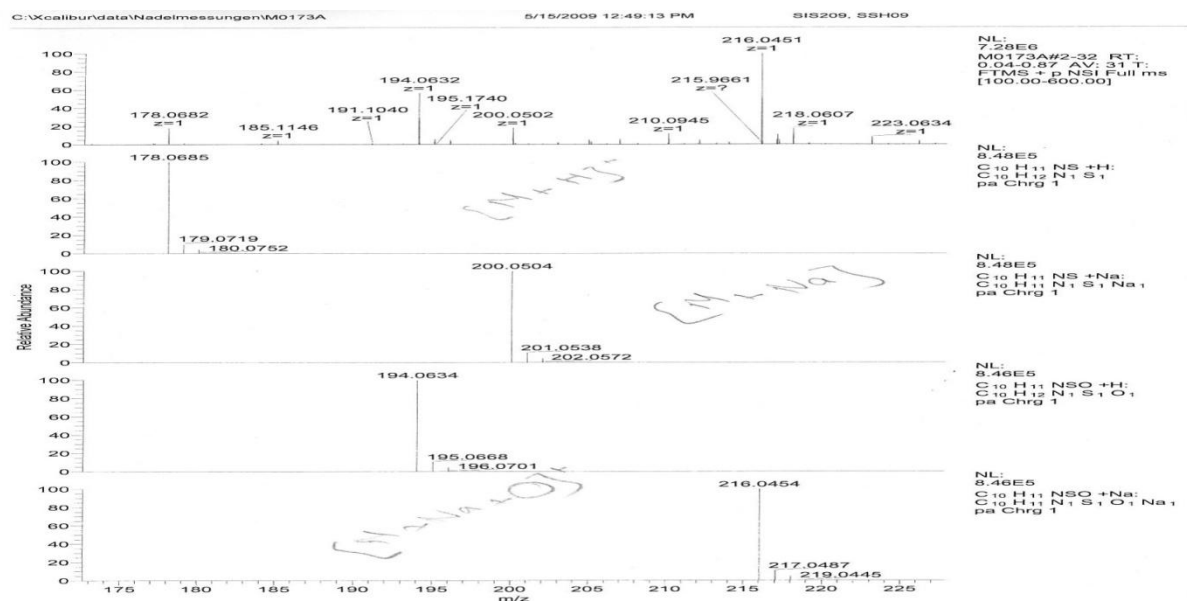


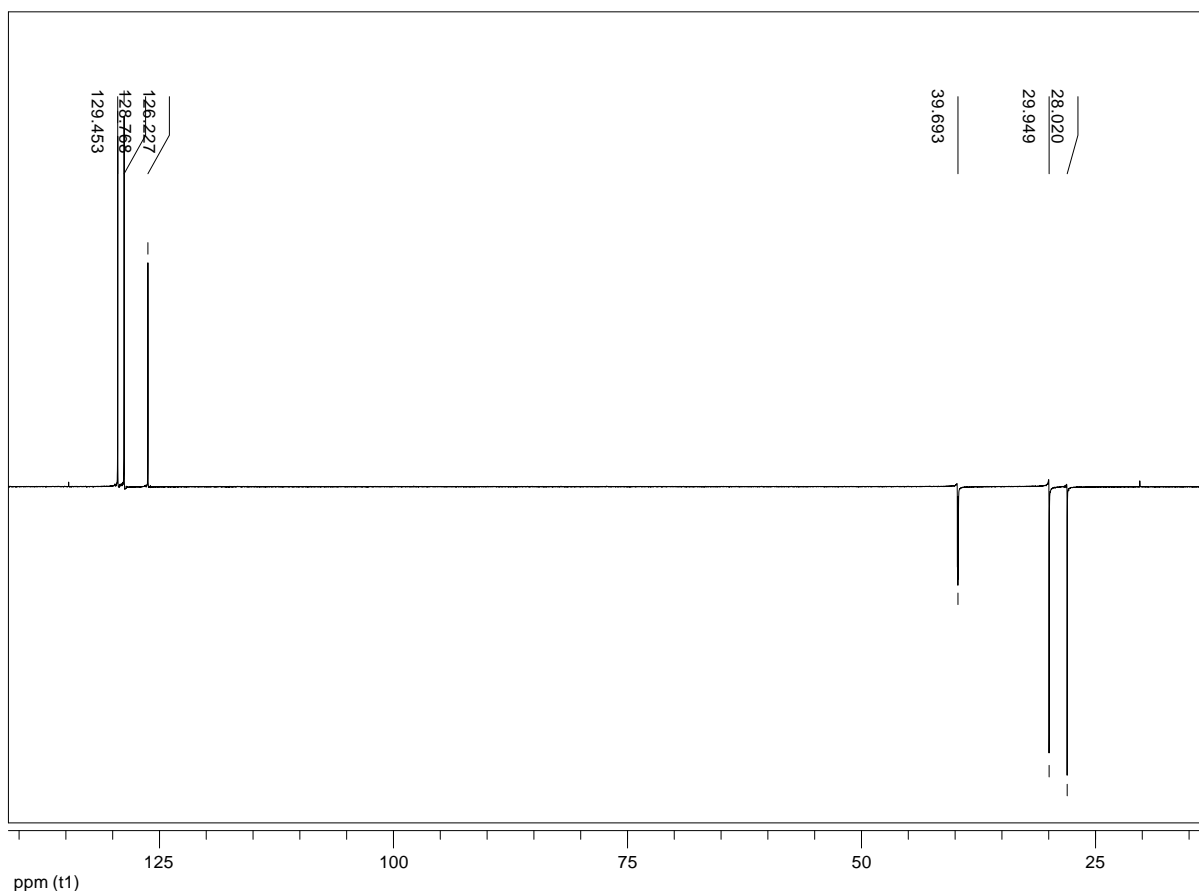
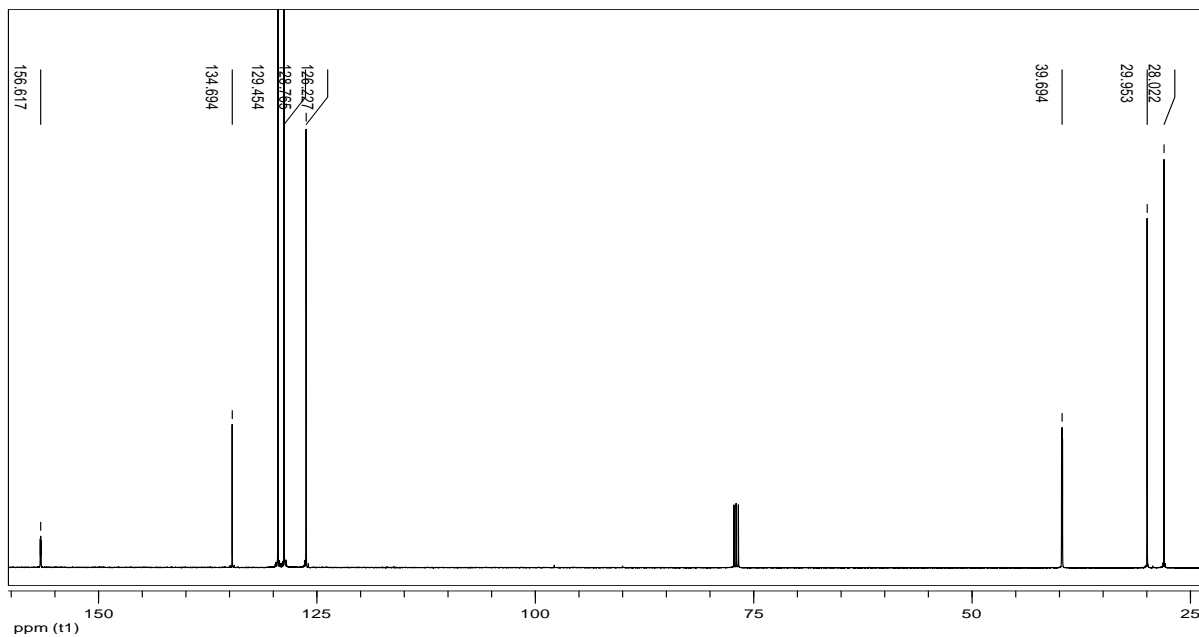
Compound 15u



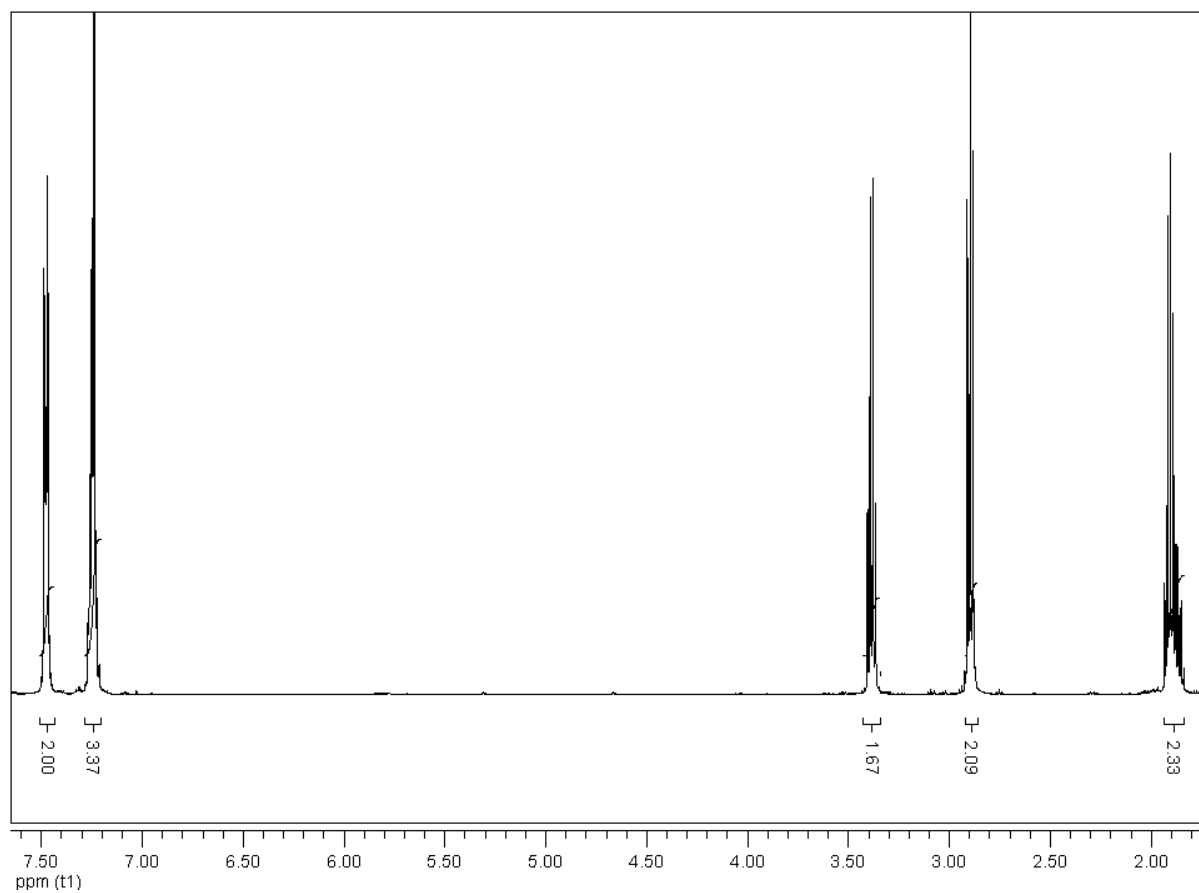
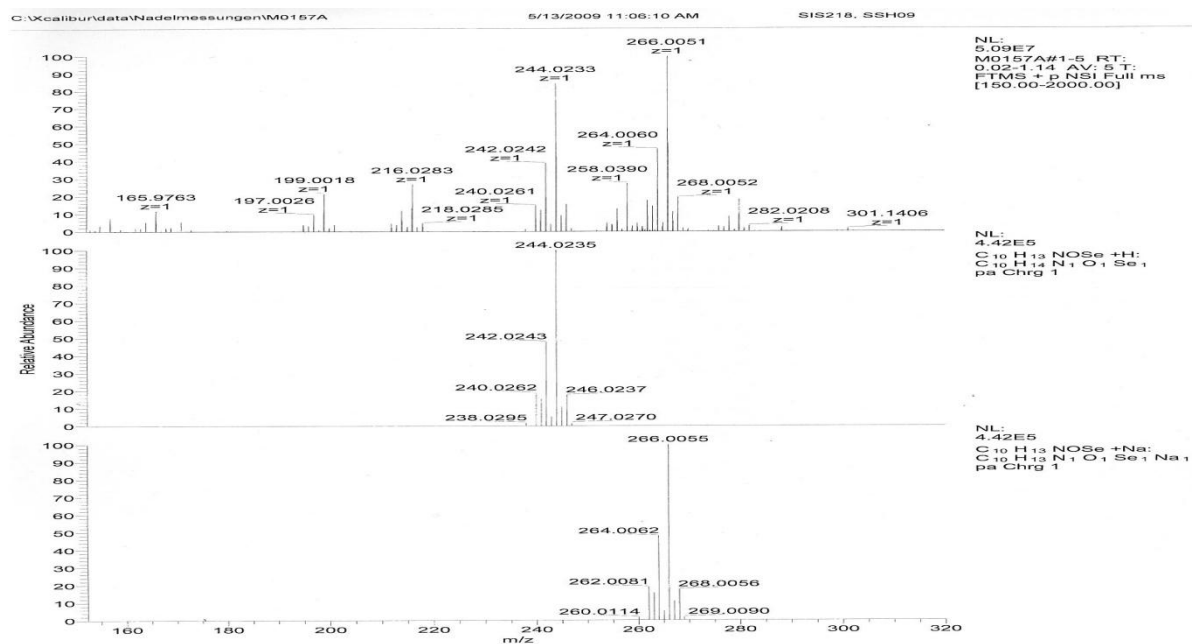


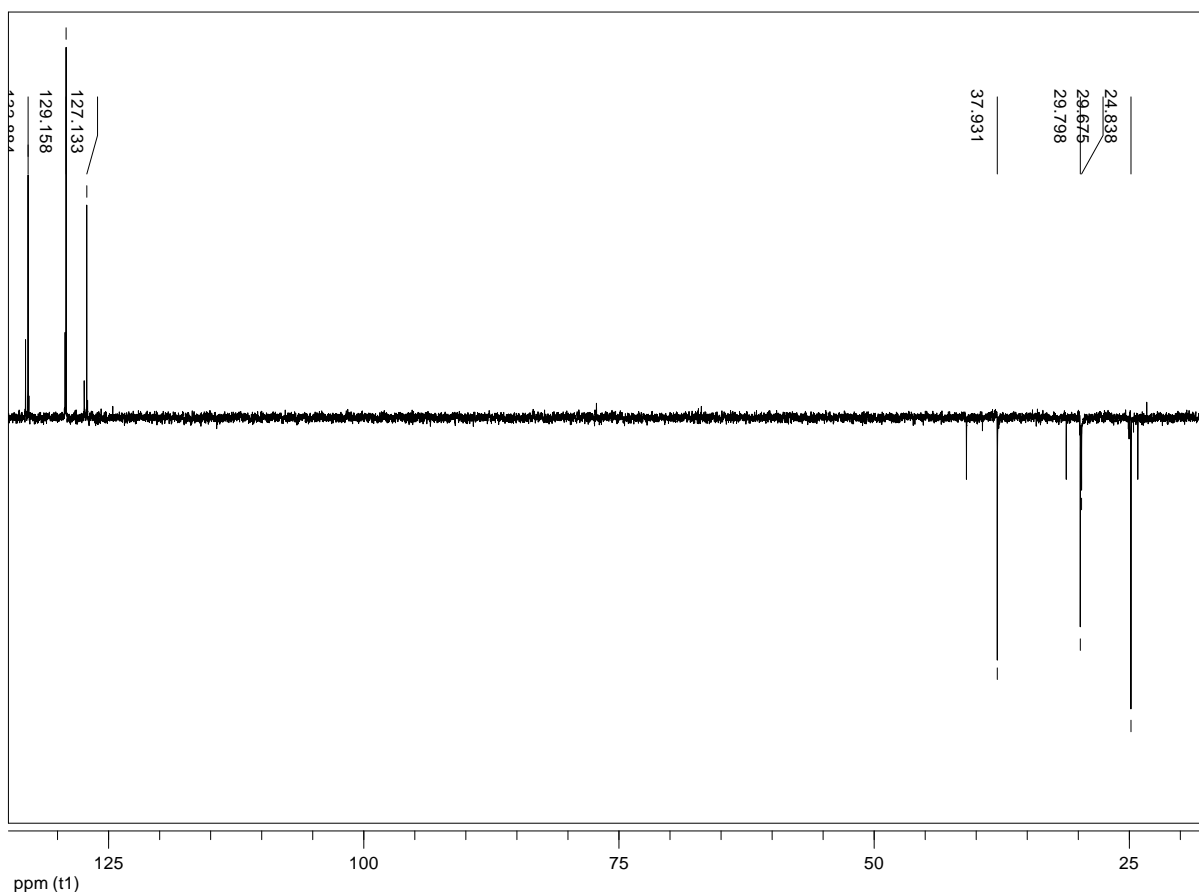
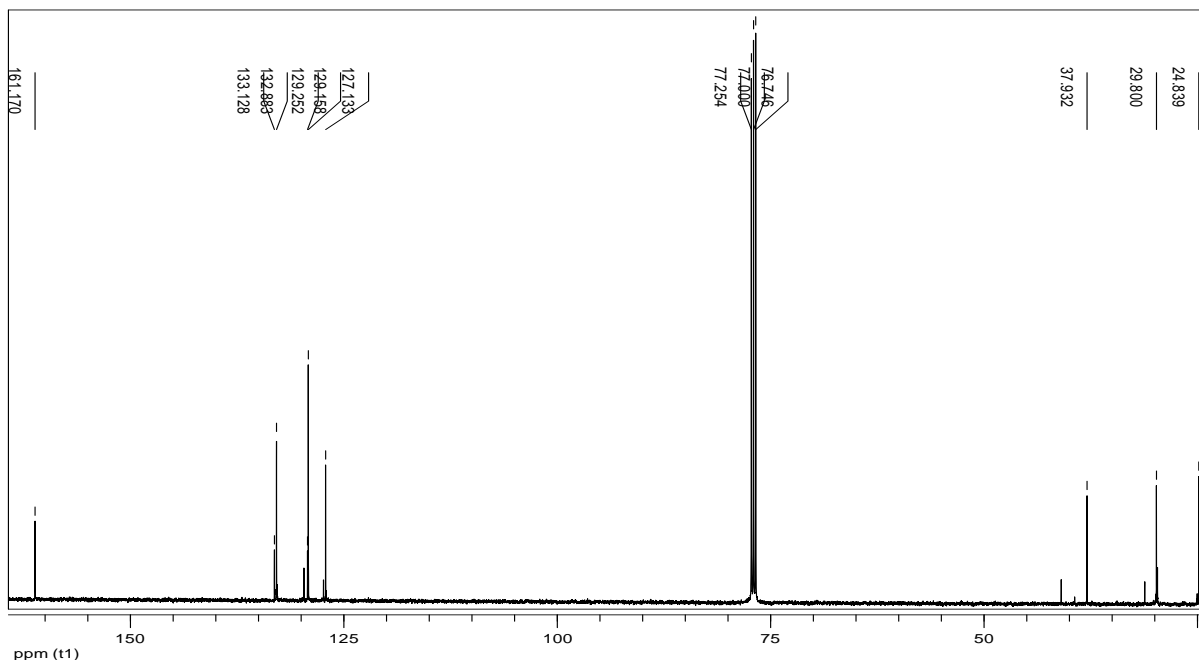
Compound 3c



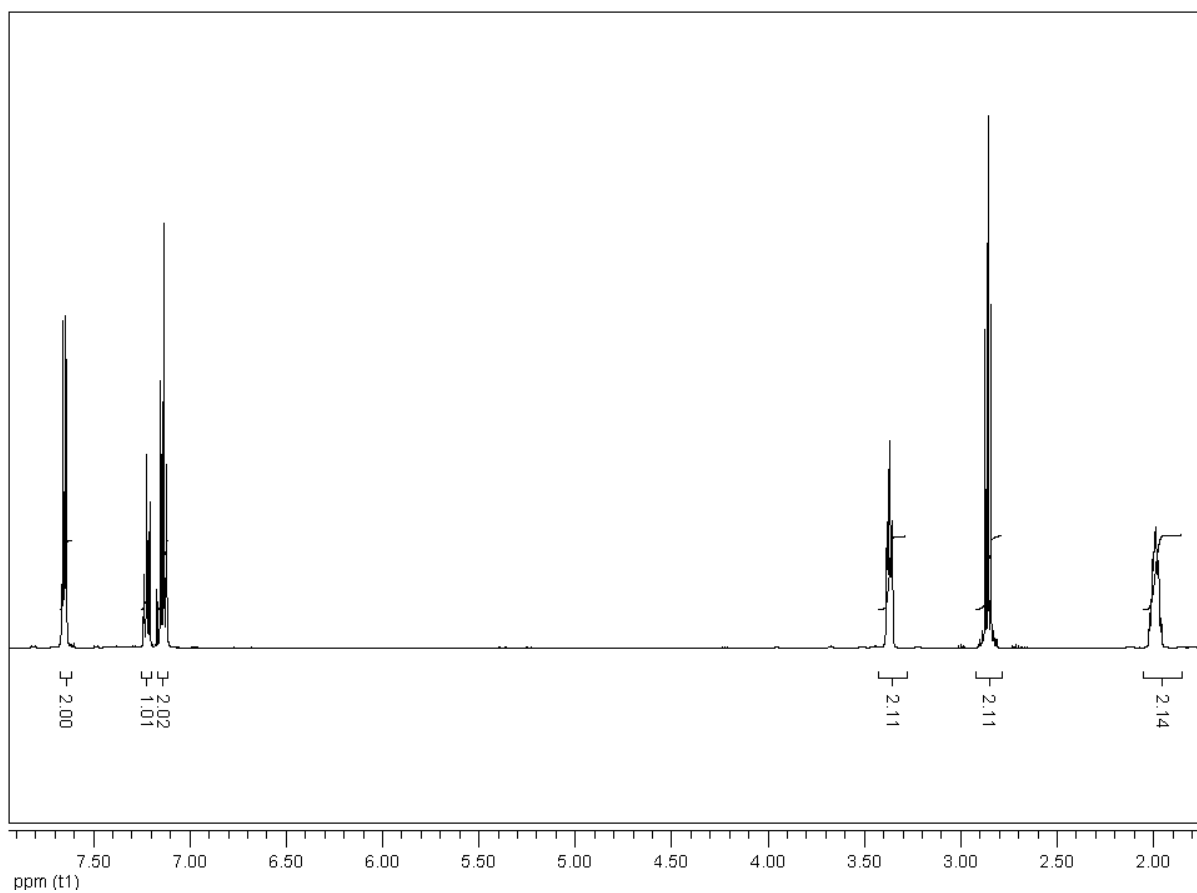
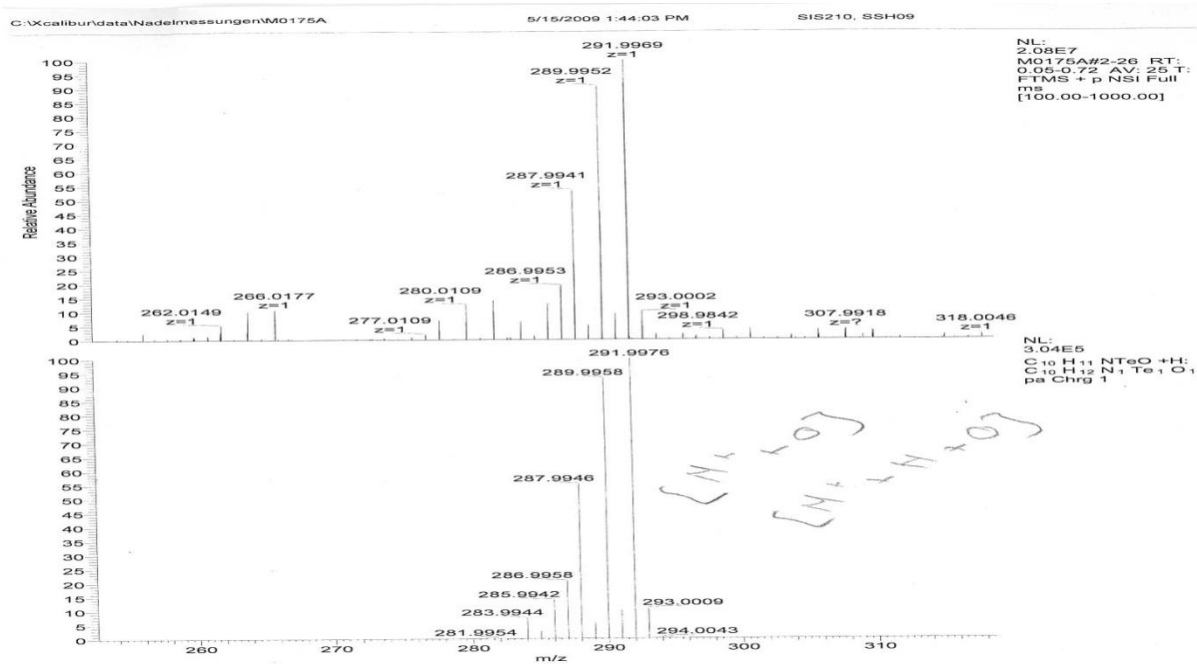


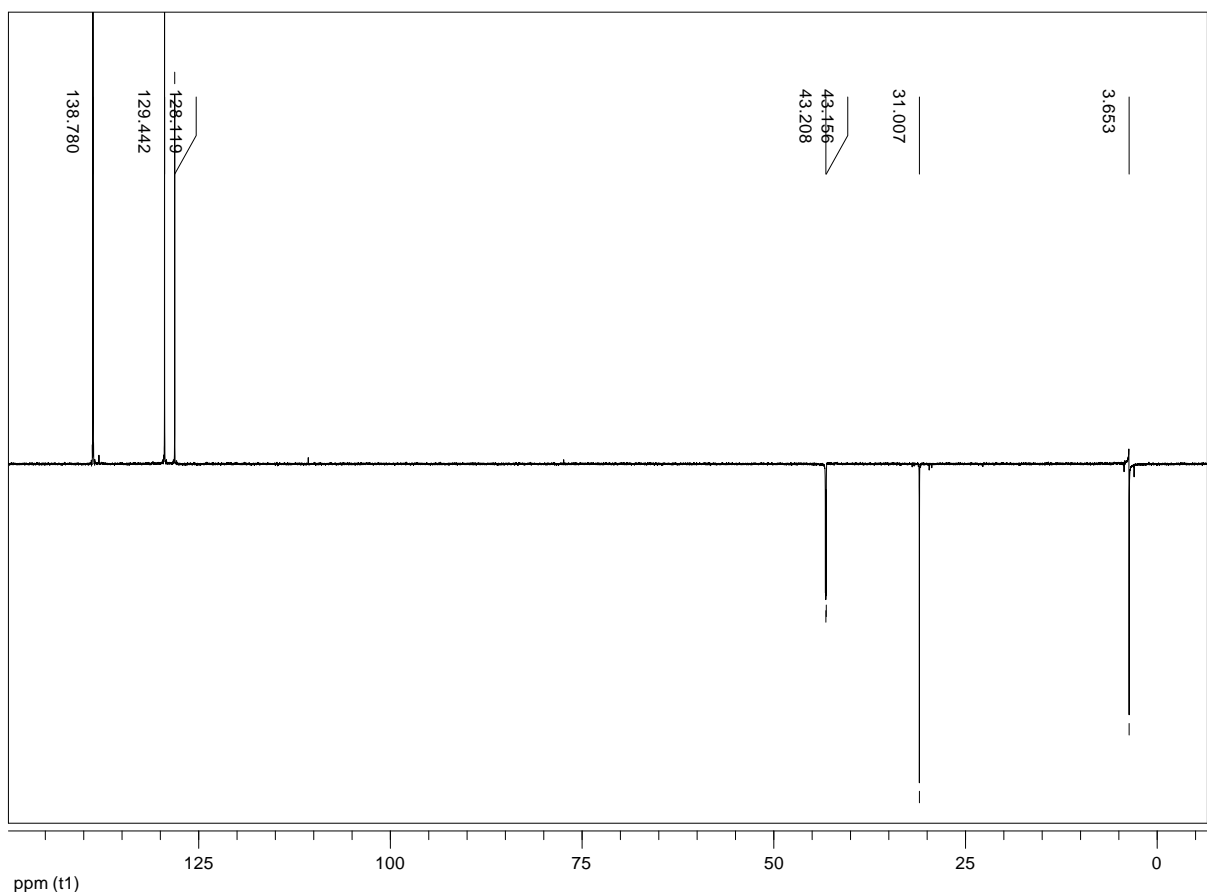
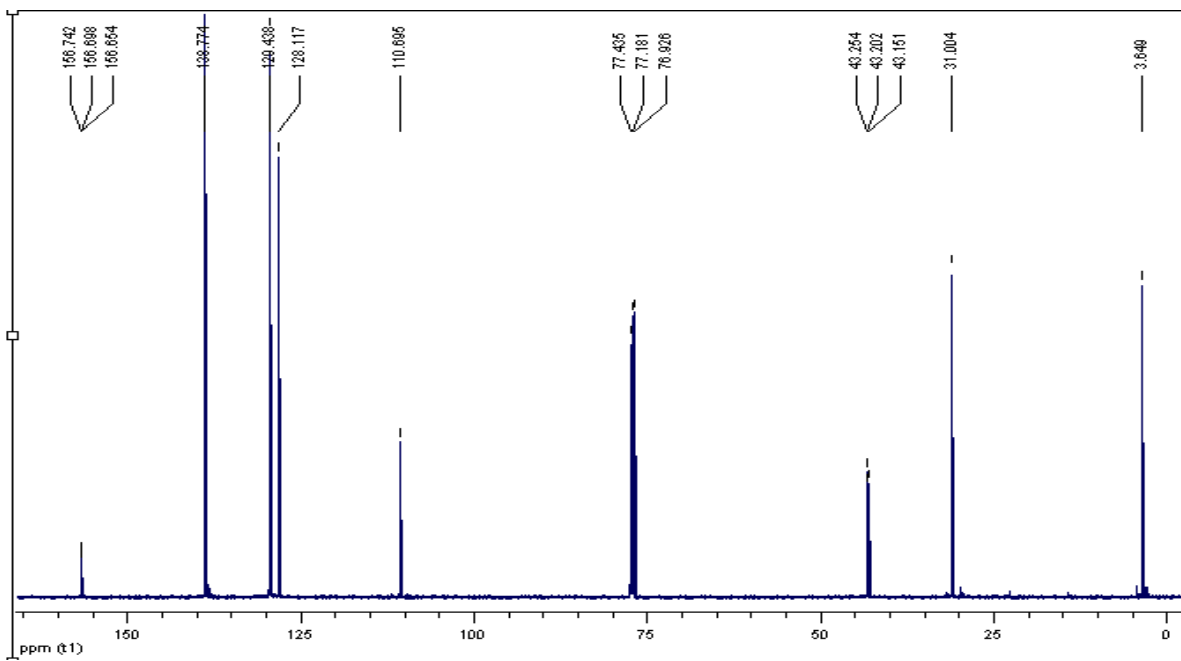
Compound 3d





Compound 3e





Saad Shaaban, M.Sc

Mansoura University
Faculty of Science
Chemistry Department
Egypt

PERSONAL

- **Date of Birth:** 01 March 1981.
- **Place of Birth:** Mansoura-Egypt.
- **Nationality:** Egyptian.
- **Marital status:** Married, and I have two childrens.
- **E-mail:** saad_shaaban@yahoo.com
- **Fax:** 050-2246781 (*work*).
- **Phone:** +2050-22410528 (*home*).

ACADEMIC

- **PhD. Dissertation** “Synthesis and Biological Activity of Multifunctional Sensor/Effector Catalysts” with Prof. Claus Jacob, University of Saarland, Germany. (2007-todate).
- **M.Sc. Dissertation** “Synthesis of some Annulated Compounds via Transformations of Nitogen Containing Heterocycles” with Prof. Hanafi H. Zoorob, Mansoura University, Egypt. (2003-2006).
- **Pri. M.Sc.** in Organic chemistry, Mansoura University, Egypt. (2003).
- **B.Sc.** in Chemistry Mansoura University, Egypt. (2001).

EXPERIENCE & TEACHING SKILLS

- **Demonstrator** at the Chemistry Department, Faculty of Science, Mansoura University. (2003- 2006)
- **Teaching** the following undergraduate practical laboratory courses

[1] Dyes.

[2] Separation of Organic Mixture.

[3] Estimation of Organic Compounds.

[4] Investigation of Organic Compounds.

[5] Study of Physical Organic Mechanisms.

[6] Simple and Complete Identification of Organic Compounds.

[7] Isolation, Purification and Identification of Natural Products.

[8] Organic Synthesis of Heterocyclic and Polymeric Compounds.

[9] Separation and Identification of acidic and basic radicals of simple salts.

[10] Qualitative and Quantitative Identification of Organic Compound by Spectroscopy Analyses.

- **Computer Skills:** (ICDL, granted in September, 2008).

HOBBIES

Traveling, Swimming, Reading, and web surfing.

SCIENTIFIC CONFERENCES

- **Dream Reactions- synthesis and Processes for sustainable Chemistry.**
Aachen, Germany April 2008.

List of Publications

- 1) **Shabaan, S.**; Ba, L. A.; Abbas, M.; Burkholz, T.; Denkert, A.; Gohr, A.; Wessjohann, L. A.; Sasse, F.; Weber, W.; Jacob, C. Multicomponent Reactions for The Synthesis of Multifunctional Agents With Activity Against Cancer Cells. *Chemical Communications* **2009**, 4702-4704.
- 2) Metwally, M. A.; **Shaaban, S.**; Abdel-Wahab, B. F.; El-Hiti, G. A. 3-Acetylindoles: Synthesis, Reactions and Biological Activities. *Current Organic Chemistry* **2009**, 13, 1475-1496.
- 3) Mecklenburg, S.; **Shaaban, S.**; Ba, L. A.; Burkholz, T.; Schneider, T.; Diesel, B.; Kiemer, A. K.; Roseler, A.; Becker, K.; Reichrath, J.; Stark, A.; Tilgen, W.; Abbas, M.; Wessjohann, L. A.; Sasse, F.; Jacob, C. Exploring Synthetic Avenues for The Effective Synthesis of Selenium- and Tellurium-Containing Multifunctional Redox Agents. *Org. Biomol. Chem.* **2009**, 7, 4753-4762.
- 4) Hamama, W. S.; Ismail, M. A.; **Shaaban, S.**; Zoorob, H. H. Progress in The Chemistry of 4- Thiazolidinones. *J. Heterocycl. Chem.* **2008**, 45, 939-956.

Under Preparation

- 1) **Saad Shaaban**, Randi Diestel, Bettina Hinkelmann, Yazh Muthukumar, Lothar Gröbe, Rajeshwar P. Verma Florenz Sasse, and Claus Jacob. Novel Peptidomimetic Compounds Containing Redox Active Chalcogens and Quinones as Potential Anticancer Agents. (Submitted to *J. Med. Chem.*)
- 2) **Saad Shaaban**, Bettina Hinkelmann, Florenz Sasse, and Claus Jacob. The use of Multicomponent Ugi Reaction in The Synthesis of Multifunctional Sensor/effector Catalysts.(Under preparation)

- 3) **Saad Shaaban**, Florenz Sasse, and Claus Jacob. Antimicrobial Evaluation of Selenium- and Tellurium-Containing Multifunctional Redox Agents.(Under preparation)
- 4) Mahmoud Fahmi Elsebai, Stefan Kehraus, Ulrike Lindequist, Florenz Sasse, **Saad Shaaban**, Michael Gütschow, Michaele Josten, Hans-Georg Sahl, and Gabriele M. König. Antimicrobial Phenalenone Derivatives from The Marine-derived Fungus *Coniothyrium Cereal*. *Organic & Biomolecular Chemistry*. (Accepted)
- 5) Wafaa S. Hamama, Mohamed A. Ismail, Mamdoh Soliman, **Saad Shaaban**, and Hanafi H. Zoorob. Behaviour of 2-Iminothiazolidin-4-one with Different Reagents. *Journal of Heterocyclic Chemistry*. (Accepted)
- 6) Wafaa S. Hamama, Mohamed A. Ismail, Mamdouh S. Soliman, **Saad Shaaban**, and Hanafi H. Zoorob. Synthesis and Characterisation *via* Molecular Quantum Parameters of 2H-Thiazolo[3,2-a]pyrimidine-3,5,7(6H)-trione. *Journal of Heterocyclic Chemistry*. (Accepted)
- 7) Wafaa S. Hamama, Mohamed A. Ismail, **Saad Shaaban**, and Hanafi H. Zoorob. Synthesis and Biological Evaluation of Some New Thiazolo[3,2-a][1,3,5]triazine Derivatives. (Submitted to *Med. Chem. Res.*)